Vers une meilleure compréhension de la tolérance aux antibiotiques de biofilms bactériens cliniques

Rym Boudjemaa

NNT : 2017SACLS241

THESE DE DOCTORAT
DE
L'UNIVERSITE PARIS-SACLAY
PREPAREE A
L'UNIVERSITE PARIS-SUD

Ecole Doctorale n° 571
Sciences chimiques : molécules, matériaux, instrumentation et biosystèmes

Spécialité de doctorat : Chimie

Par

Mme Rym Yasmine Boudjemaa

Vers une meilleure compréhension de la tolérance aux antibiotiques de biofilms bactériens cliniques

Thèse présentée et soutenue à Orsay, le 15 septembre 2017 :

Composition du Jury :

M. Bouloc, Philippe, Directeur de recherche, CNRS	Président
Mme Ishow, Elena, Professeure, Université de Nantes	Rapporteur
Mme Forestier, Christiane, Professeure, Université Clermont Auvergne	Rapporteur
M. Tramier, Marc, Ingénieur de Recherche, CNRS	Examinateur
M. Tattevin, Pierre, Professeur des universités - Praticien hospitalier, CHU de Rennes	Examinateur
Mme Fontaine-Aupart, Marie-Pierre, Directrice de recherche, CNRS	Directrice de thèse
Mme Steenkeste, Karine, Maître de conférences, Université Paris-Sud	Invitée

ÉCOLE DOCTORALE
Sciences chimiques : molécules, matériaux, instrumentation et biosystèmes

Titre : Vers une meilleure compréhension de la tolérance aux antibiotiques de biofilms bactériens cliniques

Mots clés : antibiotiques, biofilms, tolérance, imagerie multimodale

Résumé : Les bactéries sont des microorganismes capables de se développer et de proliférer indépendamment les uns des autres en milieu liquide. Mais dès qu'une surface se présente, biotique ou abiotique, les bactéries privilégient un « mode de vie en communauté » pour se protéger des agressions externes et survivre aux environnements hostiles. Ces biostructures, appelées biofilms, sont présentes dans tous les environnements naturels, y compris chez l'Homme où elles peuvent être à l'origine d'infections chroniques lorsqu'elles hébergent des germes pathogènes. Il est aujourd'hui admis que de tels édifices biologiques perdurent sous l'action des antibiotiques. Outre le très médiatique phénomène de résistance qui trouve son origine dans des mutations génétiques bactériennes, la tolérance, quant à elle, provient des spécificités de la structure et de la physiologie des bactéries organisées en biofilms. C'est dans ce contexte que s'inscrit ce travail de thèse qui vise à mieux comprendre les mécanismes sous-jacents au manque d'efficacité d'antibiotiques (vancomycine, daptomycine, rifampicine) vis-à-vis des biofilms de *S. aureus*, en s'appuyant notamment sur des techniques innovantes d'imagerie à résolution micro-nanométrique. Nous avons mis au point un modèle d'infections sur prothèse vasculaire implantable chez la souris qui a permis une toute première visualisation par imagerie de fluorescence de biofilms formés *in vivo* et soumis à l'action des antibiotiques mais aussi de montrer leur activité limitée. Nous nous sommes ensuite attachés à une meilleure compréhension de la tolérance aux antibiotiques de biofilms bactériens de *S. aureus*. Pour ce faire, nos études ont porté, d'une part, sur le rôle de la matrice extracellulaire et, d'autre part, sur le rôle de la physiologie des bactéries incluses en biofilm. Il a ainsi été mis en évidence le rôle crucial de la fluidité membranaire. Ces travaux nous ont alors permis de dégager des pistes pour améliorer l'antibiothérapie disponible mais aussi développer des alternatives à ce type de traitement.

Title: Towards a better understanding of clinical bacterial biofilms tolerance to antibiotics

Keywords: antibiotics, biofilms, tolerance, multimodal imaging

Abstract: Bacteria are microorganisms capable of growing independently in liquid media. However, as soon as they encounter a surface, either biotic or abiotic, bacteria favour a "community living" to protect themselves from external aggressions and survive in hostile environments. These bacterial communities, named biofilms, are present in all natural environments, including humans where they can cause severe infections when hosting pathogenic germs. It is now accepted that such biological edifices persist under antibiotics action. In addition to the highly mediatized resistance phenomenon, which is associated with genetic mutations of bacteria, tolerance is related with the specific structure and physiology of bacteria organized in biofilms. In this context, we took benefit from innovative high-resolution imaging techniques to better understand the mechanisms underlying antibiotics (vancomycin, daptomycin, rifampicin) (in)efficacy within *S. aureus* biofilms. In addition, we developed a model for prosthetic vascular graft infections in mice that allowed the visualization by fluorescence imaging of biofilms formed *in vivo* and subjected to the action of antibiotics. Considering the very limited antibiotics efficacy observed, we then focused on a better understanding of *S. aureus* bacterial biofilms tolerance towards antibiotics. To this purpose, our work was focused on the role of both the extracellular matrix and the physiology of bacteria included in biofilms. The crucial role of membrane fluidity was then demonstrated. This work allowed us to identify paths for the improvement of antibiotic therapy and to develop alternatives to this type of treatment.

Remerciements

Cette thèse a été financée par une bourse de l'Ecole Doctorale 571 « Sciences chimiques : molécules, matériaux, instrumentation et biosystèmes » de l'Université Paris-Saclay.

Je remercie tout d'abord M. Bernard Bourguignon, directeur de l'ISMO, de m'avoir accueillie dans son unité de recherche, au sein de laquelle j'ai pu réaliser mes travaux de thèse dans les meilleures conditions.

Je remercie Mme Elena Ishow et Mme Christiane Forestier d'avoir accepté d'évaluer mon manuscrit de thèse. J'adresse également mes remerciements à M. Pierre Tattevin, M. Philippe Bouloc et M. Marc Tramier pour avoir accepté d'examiner ce travail.

Je tiens à remercier tout particulièrement Marie-Pierre Fontaine-Aupart et Karine Steenkeste pour m'avoir encadrée et soutenue durant ces trois années, pour leur gentillesse, leur grande disponibilité et leur enthousiasme en toutes circonstances. Merci Marie-Pierre pour votre esprit critique hors pair qui a, sans cesse, contribué à l'amélioration de ces travaux de façon constructive. Karine, merci de m'avoir transmis votre savoir sur l'ensemble des techniques, aussi bien en imagerie de fluorescence qu'en microbiologie. Votre mémoire infaillible me surprendra toujours ! Merci à toutes les deux pour toutes les discussions constructives que nous avons pu avoir tous domaines confondus.

Un grand merci à Allan Rodriguez, Thibaut Troude et Laetitia Lallement qui m'ont permis d'effectuer mon sixième de temps hors-recherche au sein de leur start-up, VitaDX.

J'adresse également mes remerciements aux membres du Centre de Photonique Biomédicale, au sein duquel j'ai réalisé la plupart de mes expériences, et plus particulièrement aux personnes que j'ai côtoyées au quotidien : Sandrine Lécart, Sandrine Lévêque-Fort, Guillaume Dupuis, Chantal Jucha pour leur aide et leur sympathie au quotidien. Je remercie également les autres membres de l'équipe avec lesquels j'ai eu l'occasion de travailler : Rachel Méallet-Renault pour sa bonne humeur et Christian Marlière pour m'avoir fait découvrir la microscopie à force atomique.

Merci à l'ensemble des doctorants, post-doctorants et stagiaires avec qui j'ai partagé de très bons moments : Nicolas, Alan, Baptiste, Clément, So-Young, Marta, Lenka, Gabriela, Elisabetta, Marwa, Martina.

Mes sincères remerciements vont également aux membres de l'Institut Micalis de l'INRA qui m'ont toujours accueillie très chaleureusement au sein de leur laboratoire : Julien, Charlène, Alexis, Gilles, Jean-Christophe, Caroline, Aurélia. Un grand merci à Romain Briandet, Florence Dubois-Brissonnet et Alexandra Gruss pour leur gentillesse, leur sympathie et leur disponibilité face à mes multiples questions en tout genre sur les bactéries ! Romain, merci pour toutes vos relectures et les nombreuses discussions constructives que nous avons pu partager mais surtout pour votre créativité et l'enthousiasme que vous portez à explorer toujours plus de nouvelles pistes. Florence, un grand merci également pour votre aide dans la réalisation des expériences d'analyses en chromatographie. Sandy, je vous remercie pour les conseils et suggestions autour de la fluidité des membranes, mais aussi…des articles !

Je remercie également les membres de l'ISMO que j'ai côtoyés au quotidien : Ivan, Valéria, Christophe, Thierry, Catherine, Katia. Un grand merci également au personnel administratif qui s'est toujours montré sympathique : Annie, Valérie, Sylvie, Véronique, Stéphanie, Bernadette.

Je tiens à remercier mes colocataires de bureau pour tous les bons moments que nous avons pu passer ensemble, aussi bien au labo qu'en dehors, et les nombreuses discussions de palier en tous genres : Alexis, Velia, Gianluca.

Un grand merci aux stagiaires qui m'ont considérablement aidée à faire aboutir ces travaux : Céline, Matthieu, Félindra, Inès, Ali, Kenny et Cynthia.

Je tiens à remercier également les personnes avec lesquelles j'ai pu collaborer sur les divers projets abordés dans le cadre de ma thèse : Maryse Hoebeke de l'Université de Liège, Raphael Schneider de l'Université de Nancy, Pascal Thébault de l'Université de Rouen. Aussi, un très grand merci à l'équipe de l'Université de Nantes et du CHU de Rennes : Jocelyne Caillon, Cédric Jacqueline et Matthieu Revest.

Miryana, je te remercie tout particulièrement pour m'avoir encouragée et convaincue de me lancer dans cette aventure. Sans toi, je n'aurais sans doute pas envisagé de faire une thèse !

Merci à mes amis bordelais, marseillais et montiliens qui m'ont soutenue à tout moment au cours de ces trois années. Mais surtout un énorme merci aux parisiens : Mouni, Rym, Hannah, qui m'ont soutenue et « supportée » tout du long, aussi bien dans les bons moments que dans les moins bons ! Berdice, merci de ton écoute malgré la distance !

A mes parents, merci maman, merci papa de m'avoir toujours soutenue dans tout ce que j'ai pu entreprendre et de m'avoir appris à faire toujours plus d'efforts. Merci à mes sœurs qui, de ce côté de la Méditerranée ou de l'autre, ont toujours veillé sur « leur petite dernière. »

Et enfin, merci à toi, Tarik, de ton aide, de ton support, de ta patience mais surtout d'avoir toujours fait en sorte que je reste de bonne humeur en toutes circonstances…

Table des matières

Liste des abréviations

ADN : acide désoxyribonucléique
AFM : Atomic Force Microscopy
ANOVA : ANalysis Of VAriance
APG-2 : Asante Potassium Green -2
ARN : Acide RiboNucléique
ATCC : American Type Culture Collection

Bap : Biofilm-associated surface proteins
BCEC : 2′,7′-bis-(2-Carboxyethyl)-5-(and-6)-carboxyfluorescein
BCECF-AM BCECF : acetoxymethylester
BFA : Branched-Chain Fatty Acid
BODIPY-FL : dipyrro-metheneboron difluoride
BrdU : Bromodeoxyuridine
BSA : Bovin Serum Albumin
$CaCO_3$: carbonate de calcium
CFDA : Carboxyfluorescein Diacetate
CFU : Colony-Forming Units
ClfB : clumping factor B
CLSM : Confocal Laser Scanning Microscopy
CMI : concentration minimale inhibitrice
Cna : collagen-binding protein
CPBD : Calgary Biofilm Pin Lid Device
CTC : 5-cyano-2,3-ditoluyl Tetrazolium Chloride
DAPI : 4,6-diamidino-2-phenylindole Dihydrochloride
DMSO : dimethylsulfoxide
DONALD : Direct Optical Nanoscopy With Axially Localized Detection
EFM : Epifluorescence Microscopy
EPS : exopolysaccharides
EUCAST : European Committee on Antimicrobial Susceptibility Testing
FCM : Flow Cytometry
FCS : Fluorescence Correlation Spectroscopy
FFlucRT : Firefly Luciferase Gene
FLIM : Fluorescence Lifetime Imaging
FnBP : fibronectin-binding protein
FRAP : Fluorescence Recovery after Photobleaching
GFP : Green Fluorescent Protein
GPC : Gas Phase Chromatography
ITO : Indium-Tin Oxide
LSC : Laser Scanning Cytometer
LSM : Laser Scanning Microscopy
MBC : Minimum Bactericidal Concentration
MBEC : Minimum Biofilm Eradicating Concentrations
MBIC : Minimum Biofilm Inhibitory Concentrations
MHB : Mueller-Hinton broth
MIC : Minimum Inhibitory Concentration
MPA : Acide mercaptopropionique
MRSA : Methicillin-Resistant *S. aureus*
MSCRAMMs : Microbial Surface Components Recognizing Adhesive Matrix
MSSA : Methicillin-Susceptible *S. aureus*
MUA : Acide mercaptoundecanoique

NaCl : Chlorure de sodium
NAG : N-acetylglucosamine
Nanoscale Topography
NBD-Cl : 4-Chloro-7-nitrobenzofurazan
NIR : Near Infrared
PAINT : Point Accumulation for Imaging in
PALM : Photo-activated Localization Microscopy
PCR : Polymerase Chain Reaction
PI : Propidium Iodide
PIA : Polysaccharide Intercellular Adhesin
PNAG: poly-β(1-6)-N-acetylglucosamine
PSM : Phenol Soluble Modulins
PTFE : polytétrafluoréthylène
PVGI : Prosthetic Vascular Graft Infection
QD : quantum dots
RFP : Red Fluorescent Protein
RMS : Root Mean Square

RT-PCR: Reverse Transcription-PCR
SAF : Supercritical Angle Fluorescence
SasG : *S. aureus* surface protein G

SFA : Saturated Fatty Acid
SIM : Structured Illumination Microscopy
SMLM : Single-molecule Localization Microscopy
SOD : superoxyde dismutase
SraP : Serine-Rich Surface Protein
STED : Stimulated Emission Depletion
STORM : Stochastic Optical Resolution Microscopy
SWNT : Single-walled Carbon Nanotube
TIRF : Total Internal Reflection Fluorescence
TPE : Two-photon Excitation
TSA : Tryptic Soy Agar
TSB : Tryptic Soy Broth
VBNC : Viable But Non Culturable
ZnS : Sulfure de Zinc

INTRODUCTION GENERALE

La bio-colonisation des surfaces exposées à des environnements humides non stériles est un processus naturel et spontané, rencontré quelle que soit la nature de la bactérie (bactéries à Gram positif ou négatif, formes sporulées ou non, …), du fluide environnant (air, liquide simple ou complexe) et du support récepteur (surfaces biotiques ou abiotiques). Elle est caractérisée par l'adhésion de premières bactéries, le plus souvent suivie par la croissance de structures tridimensionnelles engluées dans une matrice polymérique, appelées biofilms. Lorsque cette biocontamination surfacique implique des germes pathogènes, elle peut être à l'origine de problèmes de santé publique sévères en milieu hospitalier ou dans l'industrie (infections nosocomiales, toxiinfections alimentaires ou cosmétiques, …etc.).

Depuis leur découverte en 1928 par Alexander Fleming, les antibiotiques ont permis de faire considérablement reculer la mortalité associée aux infections bactériennes. Hélas, selon un rapport britannique paru en 2016, les infections associées à des germes pathogènes impliquent 700 000 décès dans le monde chaque année et engendreraient, d'ici 2050, le décès de dix millions de personnes par an si aucune mesure n'est prise.

Pourquoi un tel retournement de situation ? Face à l'utilisation massive et répétée des antibiotiques, la quasi-totalité des bactéries est détruite mais il en reste toujours quelques-unes qui survivent en développant des systèmes de défense remarquables contre ces médicaments : c'est le phénomène de résistance qui défraie tant la chronique actuellement. Cette situation est encore plus criante lorsque les bactéries sont structurées en biofilm. En effet, l'adhésion des cellules aux surfaces leur confère une physiologie particulière qui leur permet de faire face aux stress environnementaux, les rendant alors insensibles aux molécules censées les détruire (système immunitaire, antibiotiques, …).

La triste réalité de cette résistance aux antibiotiques est aggravée par le manque de nouvelles molécules efficaces dans les pipelines de l'industrie pharmaceutique. Face à cette impasse thérapeutique, il apparait donc crucial de concentrer les efforts de la recherche et de l'innovation scientifiques pour apporter une meilleure compréhension de la résistance aux antibiotiques et proposer des solutions nouvelles.

C'est dans ce contexte que s'est inscrit mon travail de thèse, qui a utilisé la synergie des compétences entre physiciens, physico-chimistes de l'équipe Biophysique/Biophotonique de l'Institut des Sciences Moléculaires d'Orsay et de leurs collaborateurs médecins infectiologues du Centre Hospitalo-Universitaire de Nantes et microbiologistes de l'Institut National de la Recherche Agronomique pour développer des travaux de recherche sur les infections à biofilms induites par *Staphylococcus aureus (S. aureus),* bactérie pathogène au premier rang des germes responsables d'infections humaines graves.

Ce manuscrit se décline en trois parties principales.

La première partie correspond à une synthèse bibliographique présentant le contexte de ce travail : i) un état de l'art général sur les infections associées aux biofilms de *S. aureus* et le comportement des bactéries face au système immunitaire et à l'antibiothérapie (Chapitre 1) et ii) un état de l'art sur les performances des outils de la fluorescence pour caractériser *in vitro* et *in vivo* l'(in)action des antibiotiques sur les bactéries (Chapitre 2).

La seconde partie rassemble les résultats obtenus au cours de ce travail (Chapitres 3 à 5). Face au manque de données concernant la formation des biofilms de *S. aureus* sur implants et l'action des antibiotiques *in vivo,* nous avons mis au point un modèle d'infections sur prothèse vasculaire implantable chez la souris (Chapitre 3). Les résultats de cette étude confirment l'efficacité limitée des antibiotiques pour des infections à biofilms. Dans la suite de ce travail de thèse, nous nous sommes attachés à une meilleure compréhension de la tolérance aux antibiotiques de biofilms bactériens cliniques. Pour ce faire, nos études ont porté, d'une part, sur le rôle de la matrice extracellulaire (Chapitre 4) et, d'autre part, sur le rôle de la physiologie des bactéries incluses en biofilm (Chapitre 5).

La compréhension de l'inefficacité de traitements antibiotiques de dernière génération vis-à-vis des infections à *S. aureus* sur implants nous a alors permis de dégager des pistes pour améliorer l'antibiothérapie disponible mais aussi de développer des alternatives à ce type de traitement, qui sont proposées dans la partie « Synthèse générale et perspectives » de ce manuscrit.

SYNTHESE BIBLIOGRAPHIQUE

Chapitre 1 : Les biofilms de staphylocoques dorés : une communauté de fins stratèges à l'origine d'infections récalcitrantes

1.1. Les biofilms bactériens cliniques

Les bactéries sont des microorganismes capables de se développer et de proliférer indépendamment les uns des autres en milieu liquide. Mais dès qu'une surface se présente, biotique ou abiotique, les bactéries privilégient le « mode de vie en communauté » pour se protéger des agressions externes et survivre aux environnements hostiles. L'existence de ce mode de vie a été rapportée pour la première fois en 1933 par Arthur Henrici qui observe, à la surface d'une lame de verre plongée dans un aquarium, un dépôt de microorganismes s'épaississant au cours du temps et formant alors un film bactérien.[1] Quelques années plus tard, Claude Zobell et Esther Allen rapportent que l'essentiel de la biomasse microbienne n'est pas en suspension mais fixé à des surfaces.[2] Dans les années 80, c'est William Costerton qui introduit la notion de biofilms comme étant *« un assemblage biologique dans lequel les microorganismes forment des communautés tridimensionnelles épaisses et structurées dont les sous-populations assurent des fonctions spécifiques »*.[3,4]

Les biofilms sont présents dans tous les environnements naturels et peuvent avoir de multiples impacts : ils peuvent (i) jouer un rôle bénéfique capital au bon fonctionnement de nombreux écosystèmes comme par exemple dans le traitement des eaux usées ; (ii) être utiles, par exemple dans la flore intestinale pour la digestion des aliments ou la défense de l'organisme contre les germes pathogènes ; (iii) être désagréable comme au niveau de la plaque dentaire ; (iv) être destructeur, dans la biocorrosion des matériaux par exemple ; mais également (v) être fatals en médecine humaine et animale, à l'origine d'infections gravissimes et/ou chroniques.

En colonisant tous types de surfaces en milieu hospitalier aussi bien biotiques (tissus ou muqueuses) qu'abiotiques (prothèses, implants, cathéters ou autres équipements médicaux), les biofilms sont aujourd'hui impliqués dans plus de 65% des infections humaines et à l'origine de plus de 700 000 décès par an.[5] La colonisation bactérienne des muqueuses et des tissus a été mise en évidence pour la première fois dans les années 70 par Niels Høiby.[6] Il y démontre le lien entre la présence d'agrégats bactériens et la chronicité d'infections pulmonaires persistantes en examinant au microscope des crachats issus de patients atteints de la mucoviscidose. La colonisation de dispositifs médicaux implantés a été, quant à elle, rapportée dès le début des années 1980 grâce au développement de la microscopie électronique : des dépôts bactériens ont ainsi pu être visualisés sur la surface de cathéters intraveineux ou stimulateurs cardiaques.[7–9]

Parmi les pathogènes associés aux infections à biofilms dont la liste non exhaustive est indiquée en **Figure 1**, on retrouve le plus fréquemment les souches bactériennes de *Pseudomonas aeruginosa, Escherichia coli, Staphylococcus epidermidis* et *Staphylococcus aureus* (*S. aureus*). Si on s'intéresse plus particulièrement aux dispositifs médicaux, *S. aureus* se trouve au premier rang des germes responsables des infections associées à des biofilms. C'est une bactérie en forme de coque dont le diamètre est d'environ 1 µm et à paroi Gram positif. Elle dispose donc d'une seule membrane, cytoplasmique, et d'un peptidoglycane de nature polymérique constituant sa paroi. De plus, une capsule polysaccharidique peut englober les bactéries de *S. aureus*, jouant un rôle important dans son pouvoir pathogène.

Chez l'Homme, *S. aureus* fait partie de la flore cutanée et nasale naturelles et 30% des sujets sains en sont porteurs.[10] En revanche, dès lors que ces bactéries trouvent un point d'entrée dans l'organisme (à travers une plaie par exemple) ou qu'elles s'activent anormalement en raison d'un système immunitaire de l'hôte amoindri (interventions médicales invasives, chimiothérapie, état de fatigue, …), elles peuvent provoquer des infections au degré de gravité variable.[11,12] En particulier, les bactéries peuvent coloniser les cellules et les entités de la matrice extracellulaire de l'hôte (tissus, protéines plasmatiques, …) ou s'associer à des implants et ainsi former des biofilms à l'origine d'infections sévères. Il a ainsi déjà été montré que les microorganismes de la peau ou des tissus mous qui entrent de manière transitoire dans la circulation sanguine pouvaient coloniser des valves implantées ou encore les surfaces endothéliales du cœur, entrainant ensuite des infections chroniques graves telles que les bactériémies ou les endocardites.[12,13] La prévalence de ces infections staphylococciques provient principalement de la persistance de cette espèce bactérienne chez l'hôte : en formant des biofilms, les bactéries perdurent en résistant non seulement à l'action du système immunitaire (phagocytose, défenses inflammatoires, …) mais également à celle des antimicrobiens.

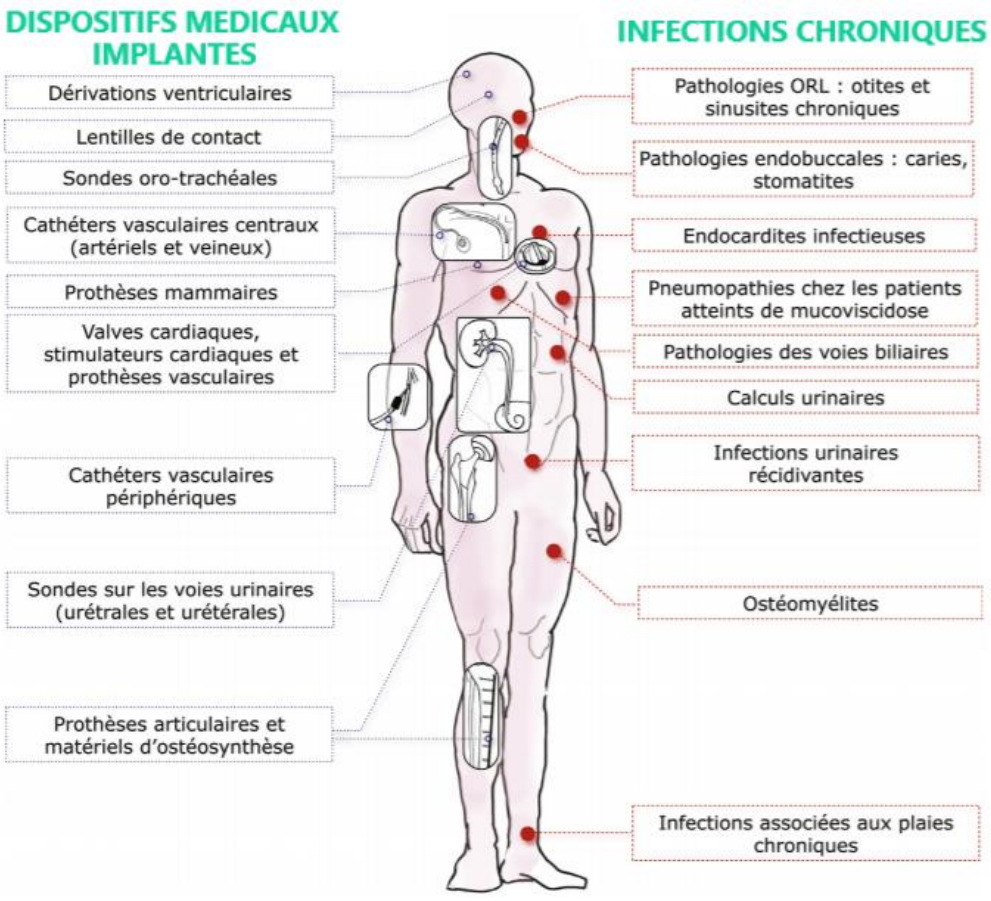

Figure 1. *Liste non exhaustive des types de dispositifs médicaux implantés ainsi que des infections sévères associées à la présence de biofilms bactériens. Reproduit de Lebeaux et al. 'Tolérance des biofilms aux antibiotiques : comprendre pour mieux traiter', Journal des anti-infectieux, 2014.*[14]

1.2. Les bactéries à la conquête des surfaces

1.2.1. La formation du biofilm *in vitro* et *in vivo*

Les mécanismes requis pour former un biofilm staphylococcique mature ont largement été décrits et revisités au fil des années et continuent de l'être aujourd'hui. Pour étudier et caractériser les facteurs gouvernant la construction de tels biofilms, de nombreux modèles expérimentaux ont été développés *in vitro*. Les connaissances ainsi acquises à travers ces modèles ont permis d'arriver à un consensus confirmant trois étapes majeures observées pour la plupart des biofilms : (i) l'adhésion initiale des bactéries planctoniques à une surface, (ii) la maturation du biofilm, caractérisée par la formation de microcolonies qui se développent et s'accumulent et dans le temps (iii) la dispersion des cellules libérant des bactéries isolées ou des microcolonies qui pourront, à leur tour, coloniser d'autres surfaces **(Figure 2)**.[12,15,16]

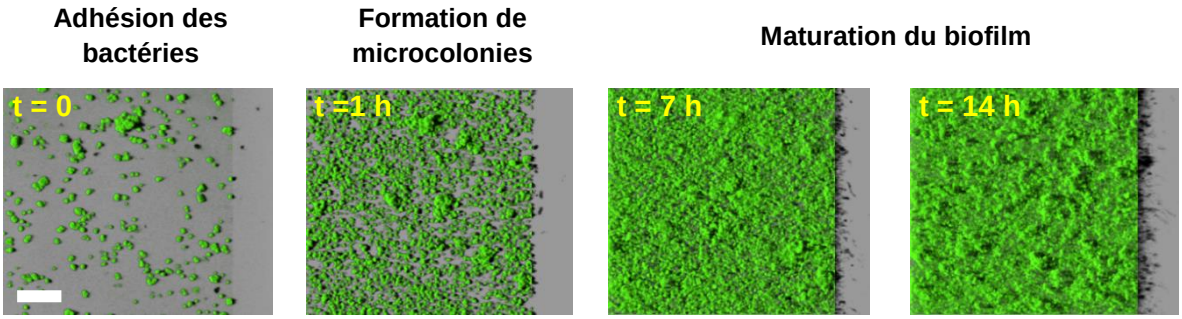

Figure 2. *Imagerie time-lapse de la formation d'un biofilm de S. aureus en microplaque par microscopie confocale de fluorescence. L'observation des bactéries est rendue possible par le marquage de leurs membranes avec le fluorophore FM4-64. L'échelle correspond à 20 µm.*

(i) L'adhésion : les bactéries se fixent aux surfaces

L'adhésion initiale des bactéries planctoniques à la surface d'un matériel est fortement conditionnée par la nature et les propriétés physicochimiques à la fois du substrat et de la surface des bactéries.[17–21] En particulier, l'hydrophobicité et la charge électrostatique influencent considérablement les premières interactions substrat-bactérie.[4] Dans le cas des bactéries de *S. aureus*, les diverses protéines ancrées à la paroi bactérienne et constituant leur enveloppe cellulaire ont été identifiées comme des paramètres-clés dans l'adhésion, non seulement au substrat mais également entre elles.[4,12,22–27] Parmi ces protéines, les autolysines permettent aux bactéries de s'associer aux surfaces abiotiques via des interactions ioniques et hydrophobes.[28] Une fois adhérées, les bactéries interagissent entre elles pour s'accumuler et former des microcolonies d'épaisseur variable. Chez *S. aureus*, les protéines responsables de l'adhésion intercellulaire sont les adhésines de la classe des MSCRAMMs « *Microbial Surface Components Recognizing Adhesive Matrix* », et en particulier, le *Polysaccharide Intercellular Adhesin* (PIA), un *poly-β(1-6)-N-acetylglucosamine* (PNAG) partiellement désacétylé, chargé positivement.[24,25,32] D'autres protéines de surface telles que les *Biofilm-associated surface proteins* (Bap), contribuent également à l'adhésion intercellulaire et promeuvent la formation du biofilm.[33–35] Lorsque l'on s'intéresse à la colonisation des surfaces biotiques,[23] on peut citer

également la *clumping factor B* (ClfB), la *fibronectin-binding protein* (FnBP), la *collagen-binding protein* (Cna) qui gouvernent respectivement l'adhésion au fibrinogène, à la fibronectine ou encore au collagène, des (glyco)protéines abondantes dans la matrice extracellulaire de l'hôte.[29–31]

(ii) La maturation : le biofilm se structure

Au sein des microcolonies bactériennes de *S. aureus* résultant de l'adhésion au substrat et de l'adhésion intercellulaire, la caractéristique la plus notable est la production d'une matrice d'exopolymères qui englobe et protège les bactéries des défenses immunitaires et des traitements antibiotiques.[36,37] Composé principalement d'eau (97%), de polysaccharides, de protéines, d'ADN extracellulaire et de lipides, ce ciment organique apporte la stabilité mécanique des biofilms, en formant un réseau polymérique tridimensionnel qui interconnecte et immobilise les cellules.[36] Nombre de ces substances polymériques extracellulaires (EPS) ont été analysées et caractérisées mais la composition de la matrice peut varier d'une souche bactérienne à une autre selon les conditions environnementales.

Chacun de ces constituants assure une fonction spécifique **(Tableau 1)**. Par exemple, les polysaccharides libres dans la matrice contribuent au maintien de la structure et de l'intégrité du biofilm. L'ADN extracellulaire, un autre constituant majeur que l'on retrouve de manière abondante dans la matrice des biofilms de *S. aureus*, renforce leur structure, agit comme source de nutriments en cas de privation, promeut la colonisation et facilite le transfert de gènes horizontal.[38,39] Plus récemment, il a été démontré que les biofilms staphylococciques contenaient des fibres amyloïdiques. Ces structures fibrillaires sont constituées de *Phenol Soluble Modulins* (PSM),[40] des petits peptides aux propriétés tensioactives qui se sont avérés impliqués dans le maintien de l'intégrité des biofilms mais aussi dans la croissance et la prolifération des bactéries.[41]

Fonction	Intérêt pour les biofilms	Constituants de la matrice impliqués
Adhésion	Permet les premières étapes d'adhésion dans la colonisation de surfaces abiotiques et biotiques par les cellules planctoniques, et l'attachement à long terme des biofilms aux surfaces	Polysaccharides, protéines, ADN et molécules amphiphiles
Agrégation des bactéries	Permet la reconnaissance et l'interaction entre les cellules, l'immobilisation temporaire des populations bactériennes et le développement d'amas denses	Polysaccharides, protéines, ADN
Cohésion du biofilm	Forme un réseau polymérique hydraté (la matrice), contribuant à la stabilité mécanique du biofilm (souvent conjointement avec les cations multivalents) et déterminant l'architecture du biofilm	Polysaccharides chargés et neutres, protéines (amyloïdes ou lectines) et ADN
Rétention d'eau	Maintient l'hydratation des microenvironnements autour des bactéries	Polysaccharides hydrophiles et probablement protéines
Barrière protectrice	Confère une diffusion de molécules antimicrobiennes ralentie	Polysaccharides et protéines

Sorption de composés organiques	Permet l'accumulation de nutriments de l'environnement	Polysaccharides chargés ou hydrophobes et protéines
Activité enzymatique	Permet la digestion de macromolécules exogènes et la dégradation de l'EPS structural pour ensuite relarguer les cellules du biofilm	Protéines
Source de nutriments	Fournit une source de composés à base de carbone, azote, phosphore pour l'utilisation par la communauté du biofilm	Potentiellement tous les composés de la matrice
Echanges d'informations génétiques	Facilite le transfert de gènes horizontal entre les cellules du biofilm	ADN
Donneur ou accepteur d'électrons	Permet l'activité rédox dans la matrice du biofilm	Protéines
Export de composants cellulaires	Relargue le matériel cellulaire	Vésicules membranaires contenant des acides nucléiques, enzymes et phospholipides
Stockage d'excès d'énergie	Stocke l'excès de carbone lorsque l'équilibre carbone, azote est rompu	Polysaccharides
Liaison aux enzymes	Résulte de l'accumulation, la rétention et la stabilisation des enzymes à travers leur interaction avec les polysaccharides	Polysaccharides et enzymes

Tableau 1. *Fonctions des substances polymériques extracellulaires présentes dans la matrice des biofilms bactériens. Traduit et adapté de Flemming et al. 'The biofilm matrix', Nat. Rev. Mic., 2010.*[36]

(iii) La dispersion du biofilm

Une fois mature, une partie du biofilm se disperse pour libérer des cellules isolées qui, à leur tour, vont coloniser d'autres surfaces.[42] C'est une étape importante dans le cycle de formation du biofilm qui contribue à la survie des bactéries et à la transmission de l'infection. Les mécanismes de dispersion des biofilms sont dépendants de la nature de l'espèce bactérienne et peu clairs pour l'instant.[42] Pour *S. aureus*, il a été démontré que cette étape était gouvernée en majeure partie par des enzymes auto-produites ou présentes dans l'environnement qui dégradent la matrice et permettent alors la dissémination des cellules.[27,43]

L'étude des biofilms de *S. aureus in vitro* sur des surfaces abiotiques est un outil précieux, en particulier dans le criblage des facteurs associés à leur formation et à leur dispersion, dans le décryptage de leur architecture et de leur physiologie. Des plus simples aux plus sophistiqués, les modèles de biofilms *in vitro* apportent de nombreux avantages, à savoir un coût modéré, une mise au point relativement facile mais surtout une grande reproductibilité.[44]

Le biofilm chez l'hôte : quelles différences ? Les systèmes *in vitro* ne sont pas toujours représentatifs de la complexité des infections à biofilm *in vivo* dans la mesure où certains paramètres majeurs, tels que l'influence du système immunitaire, ne se sont pas pris en compte.

Bien que les observations de biofilms directement chez l'hôte se fassent rares, les prélèvements de tissus sur des patients infectés révèlent des différences par rapport aux modèles *in vitro* en termes de structure et d'organisation spatiale.[45] Dans une revue récente comparant

l'ensemble de ces études, les auteurs soulignent que la structure multicouche du biofilm, habituellement observée *in vitro,* n'est pas retrouvée *in vivo* ; les biofilms sont plus souvent fins, de la taille d'agrégats ou « patchs ».[45] Les facteurs responsables de ces différences sont peu étudiés pour l'instant mais l'absence de l'action du système immunitaire *in vitro* est sans aucun doute un paramètre d'importance.[45]

Il est essentiel de noter, par ailleurs, que quelles que soient la structure et l'organisation spatiale du biofilm de *S. aureus*, les cellules qui le constituent adoptent une physiologie particulière pour s'adapter à ce mode de vie.

1.2.2. L'état physiologique des bactéries incluses en biofilms : un environnement hétérogène

Contrairement à celui des bactéries à l'état planctonique, l'environnement d'un biofilm formé aussi bien *in vitro* qu'*in vivo* n'est pas homogène. A mesure que les bactéries se développent sur des surfaces, elles expriment des propriétés phénotypiques spécifiques, très distinctes de celles des bactéries planctoniques, qui dépendent de leur microenvironnement local. Il est maintenant bien décrit dans la littérature que la croissance du biofilm et la production concomitante de matrice extracellulaire conduit à l'apparition de gradients d'oxygène et de nutriments qui confèrent aux biofilms une hétérogénéité physicochimique.[46] De nombreuses études montrent, en utilisant des microélectrodes, que la concentration d'oxygène, élevée à la surface du biofilm, décroît de manière considérable dans les couches les plus profondes.[24,46–50] Cette diffusion limitée de l'oxygène n'est pas un résultat d'exclusion physique, la matrice étant aqueuse : il s'agit plutôt de la respiration accrue des cellules présentes à la surface des biofilms, qui entraîne la consommation d'une grande partie de l'oxygène dans les premières couches.[46] Par ailleurs, il a également été démontré que le pH au sein du biofilm était variable d'une zone à l'autre ;[46] l'accumulation de déchets métaboliques provenant des bactéries diminue le pH local de manière non uniforme dans la structure du biofilm, affectant ainsi l'état physiologique des bactéries. De la même façon *in vivo,* lorsque les cellules du système immunitaire sont également présentes, le pH à l'intérieur des cellules telles que les macrophages peut modifier considérablement l'état physiologique des bactéries qui s'y trouvent.

En réponse à ces modifications physicochimiques hétérogènes à travers le biofilm, les bactéries s'adaptent. Ceci conduit alors à l'émergence de sous-populations génétiquement semblables mais physiologiquement distinctes. Lorsque le microenvironnement est favorable, les bactéries se divisent normalement comme les bactéries en phase exponentielle de croissance (division cellulaire active). En revanche, en réponse aux stress environnants (privation de nutriments, d'oxygène, baisse de pH, présence d'antimicrobiens, …), d'autres adoptent une croissance ralentie comme les bactéries en phase stationnaire.[51–58] On dit alors que ces bactéries entrent dans un état de « dormance ». Il est de plus en plus décrit dans la littérature deux types de populations en dormance pour les biofilms de *S. aureus* : les bactéries viables non cultivables (VBNC, *Viable But Non Culturable*) et les persisters.[41,52,53] Alors que les VBNC sont la conséquence d'un manque drastique de nutriments, les persisters sont associées à une

population bactérienne persistante face à l'action d'antimicrobiens et détectées malgré une abondance de nutriments dans le milieu environnant.[58] La particularité de ces populations est qu'aucune d'elles n'est le produit de mutations génétiques. De plus, leur état physiologique est réversible.[52] Toutes deux sont caractérisées par un métabolisme très fortement ralenti, maintenant un approvisionnement en énergie tout juste suffisant pour rester vivantes plusieurs jours voire plusieurs mois consécutifs.[58] Les bactéries reprennent leur métabolisme normal et continuent de se multiplier dès lors que le facteur de stress (privation en nutriments pour les VBNC et antibiotiques pour les persisters) est retiré, par exemple en renouvelant les ressources nutritives. Ce mode « d'économie d'énergie » est alors levé. Par ailleurs, les populations VBNC ne sont décrites que depuis peu de temps car elles ne sont pas identifiables par les techniques conventionnelles de microbiologie. Leur viabilité est certes conservée mais leur métabolisme ralenti ne leur permet pas de former des colonies sur des milieux gélosés classiques. Il est donc nécessaire, pour les identifier, de combiner ces techniques à l'utilisation de marqueurs de viabilité fluorescents ou aux techniques d'amplification en chaîne par polymérase (PCR) (cf. Chapitre 2).[53,59,60]

1.3. Les biofilms de *S. aureus* face au système immunitaire et aux antibiotiques : les infections résistent

Dès que le développement bactérien devient conséquent chez l'hôte, c'est le système immunitaire qui intervient en premier lieu.[22,61,62] Cependant, les bactéries déploient un arsenal de stratégies leur permettant d'échapper à son action et de survivre.[10,61–63] Bien que nombre des mécanismes impliqués aient été élucidés pour les bactéries en état planctonique, peu de données existent concernant les biofilms.[62]

1.3.1. Le système immunitaire attaque, les bactéries font diversion

Les staphylocoques, en se développant chez l'hôte, entraînent la libération massive par les bactéries de diverses entités, telles que des lipoprotéines, des formyl-peptides ou des peptidoglycanes, générant une réaction inflammatoire dans l'organisme.[10] Les neutrophiles et les macrophages répondent alors à cette inflammation et migrent jusqu'au site de l'infection pour détruire les bactéries pathogènes. La première confrontation entre les bactéries et le système immunitaire de l'hôte intervient lors de l'opsonisation : des anticorps (les opsonines), présents dans le sérum de l'hôte et susceptibles de reconnaître des récepteurs spécifiques de la surface des bactéries, se lient aux bactéries formant ainsi un complexe reconnaissable par le système immunitaire.[63] S'ensuit alors l'éradication des bactéries par phagocytose et/ou par l'action d'une multitude de composés bactéricides (tels que les peptides antimicrobiens, les protéines du complément ou les lysozymes) issus de la réaction du système immunitaire.[63–67] En outre, les neutrophiles sont connus pour leur production d'espèces réactives de l'oxygène en grande quantité et leur sécrétion de nombreuses cytokines proinflammatoires qui vont pouvoir agir sur les bactéries et les détruire.[64]

Pour faire face à ces attaques du système immunitaire, les bactéries de *S. aureus* se défendent de différentes façons :

(i) en empêchant leur reconnaissance par les neutrophiles. *S. aureus* est en effet capable d'exprimer des protéines de surface anti-opsoniques ancrées à leur peptidoglycane (protein A, Clumping factor A et B, …) qui masquent les récepteurs de reconnaissance utilisés par les neutrophiles.[63] Les bactéries peuvent aussi produire une capsule polysaccharidique épaisse en plus de leur peptidoglycane.[68,69] Sans cette reconnaissance spécifique de surface, les bactéries ne peuvent pas être phagocytées.

(ii) en s'adaptant au milieu intérieur des phagosomes. En effet, récemment, il a été mis en évidence que des bactéries de *S. aureus* pouvaient survivre à l'intérieur des cellules immunitaires. Les bactéries phagocytées sont exposées à de nombreuses entités toxiques visant à les éradiquer (espèces réactives de l'oxygène, hydrolases, enzymes protéolytiques, …). Cependant, il a été montré que *S. aureus* pouvait exprimer des enzymes et des inhibiteurs qui réduisent le stress oxydant induit par les neutrophiles.[63] Par exemple, les bactéries peuvent produire un pigment caroténoïde synthétisé par sa paroi, la staphyloxanthine, pour résister au peroxyde d'hydrogène et/ou aux radicaux hydroxyles.[10] Elles sont aussi capables d'exprimer des superoxyde dismutases (SOD) pour éliminer les radicaux superoxydes présents dans les neutrophiles. Il a été également montré que les bactéries pouvaient contrer l'attaque des lysozymes et des peptides antimicrobiens via l'acétylation de son peptidoglycane.

(iii) en sécrétant des exotoxines, des toxines superantigéniques, des exfoliationes, …etc. qui provoquent la lyse des cellules immunitaires.[10,62,63,70] Parmi elles, on retrouve les *Phenol Soluble Modulins* (PSM) dont le rôle est cette fois de détruire les neutrophiles, très probablement en perturbant leurs membranes.[70]

Il faut toutefois noter que toutes ces stratégies de défense des bactéries de *S. aureus* vis-à-vis du système immunitaire reposent essentiellement sur des études réalisées *in vitro* impliquant des bactéries, des neutrophiles et des macrophages humains.[71]

1.3.2. Antibiothérapie et résistance/tolérance

Lorsque le système immunitaire devient insuffisant pour empêcher le développement des bactéries, l'administration d'antibiotiques est la thérapie la plus couramment utilisée en pratique clinique.[72] Depuis leur découverte en 1942, les antibiotiques ont été massivement utilisés pour traiter tous types d'infections bactériennes, faisant considérablement reculer la mortalité associée aux maladies infectieuses. Malheureusement, avec leur utilisation intensive, les bactéries se montrent de plus en plus résistantes/tolérantes à leur action.[73]

Tout d'abord, qu'est-ce qu'un antibiotique ? C'est une molécule antimicrobienne naturellement synthétisée par un microorganisme pour se défendre contre les bactéries de son environnement qui lui sont néfastes. Aujourd'hui, il existe plusieurs familles d'antibiotiques comprenant des molécules naturelles, semi-synthétiques ou synthétiques qui ciblent plus ou moins spécifiquement une ou plusieurs espèces bactériennes.[74] Ils peuvent soit détruire (effet bactéricide) soit bloquer la croissance (effet bactériostatique) des microorganismes. Parmi les antibiotiques disponibles commercialement, on distingue quatre classes de molécules, (i) ceux qui inhibent la synthèse de la paroi bactérienne, (ii) ceux qui détruisent la membrane cytoplasmique, (iii) ceux qui bloquent la synthèse protéique intracellulaire ou (iv) ceux qui bloquent la synthèse des acides nucléiques (**Figure 3**).[72,75]

Parmi les antibiotiques utilisés en pratique clinique pour éradiquer les infections engendrées par les biofilms de *S. aureus*, on retrouve en première intention les β-lactamines (telles que la méticilline, l'oxacilline ou la cloxacilline). Par ailleurs, si la souche est résistante à la méticilline (*Methicillin-Resistant S. aureus*, MRSA), l'antibiotique de choix sera un glycopeptide (vancomycine, téicoplanine), utilisé seul ou en association avec une rifamycine (rifampicine) ou un aminoside (gentamicine).[77,78] Enfin, plus récemment, de nouveaux antibiotiques dits de dernière intention sont venus renforcer l'arsenal thérapeutique en cas d'échec des autres thérapies. Parmi eux, les oxazolidinones (linézolide), les lipopeptides (daptomycine) ou les glycylcyclines (tigécycline).[79]

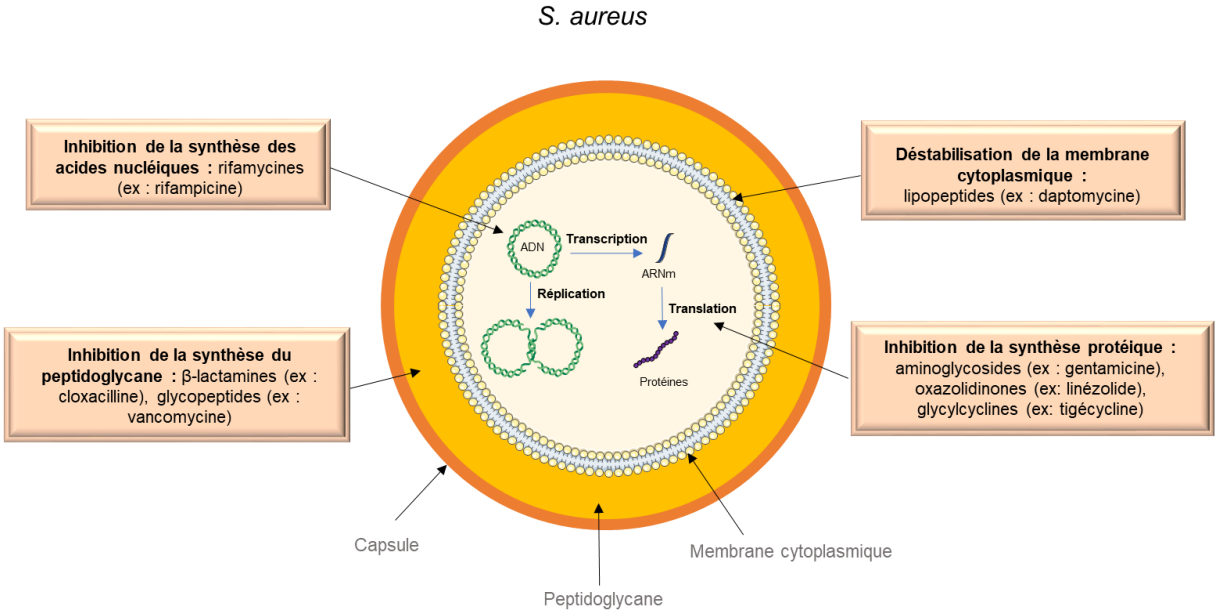

Figure 3. *Schéma représentatif des quatre types de mode d'action des antibiotiques vis-à-vis de S. aureus selon leur cible.*

L'échec des traitements antibiotiques face à certaines infections est lié aux propriétés génétiques et/ou physiologiques des bactéries ciblées.[80] En effet, certaines bactéries sont naturellement résistantes aux antibiotiques (résistance innée) tandis que d'autres développent des mécanismes de résistance suite à l'administration répétée ou prolongée d'antibiotiques par exemple (résistance acquise).[81] C'est le cas notamment des souches de *S. aureus* résistantes à la méticilline qui ont émergé très rapidement après l'introduction de l'antibiotique sur le marché.[82] Le mécanisme de résistance impliqué est induit par la synthèse d'une protéine PLP (Protéine Liant les Pénicillines), la PLP2a vis-à-vis de laquelle les pénicillines ont très peu d'affinité et dont le support génétique est transmissible.[82] Par ailleurs, un autre mécanisme largement impliqué dans la résistance des bactéries aux antibiotiques est la modification structurale de la cible de l'antibiotique. Par exemple, il existe des souches bactériennes de *S. aureus* qui résistent à la vancomycine en raison d'une substitution du dipeptide D-alanine-D-alanine par le dipeptide D-alanine-D-lactate.[82]

Ce phénomène de résistance, issu de modifications génétiques, n'est pas le seul facteur responsable de l'échec thérapeutique des antibiotiques. En effet, un autre phénomène, qualifié de tolérance, joue également un rôle majeur dans la persistance des biofilms sous l'action des

antibiotiques. Dans ce cas, le mécanisme impliqué est de nature phénotypique, induit par l'adaptation des cellules à la vie en biofilm (modifications physiologiques décrites au paragraphe 1.2.2) et est donc réversible dans la mesure où les bactéries du biofilm revenues à leur état planctonique réacquièrent leur sensibilité aux antibiotiques. [83,84] Le terme de résistance est donc restreint à des mécanismes génétiques uniquement.

Pour évaluer la sensibilité/résistance d'une souche bactérienne et choisir l'antibiotique le plus efficace, un modèle standardisé a été mis en place aussi bien en laboratoire qu'à l'hôpital : la mesure de la concentration minimale inhibitrice (CMI), c'est-à-dire la concentration minimale d'antibiotique nécessaire à l'inhibition de la croissance des microorganismes.[85] Néanmoins, la principale limite de cette mesure est qu'elle n'est pas prédictive de l'efficacité des antibiotiques *in fine* chez les patients atteints d'infections à biofilms.[84] En effet, il a été rapporté au fil des années de nombreux cas où des pathogènes, décrits comme sensibles via la mesure de CMI, ne répondaient pas du tout à l'antibiothérapie chez le patient.[84,86] Certes adaptée pour mesurer la réponse des bactéries qui se divisent activement, cette méthode ne tient pas compte de la physiologie des bactéries qui est modifiée en biofilm, comme décrit précédemment (cf. paragraphe 1.2.2.).[46] Concernant les biofilms, on détermine alors la concentration nécessaire pour que l'antibiotique ait un effet bactéricide sur les bactéries incluses en biofilms. Dans ce cas, les concentrations sont 10 à 1000 fois supérieures à celles appliquées aux bactéries planctoniques.[28,87–89] Or, l'application de telles concentrations *in vivo* est, le plus souvent, impossible à atteindre au risque d'être toxique et d'engendrer des effets secondaires trop importants chez l'hôte. Dans ce contexte, si l'antibiothérapie administrée échoue dans le traitement de l'infection, l'implant ou le tissu à l'origine de cette dernière est retiré chirurgicalement ; cette option peut être problématique pour certains dispositifs compte tenu des répercussions pour le patient.[90] Le traitement des infections à biofilms devient donc un challenge d'importance majeure qui attire l'attention de la communauté scientifique et médicale. Ainsi, de nombreuses études récentes visent à élaborer de nouvelles stratégies thérapeutiques pour combattre les infections à biofilms.

1.4. Nouvelles stratégies pour enrayer les infections à biofilms : éradication des biofilms déjà établis ou prévention ?

Afin de contrer ces infections à biofilms, deux types de stratégies sont actuellement employés. Le premier vise à éradiquer les biostructures déjà établies chez l'hôte. Le second, de plus en plus étudié, vise à maîtriser les surfaces auxquelles adhèrent les bactéries dans le but de prévenir le développement du biofilm.[91]

1.4.1. Eradication des biofilms établis

(i) Optimisation de l'antibiothérapie disponible

Pour faire face à l'échec de l'antibiothérapie classique vis-à-vis des infections à biofilms et au peu de nouvelles molécules antibiotiques mises sur le marché, de nouvelles stratégies basées sur l'amélioration de l'antibiothérapie disponible ont été développées.[88] La plus classique repose sur la combinaison de deux ou trois antibiotiques afin (i) de couvrir un plus large spectre de sensibilité, et (ii) de contrer l'émergence de résistances vis-à-vis de l'un ou l'autre des

antibiotiques.[76,92] Par exemple, la rifampicine, utilisée pour sa bonne diffusion et son action sur les bactéries au métabolisme ralenti, est souvent associée à la vancomycine ou à la daptomycine pour prévenir l'apparition de résistances.[76,93] Ces multithérapies ont fait leurs preuves et sont maintenant couramment choisies en pratique clinique. Par ailleurs, on rencontre aussi en usage clinique une nouvelle méthode qui repose sur l'injection et le maintien entre 12 et 24 h d'une concentration élevée d'antibiotiques (100 à 1000 fois la CMI) déposée localement sur une zone infectée, comme par exemple un biofilm formé sur cathéter pour éviter de le retirer. [94–98] Cette méthode nommée « lock therapy » (ou verrou d'antibiotique) est certes efficace, mais présente tout de même le risque de favoriser l'émergence de résistance bactérienne aux antibiotiques. Une autre approche proposée pour améliorer l'activité des antibiotiques vis-à-vis des biofilms concerne l'association d'aminoglycosides avec des sucres tels que le mannitol ou le fructose. L'incorporation de ces sucres par les bactéries stimule la glycolyse, entraînant *in fine* une stimulation de la force proton-motrice et par conséquent une meilleure assimilation des aminoglycosides.[88,99] Des études *in vitro* ont montré l'efficacité de cette approche pour éradiquer les persisters de *S. aureus* notamment.[100]

(ii) Utilisation d'enzymes pour la dispersion des biofilms de *S. aureus*

Comme nous l'avons vu précédemment, au sein des biofilms, les bactéries tolérantes aux antibiotiques à cause de leur adaptation aux conditions d'environnement, redeviennent sensibles lorsqu'elles recouvrent leurs conditions planctoniques. Ainsi, induire la dispersion des biofilms bactériens est une approche intéressante pour restaurer l'action des antibiotiques.[16,42,101,102] Plusieurs approches ont été proposées dans ce sens, notamment l'utilisation d'enzymes capables de dégrader les polymères ou l'ADN extracellulaire constituant la matrice sécrétée par les bactéries. Il a été par exemple démontré que la dispersine B, une enzyme produite par *Actinobacillus actinomycetemcomitans*, déstabilise les polysaccharides de la matrice des biofilms de *S. aureus.*[103–105] Une autre enzyme, la DNase I, disperse les biofilms en s'attaquant à l'ADN extracellulaire.[106,107] La trypsine et la protéinase K ont été utilisées pour déstabiliser les protéines de la matrice du biofilm.[102,108] Tel que décrit dans la partie 1.2.1., la nature de la matrice sécrétée par les bactéries peut grandement varier d'une souche bactérienne à une autre. Ainsi, l'efficacité de la dispersion des biofilms à partir d'enzymes, dépendante de la composition chimique de la matrice, peut se révéler limitée.[109] De plus, cette méthode d'éradication, en libérant rapidement une concentration élevée de bactéries planctoniques, peut induire un risque de forte réponse inflammatoire et d'infection systémique aigüe.[90]

1.4.2. Prévention : vers une maîtrise des surfaces

Les observations en pratique clinique de même que les expériences menées *in vitro* ont démontré que les biofilms pouvaient être plus facilement éradiqués par les antibiotiques en début d'infection lorsque les biofilms sont « jeunes ».[87] Cependant, le diagnostic précoce des infections à biofilms est difficile car les bactéries ne sont pas faciles à détecter à ce stade.[87,91] Dans ce contexte, il apparait crucial de développer des stratégies visant à empêcher la formation de biofilms plutôt que de les dissocier.[110]

Pour y parvenir, l'axe de recherche le plus développé actuellement est le traitement des surfaces des biomatériaux propices au développement de biofilms. On distingue alors (i) les surfaces antiadhésives, qui visent à empêcher l'adhésion bactérienne initiale en limitant les interactions bactéries-substrat, et (ii) les revêtements antibactériens qui consistent à greffer des molécules bactériostatiques ou bactéricides pour empêcher l'adhésion et la multiplication des bactéries à la surface du substrat. Cependant, ces stratégies ne sont en aucun cas applicables aux surfaces biotiques et ne peuvent donc se substituer totalement à l'optimisation de l'antibiothérapie disponible.

(i) Les surfaces antiadhésion

Une approche actuellement en développement est l'ingénierie de surfaces abiotiques dans le but de réduire ou retarder l'adhésion initiale des bactéries en combinaison avec l'administration d'antibiotiques et/ou l'action du système immunitaire.[111] Cette stratégie duelle vise à empêcher la formation du biofilm tout en ayant la possibilité d'éradiquer les bactéries planctoniques.

Un premier panel d'études s'est focalisé sur la modification des propriétés physicochimiques des surfaces, telles que la texture, la charge, la rugosité ou encore le caractère hydrophile/hydrophobe.[91] Par exemple, les surfaces aux propriétés dites « superhydrophobes », se sont révélées remarquablement efficaces dans la prévention de l'adhésion bactérienne. Pour atteindre une telle hydrophobicité, le plus souvent, des liquides fluorés sont utilisés.[112–115] Une étude récente a montré que des surfaces de ce type, constituées de liquides perfluorés ajoutés à du polytétrafluoréthylène (PTFE), étaient capables d'empêcher complètement l'adhésion et la formation de biofilm d'une multitude de souches au-delà de sept jours tout en restant très stables.[114,115] L'inconvénient majeur, en revanche, est que ces surfaces requièrent l'utilisation de substances fluorées toxiques. Plus récemment, Hu *et al.* ont rapporté la mise au point d'un revêtement biodégradable pour une utilisation *in vivo*.[116]

(ii) Les revêtements de surface antibactériens

Les traitements de surface antibactériens sont nombreux. On se limitera ici à quelques exemples clés en plein développement, à savoir les traitements par des antibiotiques, des peptides antimicrobiens et des nanoparticules.[110] Ces molécules peuvent être soit simplement immobilisées sur les surfaces, soit greffées de façon covalente.

Antibiotiques. La surface des implants osseux peut être recouverte d'un gel d'hydroxyapatite incluant des antibiotiques qui seront libérés au cours du temps pour empêcher la formation de biofilms. C'est une méthode couramment utilisée en chirurgie orthopédique.[117,118] Son inconvénient majeur repose sur le manque de contrôle de la cinétique et de la concentration d'antibiotiques libérée *in vivo*. En effet, il a été démontré qu'il pouvait y avoir une libération rapide et efficace d'antibiotique aux temps courts, suivie d'une libération de concentrations sub-inhibitrices des molécules dans le temps, ce qui peut induire des résistances bactériennes.[110] Dans ce contexte, des surfaces constituées de multicouches polymériques dégradables intégrant chacune des antibiotiques ont été mises au point de sorte à ce que la libération des molécules se fasse de façon graduelle.[119] Une autre alternative consiste cette fois à greffer les antibiotiques en forte concentration à la surface des implants, pour y minimiser l'exposition des bactéries à des concentrations sub-inhibitrices.[120,121] Un autre avantage, tel celui déjà démontré concernant

le greffage de la vancomycine sur des implants en titane, est que l'antibiotique agit sur des bactéries planctoniques montrant une efficacité largement supérieure à celle des traitements des biofilms *in situ*. [120,122,123]

Peptides antimicrobiens. Comme mentionné précédemment, les peptides antimicrobiens sont synthétisés naturellement par des organismes vivants (plantes, insectes, mammifères, …etc.) pour se défendre des bactéries pathogènes.[124] De nombreux travaux portent sur l'utilisation de ces peptides dans les revêtements de surface, pour s'en servir, sur le long terme, comme traitement préventif de l'adhésion bactérienne sur les implants.[110,125] Aujourd'hui, l'adhésion de ces peptides sur des surfaces d'or revêtues de composés sulfurés tels que l'acide mercaptoundécanoïque s'est révélée efficace.[126,127] En revanche, si ce type de traitement de surface est adaptable au milieu industriel, des développements sont encore à venir pour leur utilisation *in vivo*.[128] Une approche intéressante porte sur des implants à base de titane sur lesquels sont adsorbés des multicouches de films phospholipidiques contenant du phosphate de calcium et des peptides antimicrobiens, qui ont montré une prévention efficace de l'adhésion des bactéries et une cytotoxicité négligeable vis-à-vis des cellules de l'hôte. [129]

Nanoparticules. Les nanoparticules métalliques (d'argent, d'oxyde de titane, quantum dots et bien d'autres), initialement connues pour leur activité antibactérienne en solution, ont également fait l'objet de nombreuses études pour leur application dans le cadre de revêtements de surfaces.[130] Greffées à la surface de cathéters veineux centraux, les nanoparticules d'argent libèrent lentement des ions Ag^+ à l'origine d'une efficacité certaine dans l'éradication des bactéries avoisinant la surface des cathéters aussi bien *in vitro* qu'*in vivo*.[131] Cependant, leur utilisation en pratique clinique suscite des inquiétudes du fait de leur possible cytotoxicité vis-à-vis des tissus de l'hôte. En effet, il a été démontré que les nanoparticules d'argent accélèrent la formation de thrombine et l'activation des plaquettes, entraînant un haut risque de thrombose (formation de caillots sanguins).[132] De plus en plus d'études concentrent donc leurs efforts sur une meilleure compatibilité avec l'hôte.

En résumé, les données de la littérature démontrent que les mécanismes des infections, et en particulier de celles impliquant des biofilms, de même que la résistance/tolérance aux antibiotiques, ne sont pas complètement élucidés à ce jour. Il y a encore la place d'une recherche fondamentale dans ce domaine, ce qui constitue l'objet de ce travail de thèse.

Chapitre 2 : Les outils de la fluorescence *in vitro et in vivo* pour sonder l'(in)efficacité des antibiotiques dans l'éradication des bactéries

En microbiologie, les outils de la fluorescence ont sans aucun doute démontré leurs performances dans l'analyse en temps réel, de manière quantitative et non-invasive, de la structure, de la composition et de la dynamique des communautés microbiennes. En effet, les méthodes disponibles basées sur la fluorescence permettent de déchiffrer nombre de mécanismes impliqués dans l'(in)efficacité des traitements antibiotiques et ce, à plusieurs échelles (spatio)temporelles.

A travers l'article ci-après, nous allons examiner la vaste gamme des techniques de fluorescence ainsi que leur intérêt (i) dans l'étude de la viabilité des cellules bactériennes *in vitro* et *in vivo* sous l'action des antibiotiques, (ii) dans l'élucidation des mécanismes d'action de ces médicaments et (iii) dans la description des mécanismes employés par les bactéries pour résister et/ou tolérer l'action des antibiotiques.

2.1. Article 1: "Taking Advantage of Fluorescent-Based Tools to Puzzle out Successes and Failures of Antibiotics to Inactivate Infectious Bacteria"

Rym Boudjemaa, Romain Briandet, Karine Steenkeste, Marie-Pierre Fontaine-Aupart

Encyclopedia of Analytical Chemistry, 2017

Taking Advantage of Fluorescent-based Tools to Puzzle out Successes and Failures of Antibiotics to Inactivate Infectious Bacteria

Rym Boudjemaa, Romain Briandet, Karine Steenkeste, and Marie-Pierre Fontaine-Aupart
Université Paris-Saclay, Orsay, France

In microbiology, fluorescence tools have undoubtedly proven their performance to analyze in real-time, non-invasively and quantitatively, the structure, composition, processes, and dynamics of microbial communities. Importantly, the available fluorescence-based methods enable to decipher multiscale events implicated in the failures and successes of antibiotics treatments. The goal of this article is to review the large range of fluorescence techniques and probes and their interest (i) to study bacterial cells viability in vitro and in vivo under antibiotics exposure, (ii) to elucidate the mechanisms of action of these drugs, and (iii) to dissect bacterial mechanisms to resist and tolerate antibiotics action.

1 INTRODUCTION

Since the origin of human existence, we have suffered from infections caused by pathogenic bacteria.[1] The discovery of penicillin in 1928 by Alexander Fleming triggered a massive reduction of the mortality burden related to infectious diseases, saving countless lives.[1,2] Antibiotherapy is certainly the most successful form of chemotherapy in the history of medicine. However, the commercialization of every new antibiotic has been accompanied by the emergence and propagation of specific bacterial resistance.[3] Nine decades after the golden age of antibiotics, bacterial infections still represent a major concern both in hospital and community settings worldwide.[4] The continuous emergence of deadly nosocomial multiresistant bacteria ('super bugs'), currently implicates 700 000 deaths each year and is expected to be associated with more than 10 million deaths in 2050.[5–7] A major amplifying factor is the too few new antibiotic molecules in the pipeline, raising the awareness of the research community. Alternative approaches such as the re-emergence of phage therapy or the use of natural extracts for example are currently being tested *in vitro* and on animal models but are still not available for clinical use.[3,8–10]

Bacterial cells have been shown to employ different strategies to overcome antibiotic action.[11] Antibiotic resistance is the genetically acquired ability of a microorganism to resist the effect of an antimicrobial agent, and involves different molecular pathways including alterations in bacterial cell wall structure, efflux pump expression, molecular modification of the antibiotic target, or enzymatic alteration of the antibiotic itself.[1,12–15] For instance, methicillin-resistant *Staphylococcus aureus* (MRSA) is the best example to illustrate bacterial multidrug resistance. MRSA strains have demonstrated a unique ability to quickly circumvent the action of almost every class of anti-staphylococcal antibiotics, including β-lactams (using enzymatic inactivation by penicillinase production), glycopeptides (altering the target by producing a peptidoglycan precursor that does not have affinity for the drug), fluoroquinolones (by enhancing their efflux pumps activity) and lipopeptides (through spontaneous mutations and positive selection).[16,17]

In contrast, antibiotic tolerance is not triggered by genetic alterations or inheritance of a resistance gene.[11,18] It is a transient and nonheritable phenotype associated with the failure of antibiotic treatment and the relapse of many bacterial infections.[11] Tolerance enables bacterial cells to survive a transient exposure to antibiotics at concentrations that would otherwise be lethal.[11,19] The mechanisms of antibiotic tolerance can be mediated by 'slow-growing' bacteria, including small

Encyclopedia of Analytical Chemistry, Online © 2006–2017 John Wiley & Sons, Ltd.

This article was published in the *Encyclopedia of Analytical Chemistry* in 2017 by John Wiley & Sons, Ltd.
DOI: 10.1002/9780470027318.a9606

colony variants, persisters or viable but nonculturable cells (VBNC) that are less susceptible to antibiotics than their wild-type counterparts.[12,20,21] These variants have a low metabolism and unusual biochemical characteristics that confer them the ability to escape antibiotics action, further causing recurrent infections.[20] When attached to a surface, the formation of three-dimensional structures of bacteria (named biofilms[22]) can also be invoked in bacterial tolerance. Biofilm-associated drug tolerance plays a major role in the pathogenesis of many subacute and chronic bacterial diseases and their recalcitrance to antibiotic treatment, including medical device-related infections, chronic wounds, and intractable lung infections in cystic fibrosis patients.[19] In the case of biofilms, tolerance can also be mediated by specific characteristics that limit drug diffusion and activity.[2,12,23]

The study of antibiotics effects against pathogenic bacteria has been greatly aided by *in vitro* laboratory assays such as plate counting, minimum inhibitory concentrations (MIC) and minimum bactericidal concentrations (MBC) measurements to detect resistance,[11] and real-time-polymerase chain reaction (PCR) to probe antibiotic-resistance genes.[24] These techniques have been remarkably useful and still remain adequate and appropriate.[25] However, these assays are time-consuming and laborious, and do not give access to the subpopulations behavior. In an attempt to decipher these micro-heterogeneities and their functions, it is essential to probe the single cell level in order to explore in depth the dynamic and structural processes of subpopulations, information that are not approachable by the conventional tools described earlier.

To give deeper insights into the mechanisms underlying bacterial survival to antibiotics treatments as well as antibiotics mechanisms of action, fluorescence techniques have undoubtedly proven their necessity in microbiology. These techniques allow to analyze *in situ* and in real-time the structure, composition, processes, and dynamics of microbial communities.[26] Rapid, direct and nondestructive, *in vitro* studies using fluorescence-based methods render possible the monitoring of micro- to nanoscale molecular events qualitatively and/or quantitatively. Recent advancements in *in vivo* imaging techniques are facilitating the next logical step to visualize the dynamic infection process as it happens within the living host.[27] These new fluorescence imaging techniques allow tracking individual bacterial cells at the whole (small) animal body scale and are in some cases adaptable to clinical situations.[28–30]

2 FLUORESCENCE TOOLS IN MICROBIOLOGY

Fluorescence is now omnipresent in microbiology as a basic tool to study both single microbial cells and three-dimensional bacterial structures such as biofilms both *in vitro* and *in vivo*.[31–33] Briefly, fluorescence is a radiative relaxation process that occurs when photons from an incident light source raise electrons to a higher-energy state (excited state). Return of the molecule to a lower-energy state can then be accompanied by the emission of fluorescence, with specific properties in terms of spectra, lifetimes, or polarization.[34–37] Variables of practical importance in fluorescence include the intrinsic properties of a fluorophore: its excitation and emission spectra, molar absorbance coefficient, quantum yield and photostability.[34,35,37] Importantly, the difference in excitation and emission wavelengths is termed the 'Stokes shift', and the magnitude of this shift can be critical in ensuring spectral separation of signals from more than one fluorescent stain or when dealing with cells or sample matrices having highly auto-fluorescent backgrounds.[34] The local chemical or electronic environment and factors such as pH or physical proximity of other molecules in solution also play a fundamental role.[35–37]

Some molecules fluoresce naturally and others can be stained to make fluorescent compounds. A large panel of fluorophores is now available and facilitate the staining of microbial cells within complex mixtures, according to their individual features including biochemistry, physiology, or taxonomic properties.[32] Multiple fluorescent stains may be used simultaneously, allowing the collection of more than one parameter per cell. Furthermore, many fluorescent stains are compatible with living cells and can be used for real-time measurements.[32]

The choice of instrumentation in microbiology is mostly guided by the type of bacterial sample observed (i.e. free-floating cells, surface-attached cells or three-dimensional structures such as aggregates and biofilms) and the type of information expected from the fluorescence signal (molecular diffusion, cellular death, etc.). Furthermore, accuracy, detection limits, speed of analysis and light sources are among important selection criteria to be taken into account. In addition, the instrument chosen must be compatible with the photophysical properties of the fluorophores studied (absorption and emission spectra).[35–38]

The reference optical set-up in microbiology is the microscope. The first fluorescence apparatus was developed by Otto Heimstaedt and Heinrich Lehman in the early 1910s,[36] and used in particular to investigate the autofluorescence of bacteria. Next, Stanislas Von Prowazek employed fluorescence microscopy to study dyes binding to living cells.[36] The golden age of fluorescence microscopy came with the development of laser

Encyclopedia of Analytical Chemistry, Online © 2006–2017 John Wiley & Sons, Ltd.

This article was published in the *Encyclopedia of Analytical Chemistry* in 2017 by John Wiley & Sons, Ltd.
DOI: 10.1002/9780470027318.a9606

scanning microscopy (LSM) in the 1980s, and further use of confocal laser scanning microscopy (CLSM) have revolutionized the structural and functional investigation of hydrated microbiological samples.[39]

Epifluorescence microscopy (EFM) of fluorescently stained cells has long been the standard method to enumerate bacteria.[40] Advances in filter, mirror, and camera technologies continue to make this kind of microscopy highly sensitive.[41] However, the detection limit of EFM is low in terms of bacterial counting. Indeed, it becomes very tedious to detect less than 10^3 targeted cells per square centimeter of filter – this limit corresponding to the detection of one cell per microscopic field (typically a 246 × 246-µm image, using a ×63 objective), and bacteria often have to be much more concentrated for direct microscopic examination than for plate counting.[42] To improve bacterial counting, flow cytometry (FCM) offers the ability to analyze rapidly thousands of individual cells from an entire population of free planktonic cells (a flow rate between 10 and 100 µL min^{-1} and count rates ranging from 100 to 1000 cells min^{-1}).[43,44] Practically, the cells present in a liquid medium are passed individually in front of an intense light source. Simultaneously, data on light scattering and fluorescence are collected and saved as a data file. Detailed numerical analyses of populations and subpopulations of interest can then be carried out offline by using a number of analysis packages.[32] Thanks to its ability to collect information-rich data sets on thousands of cells, flow cytometry facilitates valuable insights into connections between single-cell and population-level processes, which are not available with other techniques.[32,42] However, FCM is not adapted to the detection of rare events since it is difficult to detect less than 100 bacteria per milliliter, which is still 10–100-fold better than current microscopic procedures.[32,42] It must also be noted that this technique is adapted for suspended cells only and is not applicable to surface-attached cells.[45] For this purpose, laser scanning cytometer (LSC) is a solid-phase cytometric technology that complements flow cytometry, allowing visualization and analysis of samples attached to solid substrates, or collected and concentrated on filters.[46] LSC is well-adapted for observing cellular properties as a function of time (kinetics of fluorescence staining such as substrate uptake, enzyme activity, etc.).[32] The beam spot size varies depending on the lens magnification, from 2.5 µm (at ×40) to 10.0 µm (at ×10), thus allowing single-cell studies.[46] However, long periods of sample exposure to the excitation source may induce photobleaching of the fluorescent stains. These deleterious effects should be minimized by using low-intensity (microwatt versus milliwatt) illumination sources and powers.[32]

To circumvent the limitations of FCM and LSC, CLSM has led to considerable progress in the study of fluorophores either in solution or in microbiological samples.[26,47] Due to the introduction of a 'pinhole' in the path of the fluorescence light emitted by the sample, only the fluorescence coming from the focal plane reaches the detector and the contribution of out-of-focus light is eliminated.[48] This optical sectioning ensures a submicron resolution compatible with observation of a single bacterium within biofilms.[47] Besides the three dimensions (x, y, and z) allowing acquisition of image stacks, CLSM gives also access to two supplementary dimensions: the time, to conduct time-lapse microscopy for example and also the wavelength for spectral imaging.[47] Another improvement aiming at imaging samples within deeper locations is the two-photon excitation (TPE) microscopy.[49] Its principle is the simultaneous absorption of two photons half the energy needed for a one photon transition by using ultra short pulse laser (typically femtosecond to picosecond pulse laser).[50,51] The TPE probabilities are very weak, thus significant two-photon absorption only occurs at the objective focal point of the microscope, a region where the temporal and spatial concentration of photons are very high.[52] This imaging technique allows an inherent optical sectioning property with a very low background production but also a greater depth in the samples and photodamages being restricted to the excitation volume.[51,52]

One limitation of light microscopy can be its resolution. This latter is given by the Ernst Abbe formula, which is about a half of the excitation wavelength used for imaging.[53] As a result, objects smaller than 200–300 nm cannot be resolved by conventional technologies. To overcome this resolution limitation, many new optical imaging techniques, called nanoscopies, have been further developed the past 20 years.[54] These techniques comprise structured illumination microscopy (SIM),[55,56] stimulated emission depletion (STED) microscopy,[57,58] and single-molecule localization microscopy (SMLM).[59,60] In this latter branch, photo-activated localization microscopy (PALM),[61] point accumulation for imaging in nanoscale topography (PAINT),[62] stochastic optical resolution microscopy (STORM)[63] all aim at localizing single fluorescent molecules with a nanoscopic resolution (20–40 nm).[39] The only difference between these three techniques is the physicochemical strategy employed to make the fluorescent molecules blink: PALM uses photoactivatable molecules such as fluorescent proteins (GFP for example); STORM uses ordinary fluorophores in combination with a special chemical buffer that allows molecules to blink between fluorescent and dark states; and PAINT uses fluorophores that bind reversibly to their target and do not fluoresce in solution but only when they are bound.[39,64,65]

Encyclopedia of Analytical Chemistry, Online © 2006–2017 John Wiley & Sons, Ltd.

This article was published in the *Encyclopedia of Analytical Chemistry* in 2017 by John Wiley & Sons, Ltd.
DOI: 10.1002/9780470027318.a9606

Table 1 Fluorescent probes of cell viability *in vitro*

	Molecular weight ($g\,mol^{-1}$)	Maximum excitation wavelength (nm)	Maximum emission wavelength (nm)
Membrane integrity			
Propidium iodide (PI)	668	533	617
PO-PRO-3	351	560	600
Sytox Green	[a]	488	514
Ethidium bromide	394	488	605
Esterase activity			
Fluorescein	332	488	496
Carboxyfluorescein	376	498	517
Calcein	623	494	520
BCECF	520	439	550
Respiratory activity			
Resorufin	235	600	615
CTC formazan	265	450	630

FDA, fluorescein diacetate; CFDA, carboxyfluorescein diacetate; CFDA-AM, carboxyfluorescein diacetate acetoxyl methyl ester; BCECF, 2′,7′-bis-(2-carboxyethyl)-5-(and-6)-carboxyfluorescein; BCECF-AM, BCECF acetoxy methyl ester; CTC, 5-cyano-2,3-ditoluyl tetrazolium chloride.
[a]Not communicated by the fabricant.
Source: Thermofischer, Biomérieux, Sigma-Aldrich.

3 VISUALIZATION AND QUANTIFICATION OF BACTERIAL INACTIVATION UNDER ANTIBIOTIC EXPOSURE

3.1 *In Vitro* Cell Viability

Conventional methods to study bacterial cells inactivation by antibiotics treatments consist in enumerating bacterial colonies that are able to reproduce on agar nutrient plates.[66] Even if these techniques are still the reference methods to determine microbial cell viability/activity, they are very time-consuming and do not allow dynamic and structural observations of the bacterial population features. It is also now acknowledged that in many conditions only a small fraction of bacterial cells are culturable on agar plate. Some bacteria can revert between states of culturability and unculturability (VBNC state, small-colony variants, etc.), a phenomenon that is of prime importance when studying bacterial response to toxic compounds such as antibiotics.[20,21] In the last decades, this raised increasing interest for the use of fluorescence techniques (FCM, LSM, EFM, CLSM) that allow to overcome this limitation by monitoring rapidly, noninvasively and in real-time the viability state of individual bacterial cells.[47,67] As defined by Joux and Lebaron,[42] the elementary requirements for viable microorganisms to survive are: (i) an intact cytoplasmic membrane that functions as a barrier between the cytoplasm and the extracellular environment; (ii) DNA transcription and RNA translation; (iii) generation of energy for maintenance of cell metabolism, biosynthesis of proteins, nucleic acids, polysaccharides, and other cell components; and, eventually, (iv) growth and multiplication. To evaluate each of these characteristics, a large panel of viability/vitality stains have been developed (Table 1). For conducting these fluorescence experiments properly, an essential requirement concerns the choice of appropriate fluorescent stains of cell viability that should not interact with each other or with the antibiotic tested. If so, the interactions should be fully characterized to interpret the results properly.[47,68] Another important aspect is the choice of an adequate instrumentation depending on the quantitative or qualitative sensitivity expected.

3.1.1 *Membrane Integrity*

Assessment of membrane integrity is the most widely spread approach to assess bacterial viability.[69] Due to the high concentrations of nucleic acids within the cells, these staining assays consist in nucleic acid dyes that, upon binding, exhibit great enhancement of fluorescence.[42] The large size of these probes (Table 1) allows them to penetrate damaged membranes cells only, leading to a specific staining of these cells.[42,70] Among the DNA probes that are routinely employed, the red dye propidium iodide (PI) is the most commonly applied for these assays, but ethidium bromide, PO-PRO®-3, and SYTOX® Green have also been used.[67] They penetrate both Gram-negative and Gram-positive bacteria with damaged cytoplasmic membranes. However, a limitation for the use of such stains has been reported by Lebaron et al. concerning death assessment in the case of treatment leading to DNA degradation (e.g. long-term starvation).[71] In this case, the fluorescent probe is unable to label DNA, cells display a low fluorescence signal and may be wrongfully considered as living cells.

Encyclopedia of Analytical Chemistry, Online © 2006–2017 John Wiley & Sons, Ltd.

This article was published in the *Encyclopedia of Analytical Chemistry* in 2017 by John Wiley & Sons, Ltd.
DOI: 10.1002/9780470027318.a9606

Simultaneously to the staining of membrane-damaged cells, smaller fluorophores that are also able to penetrate bacteria with intact membranes are often employed to obtain the total number of cells present in a sample. Among them, the 4,6-diamidino-2-phenylindole dihydrochloride (DAPI) and a wide range of SYTO® dyes are valuable to enumerate total amounts of bacterial cells.[67,70] However, attention must be given to the photophysical properties of these dyes for which absorption and fluorescence emission bands may overlap those allowing identification of damaged-membranes cells. Thus, to enumerate simultaneously bacteria with intact membranes and compromised membranes, it is necessary to make sure that no spectral overlap occurs between the fluorescence emissions of the dyes employed.

The most widely used combination of probes to assess bacterial membrane integrity is the commercial BacLight™ LIVE/DEAD viability assay.[72] It is composed of two DNA-intercalating dyes: SYTO®9, a green fluorescing permeant-membrane dye that is able to penetrate all the cells and PI that can only penetrate damaged-membranes cells.[72] Before using this assay as a viability test, it is of utmost importance to control the concentration of both dyes, their interaction with each other, and also the incorporation order.[68] Indeed, competition can occur between the two dyes since their target is DNA in both cases. Previous observations have demonstrated that when PI is incorporated into the sample prior to SYTO®9, images display distinct red-colored and green-colored bacteria. However, if the SYTO®9 dye is incorporated first, then the two dyes co-localize in the bacterial cells, displaying both yellow-colored cells and red-colored cells.[73] This lack of color differentiation can lead to possible misinterpretations of the resulting data about the physiological state of bacteria. It must also be noted that although this kit appellation 'LIVE/DEAD' suggests a differentiation between active and dead cells, it only enables the differentiation between bacteria with intact and damaged cytoplasmic membranes.

3.1.2 Esterase Activity

To ascertain cell viability, it is recommended to further investigate other physiological properties, such as the esterase activity. These enzymes are common in most living bacteria, and can be used to provide information on the metabolic state of bacterial cells. Esterase activity is measured using lipophilic, uncharged and nonfluorescent substrates; the product resulting from the enzyme-substrate reaction further exhibits fluorescence after cleavage.[42,67] Once within active cells, the substrate is cleaved by intracellular esterases, further releasing a polar fluorescent product that is retained inside cells having an intact membrane. By contrast, when cells have damaged membranes, the fluorescent product is rapidly leaked, even if the cells retain some residual esterase activity. Consequently, esterase activity dyes can serve not only to probe activity, which is required to activate their fluorescence, but also cell membrane integrity, which is required for intracellular retention of the fluorescent products. The use of fluorescein derivatives such as carboxyfluorescein (formed by the cleavage of carboxyfluorescein diacetate, CFDA), calcein (formed by the cleavage of calcein acetoxymethyl ester, calcein-AM) and 2′,7′-bis-(2-Carboxyethyl)-5-(and-6)-carboxyfluorescein, BCECF (formed by the cleavage of BCECF acetoxymethylester, BCECF-AM), is preferred over fluorescein because they have been demonstrated to accumulate more efficiently inside cells with intact membranes, reducing possible residual leakage that can occur with fluorescein.

A major limitation of this assay is that Gram-negative bacteria can be impermeable to these lipophilic probes, and a permeabilisation step of the outer membrane is often required.[42] To avoid this step, a commercial product, ChemChrome B has been shown to stain efficiently both Gram-negative and Gram-positive bacteria.[74] Other limitations such as poor dye uptake and active dye extrusion have been overcome by the further development of ChemChrome V6 (Chemunex, Biomérieux), which combines a counterstain to reduce nonspecific fluorescence and a specific buffer to reduce dye extrusion.[67,74]

3.1.3 Respiratory Activity

Another viability assay is based on the reduction of nonfluorescent stains by dehydrogenase enzymes present within metabolically active cells, to form insoluble fluorescent products.[75,76] An example of this type of assays is the resazurin (7-hydroxy-3H-phenoxazin-3-one-10-oxide) one.[77] In this test, the blue dye is nonfluorescent until it is irreversibly reduced to the pink colored and highly fluorescent resorufin by the oxydoreductases of viable cells.[76–79] The resazurin staining method was shown to provide a fast and simple assay for screening antimicrobial efficacies. However, once resorufin is formed, if the concentration and time incubation of the dye are not well adjusted, it can further be reduced to hydroresorufin, an uncolored and nonfluorescent compound.[80] This can lead to misinterpretation of the results. Thus, it is of importance that the dye concentration is well adapted prior to experiments in order to obtain meaningful results.

Other well-described probes of respiratory activity are the tetrazolium dyes.[75] As for the resazurin assay, dehydrogenase enzymes and/or components of the electron

Encyclopedia of Analytical Chemistry, Online © 2006–2017 John Wiley & Sons, Ltd.

This article was published in the *Encyclopedia of Analytical Chemistry* in 2017 by John Wiley & Sons, Ltd.
DOI: 10.1002/9780470027318.a9606

transport system of respiring cells can reduce tetrazolium dyes (such as the 5-cyano-2,3-ditoluyl tetrazolium chloride, CTC) to a brightly colored, intracellular, CTC formazan precipitate. In general, bacterial cells that reduce tetrazolium dyes are considered viable, but cells that fail to do so are not necessarily nonviable if a slow metabolism is adopted by the cells.[81]

The advantage of such methods is that they are rapid and allow analysis of individual cells. Furthermore, in contrast to the plate count method, also the nonviable cells are also analyzed. It should however be realized that all these methods have their own limitations, and it may therefore be recommended that, for a good understanding of the viability state of the cell population, the information of more than one method should be combined.

3.1.4 Viable But Nonculturable Subpopulations

The VBNC state was initially suggested by Roszak et al.[82] for readily culturable bacteria which, under stress conditions (nutrient depletion, oxygen deprivation, but also antibiotic exposure), become nonculturable but retain metabolic activity.[21,83,84] This subpopulation, under favorable conditions, can give rise to new progeny, leading to a recurrence of infection in patients who are thought to be cured. Regarding the negative impact of such bacterial population, their identification and quantification inside a biomass is of interest. This can be achieved by combining enumeration of fluorescently stained bacteria with FCM, and agar-grown bacteria with conventional plate count techniques.[83] Experiments can also be completed with the detection of mRNA gene expression by reverse transcription-PCR (RT-PCR): due to the short half-life of this molecule, only cells that carry out rapid transcription are detected, thus allowing to confirm the VBNC cells viability.[21,83,84]

3.2 *In Vivo* Bacterial Infections

Besides *in vitro* susceptibility tests, experimental animal models greatly aid to predict the outcomes of *in vivo* antibiotic treatments associated with bacterial infections.[27,85,86] Animal models have the advantage of determining antimicrobial efficacy at specific body sites such as the thigh in mice; the peritoneum in mice and rats; the lung in mice, rats and guinea pigs; endocarditis in rabbits and rats; and meningitis in rabbits.[87] Classical methods to evaluate *in vivo* bacterial inactivation under antibiotics exposure include classical Colony-Forming Units (CFU) counting on agar-plates samples collected from infected animals treated or not with antibiotics.[88] One major limitation concerning this method is that the studies are often conducted at the late and end stages of the disease process.[87,89] As a consequence, animals sacrifice and tissue removal are required at each sampling point, and in the case of implanted devices, the foreign body must be removed to estimate the *ex vivo* pathogen burden.[28,29] Therefore, such procedures can yield large animal-to-animal variations and the consumption of high numbers of experimental animals to determine treatment efficacy.[90–93] Over the last 13 years, the field of optical imaging has expanded from *in vitro* fluorescence microscopy of cells to *in vivo* imaging of living animals.[29] Recent advances in optical imaging of bacterial infections have been propelled by the invention of genetic tools producing fluorescent and bioluminescent bacteria, along with the discovery of synthetic fluorescent probes that selectively target bacterial cell surfaces. Real-time *in situ* optical imaging has shown to be an effective method for accurately monitoring, noninvasively and nondestructively, the bacterial migration, colonization, and their response to antibiotics treatment in living animals.[28,29,33] Importantly, these technologies enable to conduct longitudinal studies during extended times (typically until 30 days).[91] Each animal is then used as its own control over time without the need for sequential sacrifices, thus circumventing the critical issue of animal-to-animal variations and limiting the total number of sacrificed animals.[28,91,93]

3.2.1 Bioluminescence Imaging

To obtain an overview of how the pathogen invades and colonizes the host, one major development in live animal imaging is the use of bioluminescence.[94] The method was first described in 1995 by Contag and coauthors,[95] and has become increasingly popular in the context of numerous infections, including meningitis and urinary tract infections.[27] Bioluminescent bacteria are microorganisms that can either produce light naturally (without photonic excitation) or be engineered to express luciferase enzymes that catalyze the light-generating oxidation of substrates such as luciferin in the presence of oxygen and ATP.[94] Since the metabolic activity of viable cells can be detected directly on the support, nondestructively, and noninvasively, bioluminescent reporters offer a method of labeling pathogens, which is innocuous.[92] Interestingly, the doubling time of bacteria is the same for the native strains and the bioluminescent ones.[91] In addition, a loss of metabolic activity is characterized by a loss of luminescence until undetectable levels, enabling to monitor in real time antibiotic treatments efficacies. However, one limitation of such studies is that bacteria are able to exert very low metabolic activity even if they still remain viable. In this case, when testing an antibiotic treatment, a loss of bioluminescence could be wrongfully interpreted as a succeeding treatment. For example, Kadurugamuwa

Encyclopedia of Analytical Chemistry, Online © 2006–2017 John Wiley & Sons, Ltd.

This article was published in the *Encyclopedia of Analytical Chemistry* in 2017 by John Wiley & Sons, Ltd.
DOI: 10.1002/9780470027318.a9606

et al.[92] showed that during exponential phase of growth, bioluminescence was found to closely correlate with viable cell count. However, once the cultures reached the stationary phase, the bioluminescence decreased as expected, and was no longer correlated with the number of cells, indicating a decrease in growth and metabolic activity of the population.

A significant number of recent studies have emphasized the advantages of using *in vivo* bioluminescent imaging for real-time monitoring of bacterial infections, and their response to treatment, showing it to be noninvasive and significantly more rapid and sensitive than standard techniques.[94,96,97] In addition, the luminescence signal intensity is proportional to the number of bacterial cells having a metabolic activity, thus allowing to measure quantitatively the bacterial amounts at specific sites of infection *in vivo* without animal sacrifice.[93] Previous work by Kadurugamuwa et al.[91,92,98,99] have demonstrated the use of bioluminescent imaging techniques to monitor subcutaneous, catheter-associated bioluminescent *Staphylococcus aureus (S. aureus)* (Xen29) and *Pseudomonas aeruginosa (P. aeruginosa)* (Xen25) infection in mice. They demonstrated that the efficacies of antimicrobial agents belonging to different molecular families could be rapidly evaluated *in vivo* against such infections in real time. In particular, monitoring bacterial infections directly *in vivo* is very advantageous for the case of pathogens such as *Mycobacterium tuberculosis (M. tuberculosis),* which grow very slowly on agar *in vitro*.[100,101] For example, Andreu and coauthors developed an experimental bioluminescence-based lung infection model using a *M. tuberculosis* strain carrying a red-shifted derivative of the firefly luciferase gene (FFlucRT) to infect mice.[100] It allowed them to visualize the disease progression in living animals rapidly and noninvasively, and to quantify the effect of isoniazid, a front-line anti-tuberculosis drug. Using this model, they could detect as few as 10^4 reporter bacteria in the lungs of mice. In addition, a good correlation was found between bioluminescence and bacterial loads and a marked reduction in luminescence was observed in living mice treated with isoniazid.[100] These studies have also been conducted not only to study the efficacy of systemic and topical antibiotic treatments against community-acquired methicillin-resistant *S. aureus* wound infections,[102] but also to follow the entire process of *P. aeruginosa* and *Proteus mirabilis* urinary tract infections and antibiotic treatment effects.[99] Additional studies have reported the possibility of using bioluminescence imaging of bacteria in combination with fluorescence imaging of LysEGFP mice to image antibiotic treatments effects and immune response at the same time.[90,103]

Taken together, the bioluminescence approach enables to investigate not only the bacterial infection process and the antibiotic treatments efficacies, but also the infection-induced inflammatory response and the bacterial population rebounds, making it a valuable tool for rapid, accurate and inexpensive *in vivo* preclinical screening. One drawback of this approach is that the emission spectrum is generally broad and only a small percentage of bioluminescence emission spectra extend beyond 600 nm, which means that tissue penetration is limited and multicolor imaging is hardly feasible.[29,94,96,104,105]

3.2.2 Fluorescence Imaging

In addition to bioluminescence, bacteria can also be engineered to express fluorescent proteins. Many different mutants of the green fluorescent protein (GFP) have been developed, and there are now plenty of variants emitting at all colors in the visible spectrum.[106] A relevant example is the study of Hoffman and Zhao.[107] In this study, mice were given subcutaneous injections of *Salmonella typhimurium*–GFP and *Escherichia coli*–RFP (red fluorescent protein). Using whole-body fluorescence imaging,[108] the spatiotemporal infection process was imaged with accuracy, enabling to determine the tissue specificity of infection, the spatial migration of the infectious agents and the host response to the antimicrobial agent exposure.[107] Differential antibiotic response and resistance could then be visualized by dual-color imaging: *E. coli*-RFP, susceptible to the antibiotic administered, totally disappeared whereas *S. typhimurium*-GFP, nonsusceptible to the treatment, grew more under the antibiotic exposure.[107] Another fluorescent protein-expressing bacteria has been used in a number of studies,[101,109,110] the *M. tuberculosis* expressing tandem dimer tomato (tdTomato) fluorescent protein. The use of this intrinsic fluorescent reporter has been demonstrated *in vivo* for the detection of lung infections at a concentration as low as 10^5 CFU/lung in harvested lungs but reached a detection limit of 10^7 CFU/lung in living mice.[101] This limitation has been circumvented in a more recent study with the use of intravital microscopy, a technique that allows even greater depth penetration in living tissues.[109] A fiber-based microendoscope was coupled with a whole-animal fluorescence imager to enable intravital excitation in the mouse lung with whole-animal detection. Using this technique, the detection limit reached 10^3 CFU/lung while the threshold of detection was greater than 10^6 CFU using standard epi-illumination.[109] Furthermore, the intensity inside the animal was greatly enhanced, as the optical path length between the source and expected location of the fluorophore is minimized. These imaging assays can now reduce the time required to assess the preclinical efficacy of new drugs in animal models and

Encyclopedia of Analytical Chemistry, Online © 2006–2017 John Wiley & Sons, Ltd.

This article was published in the *Encyclopedia of Analytical Chemistry* in 2017 by John Wiley & Sons, Ltd.
DOI: 10.1002/9780470027318.a9606

enhance the progress of these candidates into clinical trials against infections.[101]

While the quest for the perfect label is far from being achieved, current reagents are undergoing development and promise to be valuable probes for *in vivo* targeting of bacteria, as long as they are selected and used properly.[86] In living animals, one constraint is that the tissue absorption limits the penetration of excitation light in the visible wavelength range, resulting in reduced excitation of the probes localized in deep targets. To cope with this problem, a large number of exogenous fluorescent probes that can be excited in the near infrared (NIR) range (700–900 nm) have been developed to reduce tissue absorbance and scattering, and thus enhance penetration and sensitivity.[111] For example, metal complexes such as cationic Zn-DPA (zinc-(II)-dipicolyamine), conjugated to NIR-cyanine or squaraine-rotaxane moieties have been developed to label both Gram-positive and Gram-negative bacteria with increased brightness.[112–115] A major limitation for their use *in vivo* is that they also have been shown to interact with apoptotic and necrotic mammalian cells, which have negatively charged membranes.[28] Other probes that can be used *in vivo* consist in targeting bacteria-specific sugar transport systems. Ning et al. reported the use of a maltodextrin-based imaging probe coupled with the IR786 NIR dye to stain both Gram-positive (*S. aureus*) and Gram-negative (*E. coli*) with a high signal to noise ratio.[116] Interestingly, this probe is dependent on the metabolic state of the bacteria and thus usable for antibiotic susceptibility testing. In a recent study, an imaging nanoprobe was synthesized with three moieties: Concanavalin A (a lectin-binding protein with a high affinity for cell-surface mannose residues and polysaccharides) as a bacterial targeting ligand, a nanoparticle carrier, and a NIR fluorescent dye (IR750).[117] This probe allowed to detect and quantify the extent of bacterial colonization in a murine wound and catheter infection model. Other nanoprobes such as single-walled carbon nanotubes (SWNTs) have shown to be attractive candidates as fluorophores for NIR-II imaging, due to their photoluminescence in the 900–1400 nm range, a large Stokes' shift, low autofluorescence background, relative insensitivity to photobleaching compared to organic dyes and the ability to be functionalized with targeting/drug delivery agents.[118] Using genetically engineered M13 virus as a multifunctional vector, Bardhan and coauthors synthesized NIR-II fluorescent SWNT probes (M13-SWNT), with additional functionalization on the virus to target effectively bacterial infections. The authors could demonstrate the nanoprobes efficiency in an endocarditis model of *S. aureus* infection to illustrate an example of deep-tissue *in vivo* imaging.[118] All these probes, developed or still undergoing development for *in vivo* purposes, are summed up in Table 2.

Advances in imaging technologies using bioluminescent and fluorescent reporters remain of great interest for better understanding fundamental processes occurring *in vivo*, such as host–pathogen interactions or preclinical therapeutic agents testing. Nevertheless, animal infection models are, in general, developed to mimic those in humans. For a further translation to human tests for localizing infectious sites during and after antibiotics treatments, only exogenous probes represent an appropriate option.

4 FLUORESCENCE TOOLS TO DISSECT ANTIBIOTICS MODE OF ACTION AND THEIR FAILURE FACE TO BACTERIAL RESISTANCE/TOLERANCE MECHANISMS

In the time when microorganisms develop multidrug resistance, dissecting the molecular processes underlying clinically used antibiotics (in)activity is becoming more and more important.[119] In this context, fluorescence techniques have been shown to be suitable tools. Most of antibiotic molecules exhibit no or very low intrinsic fluorescence or can only be excited in the deep UV–UV range (Table 3), a drawback that can be circumvented by the possibility of labeling antibiotics with fluorescent molecules such as BODIPY-FL®, NBD, Alexa Fluor® or Fluorescein (Table 3).[125]

4.1 Antibiotics Mechanisms of Action

Antibiotics can act on the protein or nucleic acid synthesis or on the bacterial cell wall and membrane.[4] Undoubtedly, the cell membrane-targeting antibiotics have been the most extensively studied ones using fluorescence-based tools.[125] A typical example is the detailed mechanism of action of daptomycin, a new generation cyclic lipopeptide antibiotic.[133] Primary studies by Lakey and Ptak[134] and Muraih et al.[135] exploiting the antibiotic fluorescence and fluorescence resonance energy transfer measurements demonstrate that this drug forms oligomers in bacterial cell membranes, depending both on calcium and phosphatidylglycerol, a major component of bacterial membranes. Further experiments aimed at elucidating the eventual role of the membrane potential in daptomycin mechanism of action.[136] Using fluorometric and flow cytometric assays combined with the concomitant use of membrane potential fluorescent probes, the authors could demonstrate a daptomycin-triggered membrane depolarization further inducing potassium release from *S. aureus* cells.[136]

Encyclopedia of Analytical Chemistry, Online © 2006–2017 John Wiley & Sons, Ltd.

This article was published in the *Encyclopedia of Analytical Chemistry* in 2017 by John Wiley & Sons, Ltd.
DOI: 10.1002/9780470027318.a9606

Table 2 Bioluminescent reporters, intrinsic fluorescent reporters and exogenous fluorescent probes adapted for *in vivo* bacteria targeting: advantages and drawbacks

	Target	Advantages	Drawbacks
Bioluminescent reporters			
Xen29	*S. aureus*	⊕ Low background ⊕ Adapted for longitudinal studies ⊕ Great ability to mimic native bacterial strains	Ø Limited tissue penetration Ø Genetic engineering of bacteria often needed Ø Limited choice of emission wavelength range
Xen25	*P. aeruginosa*	⊕ Possibility to detect infection recovery following antibiotics treatments	
FFlucRT	*M. tuberculosis*	⊕ Well adapted for antibiotic screening ⊕ Quantitative data of bacterial amounts ⊕ Real-time dependent on metabolic activity	
Intrinsic fluorescent reporters			
Green fluorescent protein (GFP)	NA	⊕ Adapted for longitudinal studies ⊕ Possibility to detect infection recovery following antibiotics treatments ⊕ Well adapted for antibiotic screening	Ø Limited tissue penetration Ø High autofluorescence-related background Ø Genetic engineering of bacteria needed Ø Not translatable to clinical use
Red fluorescent protein (RFP)	NA		
tdTomato fluorescent protein	NA		
Exogenous fluorescent probes			
Zn-DPA metal complexes conjugated to NIR-cyanine or squaraine-rotaxane	Cell membrane	⊕ Usually coupled with NIR dyes ⊕ Deeper penetration (reduced tissue absorbance and scattering) ⊕ Low autofluorescence background ⊕ Reduced sensitivity to photo-bleaching ⊕ Possible translation to clinical use	Ø Long-term possible toxicity Ø Not adapted for longitudinal studies Ø Still under development (not commercial yet)
Maltodextrin conjugated to IR786 dye	Maltodextrin transporter		
Concanavalin A conjugated to a nanoparticle carrier and an IR750 dye	Cell wall		
M13 conjugated to SWNTs	*S. aureus* and *E. coli* F'Pili		

Taken together, physical and chemical fluorescence tools allowed to demonstrate that daptomycin, in the presence of calcium, inserts into the cytoplasmic membranes of cells,[134] where it can form oligomeric pores,[135] causing membrane depolarization and subsequent potassium ion leakage.[136]

Among the antibiotics that target the cell wall, 'lantibiotics' (vancomycin, nisin, etc.) are polycyclic peptides that have a binding specificity for the lipid II component, a membrane-anchored cell-wall precursor that is essential for bacterial cell-wall biosynthesis.[137] Hasper and coauthors[124] used CLSM to evidence that the fixation of the lantibiotic leads to lipid II displacement at the cell division site (or septum) and thus block the cell wall synthesis.

A significant advance was also achieved in the identification of the intracellular protein target of antibiotics. In this domain, we can cite the work of Llano-Sotelo et al. that identified the specific ribosomal protein target of aminoglycosides such as streptomycin and neomycin, using steady-state fluorescence spectroscopy.[138]

Another interesting highlight was the intracellular hydroxyl radical production following *E. coli* exposure to various classes of bactericidal antibiotics (quinolones, β-lactam, aminoglycoside) and bacteriostatic drugs (chloramphenicol, spectinomycin, tetracycline, and the macrolide erythromycin).[139] The radical quantification was obtained by combining cells staining with (hydroxyphenyl fluorescein, HPF), a reporter dye of hydroxyl radical and flow cytometry. It was proven that only application of lethal doses of bactericidal antibiotics promote the formation of highly deleterious oxidative radical species.[139]

Encyclopedia of Analytical Chemistry, Online © 2006–2017 John Wiley & Sons, Ltd.

This article was published in the *Encyclopedia of Analytical Chemistry* in 2017 by John Wiley & Sons, Ltd.
DOI: 10.1002/9780470027318.a9606

Table 3 Principal clinically used antibiotics and their visible-fluorescent derivatives

Antibiotic	Target	Maximum absorption of the native antibiotic	Grafted fluorophore for fluorescence imaging	References
Penicillin	Cell wall	260 nm	BODIPY-FL	(120,121)
Ramoplanin	Cell wall	[a]	Fluorescein, BODIPY-FL	(122)
Vancomycin	Cell wall	280 nm	Fluorescein, BODIPY-FL	(122)
Polymyxin	Cell membrane	260 nm	DANSYL	(123)
Nisin	Cell membrane	[a]	Fluorescein	(124)
Daptomycin	Cell membrane	360 nm	BODIPY-FL, NBD, Alexa-Fluor 350	(125)
Ciprofloxacin	Nucleic acids	280 nm	NBP, DBD-COCl	(126,127)
Norfloxacin	Nucleic acids	[a]	NBP, DBD-COCl	(127)
Fleroxacin	Nucleic acids	280 nm	Not needed	(128)
Tetracycline	Protein synthesis	490 nm	Not needed	(129–131)
Paromomycin	Protein synthesis	[a]	DANSYL	(132)

BODIPY-FL, 4,4-difluoro-5,7-dimethyl-4-bora-3a,4a-diaza-s-indacene-3-propionic acid; DANSYL, 1-dimethylaminonaphthalene-5-sulphonyl chloride; NBD, nitrobenzoxadiazole; NBP, nile blue perchlorate; DBD-COCI, 4-(*N*,*N*-Dimethylaminosulfonyl)-7-(*N*-chloroformylmethyl-*N*-methylamino)-2,1,3-benzoxadiazole.
[a]Unpublished.

4.2 Bacterial Resistance to Antibiotics

Bacteria are able to protect themselves from external aggressions by acquiring or developing resistance to antibiotics. One of the major lines of defense of bacteria is to limit the intracellular concentrations of the drug by its extrusion via efflux pumps.(15) This results in a sublethal concentration of the drug present at the target site, leading to treatment failure. In this context, Kascakova and coauthors measured for the first time the intracellular concentration of the antibiotic, fleroxacin, by quantifying its intrinsic fluorescence after deep UV excitation from a synchrotron beamline.(140) They were able to assess the threshold of intracellular accumulation required for antibacterial activity. When concentrations were too important, efflux pumps were activated, inhibiting antibiotics effects.(141)

In specific cases, infection treatments require prolonged drug exposure that can lead to the apparition of bacterial persisters, a slow-growing/dormant subpopulation. In addition to this physiological quiescence, it was recently demonstrated that this subpopulation exhibits intracellular accumulation of the fluorescently labeled penicillin that was correlated to an overexpression of a specific efflux gene.(142) Persistent bacteria were shown to ensure a double protective strategy to survive under antibiotic attack and appear to be at risk for the host since they can constitute a reservoir of pathogens triggering recurrent chronic infections.(142)

Another bacterial path to circumvent antibiotics action consists in reducing the bacterial membrane permeability, thus limiting the incorporation of drugs (e.g. daptomycin) into the cells. This was highlighted by comparing the degree of fluorescence polarization (polarization index) values of daptomycin-susceptible and daptomycin-resistant strains labeled with a fluorescent probe that incorporates into cell membranes (DPH, 1,6-diphenyl-1,3,5-hexatriene): an inverse correlation exists between the polarization index values and membrane fluidity.(136,143–150) Another strategy employed by daptomycin-resistant bacteria is to 'mask' the drug target to divert the antibiotic. In this context, Tran et al. used fluorescence imaging to discriminate daptomycin localization between susceptible and resistant strains: a homogenous cell membrane distribution in the case of susceptible strains and a localization in a spotty pattern for the resistant cells.(151) This diversion of the antibiotic localization was mediated by a redistribution and an increasing of cell membrane cardiolipin-rich microdomains in resistant cells.(152–154)

4.3 Bacterial Tolerance to Antibiotics

Besides bacterial resistance mechanisms, a myriad of physiological changes can occur in a bacterial community. This is especially evident when a bacterial population is included in spatially organized biofilms. In hospital and communities, biofilms are frequently associated with chronic infections such as endocarditis, sinusitis, osteomyelitis, and various implant-associated infections. Antibiotic-susceptible planktonic bacteria can be eradicated with the combined action of antibiotics and host immune responses, whereas biofilm-enclosed bacteria can show a significant recalcitrance to antibiotics.(2) The mechanism of protection involved in this case is called 'tolerance', and is reversible when bacteria are resuspended. This altered biofilm susceptibility toward antibiotics

Encyclopedia of Analytical Chemistry, Online © 2006–2017 John Wiley & Sons, Ltd.

This article was published in the *Encyclopedia of Analytical Chemistry* in 2017 by John Wiley & Sons, Ltd.
DOI: 10.1002/9780470027318.a9606

is attributed to multiple factors. One of them is the inability of the drugs to penetrate to all areas of the biofilm. Several studies aimed at verifying if the antibiotic could reach the biofilms depth in order to address the role of penetration barrier in biofilm-associated drug tolerance.[129,155–158] Besides a variety of nonfluorescent-based methods such as agar disk-diffusion assays,[159] time-lapse fluorescence imaging gives access in real time to the penetration rate and the overall distribution of the antibiotic through the three dimensions of biofilms.[129,156–158,160] It was shown that even if the antibiotic penetration can be significantly delayed in certain cases, the drug readily penetrates the deepest layers of the biomass, and can generally not account for the overall tolerance of biofilms to antibiotic treatment.[13]

Another factor that is generally invoked to have a role in antibiotics tolerance by biofilms is the lack of drug bioavailability. This can be accessed by image-based fluorescence recovery after photobleaching (FRAP), a method routinely implemented on commercial CLSMs.[47,161] It is based on a brief excitation of fluorescent molecules by a very intense light source in a user-defined region to irreversibly photobleach their fluorescence.[162] Fluorescence recovery is then probed over time at a low light power in the same photobleached region. The time course of fluorescence intensity recovery can then be analyzed with analytical models, giving access to the quantitative mobility of the fluorescent molecules, and allowing the diffusion coefficients determination. If most of the antibiotics molecules are linked to their environment, no recovery of the fluorescence is observed. By contrast, if a partial or total recovery of the fluorescence is observed, this means that a proportion of antibiotic molecules are diffusing freely and are thus bioavailable. Previous studies were conducted to examine the penetration, diffusion, and bioavailability of clinically-used antibiotics, vancomycin and daptomycin.[156,157] The authors demonstrated that neither the penetration nor the bioavailability of the antibiotics were responsible for biofilms tolerance toward antibiotics.

To analyze the interaction occurring between antibiotics and biofilm cells, fluorescence correlation spectroscopy (FCS) is a well-adapted technique that benefits of a single molecule resolution.[47,163] This fluorescence-based technique consists in monitoring the emission intensity fluctuations of fluorophores due to a small number of molecules passing through the confocal excitation volume; these fluctuations can then be quantified in their amplitude and duration by temporally autocorrelating the recorded intensity signal. Daddi-Oubekka et al. used FCS to study the diffusion/reaction process of a fluorescent vancomycin derivative inside live *S. aureus* biofilms.[156] They demonstrated that at nanomolar concentrations, no free diffusion of the antibiotic occurred, strongly suggesting that the bacterial receptors were saturated.

A complementary technique that can be used to study the interaction of antibiotics fluorescent derivatives with biofilm-encased bacteria is fluorescence lifetime IMaging (FLIM).[47,156] This approach consists in measuring the fluorescence decay of a fluorophore over time[163,164] in each point of the whole volume, giving access to a 'map' of fluorescence lifetimes. This parameter is independent of the fluorescent molecules concentrations but can vary when an interaction occurs with the environment, allowing to highlight for example the interaction of a fluorescent antibiotic with its biological target as reported for *S. aureus* cells with vancomycin.[47,156,163]

5 CONCLUSION AND FUTURE PROSPECTS

Recent advances in fluorescence tools and in particular fluorescence microscopy, together with the large panel of fluorescent probes already developed or under development have undoubtedly transformed the study of antibiotics effects on infectious bacteria, both *in vitro* and *in vivo*. Fluorescence tools have also demonstrated their value to dissect molecular events involved in antibiotic action, but also to explore the panel of strategies employed by bacteria to circumvent antibiotics actions. One major challenge of current research in microbiology is the micro- to submicrometric size of bacteria that renders the use of fluorescence microscopy very challenging in probing nanoscale molecular events. To achieve such a scale, nanoscopy technologies are emerging in microbiology. The resolution improvements enabled by these techniques will be very useful to address questions such as antibiotics localization and further modifications induced inside bacteria with a nanometric resolution. Another development considered is the coupling of fluorescence microscopy with nonfluorescent ones such as atomic force microscopy to complement information about biological processes.

In animal models, the development of new technologies such as whole-animal bioluminescence and fluorescence imaging, together with the development of ever-new fluorescent reporter strategies have made the study of disease progression and the efficacy of antibiotics treatments more precise and accurate. Nevertheless, the use of whole-animal imagers gives access to macroscale events only. To circumvent this limitation, implementations such as the coupling of dorsal chambers to CLSM or TPE microscopy, already performed in the context of cancer diseases, would allow to reach the single cell cellular scale. Another big challenge in animal imaging is the tissue

Encyclopedia of Analytical Chemistry, Online © 2006–2017 John Wiley & Sons, Ltd.

This article was published in the *Encyclopedia of Analytical Chemistry* in 2017 by John Wiley & Sons, Ltd.
DOI: 10.1002/9780470027318.a9606

scattering of excitation light, preventing the imaging of deep targets. To cope with this issue, the application of TPE microscopy for example could allow effective deeper localization of a wider panel of probes independent on their excitation and emission wavelengths. Taken together, fluorescence tools have greatly contributed to a better knowledge of the microbial world, and undergoing developments show to be promising for pursuing research in this sense.

ABBREVIATIONS AND ACRONYMS

BCECF	2′,7′-bis-(2-Carboxyethyl)-5-(and-6)-carboxyfluorescein
BCECF-AM	BCECF acetoxymethylester
CFDA	Carboxyfluorescein Diacetate
CLSM	Confocal Laser Scanning Microscopy
CTC	5-cyano-2,3-ditoluyl Tetrazolium Chloride
DAPI	4,6-diamidino-2-phenylindole Dihydrochloride
EFM	Epifluorescence Microscopy
FCM	Flow Cytometry
FCS	Fluorescence Correlation Spectroscopy
FFlucRT	Firefly Luciferase Gene
FLIM	Fluorescence Lifetime Imaging
FRAP	Fluorescence Recovery after Photobleaching
GFP	Green Fluorescent Protein
LSC	Laser Scanning Cytometer
LSM	Laser Scanning Microscopy
MBC	Minimum Bactericidal Concentration
MIC	Minimum Inhibitory Concentration
MRSA	Methicillin-resistant *Staphylococcus aureus*
NIR	Near Infrared
PAINT	Point Accumulation for Imaging in Nanoscale Topography
PALM	Photo-activated Localization Microscopy
PCR	Polymerase Chain Reaction
PI	Propidium Iodide
RFP	Red Fluorescent Protein
RT-PCR	Reverse Transcription-PCR
SIM	Structured Illumination Microscopy
SMLM	Single-molecule Localization Microscopy
STED	Stimulated Emission Depletion
STORM	Stochastic Optical Resolution Microscopy
SWNT	Single-walled Carbon Nanotube
TPE	Two-photon Excitation
VBNC	Viable But Nonculturable

RELATED ARTICLES

Biomedical Spectroscopy
Fluorescence Spectroscopy In Vivo • Single-molecule Fluorescence Imaging Techniques • Biomedical Spectroscopy: Introduction

Electronic Absorption and Luminescence
Fluorescence Imaging Microscopy • Fluorescence Lifetime Measurements, Applications of

Pharmaceuticals and Drugs
Antibiotics, Pharmaceutical Analysis of

Clinical Chemistry
Phosphorescence, Fluorescence, and Chemiluminescence in Clinical Chemistry

Nucleic Acids Structure and Mapping
High-Resolution 4D Imaging in Live Cells

REFERENCES

1. D. Debabov, 'Antibiotic Resistance: Origins, Mechanisms, Approaches to Counter', *Appl. Biochem. Microbiol.*, **49**(8), 665–671 (2013).
2. D. Lebeaux, J.-M. Ghigo, C. Beloin, 'Biofilm-related Infections: Bridging the Gap between Clinical Management and Fundamental Aspects of Recalcitrance toward Antibiotics', *Microbiol. Mol. Biol. Rev.*, **78**(3), 510–543 (2014).
3. R.J. Fair, Y. Tor, 'Antibiotics and Bacterial Resistance in the 21st Century', *Perspect. Med. Chem.*, **6**, 25–64 (2014).
4. M.S. Butler, M.A. Blaskovich, M.A. Cooper, 'Antibiotics in the Clinical Pipeline at the End of 2015', *J. Antibiot. (Tokyo)*, **70**, 3–24 (2016).
5. Publications|AMR Review. http://amr-review.org/Publications.
6. S.S. Shetty, P. Shetty, S.R. Uchil, 'War of Humans and Superbugs: Have We Depleted Our Resources?', *Br. Med. J.*, **351**, (2015).
7. K. Kupferschmidt, 'Superbugs Predate Wonder Drugs', Science AAAS website. http://www.sciencemag.org/news/2011/08/superbugs-predate-wonder-drugs (2011).
8. L.J. Piddock, 'The Crisis of No New Antibiotics — What is the Way Forward?', *Lancet Infect. Dis.*, **12**(3), 249–253 (2012).
9. T.B. Stanton, 'A Call for Antibiotic Alternatives Research', *Trends Microbiol.*, **21**(3), 111–113 (2013).
10. H.K. Allen, J. Trachsel, T. Looft, T.A. Casey, 'Finding Alternatives to Antibiotics', *Ann. N. Y. Acad. Sci.*, **1323**(1), 91–100 (2014).

Encyclopedia of Analytical Chemistry, Online © 2006–2017 John Wiley & Sons, Ltd.

This article was published in the *Encyclopedia of Analytical Chemistry* in 2017 by John Wiley & Sons, Ltd.
DOI: 10.1002/9780470027318.a9606

11. A. Brauner, O. Fridman, O. Gefen, N.Q. Balaban, 'Distinguishing Between Resistance, Tolerance and Persistence to Antibiotic Treatment', *Nat. Rev. Microbiol.*, **14**(5), 320–330 (2016).
12. H. Van Acker, P. Van Dijck, T. Coenye, 'Molecular Mechanisms of Antimicrobial Tolerance and Resistance in Bacterial and Fungal Biofilms', *Trends Microbiol.*, **22**(6), 326–333 (2014).
13. D. Davies, 'Understanding Biofilm Resistance to Antibacterial Agents', *Nat. Rev. Drug Discov.*, **2**(2), 114–122 (2003).
14. J. Davies, D. Davies, 'Origins and Evolution of Antibiotic Resistance', *Microbiol. Mol. Biol. Rev.*, **74**(3), 417–433 (2010).
15. J.M.A. Blair, M.A. Webber, A.J. Baylay, D.O. Ogbolu, L.J.V. Piddock, 'Molecular Mechanisms of Antibiotic Resistance', *Nat. Rev. Microbiol.*, **13**(1), 42–51 (2015).
16. P.D. Stapleton, P.W. Taylor, 'Methicillin Resistance in *Staphylococcus aureus*: Mechanisms and Modulation', *Sci. Prog.*, **85**(Pt 1), 57–72 (2002).
17. C.L. Ventola, 'The Antibiotic Resistance Crisis', *Pharm. Ther.*, **40**(4), 277–283 (2015).
18. N. Dhar, J.D. McKinney, 'Microbial Phenotypic Heterogeneity and Antibiotic Tolerance', *Curr. Opin. Microbiol.*, **10**(1), 30–38 (2007).
19. S. Hathroubi, M.A. Mekni, P. Domenico, D. Nguyen, M. Jacques, 'Biofilms: Microbial Shelters Against Antibiotics', *Microb. Drug Resist.*, Epub ahead of print (2016).
20. R.A. Proctor, C. von Eiff, B.C. Kahl, K. Becker, P. McNamara, M. Herrmann, G. Peters, 'Small Colony Variants: A Pathogenic Form of Bacteria that Facilitates Persistent and Recurrent Infections', *Nat. Rev. Microbiol.*, **4**(4), 295–305 (2006).
21. M. Ayrapetyan, T.C. Williams, J.D. Oliver, 'Bridging the Gap Between Viable But Non-culturable and Antibiotic Persistent Bacteria', *Trends Microbiol.*, **23**, 7–13 (2014).
22. C.E. Zobell, D.Q. Anderson, 'Observations on the Multiplication of Bacteria in Different Volumes of Stored Sea Water and the Influence of Oxygen Tension and Solid Surfaces', *Biol. Bull.*, **71**(2), 324–342 (1936).
23. P.S. Stewart, 'Mechanisms of Antibiotic Resistance in Bacterial Biofilms', *Int. J. Med. Microbiol.*, **292**(2), 107–113 (2002).
24. T.-F. Mah, B. Pitts, B. Pellock, G.C. Walker, P.S. Stewart, G.A. O'Toole, 'A Genetic Basis for *Pseudomonas aeruginosa* Biofilm Antibiotic Resistance', *Nature*, **426**(6964), 306–310 (2003).
25. S. Aellen, Y.-A. Que, B. Guignard, M. Haenni, P. Moreillon, 'Detection of Live and Antibiotic-killed Bacteria by Quantitative Real-time PCR of Specific Fragments of rRNA', *Antimicrob. Agents Chemother.*, **50**(6), 1913–1920 (2006).
26. T.R. Neu, B. Manz, F. Volke, J.J. Dynes, A.P. Hitchcock, J.R. Lawrence, 'Advanced Imaging Techniques for Assessment of Structure, Composition and Function in Biofilm Systems', *FEMS Microbiol. Ecol.*, **72**(1), 1–21 (2010).
27. K. Melican, A. Richter-Dahlfors, 'Real-time Live Imaging to Study Bacterial Infections In Vivo', *Curr. Opin. Microbiol.*, **12**(1), 31–36 (2009).
28. B. Mills, M. Bradley, K. Dhaliwal, 'Optical Imaging of Bacterial Infections', *Clin. Transl. Imaging*, **4**, 163–174 (2016).
29. W.M. Leevy, N. Serazin, B.D. Smith, 'Optical Imaging of Bacterial Infection Models', *Drug Discov. Today Dis. Models*, **4**(3), 91–97 (2007).
30. S.K. Piper, C. Habermehl, C.H. Schmitz, W.M. Kuebler, H. Obrig, J. Steinbrink, J. Mehnert, 'Towards Whole-body Fluorescence Imaging in Humans', *PLoS One*, **8**(12), e83749 (2013).
31. A. Bridier, F. Hammes, A. Canette, T. Bouchez, R. Briandet, 'Fluorescence-based Tools for Single-cell Approaches in Food Microbiology', *Int. J. Food Microbiol.*, **213**, 2–16 (2015).
32. B.F. Brehm-Stecher, E.A. Johnson, 'Single-cell Microbiology: Tools, Technologies, and Applications', *Microbiol. Mol. Biol. Rev.*, **68**(3), 538–559 (2004).
33. G.C. Kagadis, N.L. Ford, D.N. Karnabatidis, G.K. Loudos, *Handbook of Small Animal Imaging: Preclinical Imaging, Therapy, and Applications*, CRC Press, Boca Raton, 2016.
34. M. Sauer, J. Hofkens, J. Enderlein, 'Basic Principles of Fluorescence Spectroscopy', in *Handbook of Fluorescence Spectroscopy and Imaging*, Wiley-VCH Verlag GmbH & Co. KGaA, Weinheim, Germany, 1–30, 2011.
35. J.R. Lakowicz (ed), *Principles of Fluorescence Spectroscopy*, Springer US, Boston, MA, 2006.
36. D.M. Jameson, *Introduction to Fluorescence*, CRC Press Book, Boca Raton, 2014.
37. B. Valeur, M.N. Berberan-Santos, *Molecular Fluorescence: Principles and Applications*, John Wiley & Sons, Weinheim, Germany, 2012.
38. G.G. Guilbault, *Practical Fluorescence*, CRC Press, Boca Raton, 2nd edition, 1990.
39. T.R. Neu, J.R. Lawrence, 'Innovative Techniques, Sensors, and Approaches for Imaging Biofilms at Different Scales', *Trends Microbiol.*, **23**(4), 233–242 (2015).
40. J.T. Lisle, M.A. Hamilton, A.R. Willse, G.A. McFeters, 'Comparison of Fluorescence Microscopy and Solid-phase Cytometry Methods for Counting Bacteria in Water', *Appl. Environ. Microbiol.*, **70**(9), 5343–5348 (2004).
41. D.J. Webb, C.M. Brown, 'Epi-fluorescence Microscopy', *Methods Mol. Biol. Clifton NJ*, **931**, 29–59 (2013).

Encyclopedia of Analytical Chemistry, Online © 2006–2017 John Wiley & Sons, Ltd.

This article was published in the *Encyclopedia of Analytical Chemistry* in 2017 by John Wiley & Sons, Ltd.
DOI: 10.1002/9780470027318.a9606

42. F. Joux, P. Lebaron, 'Use of Fluorescent Probes to Assess Physiological Functions of Bacteria at Single-cell Level', *Microbes Infect. Inst. Pasteur*, **2**(12), 1523–1535 (2000).
43. J.L. Collier, L. Campbell, 'Flow Cytometry in Molecular Aquatic Ecology', *Hydrobiologia*, **401**(0), 34–54 (1999).
44. S. Müller, G. Nebe-von-Caron, 'Functional Single-Cell Analyses: Flow Cytometry and Cell Sorting of Microbial Populations and Communities', *FEMS Microbiol. Rev.*, **34**(4), 554–587 (2010).
45. M. Henriksen, 'Quantitative Imaging Cytometry: Instrumentation of Choice for Automated Cellular and Tissue Analysis', *Nat. Methods*, **7**, 4 (2010).
46. P. Pozarowski, E. Holden, Z. Darzynkiewicz, 'Laser Scanning Cytometry: Principles and Applications—An Update', *Methods Mol. Biol. Clifton NJ*, **931**, 187–212 (2013).
47. A. Bridier, E. Tischenko, F. Dubois-Brissonnet, J.-M. Herry, V. Thomas, S. Daddi-Oubekka, F. Waharte, K. Steenkeste, M.-P. Fontaine-Aupart, R. Briandet, 'Deciphering Biofilm Structure and Reactivity by Multiscale Time-resolved Fluorescence Analysis', *Adv. Exp. Med. Biol.*, **715**, 333–349 (2011).
48. K. Carlsson, P.E. Danielsson, A. Liljeborg, L. Majlöf, R. Lenz, N. Åslund, 'Three-dimensional Microscopy Using a Confocal Laser Scanning Microscope', *Opt. Lett.*, **10**(2), 53 (1985).
49. W. Denk, J.H. Strickler, W.W. Webb, 'Two-photon Laser Scanning Fluorescence Microscopy', *Science*, **248**(4951), 73–76 (1990).
50. M. Oheim, D.J. Michael, M. Geisbauer, D. Madsen, R.H. Chow, 'Principles of Two-photon Excitation Fluorescence Microscopy and Other Nonlinear Imaging Approaches', *Adv. Drug Deliv. Rev.*, **58**(7), 788–808 (2006).
51. V. Konjufca, M.J. Miller, 'Two-photon Microscopy of Host–Pathogen Interactions: Acquiring a Dynamic Picture of Infection In Vivo', *Cell. Microbiol.*, **11**(4), 551–559 (2009).
52. R. Briandet, P. Lacroix-Gueu, M. Renault, S. Lecart, T. Meylheuc, E. Bidnenko, K. Steenkeste, M.-N. Bellon-Fontaine, M.-P. Fontaine-Aupart, 'Fluorescence Correlation Spectroscopy to Study Diffusion and Reaction of Bacteriophages inside Biofilms', *Appl. Environ. Microbiol.*, **74**(7), 2135–2143 (2008).
53. E. Abbe, 'Beiträge zur Theorie des Mikroskops und der mikroskopischen Wahrnehmung', *Arch. Für Mikrosk. Anat.*, **9**(1), 413–418 (1873).
54. Method of the Year 2008', *Nat. Methods*, **6**(1), 1 (2009).
55. M.G.L. Gustafsson, L. Shao, P.M. Carlton, C.J.R. Wang, I.N. Golubovskaya, W.Z. Cande, D.A. Agard, J.W. Sedat, 'Three-dimensional Resolution Doubling in Wide-Field Fluorescence Microscopy by Structured Illumination', *Biophys. J.*, **94**(12), 4957–4970 (2008).
56. L. Schermelleh, P.M. Carlton, S. Haase, L. Shao, L. Winoto, P. Kner, B. Burke, M.C. Cardoso, D.A. Agard, M.G.L. Gustafsson, H. Leonhardt, J.W. Sedat, 'Subdiffraction Multicolor Imaging of the Nuclear Periphery with 3D Structured Illumination Microscopy', *Science*, **320**(5881), 1332–1336 (2008).
57. G. Vicidomini, G. Moneron, K.Y. Han, V. Westphal, H. Ta, M. Reuss, J. Engelhardt, C. Eggeling, S.W. Hell, 'Sharper Low-power STED Nanoscopy by Time Gating', *Nat. Methods*, **8**(7), 571–573 (2011).
58. K.I. Willig, B. Harke, R. Medda, S.W. Hell, 'STED Microscopy with Continuous Wave Beams', *Nat. Methods*, **4**(11), 915–918 (2007).
59. U. Endesfelder, S. Malkusch, B. Flottmann, J. Mondry, P. Liguzinski, P.J. Verveer, M. Heilemann, 'Chemically Induced Photoswitching of Fluorescent Probes – A General Concept for Super-resolution Microscopy', *Mol. Basel Switz.*, **16**(4), 3106–3118 (2011).
60. E. Betzig, G.H. Patterson, R. Sougrat, O.W. Lindwasser, S. Olenych, J.S. Bonifacino, M.W. Davidson, J. Lippincott-Schwartz, H.F. Hess, 'Imaging Intracellular Fluorescent Proteins at Nanometer Resolution', *Science*, **313**(5793), 1642–1645 (2006).
61. S.T. Hess, T.P.K. Girirajan, M.D. Mason, 'Ultra-high Resolution Imaging by Fluorescence Photoactivation Localization Microscopy', *Biophys. J.*, **91**(11), 4258–4272 (2006).
62. R. Jungmann, M.S. Avendaño, J.B. Woehrstein, M. Dai, W.M. Shih, P. Yin, 'Multiplexed 3D Cellular Super-resolution Imaging with DNA-PAINT and Exchange-PAINT', *Nat. Methods*, **11**(3), 313–318 (2014).
63. M.J. Rust, M. Bates, X. Zhuang, 'Sub-diffraction-limit Imaging by Stochastic Optical Reconstruction Microscopy (STORM)', *Nat. Methods*, **3**(10), 793–796 (2006).
64. J.S. Biteen, W.E. Moerner, 'Single-molecule and Super-resolution Imaging in Live Bacteria Cells', *Cold Spring Harb. Perspect. Biol.*, **2**, 3 (2010).
65. C. Coltharp, J. Xiao, 'Superresolution Microscopy for Microbiology', *Cell. Microbiol.*, **14**(12), 1808–1818 (2012).
66. L.B. Reller, M. Weinstein, J.H. Jorgensen, M.J. Ferraro, 'Antimicrobial Susceptibility Testing: A Review of General Principles and Contemporary Practices', *Clin. Infect. Dis.*, **49**(11), 1749–1755 (2009).
67. P. Breeuwer, T. Abee, 'Assessment of Viability of Microorganisms Employing Fluorescence Techniques', *Int. J. Food Microbiol.*, **55**(1–3), 193–200 (2000).
68. M. Berney, F. Hammes, F. Bosshard, H.-U. Weilenmann, T. Egli, 'Assessment and Interpretation of Bacterial Viability by Using the LIVE/DEAD BacLight Kit in Combination with Flow Cytometry', *Appl. Environ. Microbiol.*, **73**(10), 3283–3290 (2007).

Encyclopedia of Analytical Chemistry, Online © 2006–2017 John Wiley & Sons, Ltd.

This article was published in the *Encyclopedia of Analytical Chemistry* in 2017 by John Wiley & Sons, Ltd.
DOI: 10.1002/9780470027318.a9606

69. G.A. Cangelosi, J.S. Meschke, 'Dead or Alive: Molecular Assessment of Microbial Viability', *Appl. Environ. Microbiol.*, **80**(19), 5884–5891 (2014).
70. E.J. Wood, R.P. Haugland, Molecular Probes: Handbook of Fluorescent Probes and Research Chemicals, *Biochem. Educ.*, **22** 83, (1994).
71. P. Lebaron, P. Catala, N. Parthuisot, 'Effectiveness of SYTOX Green Stain for Bacterial Viability Assessment', *Appl. Environ. Microbiol.*, **64**(7), 2697–2700 (1998).
72. L. Boulos, M. Prévost, B. Barbeau, J. Coallier, R. Desjardins, 'LIVE/DEAD® BacLight™: Application of a New Rapid Staining Method for Direct Enumeration of Viable and Total Bacteria in Drinking Water', *J. Microbiol. Methods*, **37**(1), 77–86 (1999).
73. P. Stiefel, S. Schmidt-Emrich, K. Maniura-Weber, Q. Ren, 'Critical Aspects of using Bacterial Cell Viability Assays with the Fluorophores SYTO9 and Propidium Iodide', *BMC Microbiol.*, **15**, 36 (2015).
74. N. Parthuisot, P. Catala, K. Lemarchand, J. Baudart, P. Lebaron, 'Evaluation of ChemChrome V6 for Bacterial Viability Assessment in Waters', *J. Appl. Microbiol.*, **89**(2), 370–380 (2000).
75. M.V. Berridge, P.M. Herst, A.S. Tan, 'Tetrazolium Dyes as Tools in Cell Biology: New Insights into their Cellular Reduction', *Biotechnol. Annu. Rev.*, **11**, 127–152 (2005).
76. E. Peeters, H.J. Nelis, T. Coenye, 'Comparison of Multiple Methods for Quantification of Microbial Biofilms Grown in Microtiter Plates', *J. Microbiol. Methods*, **72**(2), 157–165 (2008).
77. A. Mariscal, R.M. Lopez-Gigosos, M. Carnero-Varo, J. Fernandez-Crehuet, 'Fluorescent Assay Based on Resazurin for Detection of Activity of Disinfectants Against Bacterial Biofilm', *Appl. Microbiol. Biotechnol.*, **82**(4), 773–783 (2009).
78. J. O'Brien, I. Wilson, T. Orton, F. Pognan, 'Investigation of the Alamar Blue (Resazurin) Fluorescent Dye for the Assessment of Mammalian Cell Cytotoxicity', *Eur. J. Biochem. FEBS*, **267**(17), 5421–5426 (2000).
79. M.E. Sandberg, D. Schellmann, G. Brunhofer, T. Erker, I. Busygin, R. Leino, P.M. Vuorela, A. Fallarero, 'Pros and Cons of Using Resazurin Staining for Quantification of Viable *Staphylococcus aureus* Biofilms in a Screening Assay', *J. Microbiol. Methods*, **78**(1), 104–106 (2009).
80. S.D. Sarker, L. Nahar, Y. Kumarasamy, 'Microtitre Plate-based Antibacterial Assay Incorporating Resazurin as an Indicator of Cell Growth, and Its Application in the In Vitro Antibacterial Screening of Phytochemicals', *Methods*, **42**(4), 321–324 (2007).
81. G.G. Rodriguez, D. Phipps, K. Ishiguro, H.F. Ridgway, 'Use of a Fluorescent Redox Probe for Direct Visualization of Actively Respiring Bacteria', *Appl. Environ. Microbiol.*, **58**(6), 1801–1808 (1992).
82. D.B. Roszak, D.J. Grimes, R.R. Colwell, 'Viable But Nonrecoverable Stage of *Salmonella enteritidis* in Aquatic Systems', *Can. J. Microbiol.*, **30**(3), 334–338 (1984).
83. L. Li, N. Mendis, H. Trigui, J.D. Oliver, S.P. Faucher, 'The Importance of the Viable But Non-culturable State in Human Bacterial Pathogens', *Microb. Physiol. Metab.*, **5**, 258 (2014).
84. T. Ramamurthy, A. Ghosh, G.P. Pazhani, S. Shinoda, 'Current Perspectives on Viable but Non-culturable (VBNC) Pathogenic Bacteria', *Front. Public Health*, **2**:103 (2014).
85. M. van Oosten, M. Hahn, L.M.A. Crane, R.G. Pleijhuis, K.P. Francis, J.M. van Dijl, G.M. van Dam, 'Targeted Imaging of Bacterial Infections: Advances, Hurdles and Hopes', *FEMS Microbiol. Rev.*, **39**(6), 892–916 (2015).
86. M. Heuker, A. Gomes, J.M. van Dijl, G.M. van Dam, A.W. Friedrich, B. Sinha, M. van Oosten, 'Preclinical Studies and Prospective Clinical Applications for Bacteria-targeted Imaging: The Future is Bright', *Clin. Transl. Imaging*, **4**, 253–264 (2016).
87. W.A. Craig, 'In Vitro and Animal PK/PD Models', in *Fundamentals of Antimicrobial Pharmacokinetics and Pharmacodynamics*, eds A.A. Vinks, H. Derendorf, J.W. Mouton, Springer, New York, 23–44, 2014.
88. M. Revest, C. Jacqueline, R. Boudjemaa, J. Caillon, V. Le Mabecque, A. Breteche, K. Steenkeste, P. Tattevin, G. Potel, C. Michelet, M.P. Fontaine-Aupart, D. Boutoille, 'New In Vitro and In Vivo Models to Evaluate Antibiotic Efficacy in *Staphylococcus aureus* Prosthetic Vascular Graft Infection', *J. Antimicrob. Chemother.*, **71**(5), 1291–1299 (2016).
89. G. Brackman, T. Coenye, 'In Vitro and In Vivo Biofilm Wound Models and Their Application', *Adv. Exp. Med. Biol.*, **897**, 15–32 (2016).
90. J.S. Cho, J. Zussman, N.P. Donegan, R. Irene Ramos, N.C. Garcia, D.Z. Uslan, Y. Iwakura, S.I. Simon, A.L. Cheung, R.L. Modlin, J. Kim, L.S. Miller, 'Noninvasive In Vivo Imaging to Evaluate Immune Responses and Antimicrobial Therapy against *Staphylococcus aureus* and USA300 MRSA Skin Infections', *J. Invest. Dermatol.*, **131**(4), 907–915 (2011).
91. J.L. Kadurugamuwa, L.V. Sin, J. Yu, K.P. Francis, R. Kimura, T. Purchio, P.R. Contag, 'Rapid Direct Method for Monitoring Antibiotics in a Mouse Model of Bacterial Biofilm Infection', *Antimicrob. Agents Chemother.*, **47**(10), 3130–3137 (2003).
92. J.L. Kadurugamuwa, L. Sin, E. Albert, J. Yu, K. Francis, M. DeBoer, M. Rubin, C. Bellinger-Kawahara, J.T.R. Parr, P.R. Contag, 'Direct Continuous Method for Monitoring Biofilm Infection in a Mouse Model', *Infect. Immun.*, **71**(2), 882–890 (2003).

Encyclopedia of Analytical Chemistry, Online © 2006–2017 John Wiley & Sons, Ltd.

This article was published in the *Encyclopedia of Analytical Chemistry* in 2017 by John Wiley & Sons, Ltd.
DOI: 10.1002/9780470027318.a9606

93. Y.Q. Xiong, J. Willard, J.L. Kadurugamuwa, J. Yu, K.P. Francis, A.S. Bayer, 'Real-time In Vivo Bioluminescent Imaging for Evaluating the Efficacy of Antibiotics in a Rat *Staphylococcus aureus* Endocarditis Model', *Antimicrob. Agents Chemother.*, **49**(1), 380–387 (2005).

94. Y. Kong, Y. Shi, M. Chang, A.R. Akin, K.P. Francis, N. Zhang, T.L. Troy, H. Yao, J. Rao, S.L.G. Cirillo, J.D. Cirillo, 'Whole-body Imaging of Infection Using Bioluminescence', *Curr. Protoc. Microbiol.*, 21:C:2C.4:2C.4.1–2C.4.17 (2011).

95. C.H. Contag, P.R. Contag, J.I. Mullins, S.D. Spilman, D.K. Stevenson, D.A. Benaron, 'Photonic Detection of Bacterial Pathogens in Living Hosts', *Mol. Microbiol.*, **18**(4), 593–603 (1995).

96. M. Hutchens, G.D. Luker, 'Applications of Bioluminescence Imaging to the Study of Infectious Diseases', *Cell. Microbiol.*, **9**(10), 2315–2322 (2007).

97. S. Massey, K. Johnston, T.M. Mott, B.M. Judy, B.H. Kvitko, H.P. Schweizer, D.M. Estes, A.G. Torres, 'In Vivo Bioluminescence Imaging of Burkholderia mallei Respiratory Infection and Treatment in the Mouse Model', *Cell. Infect. Microbiol. – Closed Sect.*, **2**, 174 (2011).

98. J.L. Kadurugamuwa, L.V. Sin, J. Yu, K.P. Francis, T.F. Purchio, P.R. Contag, 'Noninvasive Optical Imaging Method To Evaluate Postantibiotic Effects on Biofilm Infection In Vivo', *Antimicrob. Agents Chemother.*, **48**(6), 2283–2287 (2004).

99. J.L. Kadurugamuwa, K. Modi, J. Yu, K.P. Francis, T. Purchio, P.R. Contag, 'Noninvasive Biophotonic Imaging for Monitoring of Catheter-associated Urinary Tract Infections and Therapy in Mice', *Infect. Immun.*, **73**(7), 3878–3887 (2005).

100. N. Andreu, A. Zelmer, S.L. Sampson, M. Ikeh, G.J. Bancroft, U.E. Schaible, S. Wiles, B.D. Robertson, 'Rapid In Vivo Assessment of Drug Efficacy Against *Mycobacterium tuberculosis* using an Improved Firefly Luciferase', *J. Antimicrob. Chemother.*, **68**(9), 2118–2127 (2013).

101. A. Zelmer, P. Carroll, N. Andreu, K. Hagens, J. Mahlo, N. Redinger, B.D. Robertson, S. Wiles, T.H. Ward, T. Parish, J. Ripoll, G.J. Bancroft, U.E. Schaible, 'A New In Vivo Model to Test Anti-tuberculosis Drugs using Fluorescence Imaging', *J. Antimicrob. Chemother.*, **67**(8), 1948–1960 (2012).

102. Y. Guo, R.I. Ramos, J.S. Cho, N.P. Donegan, A.L. Cheung, L.S. Miller, 'In Vivo Bioluminescence Imaging To Evaluate Systemic and Topical Antibiotics against Community-acquired Methicillin-resistant *Staphylococcus aureus*-infected Skin Wounds in Mice', *Antimicrob. Agents Chemother.*, **57**(2), 855–863 (2013).

103. N.M. Bernthal, A.I. Stavrakis, F. Billi, J.S. Cho, T.J. Kremen, S.I. Simon, A.L. Cheung, G.A. Finerman, J.R. Lieberman, J.S. Adams, L.S. Miller, 'A Mouse Model of Post-arthroplasty *Staphylococcus aureus* Joint Infection to Evaluate In Vivo the Efficacy of Antimicrobial Implant Coatings', *PLoS One*, **5**(9), e12580 (2010).

104. C.H. Contag, M.H. Bachmann, 'Advances in In Vivo Bioluminescence Imaging of Gene Expression', *Annu. Rev. Biomed. Eng.*, **4**(1), 235–260 (2002).

105. T.C. Doyle, S.M. Burns, C.H. Contag, 'Technoreview: In Vivo Bioluminescence Imaging for Integrated Studies of Infection', *Cell. Microbiol.*, **6**(4), 303–317 (2004).

106. N.C. Shaner, P.A. Steinbach, R.Y. Tsien, 'A Guide to Choosing Fluorescent Proteins', *Nat. Methods*, **2**(12), 905–909 (2005).

107. R.M. Hoffman, M. Zhao, 'Whole-body Imaging of Bacterial Infection and Antibiotic Response', *Nat. Protoc.*, **1**(6), 2988–2994 (2007).

108. F. Leblond, S.C. Davis, P.A. Valdés, B.W. Pogue, 'Preclinical Whole-body Fluorescence Imaging: Review of Instruments, Methods and Applications', *J. Photochem. Photobiol. B*, **98**(1), 77–94 (2010).

109. F. Nooshabadi, H.-J. Yang, J.N. Bixler, Y. Kong, J.D. Cirillo, K.C. Maitland, 'Intravital Fluorescence Excitation in Whole-animal Optical Imaging', *PLoS One*, **11**, 2 (2016).

110. F. Nooshabadi, H. Yang, J. Cirillo, and K. C. Maitland, In-vivo Fluorescence Imaging of Bacterial Infection in the Mouse Lung, 2015, OW1D.3.

111. D.D. Nolting, J.C. Gore, W. Pham, 'Near-infrared Dyes: Probe Development and Applications in Optical Molecular Imaging', *Curr. Org. Synth.*, **8**(4), 521–534 (2011).

112. K.M. DiVittorio, W.M. Leevy, E.J. O'Neil, J.R. Johnson, S. Vakulenko, J.D. Morris, K.D. Rosek, N. Serazin, S. Hilkert, S. Hurley, M. Marquez, B.D. Smith, 'Zinc(II) Coordination Complexes as Membrane-active Fluorescent Probes and Antibiotics', *ChemBioChem*, **9**(2), 286–293 (2008).

113. W.M. Leevy, S.T. Gammon, J.R. Johnson, A.J. Lampkins, H. Jiang, M. Marquez, D. Piwnica-Worms, M.A. Suckow, B.D. Smith, 'Non-invasive Optical Imaging of *Staphylococcus aureus* Bacterial Infection in Living Mice using a Bis-dipicolylamine-zinc(II) Affinity Group Conjugated to a Near Infrared Fluorophore', *Bioconjug. Chem.*, **19**(3), 686–692 (2008).

114. W.M. Leevy, J.R. Johnson, C. Lakshmi, J. Morris, M. Marquez, B.D. Smith, 'Selective Recognition of Bacterial Membranes by Zinc(II)-coordination Complexes', *Chem. Commun. Camb. Engl.*, **15**, 1595–1597 (2006).

115. A.G. White, N. Fu, W.M. Leevy, J.-J. Lee, M.A. Blasco, B.D. Smith, 'Optical Imaging of Bacterial Infection in Living Mice Using Deep-red Fluorescent Squaraine Rotaxane Probes', *Bioconjug. Chem.*, **21**(7), 1297–1304 (2010).

116. X. Ning, S. Lee, Z. Wang, D. Kim, B. Stubblefield, E. Gilbert, N. Murthy, 'Maltodextrin-based Imaging

Encyclopedia of Analytical Chemistry, Online © 2006–2017 John Wiley & Sons, Ltd.

This article was published in the *Encyclopedia of Analytical Chemistry* in 2017 by John Wiley & Sons, Ltd.
DOI: 10.1002/9780470027318.a9606

Probes Detect Bacteria In Vivo with High Sensitivity and Specificity', *Nat. Mater.*, **10**(8), 602–607 (2011).

117. E.N. Tang, A. Nair, D.W. Baker, W. Hu, J. Zhou, 'In Vivo Imaging of Infection using a Bacteria-targeting Optical Nanoprobe', *J. Biomed. Nanotechnol.*, **10**(5), 856–863 (2014).
118. N.M. Bardhan, D. Ghosh, A.M. Belcher, 'Carbon Nanotubes as In Vivo Bacterial Probes', *Nat. Commun.*, **5**, 4918 (2014).
119. M.A. Kohanski, D.J. Dwyer, J.J. Collins, 'How Antibiotics Kill Bacteria: From Targets to Networks', *Nat. Rev. Microbiol.*, **8**(6), 423–435 (2010).
120. S.G. Waley, 'A Spectrophotometric Assay of β-lactamase Action on Penicillins', *Biochem. J.*, **139**(3), 789–790 (1974).
121. G. Zhao, T.I. Meier, S.D. Kahl, K.R. Gee, L.C. Blaszczak, 'BOCILLIN FL, A Sensitive and Commercially Available Reagent for Detection of Penicillin-binding Proteins', *Antimicrob. Agents Chemother.*, **43**(5), 1124–1128 (1999).
122. K. Tiyanont, T. Doan, M.B. Lazarus, X. Fang, D.Z. Rudner, S. Walker, 'Imaging Peptidoglycan Biosynthesis in *Bacillus subtilis* with Fluorescent Antibiotics', *Proc. Natl. Acad. Sci.*, **103**(29), 11033–11038 (2006).
123. B.A. Newton, 'A Fluorescent Derivative of Polymyxin: Its Preparation and Use in Studying the Site of Action of the Antibiotic', *Microbiology*, **12**(2), 226–236 (1955).
124. H.E. Hasper, N.E. Kramer, J.L. Smith, J.D. Hillman, C. Zachariah, O.P. Kuipers, B. de Kruijff, E. Breukink, 'An Alternative Bactericidal Mechanism of Action for Lantibiotic Peptides that Target Lipid II', *Science*, **313**(5793), 1636–1637 (2006).
125. J. K. Muraih, Mode of Action of Daptomycin, a Lipopeptide Antibiotic, 2013.
126. M.-T. Château, R. Caravano, 'Rapid Fluorometric Measurement of the Intra-cellular Concentration of Ciprofloxacin in Mouse Peritoneal Macrophages', *J. Antimicrob. Chemother.*, **31**(2), 281–287 (1993).
127. B. Prutthiwanasan, C. Phechkrajang, L. Suntornsuk, 'Fluorescent Labelling of Ciprofloxacin and Norfloxacin and Its Application for Residues Analysis in Surface Water', *Talanta*, **159**, 74–79 (2016).
128. D.R. Korber, G.A. James, J.W. Costerton, 'Evaluation of Fleroxacin Activity against Established *Pseudomonas fluorescens* Biofilms', *Appl. Environ. Microbiol.*, **60**(5), 1663–1669 (1994).
129. G. Stone, P. Wood, L. Dixon, M. Keyhan, A. Matin, 'Tetracycline Rapidly Reaches All the Constituent Cells of Uropathogenic *Escherichia coli* Biofilms', *Antimicrob. Agents Chemother.*, **46**(8), 2458–2461 (2002).
130. R.A. Milch, D.P. Rall, J.E. Tobie, 'Fluorescence of Tetracycline Antibiotics in Bone', *J. Bone Jt. Surg. Am.*, **40**(4), 897–910 (1958).
131. C.U. Chukwudi, L. Good, 'Interaction of the Tetracyclines with Double-stranded RNAs of Random Base Sequence: New Perspectives on the Target and Mechanism of Action', *J. Antibiot. (Tokyo)*, **69**(8), 622–30 (2016).
132. J.H. Buchanan, S.I. Rattan, A. Stevens, R. Holliday, 'Intracellular Accumulation of a Fluorescent Derivative of Paromomycin in Human Fibroblasts', *J. Cell. Biochem.*, **20**(1), 71–80 (1982).
133. R.M. Humphries, S. Pollett, G. Sakoulas, 'A Current Perspective on Daptomycin for the Clinical Microbiologist', *Clin. Microbiol. Rev.*, **26**(4), 759–780 (2013).
134. J.H. Lakey, M. Ptak, 'Fluorescence Indicates a Calcium-dependent Interaction between the Lipopeptide Antibiotic LY 146032 and Phospholipid Membranes', *Biochemistry (Mosc.)*, **27**(13), 4639–4645 (1988).
135. J.K. Muraih, A. Pearson, J. Silverman, M. Palmer, 'Oligomerization of Daptomycin on Membranes', *Biochim. Biophys. Acta BBA – Biomembr.*, **1808**(4), 1154–1160 (2011).
136. J.A. Silverman, N.G. Perlmutter, H.M. Shapiro, 'Correlation of Daptomycin Bactericidal Activity and Membrane Depolarization in *Staphylococcus aureus*', *Antimicrob. Agents Chemother.*, **47**(8), 2538–2544 (2003).
137. E. Breukink, B. de Kruijff, 'Lipid II as a Target for Antibiotics', *Nat. Rev. Drug Discov.*, **5**(4), 321–323 (2006).
138. B. Llano-Sotelo, R.P. Hickerson, L. Lancaster, H.F. Noller, A.S. Mankin, 'Fluorescently Labeled Ribosomes as a Tool for Analyzing Antibiotic Binding', *RNA*, **15**(8), 1597–1604 (2009).
139. M.A. Kohanski, D.J. Dwyer, B. Hayete, C.A. Lawrence, J.J. Collins, 'A Common Mechanism of Cellular Death Induced by Bactericidal Antibiotics', *Cell*, **130**(5), 797–810 (2007).
140. S. Kaščáková, L. Maigre, J. Chevalier, M. Réfrégiers, J.-M. Pagès, 'Antibiotic Transport in Resistant Bacteria: Synchrotron UV Fluorescence Microscopy to Determine Antibiotic Accumulation with Single Cell Resolution', *PLoS One*, **7**(6), e38624 (2012).
141. B. Cinquin, L. Maigre, E. Pinet, J. Chevalier, R.A. Stavenger, S. Mills, M. Réfrégiers, J.-M. Pagès, 'Microspectrometric Insights on the Uptake of Antibiotics at the Single Bacterial Cell Level', *Sci. Rep.*, **5**, 17968 (2015).
142. Y. Pu, Z. Zhao, Y. Li, J. Zou, Q. Ma, Y. Zhao, Y. Ke, Y. Zhu, H. Chen, M.A.B. Baker, H. Ge, Y. Sun, X.S. Xie, F. Bai, 'Enhanced Efflux Activity Facilitates Drug Tolerance in Dormant Bacterial Cells', *Mol. Cell*, **62**(2), 284–294 (2016).
143. A.S. Bayer, R. Prasad, J. Chandra, A. Koul, M. Smriti, A. Varma, R.A. Skurray, N. Firth, M.H. Brown, S.-P. Koo, M.R. Yeaman, 'In Vitro Resistance of *Staphylococcus aureus* to Thrombin-induced Platelet Microbicidal Protein is Associated with Alterations in Cytoplasmic

Encyclopedia of Analytical Chemistry, Online © 2006–2017 John Wiley & Sons, Ltd.

This article was published in the *Encyclopedia of Analytical Chemistry* in 2017 by John Wiley & Sons, Ltd.
DOI: 10.1002/9780470027318.a9606

Membrane Fluidity', *Infect. Immun.*, **68**(6), 3548–3553 (2000).

144. A.S. Bayer, T. Schneider, H.-G. Sahl, 'Mechanisms of Daptomycin Resistance in *Staphylococcus aureus*: Role of the Cell Membrane and Cell Wall', *Ann. N. Y. Acad. Sci.*, **1277**(1), 139–158 (2013).
145. T. Jones, M.R. Yeaman, G. Sakoulas, S.-J. Yang, R.A. Proctor, H.-G. Sahl, J. Schrenzel, Y.Q. Xiong, A.S. Bayer, 'Failures in Clinical Treatment of *Staphylococcus aureus* Infection with Daptomycin are Associated with Alterations in Surface Charge, Membrane Phospholipid Asymmetry, and Drug Binding', *Antimicrob. Agents Chemother.*, **52**(1), 269–278 (2008).
146. N.N. Mishra, A.S. Bayer, 'Correlation of Cell Membrane Lipid Profiles with Daptomycin Resistance in Methicillin-resistant *Staphylococcus aureus*', *Antimicrob. Agents Chemother.*, **57**(2), 1082–1085 (2013).
147. N.N. Mishra, S.-J. Yang, A. Sawa, A. Rubio, C.C. Nast, M.R. Yeaman, A.S. Bayer, 'Analysis of Cell Membrane Characteristics of In Vitro-selected Daptomycin-resistant Strains of Methicillin-resistant *Staphylococcus aureus*', *Antimicrob. Agents Chemother.*, **53**(6), 2312–2318 (2009).
148. N.N. Mishra, G.Y. Liu, M.R. Yeaman, C.C. Nast, R.A. Proctor, J. McKinnell, A.S. Bayer, 'Carotenoid-related Alteration of Cell Membrane Fluidity Impacts *Staphylococcus aureus* Susceptibility to Host Defense Peptides', *Antimicrob. Agents Chemother.*, **55**(2), 526–531 (2011).
149. N.N. Mishra, A.S. Bayer, T.T. Tran, Y. Shamoo, E. Mileykovskaya, W. Dowhan, Z. Guan, C.A. Arias, 'Daptomycin Resistance in Enterococci is Associated with Distinct Alterations of Cell Membrane Phospholipid Content', *PLoS One*, **7**(8), e43958 (2012).
150. J.T. Trevors, 'Fluorescent Probes for Bacterial Cytoplasmic Membrane Research', *J. Biochem. Biophys. Methods*, **57**(2), 87–103 (2003).
151. T.T. Tran, J.M. Munita, C.A. Arias, 'Mechanisms of Drug Resistance: Daptomycin Resistance', *Ann. N. Y. Acad. Sci.*, **1354**(1), 32–53 (2015).
152. D. Panesso, J. Reyes, E.P. Gaston, M. Deal, A. Londoño, M. Nigo, J.M. Munita, W.R. Miller, Y. Shamoo, T.T. Tran, C.A. Arias, 'Deletion of liaR Reverses Daptomycin Resistance in *Enterococcus faecium* Independent of the Genetic Background', *Antimicrob. Agents Chemother.*, **59**(12), 7327–7334 (2015).
153. T.T. Tran, D. Panesso, N.N. Mishra, E. Mileykovskaya, Z. Guan, J.M. Munita, J. Reyes, L. Diaz, G.M. Weinstock, B.E. Murray, Y. Shamoo, W. Dowhan, A.S. Bayer, C.A. Arias, 'Daptomycin-resistant *Enterococcus faecalis* Diverts the Antibiotic Molecule from the Division Septum and Remodels Cell Membrane Phospholipids', *mBio*, **4**(4), e00281–13 (2013).
154. T. Zhang, J.K. Muraih, N. Tishbi, J. Herskowitz, R.L. Victor, J. Silverman, S. Uwumarenogie, S.D. Taylor, M. Palmer, E. Mintzer, 'Cardiolipin Prevents Membrane Translocation and Permeabilization by Daptomycin', *J. Biol. Chem.*, **289**(17), 11584–11591 (2014).
155. P.S. Stewart, 'Diffusion in Biofilms', *J. Bacteriol.*, **185**(5), 1485–1491 (2003).
156. S. Daddi Oubekka, R. Briandet, M.-P. Fontaine-Aupart, K. Steenkeste, 'Correlative Time-resolved Fluorescence Microscopy to Assess Antibiotic Diffusion–Reaction in Biofilms', *Antimicrob. Agents Chemother.*, **56**(6), 3349–3358 (2012).
157. R. Boudjemaa, R. Briandet, M. Revest, C. Jacqueline, J. Caillon, M.-P. Fontaine-Aupart, K. Steenkeste, 'New Insight into Daptomycin Bioavailability and Localization in *Staphylococcus aureus* Biofilms by Dynamic Fluorescence Imaging', *Antimicrob. Agents Chemother.*, **60**(8), 4983–4990 (2016).
158. K.K. Jefferson, D.A. Goldmann, G.B. Pier, 'Use of Confocal Microscopy To Analyze the Rate of Vancomycin Penetration through *Staphylococcus aureus* Biofilms', *Antimicrob. Agents Chemother.*, **49**(6), 2467–2473 (2005).
159. R. Singh, S. Sahore, P. Kaur, A. Rani, P. Ray, 'Penetration Barrier Contributes to Bacterial Biofilm-associated Resistance Against Only Select Antibiotics, and Exhibits Genus-, Strain- and Antibiotic-specific Differences', *Pathog. Dis.*, **74**(6), ftw056 (2016).
160. P.S. Stewart, W.M. Davison, J.N. Steenbergen, 'Daptomycin Rapidly Penetrates a *Staphylococcus epidermidis* Biofilm', *Antimicrob. Agents Chemother.*, **53**(8), 3505–3507 (2009).
161. F. Waharte, K. Steenkeste, R. Briandet, M.-P. Fontaine-Aupart, 'Diffusion Measurements Inside Biofilms by Image-based Fluorescence Recovery after Photobleaching (FRAP) Analysis with a Commercial Confocal Laser Scanning Microscope', *Appl. Environ. Microbiol.*, **76**(17), 5860–5869 (2010).
162. S. Daddi Oubekka, R. Briandet, F. Waharte, M.-P. Fontaine-Aupart, and K. Steenkeste, Image-based fluorescence recovery after photobleaching (FRAP) to dissect vancomycin diffusion–reaction processes in *Staphylococcus aureus*, in *Proc. SPIE 8087, Clinical and Biomedical Spectroscopy and Imaging II,* 80871I–7, 2011.
163. S. D. Oubekka, Dynamique réactionnelle d'antibiotiques au sein des biofilms de *Staphylococcus aureus*: apport de la microscopie de fluorescence multimodale, Ph.D. Thesis, Université Paris Sud – Paris XI, France, 2012.
164. F.V. Bright, S. Pandey, G.A. Baker, 'Applications of Fluorescence Lifetime Measurements', in *Encyclopedia of Analytical Chemistry*, John Wiley & Sons, Ltd, Weinheim, Germany, 2006.

Encyclopedia of Analytical Chemistry, Online © 2006–2017 John Wiley & Sons, Ltd.

This article was published in the *Encyclopedia of Analytical Chemistry* in 2017 by John Wiley & Sons, Ltd.
DOI: 10.1002/9780470027318.a9606

RESULTATS

Chapitre 3. Infections de prothèses vasculaires à *S. aureus* : apport d'un modèle animal pour évaluer l'efficacité d'antibiotiques sur les biofilms *in vivo*

Parmi les complications associées à la pose de prothèses vasculaires, les infections à biofilms de *S. aureus* font partie des plus sévères et conduisent généralement à l'exérèse de la prothèse infectée. Ce type d'infections ne bénéficie aujourd'hui d'aucune prise en charge médicale standardisée (choix de l'antibiotique, concentration), sans doute faute de données suffisantes sur les biofilms *in vivo*. Il apparaît donc nécessaire de développer des modèles dans le but de caractériser leur structure et d'identifier le (ou les) antibiotique(s) et la(les) concentration(s) les plus adaptés pour les éradiquer.

C'est dans ce contexte que s'inscrit la première partie de ce travail de thèse, dont les résultats sont rapportés dans les articles 1 et 2. Réalisée en collaboration avec des chercheurs cliniciens du Laboratoire de Thérapeutique Expérimentale et Clinique des Infections du CHU de Nantes, l'objectif de cette étude a été de mettre au point un modèle animal d'infections sur prothèse vasculaire à travers lequel il est possible de décrire la structure des biofilms *in vivo* et d'évaluer quantitativement et visuellement l'activité et les effets des traitements antibiotiques.

Pour ce faire, Matthieu Revest, médecin spécialisé en infectiologie, a développé un modèle expérimental d'infection à biofilms de *S. aureus* sur prothèse vasculaire en Dacron® (polyéthylène téréphtalate) implantable chez la souris. Il a ainsi été possible de comparer différents traitements antibiotiques à base de cloxacilline, vancomycine et daptomycine, seules ou en association avec la rifampicine (**Figure 4**). La cloxacilline est une β-lactamine prescrite en première intention dans le traitement des infections staphylococciques. La vancomycine (un glycopeptide) et la daptomycine (un lipopeptide cyclique) sont indiquées dans le traitement d'infections multirésistantes. Concernant, la rifampicine, il s'agit d'une rifamycine le plus souvent utilisée en l'associant avec un autre antibiotique du fait de sa capacité à générer très rapidement des mutants résistants. Dans notre étude, différentes souches de *S. aureus* ont été utilisées, sensibles ou résistantes à la méticilline (MSSA ou MRSA), qu'elles soient de collection ou cliniques. Les résultats obtenus à travers cette étude nous ont permis de montrer d'une part que les concentrations nécessaires pour inhiber la croissance des biofilms formés sur pastilles de Dacron® *in vitro* (notées dMBIC dans l'article 2) étaient très largement supérieures aux concentrations minimales inhibitrices (notées MIC dans l'article 2) mesurées classiquement sur des bactéries planctoniques. Par ailleurs, la mesure de l'activité des antibiotiques dans l'éradication des infections à biofilms chez la souris a montré que les antibiotiques seuls étaient globalement moins actifs que leurs associations avec la rifampicine. Une particularité concerne la daptomycine, dont l'efficacité est similaire qu'il s'agisse de souches MSSA ou MRSA. Un seul cas se distingue, celui de la souche MRSA clinique (BCB8) qui s'est révélée particulièrement sensible à l'antibiotique.

Quelle est la structure du biofilm *in vivo* ? Dans quelle mesure interagit-il avec les cellules immunitaires et la matrice extracellulaire (tissus, …) de l'hôte ? Pour répondre à ces questions, nous avons explanté les implants de souris infectées, traitées ou non par antibiothérapie et les avons visualisés par microscopie confocale de fluorescence. Grâce à l'utilisation de marqueurs fluorescents des bactéries, nous avons pu mettre en évidence une structure de biofilms beaucoup moins épaisse que celle des biofilms modèles qui se développent *in vitro*. Un autre résultat d'intérêt obtenu grâce à l'utilisation de sondes fluorescentes spécifiques est la mise en évidence de la présence des cellules immunitaires (polynucléaires et

macrophages) sur le site de l'infection mais aussi la présence de bactéries vivantes à l'intérieur des macrophages, là où les antibiotiques (vancomycine et daptomycine) ne pénètrent pas. Les macrophages apparaissent ainsi comme un potentiel réservoir de bactéries de *S. aureus*, à l'origine de la résurgence des infections chez l'hôte.

Les résultats sont présentés sous la forme de deux publications, un article paru dans *Journal of Antimicrobial Chemotherapy*, 2016 (doi:10.1093/jac/dkv496), *« **New in vitro and in vivo models to evaluate antibiotic efficacy in Staphylococcus aureus prosthetic vascular graft infection**»* et un autre en cours de soumission à *Journal of Infectious Diseases : **« Intramacrophagic Staphylococcus aureus in prosthetic vascular graft infections as potential responsible of antibiotic therapy failure : observations of an ex-vivo model. »***

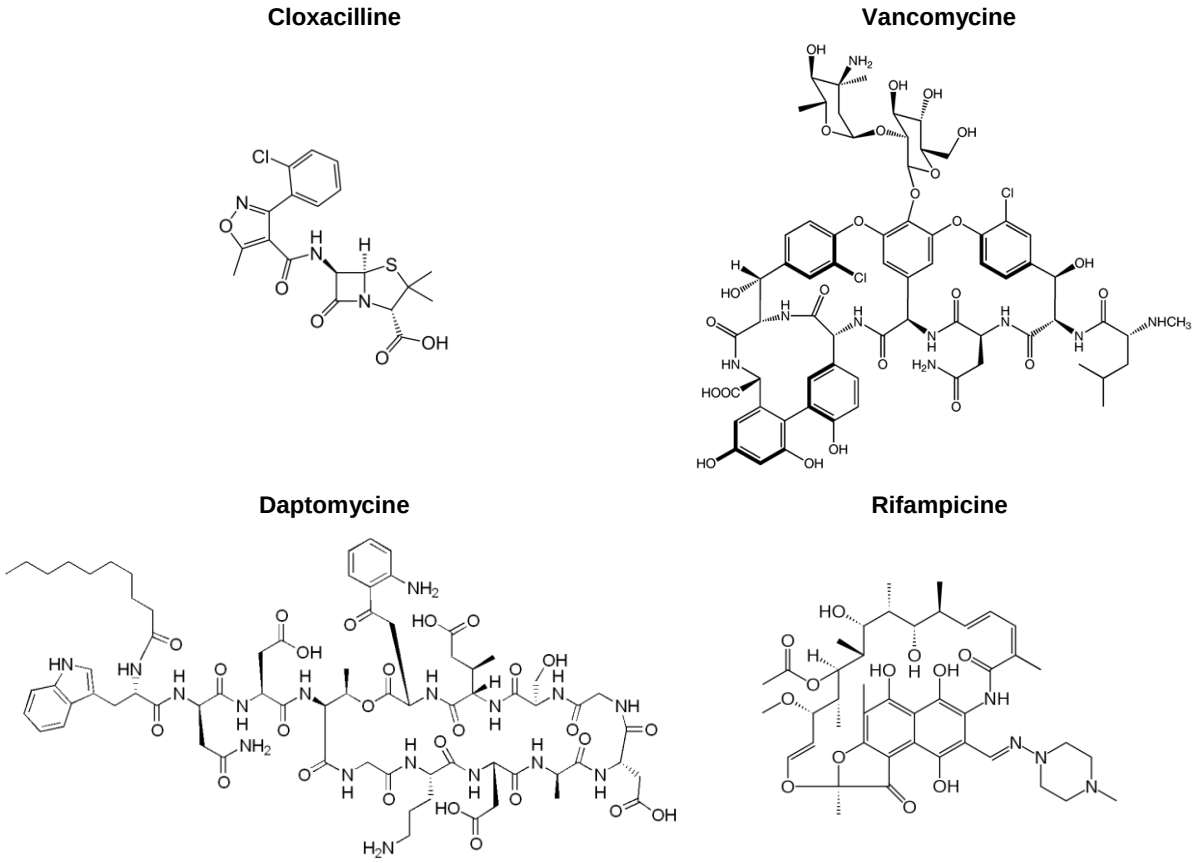

Figure 4. *Structures chimiques des antibiotiques étudiés.*

3.1. Article 2 : "New *in vitro* and *in vivo* models to evaluate antibiotic efficacy in *Staphylococcus aureus* prosthetic vascular graft infection"

Matthieu Revest, Cédric Jacqueline, Rym Boudjemaa, Jocelyne Caillon, Valérie Le Mabecque, Anne Bretéché, Karine Steenkeste, Pierre Tattevin, Gilles Potel, Christian Michelet, Marie-Pierre Fontaine-Aupart, David Boutoille

Journal of Antimicrobial Chemotherapy, 2016

J Antimicrob Chemother 2016; **71**: 1291–1299
doi:10.1093/jac/dkv496 Advance Access publication 6 February 2016

Journal of Antimicrobial Chemotherapy

New *in vitro* and *in vivo* models to evaluate antibiotic efficacy in *Staphylococcus aureus* prosthetic vascular graft infection

M. Revest[1–3]*, C. Jacqueline[1], R. Boudjemaa[4], J. Caillon[1], V. Le Mabecque[1], A. Breteche[1], K. Steenkeste[4], P. Tattevin[2,3], G. Potel[1], C. Michelet[2,3], M. P. Fontaine-Aupart[4] and D. Boutoille[1,5]

[1]*Université Nantes, Faculté Médecine EA3826 Nantes, France;* [2]*CHU Rennes Infectious Diseases and Intensive Care Unit, Pontchaillou Hospital, 35033 Rennes Cedex, France;* [3]*CIC Inserm 1414, Rennes 1 University, Pontchaillou Hospital, 35033 Rennes Cedex, France;* [4]*Institut des Sciences Moléculaires Orsay, CNRS, Université Paris-Sud, 91405 Orsay, France;* [5]*CHU Nantes, Infectious Diseases Unit, Hôtel Dieu, Nantes, France*

*Corresponding author. CHU Rennes Infectious Diseases and Intensive Care Unit, Pontchaillou Hospital, 35033 Rennes Cedex, France. Tel: +33-2-99-28-37-98; Fax: +33-2-99-28-94-64; E-mail: matthieu.revest@chu-rennes.fr

Received 17 September 2015; returned 1 October 2015; revised 14 December 2015; accepted 19 December 2015

Objective: Prosthetic vascular graft infection (PVGI) is an emerging disease, mostly caused by staphylococci, with limited data regarding efficacy of current antistaphylococcal agents. We aimed to assess the efficacy of different antibiotic regimens.

Methods: Six different strains of MSSA and MRSA were used. We compared results of minimal biofilm inhibitory and eradicating concentrations (MBICs and MBECs) obtained with a Calgary Biofilm Pin Lid Device (CBPD) with those yielded by an original Dacron®-related minimal inhibitory and eradicating concentration measure model. We then used a murine model of *Staphylococcus aureus* vascular prosthetic material infection to evaluate efficacy of different antibiotic regimens: vancomycin and daptomycin combined or not with rifampicin for MRSA and the same groups with cloxacillin and cloxacillin combined with rifampicin for MSSA.

Results: We demonstrated that classical measures of MBICs and MBECs obtained with a CPBD could overestimate the decrease in antibiotic susceptibility in material-related infections and that the nature of the support used might influence the measure of biofilm susceptibility, since results yielded by our Dacron®-related minimal eradicating assay were lower than those found with a plastic device. In our *in vivo* model, we showed that daptomycin was significantly more bactericidal than comparators for some strains of MRSA or MSSA but not for all. For the majority of strains, it was as efficient as comparators. The addition of rifampicin to daptomycin did not enhance daptomycin efficacy.

Conclusions: Despite the heterogeneity of results according to bacterial strains, these innovative models represent an option to better evaluate the *in vitro* efficacy of antibiotics on Dacron®-related biofilm *S. aureus* infections, and to screen different antibiotic regimens in a mouse model of PVGIs.

Introduction

More than 400000 vascular grafts are inserted annually in the USA[1] and ~50000 in France.[2] Prosthetic vascular graft infections (PVGIs) are among the most serious complications associated with these procedures,[1] with 30 day and 1 year mortality rates of 10%–25% and 50%, respectively.[3] *Staphylococcus aureus* is the main pathogen, and MRSA accounts for almost 50% of *S. aureus* PVGIs in North America.[4] Clinical data regarding the optimal antibiotic therapy for these infections are scarce, in the absence of any comparative clinical trial dealing with the treatment of PVGIs.[5] Hence, experimental data are needed to better identify the optimal antibiotic regimens for PVGIs.

Biofilm development on the vascular prosthesis plays a significant role in the difficulties encountered when treating PVGIs. Firstly, biofilm acts as a mechanical barrier against antibiotic penetration. Secondly, bacteria embedded in a mature biofilm enter into an altered metabolic state associated with a dramatic decrease in susceptibility to most antibiotics.[6,7] Many studies showed that minimal biofilm inhibitory concentrations (MBICs) and minimal biofilm eradicating concentrations (MBECs) of antibiotics are much higher than their respective MICs, and their MBCs as measured in planktonic bacteria.[8–10] However, most studies evaluated antibiotic efficacy on artificial materials not used in clinical practice, although the nature of the material may influence these results. In addition, although helpful,

in vitro data may fail to capture what happens *in vivo*. Animal models of PVGIs have mainly been used to evaluate techniques to prevent PVGIs,[11–14] but no animal model assessing the efficacy of antibiotics against infection of the Dacron® vascular prosthesis used in clinical daily practice has been described so far.

In this study, we investigated the activities of cloxacillin, vancomycin, daptomycin and rifampicin against different strains of MSSA and MRSA *in vitro*. Those activities were determined against planktonic bacteria (MIC and MBC) and adherent bacteria (MBIC and MBEC). To evaluate whether the nature of the support influences MBIC and MBEC results, two different techniques were used: a widely used modified version of the Calgary Biofilm Pin Lid Device (CBPD) and an original model of Dacron®-related biofilm. Then, cloxacillin, vancomycin and daptomycin, combined or not with rifampicin, were evaluated in a new mouse model of vascular prosthetic material infection, using the same strains of *S. aureus*.

Materials and methods

Bacterial strains

Six different strains of *S. aureus* were used for all experiments. For MSSA we used two clinical strains, hereafter named 171 and 176, isolated from patients with *S. aureus* bloodstream infections, and one strain from the American Type Culture Collection: ATCC 27217. For MRSA we used two strains, hereafter named BCB8 and 117, also isolated from blood cultures, and one ATCC strain: ATCC 33591. Bacteria were stored in a cryovial bead preservation system at −80°C.

Antimicrobial agents

Clinical forms of the following antibiotics were used: cloxacillin (Astellas Pharma, Levallois-Perret, France), stored in a 100 mg/mL stock solution; vancomycin (Sandoz, Levallois-Perret, France), stored in a 50 mg/mL stock solution; daptomycin (Novartis Pharma SAS, Rueil-Malmaison, France), stored in a 50 mg/mL stock solution; and rifampicin (Sanofi-Aventis, Paris, France), stored in a 60 mg/mL stock solution. All stock solutions were prepared in sterile, pyrogen-free 0.9% saline except for rifampicin, which was prepared in sterile water, and stored at −80°C before utilization.

In vitro experiments

All the following experiments were performed at least in duplicate, with all the staphylococcal strains evaluated. Biofilm formation was compared between polystyrene (CPBD) and Dacron® using confocal microscopy.

MICs and MBCs

The MIC and the MBC values for cloxacillin, vancomycin, daptomycin and rifampicin were determined by the broth macrodilution method in CAMHB, according to EUCAST. Media were supplemented with 50 mg/L Ca^{2+} for daptomycin.

MBICs and MBECs

A modified Calgary device was used as previously described.[8,15] Briefly, biofilm was formed by immersing pegs of a modified microtitre lid into wells of a flat-bottom 96-well microtitre plate. Each well was filled with 150 μL of a 3 McFarland *S. aureus* broth medium solution. After 24 h of incubation at 37°C, peg lids were rinsed three times in sterile water, placed onto flat-bottom microtitre plates containing 2-fold dilutions of antibiotic in 150 μL of CAMHB per well, and incubated for 24 h at 37°C. The MBIC was defined as the minimal concentration of antibiotic inhibiting bacterial growth, as determined by reading the turbidity of the medium at 650 nm. Pegs with no bacterial growth were again rinsed three times with sterile water and sonicated (Aquasonic sonicator, 35 kHz for 5 min) followed by vortexing for 30 s to remove biofilm from the support. A new cover plate was added and this new device was cultured for 24 h at 37°C in CAMHB. The MBEC was defined as the minimal concentration of antibiotic where no bacterial growth was documented.

Dacron®-related minimal biofilm inhibitory concentrations (dMBICs) and Dacron®-related minimal biofilm eradicating concentrations (dMBECs)

Commercially available woven Dacron® grafts (Cardial™, Bard, Saint-Etienne, France) were cut into 1 cm×1 cm squares and sterilized. To cover the biomaterial with proteins and thus to facilitate the bacterial graft, these Dacron® sheets were incubated at 37°C under sterile conditions with horse serum for 24 h. They were rinsed three times with sterile water to remove the horse serum and then incubated for 24 h at 37°C with 1 mL per patch of Mueller–Hinton broth (MHB) containing 10^8 cfu/mL of *S. aureus*. Again, they were rinsed three times in sterile water to eliminate planktonic bacteria, dried with a sterile gauze compress and plunged into tubes filled with CAMHB containing no antibiotic (control groups) or serial antibiotic dilutions, and incubated for 24 h at 37°C. dMBIC for each antibiotic and strain couple was defined as the antibiotic concentration of the first tube with no visible bacterial growth. Then, Dacron® patches with no bacterial growth were removed from their tubes, rinsed three times in sterile water, dried with a sterile gauze compress and plunged again into MHB. Sonication (35 kHz for 5 min) was performed followed by vortexing for 30 s. MHB containing the Dacron® sheets was incubated for 24 h at 37°C. dMBEC was defined as the antibiotic concentration of the first tube with no bacterial growth.

Confocal microscopy evaluating biofilm formation depending on the support

Twenty-four hour biofilms prepared as previously described were observed using a Leica TCS SP5 confocal laser-scanning microscope (Leica Microsystems, France). Bacteria were stained with 2.5 μM Syto9® (Invitrogen), which is able to penetrate all bacteria, and 5 μL of 1 mg/mL propidium iodide (PI, Invitrogen), which can only penetrate dead cells. Syto9® and PI were excited at 488 and 543 nm, respectively, and their fluorescence emissions were collected between 500 and 600 nm for Syto9® and between 640 and 750 nm for PI. Images were acquired using a ×63 oil immersion objective with a numerical aperture of 1.4. The size of the confocal images was 512×512 pixels (82×82 μm^2), recorded with a *z*-step of 1 μm and a ×3 zoom. For each biofilm, at least four different regions were analysed.

In vivo experiments

All experiments were approved by the French Ministry of Research and the regional animal ethics committee and animals were cared for in line with national guidelines.

Animals

Four-week-old female Swiss mice (RjOrl/SWISS, Janvier Laboratory, St Berthevin, France) weighing ∼20 g were maintained on a 12 h light/dark cycle with free access to food and water. Eight to 15 animals per group were used for analysis.

Biomaterial

Sterile 1 cm^2 squares of commercially used Dacron® were incubated with sterile serum from healthy female Swiss mice for 24 h at 37°C. Then, they were implanted into mice.

Surgical procedures

Mice were anaesthetized with ketamine (70 mg/kg) and xylazine (10 mg/kg) through intraperitoneal (ip) injection. Under sterile conditions, a 10 mm horizontal incision in the centre of the back was made to create a subcutaneous pocket. A sterile Dacron® patch was implanted into this pocket. Skin was closed with sutures (Vicryl 5/0). Two days after Dacron® implantation, a saline solution (0.2 mL) containing 10^7 cfu of *S. aureus* was transcutaneously inoculated onto the graft surface. During inoculation, mice were anaesthetized with isoflurane (0.8 L/min, 3%).

Antimicrobial treatment regimens

All the antibiotics used were administered at dose regimens resulting in serum concentrations similar to those obtained in humans. Mice were randomized into 14 groups. For MRSA the groups were as follows: no treatment (controls); vancomycin group [subcutaneous (sc) injection, 110 mg/kg/12 h];[16] daptomycin group (50 mg/kg/24 h, sc);[17] rifampicin group (30 mg/kg/12 h, ip);[18] vancomycin/rifampicin group; and daptomycin/rifampicin group. For MSSA we used the same groups plus a cloxacillin group (200 mg/kg/12 h, sc)[19] and a cloxacillin/rifampicin group. Vancomycin and cloxacillin solutions were prepared in sterile 0.9% saline, daptomycin in sterile Ringer–lactate solution and rifampicin in sterile 5% glucose serum. Mice were treated for 48 h and then euthanized following international guidelines.

Bacterial counts

Dacron® patches were removed under aseptic conditions, homogenized in 0.5 mL of saline buffer and vortexed for 30 s. Fifty microlitres of this solution was used for quantitative bacterial cultures. The Dacron® patches were then sonicated (35 kHz for 5 min) and 50 μL of the supernatant

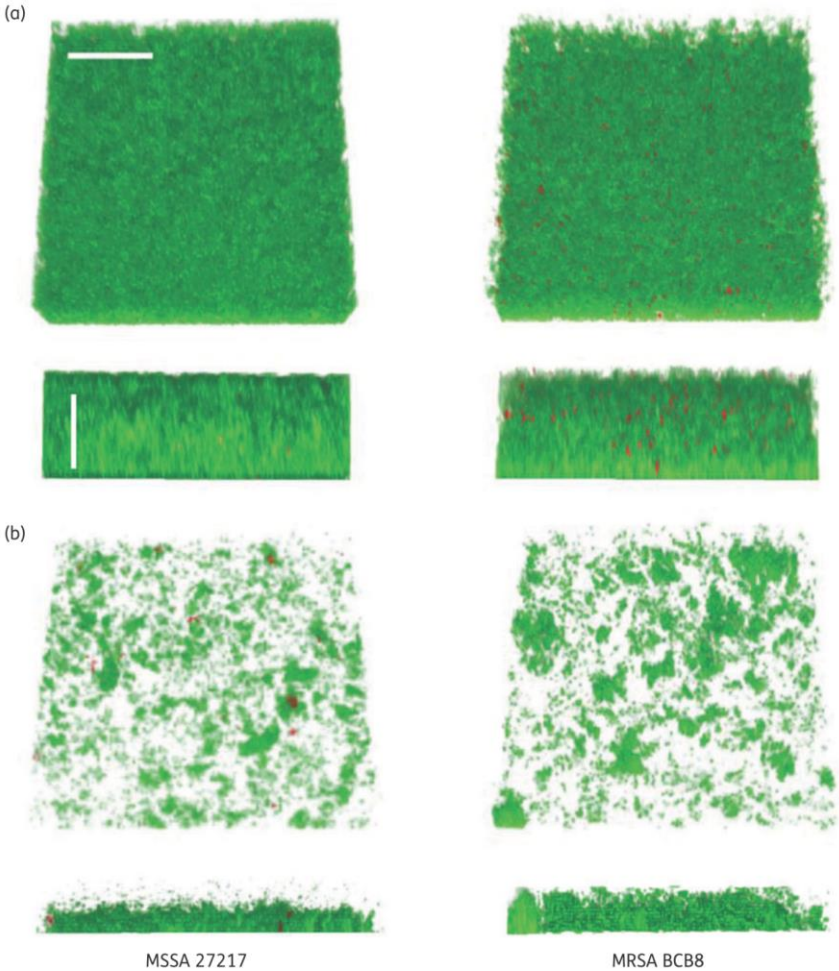

Figure 1. Visualization of MSSA and MRSA 24 h biofilms on polystyrene (a) and on Dacron (b) using section views to observe biofilm thickness. All bacteria were stained green with Syto9®. Acquisition was performed on the whole biofilm thickness with an axial displacement of 1 μm. Image dimension is 82×82 μm. Scale bars correspond to 20 μm. Only biofilms for MSSA 27217 and MRSA BCB8 are represented since they were representative of all biofilms visualized for other strains. This figure appears in colour in the online version of *JAC* and in black and white in the print version of *JAC*.

was inoculated for cultures on tryptic soy and Chapman agar plates, incubated at 37°C. The bacterial count was performed after 48 h of incubation. Spleens were also homogenized in 1 mL of saline buffer for bacterial cultures. Animals for which the spleen bacterial cultures were positive were considered to be bacteraemic. When there was a positive bacterial culture, *in vitro* drug susceptibility testing was performed using the Vitek 2 automated identification and susceptibility testing system with the Advanced Expert System (bioMérieux, Lyon, France), and results were interpreted according to the EUCAST criteria.

Statistical analysis

GraphPad Prism software (version 6.0; GraphPad Software, San Diego, CA, USA) was used. Normally distributed data were analysed using analysis of variance to compare effects between the different groups, followed by Bonferroni's test to compare the groups two by two. $P<0.05$ was considered to be statistically significant.

Results

In vitro efficacy of antibiotics in biofilms is influenced by the nature of the support

Confocal microscopy confirmed biofilm formation for all strains on polystyrene (Figure 1a) or Dacron® (Figure 1b). However, biofilms formed on Dacron® sheets were less dense and thick compared with those found with the modified CPBD.

MBIC and MBEC measures demonstrated a dramatic reduction in bacterial susceptibilities to all antibiotics tested, for all strains. dMBICs and dMBECs were also higher than MICs and MBCs for all strains tested. However, decreases in susceptibilities were less pronounced on Dacron® than on polystyrene, with the modified Calgary device (Table 1); for all conditions evaluated, MBECs were much higher than dMBECs.

Daptomycin efficacy on MRSA vascular prosthetic material infection is superior to comparators for one strain but not for others

There was no difference between bacterial cultures before and after Dacron® sonication. For MRSA BCB8, daptomycin was significantly more bactericidal than vancomycin, with a dramatic reduction of bacterial load after 48 h of treatment (-5.85 $\log_{10}$ cfu/cm^2 compared with the control group, $P<0.001$; -3.47 $\log_{10}$ cfu/cm^2 compared with vancomycin, $P<0.001$), whether or not it was combined with rifampicin. The bactericidal activity of vancomycin was significantly improved when combined with rifampicin, although this combination remained less bactericidal than daptomycin alone against this isolate ($P<0.001$). Rifampicin monotherapy demonstrated good efficacy (-4.5 $\log_{10}$ cfu/cm^2 versus control group, $P<0.001$) (Figure 2). No emergence of antibiotic resistance was observed on bacteria recovered from positive cultures.

For MRSA 117 and 33591, results were strikingly different. For both strains, there were no significant differences between daptomycin, vancomycin and rifampicin monotherapies. Combined therapies demonstrated no significant benefit compared with monotherapies (Figure 2). Although not statistically significant, there was a trend towards higher efficacy of vancomycin/rifampicin compared with daptomycin/rifampicin. Once again, no antibiotic resistance was documented after treatment for both strains.

Table 1. *In vitro* drug susceptibility testing for the bacterial strains used in this study (mg/L)

			Classical methods		Biofilm on Dacron		Biofilm on polystyrene	
Bacterial strains		Antibiotic	MIC	MBC	dMBIC	dMBEC	MBIC	MBEC
MRSA	BCB8	vancomycin	1	1	1	>32	1	>256
		daptomycin	0.125	0.125	0.5	8	1	>256
		rifampicin	<0.06	<0.06	<0.125	>1	0.015	>8
	117	vancomycin	1	4	4	16	1	>256
		daptomycin	1	2	2	64	1	>256
		rifampicin	0.015	0.03	0.015	>0.5	0.015	>8
	33591	vancomycin	1	2	4	16	2	>256
		daptomycin	0.25	0.5	2	>16	1	>256
		rifampicin	0.0075	0.015	0.015	0.5	0.0075	>8
MSSA	171	cloxacillin	0.25	0.5	2	>32	0,25	>256
		vancomycin	1	1	8	32	4	>256
		daptomycin	0.5	0.5	4	>32	4	>256
		rifampicin	0.015	0.03	0.125	>0.25	0.015	>8
	176	cloxacillin	0.5	0.5	2	>32	0.5	>256
		vancomycin	1	1	2	16	1	>256
		daptomycin	0.5	0.5	2	>64	0.5	>256
		rifampicin	0.015	0.03	0.125	>0.5	0.015	>8
	27217	cloxacillin	0.5	0.5	1	16	0.25	>256
		vancomycin	1	1	8	>32	8	>256
		daptomycin	0.25	0.25	1	>8	2	>256
		rifampicin	<0.06	0.125	2	2	0.03	>8

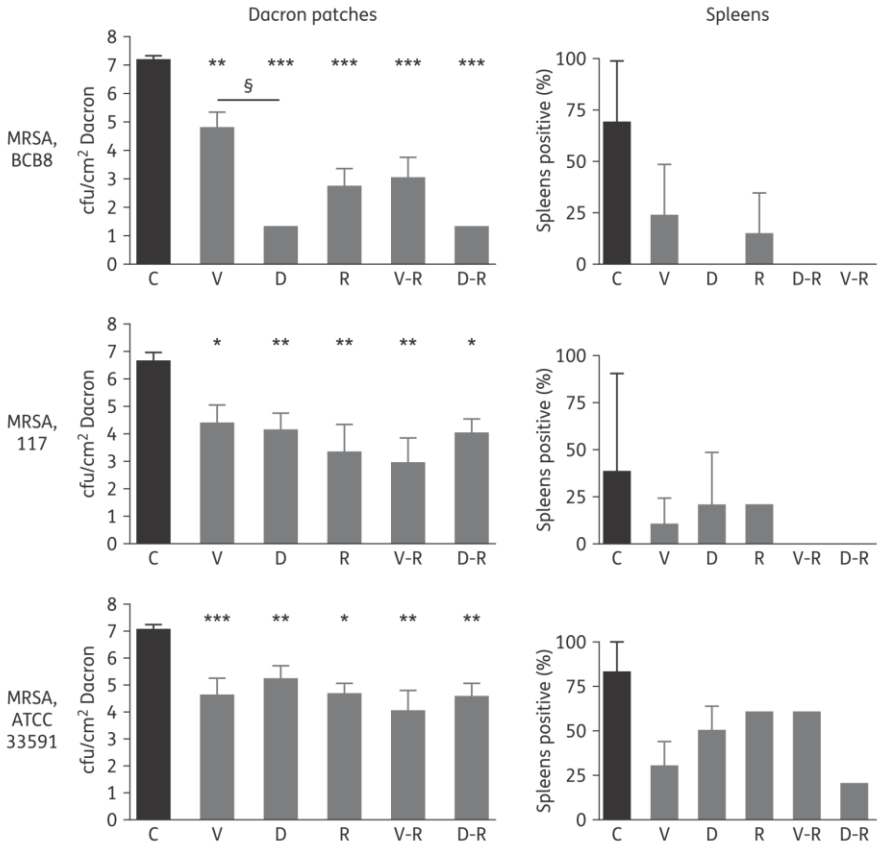

Figure 2. Bacterial counts on Dacron patches and spleens after 48 h of treatment for MRSA infection. C, controls; V, vancomycin; D, daptomycin; R, rifampicin; V-R: vancomycin/rifampicin; D-R, daptomycin/rifampicin. Asterisks represent results of comparisons between control groups and each therapeutic group (*$P<0.05$; **$P<0.01$; ***$P<0.001$); § $P<0.001$, comparison between vancomycin and daptomycin for MRSA BCB8. Number of mice per antibiotic regimen: strain BCB8, 12; strain 117, 10; and strain 33591, 14.

Spleen cultures were more frequently positive for controls than for therapeutic groups. There was no significant difference between therapeutic groups.

Daptomycin efficacy against MSSA vascular prosthetic material infection also depends on bacterial strains

As for MRSA, bacterial cultures after sonication did not differ from those without sonication. Daptomycin was significantly more bactericidal than cloxacillin for MSSA 176 (-1.27 $\log_{10}$ cfu/cm^2, 95% CI 0.32–2.22, $P<0.05$), but not for MSSA 27217 and MSSA 171 (Figure 3). A trend towards better efficacy of daptomycin versus vancomycin against MSSA 176 (-1.1 $\log_{10}$ cfu/cm^2, 95% CI -0.16 to 2.37) was observed. Daptomycin and cloxacillin demonstrated higher efficacy than vancomycin against MSSA 171 [-2.72 $\log_{10}$ cfu/cm^2 (95% CI 0.75–3.79) and -2.1 $\log_{10}$ cfu/cm^2 (95% CI 0.55–3.65), respectively; $P<0.001$ for both]. Combination of cloxacillin, vancomycin or daptomycin with rifampicin was more bactericidal than monotherapies for the 27217 strain. This effect was less pronounced for strains 171 and 176. Surprisingly, the combination of daptomycin with rifampicin was less efficient than cloxacillin/rifampicin (-1.76 $\log_{10}$ cfu/cm^2, 95% CI 0.61–2.9, $P<0.01$) or vancomycin/rifampicin (-2.17 $\log_{10}$ cfu/cm^2, 95% CI 1.1–3.25, $P<0.001$) for MSSA 27217. No emergence of antibiotic resistance was documented for any of the conditions tested.

Spleen cultures were less often positive for MSSA than for MRSA, and no significant difference between the different conditions was noticed.

Discussion

The main findings of these experimental studies are: (i) the results of *in vitro* biofilm antibiotic susceptibility assays may vary according to the nature of the support used; (ii) our mouse model of *S. aureus* vascular graft infection allowed us to test a large number of bacterial strains and antibiotic regimens and could pave the way towards a better understanding of antibiotic efficacy in PVGIs; (iii) although more efficient than comparators for some bacterial strains, daptomycin was most of the time not superior

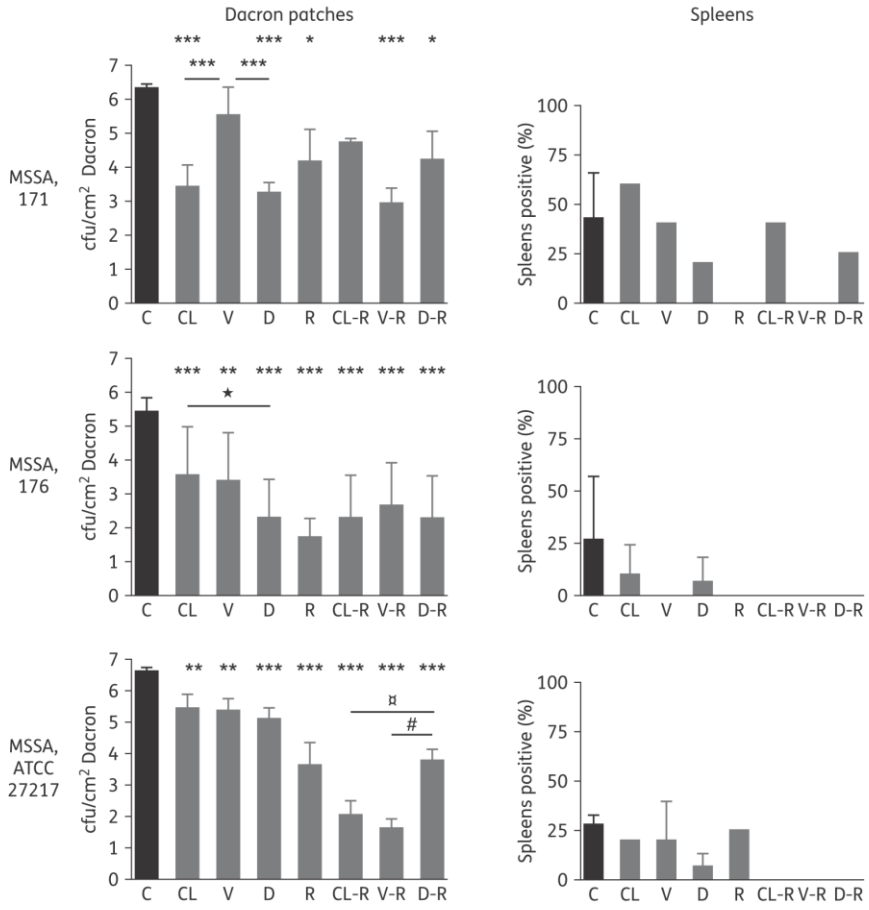

Figure 3. Bacterial count on Dacron sheets and spleen after 48 h of treatment for MRSA infection. CL, cloxacillin; C, controls; V, vancomycin; D, daptomycin; R, rifampicin; V-R, vancomycin/rifampicin; D-R, daptomycin/rifampicin. Asterisks represent results of comparisons between control groups and each therapeutic group (*$P<0.05$; ***$P<0.001$); ★ $P<0.05$, comparison between controls and daptomycin for MSSA 176; ¤ $P<0.01$, comparison between cloxacillin/rifampicin and daptomycin/rifampicin for MSSA 27217; # $P<0.001$, comparison between vancomycin/rifampicin and daptomycin/rifampicin for MSSA 27217. Number of mice per antibiotic regimen: strain 171, 8–12; strain 176, 10–15; strain 27217, 12–15.

to vancomycin or cloxacillin; and (iv) combination with rifampicin did not enhance the bactericidal effect of daptomycin in this model.

Decreased antibiotic efficacy in material-related infections has been highlighted by many studies using biofilm susceptibility tests, including the Calgary device.[8,15,20,21] Although not recommended routinely,[22] these techniques illustrate that MBICs and MBECs are much higher than MICs and MBCs, with limited prospects for clinical cure since these concentrations are not achievable in humans.[9,21] However, these techniques use polystyrene devices, which are significantly different from the biomaterials used for vascular prostheses. Therefore, results obtained with these procedures may not be relevant for PVGIs. We developed a model to evaluate specific MBICs and MBECs on Dacron®, referred as dMBICs and dMBECs, to better assess the decrease in antibiotic efficacy on bacteria embedded inside the biofilm on vascular prostheses. In this model, while dMBICs and MBICs were comparable, dMBECs were lower than MBECs, although higher than MBCs. For instance, dMBICs and dMBECs of rifampicin were in the range of concentrations achievable in humans for most bacterial strains tested. Biofilm developed on plastic was more dense, and thicker, than that found on Dacron® (Figure 1), and adhesion of bacteria to Dacron® appeared weaker, explaining why antibiotics are less efficient in the polystyrene model. Our results demonstrated that classical techniques used to measure MBICs and MBECs could overestimate the decrease in antibiotic efficacy in the particular context of PVGIs, and that our model, specific to PVGIs, could yield more relevant findings. They do not question the recommendation to remove all infected material whenever possible for PVGI.[23,24] However, our data suggest that antibiotics alone may be a reasonable therapeutic option in selected cases when surgery would be associated with a high probability of severe adverse outcomes.[25–27]

Animal models constitute a critical step in the evaluation of antibiotics for PVGIs. A rat model of PVGI using a Dacron® patch implanted in a dorsal subcutaneous pouch evaluated different prophylactic procedures.[13,28–30] Other models mimicked prosthetic joint infections using a Teflon® cage implanted in a dorsal subcutaneous pouch in guinea-pigs[31–35] or rats.[10] To our knowledge, no specific model has evaluated the curative treatment of PVGI so far. We combined these two approaches to evaluate different antibiotic regimens in a PVGI mouse model. For technical reasons, it was impossible to implant our Dacron® along the vascular system, and this represents one weakness of our work. Some authors have described rabbit,[36] pig[14] or dog[11] models of aortic graft infections, but these models do not allow the use of a large number of animals, and consequently are not appropriate for the screening of antibiotic strategies in different bacterial strains. Moreover, in a clinical setting, most PVGIs arise from the wound or from an adjacent infectious focus, and not through a haematogenous route.[37] Therefore, the infection process usually starts along the external part of the vascular prosthesis, not the endoluminal layer. Our model reproduces this pathway.

Although all antibiotics tested in this model demonstrated efficacy when compared with controls, antibiotic efficacy varied according to bacterial strains. For instance, daptomycin was more bactericidal than vancomycin for MRSA BCB8 and MSSA 171, and more bactericidal than cloxacillin for MSSA 176, but was not superior to other antibiotics for other strains. For MRSA BCB8, dMBIC and dMBEC were lower for daptomycin than for vancomycin and this could partially explain the differences noticed. One other explanation could be the different capabilities of antibiotics to penetrate the biofilm *in vivo*, although this would not explain the striking differences observed between strains.[38] Daptomycin has already demonstrated better efficacy against MRSA than vancomycin *in vitro*[39,40] and in animal models.[40,41] This higher efficacy is thought to be linked to better biofilm penetration for daptomycin than for vancomycin[42] and better bactericidal activity against bacteria in stationary phase.[40] However, some authors did not find any difference between daptomycin and vancomycin efficacy.[43,44] Our results highlight a possible differential activity of daptomycin according to bacterial strain, which may explain the discrepancies between previous studies.

Rifampicin has demonstrated its efficacy for the treatment of material-related staphylococcal infection[45] and its use in combination is widely recommended. In the present study, we did not find any improvement of therapeutic efficacy when rifampicin was added to daptomycin for MRSA, but rifampicin enhanced the activity of vancomycin. The combination of daptomycin and rifampicin increased the bactericidal activity of daptomycin against MSSA 27217 only moderately, while the addition of rifampicin to vancomycin or cloxacillin strongly enhanced their bactericidal effect on this strain. These results are in contrast with those of Sakoulas *et al.*,[46] who demonstrated in a rat model of MRSA endocarditis a synergistic effect of daptomycin plus rifampicin. Saleh-Mghir *et al.*[47] found similar results in a rabbit model of prosthetic joint infection. However, an *in vitro* pharmacodynamic model evaluating daptomycin and rifampicin against different MRSA strains found variable activity of this association (i.e. increased bactericidal activity with combinations in some, but not all, strains tested).[48] Likewise, the addition of rifampicin to daptomycin did not enhance the bactericidal activity of daptomycin in a rabbit model of MRSA endocarditis.[49] Some studies suggested that daptomycin/fosfomycin or daptomycin/cloxacillin may be more synergistic.[10,50]

Our model could not capture the utility of combinations to prevent the emergence of resistance. Indeed, even when bacterial load was high after treatment, we did not document any bacterial resistance. This was unexpected, since emergence of resistance under treatment is one of the main caveats with rifampicin[41] or daptomycin monotherapies.[41,47] An experimental study evaluating the *in vivo* fitness of rifampicin-resistant *S. aureus* mutants in a mouse biofilm infection model found that rifampicin-resistant strains appeared after 3–9 days of treatment.[18] This delay may explain why our 48 h treatment regimens were not associated with emergence of resistance. Thus, although no resistance was documented in our model, clinical data indicate that rifampicin must be used in combination for PVGI, as for any other infection.

In conclusion, we found that biofilm formation and bacterial adhesion are weaker on Dacron® than on polystyrene devices, resulting in a less pronounced biofilm-related decrease in antibiotic efficacy in the particular setting of PVGIs. We implemented an innovative mouse model of PVGI allowing the evaluation of a large number of antibiotic regimens. In this model, we demonstrated that daptomycin was more efficient than comparators for some strains but not all, and that the addition of rifampicin did not enhance daptomycin efficacy. However, due to the variability of findings according to bacterial strains, we were not able to determine the best antibiotic regimen for PVGIs.

Acknowledgements

We thank the Collège des enseignants des Maladies Infectieuses et Tropicales (CMIT) and the Société Française de Pathologie Infectieuse de Langue Française (SPILF) for their support. We also thank Prof. Erwan Flecher, who kindly provided the Dacron®.

Funding

This work was supported by a grant from Novartis and a grant from the Collège des enseignants des Maladies Infectieuses et Tropicales (CMIT). Sponsors had no role in the design and the realization of this work, and had no access to results until this work was submitted.

Transparency declarations

M. R. has been supported by MSD and Pfizer Laboratories to attend international conferences. The other authors have nothing to declare.

References

1 Darouiche RO. Treatment of infections associated with surgical implants. *N Engl J Med* 2004; **350**: 1422–9.

2 HAS. *Implants vasculaires. Révision de Catégories Homogènes de Dispositifs Médicaux*. Saint-Denis La Plaine: Haute Autorité de Santé, 2013.

3 FitzGerald SF, Kelly C, Humphreys H. Diagnosis and treatment of prosthetic aortic graft infections: confusion and inconsistency in the absence of evidence or consensus. *J Antimicrob Chemother* 2005; **56**: 996–9.

4 Jansen KU, Girgenti DQ, Scully IL *et al*. Vaccine review: "*Staphylococcus aureus* vaccines: problems and prospects". *Vaccine* 2013; **31**: 2723–30.

5 Revest M, Camou F, Senneville E *et al*. Medical treatment of prosthetic vascular graft infections: review of the literature and proposals of a Working Group. *Int J Antimicrob Agents* 2015; **46**: 254–65.

6 Stewart PS, Franklin MJ. Physiological heterogeneity in biofilms. *Nat Rev Microbiol* 2008; **6**: 199–210.

7 Richards JJ, Melander C. Controlling bacterial biofilms. *Chembiochem* 2009; **10**: 2287–94.

8 Ceri H, Olson ME, Stremick C *et al*. The Calgary Biofilm Device: new technology for rapid determination of antibiotic susceptibilities of bacterial biofilms. *J Clin Microbiol* 1999; **37**: 1771–6.

9 LaPlante KL, Mermel LA. *In vitro* activities of telavancin and vancomycin against biofilm-producing *Staphylococcus aureus*, *S. epidermidis*, and *Enterococcus faecalis* strains. *Antimicrob Agents Chemother* 2009; **53**: 3166–9.

10 Garrigos C, Murillo O, Lora-Tamayo J *et al*. Fosfomycin-daptomycin and other fosfomycin combinations as alternative therapies in experimental foreign-body infection by methicillin-resistant *Staphylococcus aureus*. *Antimicrob Agents Chemother* 2013; **57**: 606–10.

11 Javerliat I, Goeau-Brissonniere O, Sivadon-Tardy V *et al*. Prevention of *Staphylococcus aureus* graft infection by a new gelatin-sealed vascular graft prebonded with antibiotics. *J Vasc Surg* 2007; **46**: 1026–31.

12 Hirose K, Marui A, Arai Y *et al*. Sustained-release vancomycin sheet may help to prevent prosthetic graft methicillin-resistant *Staphylococcus aureus* infection. *J Vasc Surg* 2006; **44**: 377–82.

13 Cirioni O, Mocchegiani F, Ghiselli R *et al*. Daptomycin and rifampin alone and in combination prevent vascular graft biofilm formation and emergence of antibiotic resistance in a subcutaneous rat pouch model of staphylococcal infection. *Eur J Vasc Endovasc Surg* 2010; **40**: 817–22.

14 Gao H, Sandermann J, Prag J *et al*. Rifampicin-soaked silver polyester versus expanded polytetrafluoro-ethylene grafts for *in situ* replacement of infected grafts in a porcine randomised controlled trial. *Eur J Vasc Endovasc Surg* 2012; **43**: 582–7.

15 Moskowitz SM, Foster JM, Emerson J *et al*. Clinically feasible biofilm susceptibility assay for isolates of *Pseudomonas aeruginosa* from patients with cystic fibrosis. *J Clin Microbiol* 2004; **42**: 1915–22.

16 Crandon JL, Kuti JL, Nicolau DP. Comparative efficacies of human simulated exposures of telavancin and vancomycin against methicillin-resistant *Staphylococcus aureus* with a range of vancomycin MICs in a murine pneumonia model. *Antimicrob Agents Chemother* 2010; **54**: 5115–9.

17 Dandekar PK, Tessier PR, Williams P *et al*. Pharmacodynamic profile of daptomycin against *Enterococcus* species and methicillin-resistant *Staphylococcus aureus* in a murine thigh infection model. *J Antimicrob Chemother* 2003; **52**: 405–11.

18 Yu J, Wu J, Francis KP *et al*. Monitoring *in vivo* fitness of rifampicin-resistant *Staphylococcus aureus* mutants in a mouse biofilm infection model. *J Antimicrob Chemother* 2005; **55**: 528–34.

19 Domenech A, Ribes S, Cabellos C *et al*. Experimental study on the efficacy of combinations of glycopeptides and β-lactams against *Staphylococcus aureus* with reduced susceptibility to glycopeptides. *J Antimicrob Chemother* 2005; **56**: 709–16.

20 Hengzhuang W, Wu H, Ciofu O *et al*. *In vivo* pharmacokinetics/pharmacodynamics of colistin and imipenem in *Pseudomonas aeruginosa* biofilm infection. *Antimicrob Agents Chemother* 2012; **56**: 2683–90.

21 Abbanat D, Shang W, Amsler K *et al*. Evaluation of the in vitro activities of ceftobiprole and comparators in staphylococcal colony or microtitre plate biofilm assays. *Int J Antimicrob Agents* 2014; **43**: 32–9.

22 Hoiby N, Bjarnsholt T, Moser C *et al*. ESCMID guideline for the diagnosis and treatment of biofilm infections 2014. *Clin Microbiol Infect* 2015; **21** Suppl 1: S1–S25.

23 Lyons OT, Patel AS, Saha P *et al*. A 14-year experience with aortic endograft infection: management and results. *Eur J Vasc Endovasc Surg* 2013; **46**: 306–13.

24 Tong SY, Davis JS, Eichenberger E *et al*. *Staphylococcus aureus* infections: epidemiology, pathophysiology, clinical manifestations, and management. *Clin Microbiol Rev* 2015; **28**: 603–61.

25 Maze MJ, Laws P, Buckenham T *et al*. Outcomes of infected abdominal aortic grafts managed with antimicrobial therapy and graft retention in an unselected cohort. *Eur J Vasc Endovasc Surg* 2013; **45**: 373–80.

26 Erb S, Sidler JA, Elzi L *et al*. Surgical and antimicrobial treatment of prosthetic vascular graft infections at different surgical sites: a retrospective study of treatment outcomes. *PLoS One* 2014; **9**: e112947.

27 Legout L, Sarraz-Bournet B, D'Elia PV *et al*. Characteristics and prognosis in patients with prosthetic vascular graft infection: a prospective observational cohort study. *Clin Microbiol Infect* 2012; **18**: 352–8.

28 Giacometti A, Cirioni O, Ghiselli R *et al*. Temporin A soaking in combination with intraperitoneal linezolid prevents vascular graft infection in a subcutaneous rat pouch model of infection with *Staphylococcus epidermidis* with intermediate resistance to glycopeptides. *Antimicrob Agents Chemother* 2004; **48**: 3162–4.

29 Turgut H, Sacar S, Kaleli I *et al*. Systemic and local antibiotic prophylaxis in the prevention of *Staphylococcus epidermidis* graft infection. *BMC Infect Dis* 2005; **5**: 91.

30 Atahan E, Gul M, Ergun Y *et al*. Vascular graft infection by *Staphylococcus aureus*: efficacy of cefazolin, teicoplanin and vancomycin prophylaxis protocols in a rat model. *Eur J Vasc Endovasc Surg* 2007; **34**: 182–7.

31 Oliva A, Furustrand Tafin U, Maiolo EM *et al*. Activities of fosfomycin and rifampin on planktonic and adherent *Enterococcus faecalis* strains in an experimental foreign-body infection model. *Antimicrob Agents Chemother* 2014; **58**: 1284–93.

32 Furustrand Tafin U, Majic I, Zalila Belkhodja C *et al*. Gentamicin improves the activities of daptomycin and vancomycin against *Enterococcus faecalis in vitro* and in an experimental foreign-body infection model. *Antimicrob Agents Chemother* 2011; **55**: 4821–7.

33 Furustrand Tafin U, Corvec S, Betrisey B *et al*. Role of rifampin against *Propionibacterium acnes* biofilm in vitro and in an experimental foreign-body infection model. *Antimicrob Agents Chemother* 2012; **56**: 1885–91.

34 Zimmerli W, Waldvogel FA, Vaudaux P *et al*. Pathogenesis of foreign body infection: description and characteristics of an animal model. *J Infect Dis* 1982; **146**: 487–97.

35 Schwank S, Rajacic Z, Zimmerli W *et al*. Impact of bacterial biofilm formation on *in vitro* and *in vivo* activities of antibiotics. *Antimicrob Agents Chemother* 1998; **42**: 895–8.

36 Shimabukuro K, Hirose H, Mori Y *et al*. Local treatment of Dacron patch graft infected with biofilm-producing *Staphylococcus epidermidis* using antibiotic-releasing porous apatite ceramic: an experimental study in the rabbit. *J Vasc Surg* 2004; **39**: 1361.

37 Jones L, Braithwaite BD, Davies B *et al*. Mechanism of late prosthetic vascular graft infection. *Cardiovasc Surg* 1997; **5**: 486–9.

38 Boudjemaa R, Briandet R, Fontaine-Aupart M *et al*. Diffusion, bioavailability and reactivity of antibiotics against *Staphylococcus aureus* biofilms: a new approach by dynamic fluorescence imaging. In: *Abstracts of the Fifty-fourth Interscience Conference on Antimicrobial Agents and Chemotherapy, Washington, DC, 2014*. Abstract C-1415. American Society for Microbiology, Washington, DC, USA.

39 Edmiston CE Jr, Goheen MP, Seabrook GR *et al*. Impact of selective antimicrobial agents on staphylococcal adherence to biomedical devices. *Am J Surg* 2006; **192**: 344–54.

40 Murillo O, Garrigos C, Pachon ME *et al*. Efficacy of high doses of daptomycin versus alternative therapies against experimental foreign-body

infection by methicillin-resistant *Staphylococcus aureus*. *Antimicrob Agents Chemother* 2009; **53**: 4252–7.

41 Garrigos C, Murillo O, Euba G *et al*. Efficacy of usual and high doses of daptomycin in combination with rifampin versus alternative therapies in experimental foreign-body infection by methicillin-resistant *Staphylococcus aureus*. *Antimicrob Agents Chemother* 2010; **54**: 5251–6.

42 Stewart PS, Davison WM, Steenbergen JN. Daptomycin rapidly penetrates a *Staphylococcus epidermidis* biofilm. *Antimicrob Agents Chemother* 2009; **53**: 3505–7.

43 Smith K, Perez A, Ramage G *et al*. Comparison of biofilm-associated cell survival following *in vitro* exposure of meticillin-resistant *Staphylococcus aureus* biofilms to the antibiotics clindamycin, daptomycin, linezolid, tigecycline and vancomycin. *Int J Antimicrob Agents* 2009; **33**: 374–8.

44 Lefebvre M, Jacqueline C, Amador G *et al*. Efficacy of daptomycin combined with rifampicin for the treatment of experimental meticillin-resistant *Staphylococcus aureus* (MRSA) acute osteomyelitis. *Int J Antimicrob Agents* 2010; **36**: 542–4.

45 Senneville E, Joulie D, Legout L *et al*. Outcome and predictors of treatment failure in total hip/knee prosthetic joint infections due to *Staphylococcus aureus*. *Clin Infect Dis* 2011; **53**: 334–40.

46 Sakoulas G, Eliopoulos GM, Alder J *et al*. Efficacy of daptomycin in experimental endocarditis due to methicillin-resistant *Staphylococcus aureus*. *Antimicrob Agents Chemother* 2003; **47**: 1714–8.

47 Saleh-Mghir A, Muller-Serieys C, Dinh A *et al*. Adjunctive rifampin is crucial to optimizing daptomycin efficacy against rabbit prosthetic joint infection due to methicillin-resistant *Staphylococcus aureus*. *Antimicrob Agents Chemother* 2011; **55**: 4589–93.

48 Rose WE, Leonard SN, Rybak MJ. Evaluation of daptomycin pharmacodynamics and resistance at various dosage regimens against *Staphylococcus aureus* isolates with reduced susceptibilities to daptomycin in an *in vitro* pharmacodynamic model with simulated endocardial vegetations. *Antimicrob Agents Chemother* 2008; **52**: 3061–7.

49 Miro JM, Garcia-de-la-Maria C, Armero Y *et al*. Addition of gentamicin or rifampin does not enhance the effectiveness of daptomycin in treatment of experimental endocarditis due to methicillin-resistant *Staphylococcus aureus*. *Antimicrob Agents Chemother* 2009; **53**: 4172–7.

50 Garrigos C, Murillo O, Lora-Tamayo J *et al*. Efficacy of daptomycin-cloxacillin combination in experimental foreign-body infection due to methicillin-resistant *Staphylococcus aureus*. *Antimicrob Agents Chemother* 2012; **56**: 3806–11.

3.2. Article 3 : "Intramacrophagic *Staphylococcus aureus* in prosthetic vascular graft infections as potential responsible of antibiotic therapy failure: observations of an *ex-vivo* mouse model "

Rym Boudjemaa, Karine Steenkeste, Cédric Jacqueline, Romain Briandet, Jocelyne Caillon, David Boutoille, Pierre Tattevin, Marie-Pierre Fontaine-Aupart, Matthieu Revest

Soumis à Journal of Infectious Diseases

Intramacrophagic *Staphylococcus aureus* in prosthetic vascular graft infections as potential responsible of antibiotic therapy failure: observations of an *ex-vivo* mouse model

Rym Boudjemaa,[a] Karine Steenkeste,[a] Cédric Jacqueline,[b] Romain Briandet,[c] Jocelyne Caillon,[b] David Boutoille,[b,d] Pierre Tattevin,[e,f] Marie-Pierre Fontaine-Aupart,[a] Matthieu Revest [b,e,f]

[a] Institut des Sciences Moléculaires d'Orsay, CNRS, Université Paris-Sud, Université Paris-Saclay, F-91405 Orsay cedex ; [b] Université Nantes, Faculté médecine, EA3826 Nantes, France ; [c] Micalis Institute, INRA, AgroParisTech, Université Paris-Saclay, 78350 Jouy-en-Josas, France; [d] CHU Nantes, Infectious Diseases Unit, Hôtel Dieu, Nantes, France ; e CHU Rennes Infectious Diseases and Intensive Care Unit, Pontchaillou Hospital, 35033 Rennes Cedex, France ; [f] CIC Inserm 1414, Rennes 1 University, Pontchaillou Hospital, 35033 Rennes Cedex, France

BACKGROUND

Prosthetic vascular graft infections (PVGIs) are major complications of vascular surgery, but little is known regarding their pathophysiology, and their optimal antibiotic treatment. Their management is currently mostly based on expert advises, and poorly supported by evidence-based medicine. As for most other foreign device infections, the removal of all infected material is of primary importance for cure, although complete removal of infected device may not be always technically feasible. In these not uncommon situations, patients can sometimes be cured by an appropriate bactericidal regimen[1]. Unfortunately, very limited data are available to select the optimal antibacterial regimen for treatment of PVGIs, as drug susceptibility testing routinely performed for bacteria involved in PVGIs, such as *Staphylococcus* sp., provide only limited data on the bactericidal activity of antibiotics on biofilm.

Biofilm development on vascular graft plays a significant role in the difficulties encountered when treating PVGIs and more information are needed regarding the interactions between antibiotics and bacteria embedded inside the biofilm. We recently demonstrated that the limited efficacy of antibiotics in biofilm was not necessarily due to a weak penetration[2] or bioavailability of antibiotics within this biofilm,[3] and that the barrier-effect could not be taken as the only responsible for the striking loss of efficacy documented with most antistaphylococccal agents. *S. aureus* can invade and survive inside mammalian cells, including the phagocytic cells[4].

We can hypothesize that this could be responsible for the lack of antibiotics efficiency and/or delayed PVGIs, but data are lacking regarding the interactions between *S. aureus* and mammalian tissues in the particular setting of PVGIs, since most available studies use *in-vitro* models.

Thus, we developed an *ex-vivo* mouse model of *S. aureus* PVGIs, allowing direct observation of the biofilm developed onto a Dacron® vascular material by confocal microscopy, to better characterize the efficacy of antibiotics and to analyze the influence of the host tissues and cells during PVGIs.

MATERIALS

Two different bacterial strains were used for all the experiments: Methicillin-Susceptible *S. aureus* (MSSA) ATCC 27217 and Methicillin-Resistant *S. aureus* (MRSA) BCB8 isolated from blood cultures. Both strains were susceptible to vancomycin (MIC, 1 mg/L for both), daptomycin (respective MIC 0.125 mg/L, and 0.25 mg/L), and rifampicin (MIC <0.06 mg/L for both). The following antistaphylococcal agents were bought from local drug purchases companies and prepared following label instructions for clinical use in humans: vancomycin (Sandoz, Levallois-Perret, France), daptomycin (Novartis Pharma SAS, Rueil-Malmaison, France) and rifampicin

(Sanofi-Aventis, Paris, France). All *in-vivo* experiments were approved by the French ministry of research review board. Four-week old female Swiss mice (RjOrl/SWISS, Janvier laboratory St Berthevin, France) were maintained on a 12-hour light/dark cycle with free access to food and water. At least 4 animals per group were used for the experiments. Mice were anesthetized with ketamine (70 mg/kg) and Xylazine (10 mg/kg) through intraperitoneal (IP) injection. Sterile 1 cm^2 squares of commercially used Dacron® were incubated with sterile serum of healthy female Swiss mice during 24 h at 37°C. Then, they were implanted into a subcutaneous pocket (10-mm horizontal incision) created in the centre of the mice back. Skin was closed with sutures (Vicryl 5/0). Two days after Dacron® implantation, a saline solution (0.2 mL) containing 10^7 CFU of *S. aureus* was transcutaneously inoculated onto the graft surface with a tuberculin syringe. During inoculation, mice were anesthetized with isoflurane (0.8 L/min, 3%). Antibiotics treatment started two days later. All the antibiotics used were administered at appropriate dose regimens resulting in serum concentrations similar to those in humans. For both staphylococcal strains, mice were randomized into different groups: no treatment (controls); vancomycin group (subcutaneous injection (SC), 110 mg/kg/12 h); daptomycin group (50 mg/kg/24 h, SC); rifampicin group (30 mg/kg/12 h, IP); vancomycin-rifampicin group; and daptomycin-rifampicin group. Mice were treated for 48 h and then euthanized following international guidelines. Immediately after the procedure, Dacron® patches were removed under aseptic conditions, homogenized in 0.5 mL of saline buffer, vortexed during 30 seconds and analysed with a confocal laser scanning microscope (Leica TCS SP5 Microsystems, France). Results of Dacron® bacterial culture obtained during previous equivalent experiments are displayed in supplemental materials. The first step of imaging experiments consisted in visualising the biofilm formed onto the Dacron® patches according to the different antibiotics. Bacteria were stained with 2.5 µM Syto9® (Invitrogen), which is able to penetrate all bacteria, and 5 µL of 1-mg/mL propidium iodide (PI, Invitrogen), which can only penetrate damaged-membrane cells. Syto9® and PI were excited at 488 and 543 nm, respectively, and their fluorescence emissions were collected between 500 and 600 nm for Syto9® and between 640 and 750 nm for PI. Images were acquired using a ×63 oil immersion objective with a numerical aperture of 1.4. The size of the confocal images was 512 x 512 pixels, recorded with a z-step of 1 µm and a 3x zoom. Fluorescence images were obtained using ImageJ software. For each biofilm, at least four different regions were analysed.

A second group of the same experiments were therefore performed to identify the eukaryote cells visualised, using three different stainings: Ly-6G®/Mouse neutrophil-specific marker (GR-1, Pacific Blue™ conjugate RB6-8C5, excitation: 361 nm, emission: 400-450 nm), F4/80® macrophage-specific antibody (Alexa Fluor® 647 conjugate BM8, excitation: 633 nm, emission: 650-750 nm) and Syto9® for bacteria. Then, the same experiments were performed with BODIPY-FL-daptomycin and BODIPY-FL-vancomycin (excitation: 488 nm, emission: 500-550 nm). Confocal laser scanning microscopy was performed the same way as the previous experiments.

RESULTS AND DISCUSSION

The visualization of antibiotics within biofilm-associated bacteria may contribute to our understanding of the differential effects of antistaphylococcal agents on material-associated *S. aureus* infections. Previous studies mostly used *in-vitro* models. However, those *in-vitro* models do not allow the observation of what happens *in-vivo*. In addition, most *in-vivo* models rely on bacterial counts within infected materials, but very few experiments include imaging techniques to visualize the effect of antibiotics on *in-vivo* biofilm[5]. The *ex vivo S. aureus* PVGI mouse

model presented herein may provide original data in this field.

We found that the differential effect of antistaphylococcal agents is strikingly different from one *S. aureus* isolate to another. We used the green staining Syto9® that only colours nucleic acids[6]. A green reticular structure was found with all experiments, which allows to visualize the biofilm developed onto the Dacron®. Inside those structures, bacteria were observed (figure 1 for the control and the most relevant groups, supplemental data for the other groups).

In both control groups (*i.e.*, MSSA and MRSA), the biofilm was dense and thick. For treatment groups, results were markedly different according to the molecules tested, and the isolate: for MRSA BCB8, vancomycin had almost no significant effect on biofilm as compared to control, while rifampicin and daptomycin displayed a dramatic effect on the biofilm, that could not even be visualized except in a unique place for the daptomycin group (Figure 1 and supplemental data). For MSSA 27217, the effect of daptomycin was much more limited. Vancomycin and daptomycin yielded similar effect, only mildly different from the control group, while rifampicin was by far the most active on biofilm reduction. Combinations of rifampicin to vancomycin dramatically increased the effect on biofilm, but this was not the case for the daptomycin-rifampicin combination: Indeed, the biofilm remain dense and thick with this combination (figure 1 and supplemental data). Of note, these results are in total agreement with bacterial counts after 48-hour incubation on Dacron® cultures (supplemental data).

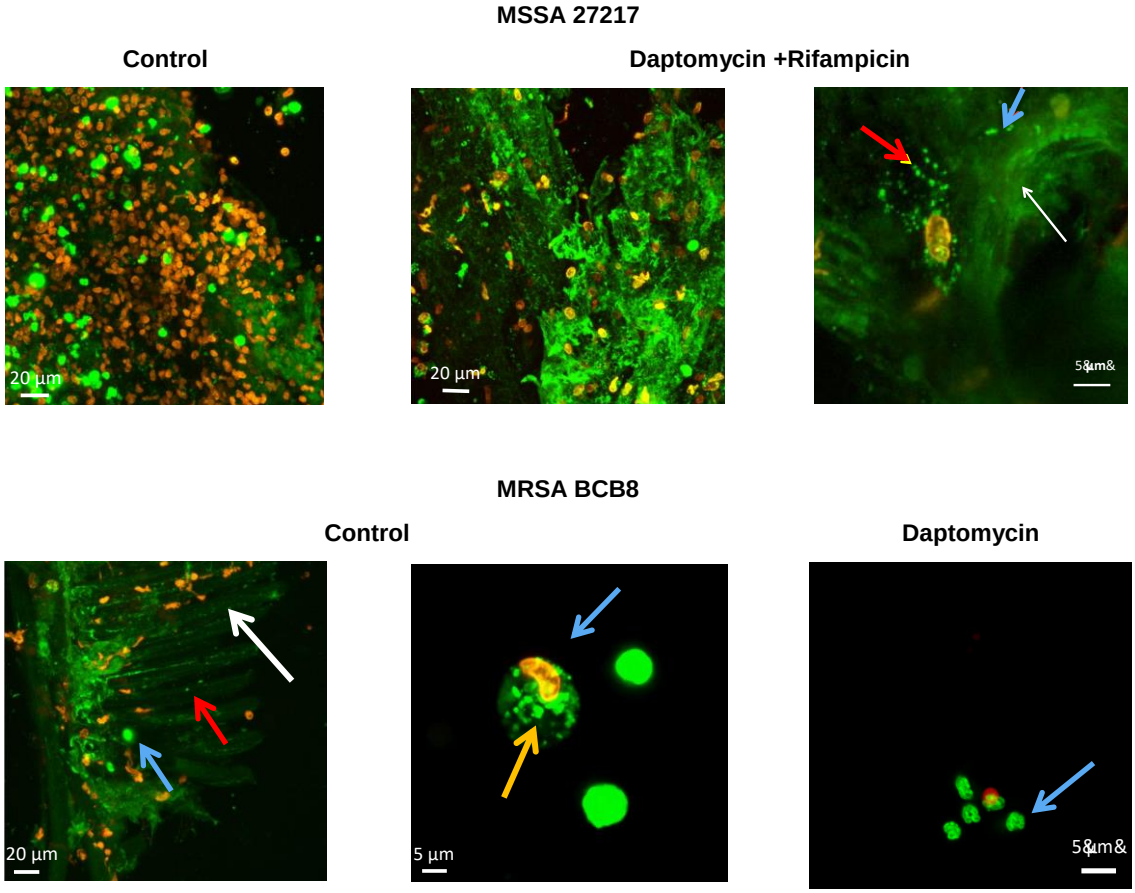

Figure 1: *Visualization of Dacron®-related S. aureus biofilms depending on treatment group by confocal laser scanning microscope. Green staining: Syto9® (Live cells), Red staining: propidium iodide (Dead cells).White arrow: reticular structures corresponding to the extra-cellular S. aureus biofilm; Red arrow: Bacterial cells included within this structure; Blue arrow: eukaryote cell; Yellow arrow: intracellular S. aureus.*

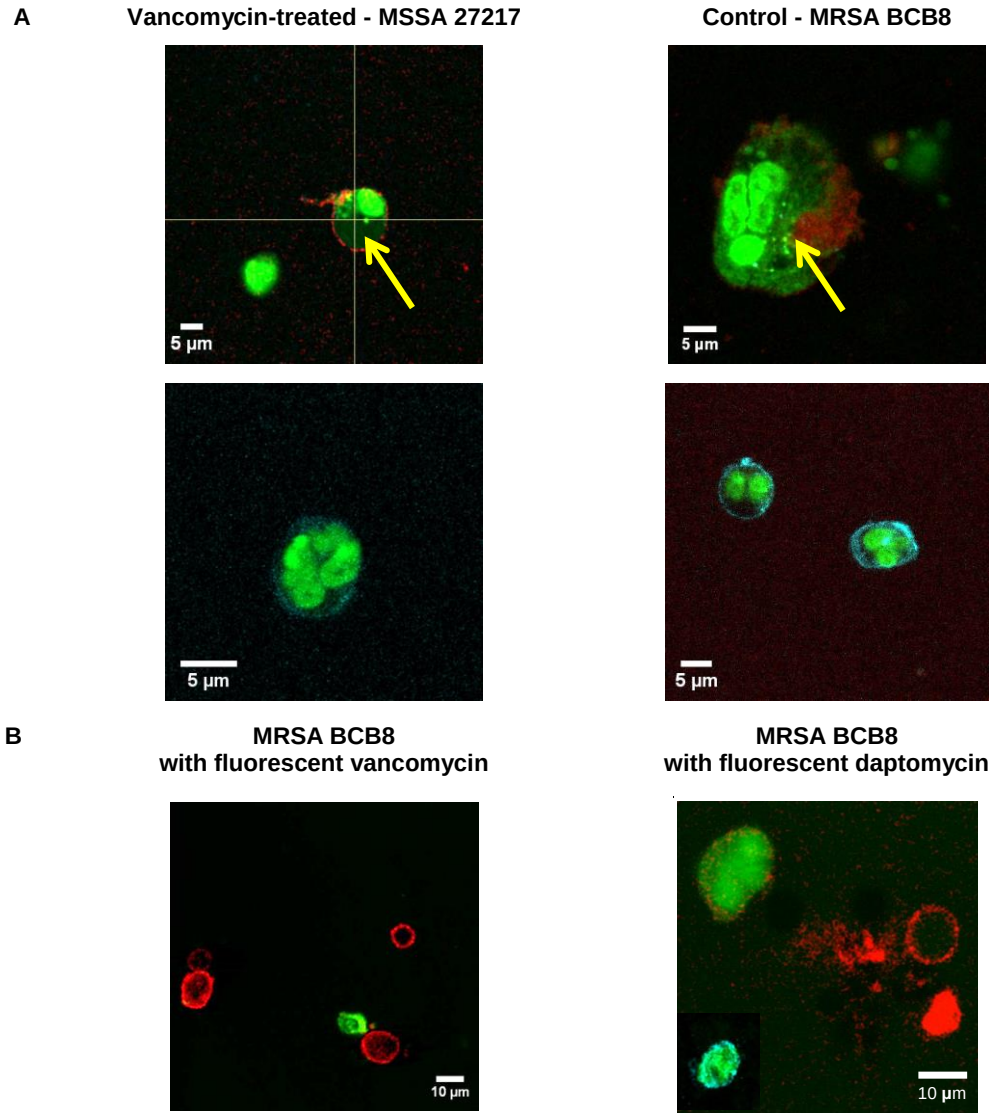

Figure 2: *Visualization of eukaryotic cells and antibiotic-staining.* ***(A)*** *Identification of eukaryotic cells. Green staining: Syto9®; Blue staining: Ly6G® (neutrophil polynuclear specific staining); Red staining: F4/80 (macrophages specific staining). Yellow arrow: intracellular S. aureus.* ***(B)*** *Antibiotic staining. Green staining: BODIPY-FL-vancomycin or daptomycin; Blue staining: Ly6G® (neutrophil polynuclear specific staining); Red staining: F4/80 (macrophages specific staining).*

Our results confirm the dramatic efficacy of rifampicin against biofilm-associated *S. aureus*[7, 8]. Our findings were however more unexpected for daptomycin, often referred to as one of the most active antistaphylococcal agent on biofilm, with much better penetration than vancomycin,[9] and significant activity against bacteria in stationary phase[10]. Although daptomycin was highly active on MRSA BCB8-related biofilm onto Dacron®, this was definitely not the case for MSSA 27217, which confirms previous findings from us[3], and from others, who found no difference between vancomycin and daptomycin *in-vitro*[11] or *in-vivo*[12].

We analyzed the Dacron® immediately after mice were euthanized. Thus, the biofilm we observed was a reliable image of the biofilm *in-vivo*, while the mice were alive. These procedures allow direct observation of interactions between the bacteria, the biomaterial and the host. Besides, eukaryote cells were observed for all the conditions tested,

either alive (colored in green), or dead (in red), and presented with characteristic features of polynuclear cells and macrophages. This was confirmed by specific staining, for polynuclear cells (Ly-6G® positive), and macrophages (F4/80® positive) (figure 2). This demonstrates that, despite a protective effect from the immune system conferred by biofilm to bacteria, major players of cellular immunity interact *in-situ* with bacteria, onto the biomaterial. Interestingly, we could observe bacteria inside macrophages, but never inside polynuclear cells (figure 2). *S. aureus* is able to invade and survive within mammalians host cells, resulting in persistent and relapsing infections, especially in the particular setting of material-associated infections[4]. This has been well described for bone and joint infections, with the capability of *S. aureus* to survive within osteoblast[13]. To our knowledge, we describe here for the first time the same capacity to survive inside host cells (i.e., macrophages), in an *ex-vivo* model of *S. aureus* PVGIs. Intramacrophagic *S. aureus* are able to escape the phagolysosome, to replicate freely in the cytoplasm. *S. aureus* can trigger cell death mechanisms from its host cell, multiply actively and disseminate, but it can also activate anti-apoptotic programs to persist hidden in intracellular position and induce chronic or relapsing infections. Besides, the figure 2 shows that some host cells of *S. aureus* are alive, coloured in green, while others are dead or nearly dead (coloured in red or orange). In addition, intramacrophagic position could represent a shelter for *S. aureus* against antibiotics: the less able to penetrate host eukaryotic cells they are, the less efficient they will be. And as shown in figure 2, vancomycin and daptomycin do not seem to penetrate macrophages within which *S. aureus* are found, while they are visualized inside polynuclear cells.

Thus, we hypothesize that *S. aureus* can persist inside macrophage during PVGIs. This could be an explanation to the relative inefficacy of antibiotics without surgery during these infections, and to the high risk of relapse when the infected material is not removed. This could also explain why antibiotic efficacy could be different according to the strain involved (i.e., daptomycin efficacy on BCB8 strain vs 27217), since the capability of *S. aureus* to invade mammalian cells could vary from one strain to another[14]. Finally, this highlights the particular importance of rifampicin for this kind of infections, due to its well-known great intracellular activity.

In conclusion, this *ex-vivo* mouse model of *S. aureus* PVGIs allows the direct observation of the impact of major antistaphylococcal agents on Dacron®-related biofilm. It allowed us to better understand the differential effect of antibiotics in PVGIs. We found that *S. aureus* is able to invade and persist into macrophages onto the biomaterial during PVGIs, which may explain why bacteria may persist, and relapse, even after prolonged and appropriate antibacterial therapy. More studies are needed, but we can postulate that the use of antibiotics active against biofilm-embedded and intracellular bacteria such as rifampicin could be a very good option in PVGIs.

References

1 FitzGerald SF, Kelly C and Humphreys H. Diagnosis and treatment of prosthetic aortic graft infections: confusion and inconsistency in the absence of evidence or consensus. *J Antimicrob Chemother* 2005; **56**: 996-9.

2 Daddi Oubekka S, Briandet R, Fontaine-Aupart MP *et al.* Correlative time-resolved fluorescence microscopy to assess antibiotic diffusion-reaction in biofilms. *Antimicrob Agents Chemother* 2012; **56**: 3349-58.

3 Boudjemaa R, Briandet R, Revest M *et al.* New Insight into Daptomycin Bioavailability and Localization in *Staphylococcus aureus* Biofilms by Dynamic Fluorescence Imaging. *Antimicrob Agents Chemother* 2016; **60**: 4983-90.

4 Fraunholz M and Sinha B. Intracellular *Staphylococcus aureus*: live-in and let die. *Front Cell Infect Microbiol* 2012; **2**: 43.

5 Nishitani K, Sutipornpalangkul W, de Mesy Bentley KL *et al.* Quantifying the natural history of biofilm formation *in vivo* during the establishment of chronic implant-associated *Staphylococcus aureus* osteomyelitis in mice to identify critical pathogen and host factors. *J Orthop Res* 2015; **33**: 1311-9.

6 Mann EE, Rice KC, Boles BR *et al.* Modulation of eDNA release and degradation affects *Staphylococcus aureus* biofilm maturation. *PLoS One* 2009; **4**: e5822.

7 Edmiston CE, Jr., Goheen MP, Seabrook GR *et al.* Impact of selective antimicrobial agents on staphylococcal adherence to biomedical devices. *Am J Surg* 2006; **192**: 344-54.

8 Senneville E, Joulie D, Legout L *et al.* Outcome and predictors of treatment failure in total hip/knee prosthetic joint infections due to *Staphylococcus aureus*. *Clin Infect Dis* 2011; **53**: 334-40.

9 Stewart PS, Davison WM and Steenbergen JN. Daptomycin rapidly penetrates a *Staphylococcus epidermidis* biofilm. *Antimicrob Agents Chemother* 2009; **53**: 3505-7.

10 Murillo O, Garrigos C, Pachon ME *et al.* Efficacy of high doses of daptomycin *versus* alternative therapies against experimental foreign-body infection by methicillin-resistant *Staphylococcus aureus*. *Antimicrob Agents Chemother* 2009; **53**: 4252-7.

11 Smith K, Perez A, Ramage G *et al.* Comparison of biofilm-associated cell survival following *in vitro* exposure of meticillin-resistant *Staphylococcus aureus* biofilms to the antibiotics clindamycin, daptomycin, linezolid, tigecycline and vancomycin. *Int J Antimicrob Agents* 2009; **33**: 374-8.

12 Lefebvre M, Jacqueline C, Amador G *et al.* Efficacy of daptomycin combined with rifampicin for the treatment of experimental meticillin-resistant *Staphylococcus aureus* (MRSA) acute osteomyelitis. *Int J Antimicrob Agents* 2010; **36**: 542-4.

13 Valour F, Rasigade JP, Trouillet-Assant S *et al.* Delta-toxin production deficiency in *Staphylococcus aureus*: a diagnostic marker of bone and joint infection chronicity linked with osteoblast invasion and biofilm formation. *Clin Microbiol Infect* 2015; **21**: 568 e1- e11.

14 Scherr TD, Hanke ML, Huang O *et al.* *Staphylococcus aureus* Biofilms Induce Macrophage Dysfunction Through Leukocidin AB and Alpha-Toxin. *MBio* 2015; **6**.

Supplemental material

Table S1: *Bactericidal activity of antistaphylococcal agents on Dacron®*

Bacterial load decrease as compared to the control group: mean (CI 95%)		
Antibiotic regimen	MSSA 27217	MRSA BCB8
Vancomycin	- 1.24 (0.30; 2.20)**	- 2.38 (1.00; 3.73)**
Daptomycin	- 1.52 (0.68; 2.36)***	- 5.85 (4.34; 7.36)***
Rifampicin	- 2.99 (2.01; 3.97)***	- 4.45 (3.04; 5.85)***
Vancomycin-rifampicin	- 5.00 (4.05; 5.94)***	- 4.14 (2.67; 5.61)***
Daptomycin-rifampicin	- 2.82 (1,91; 3.74)***	- 5.85 (4.34; 7.36)***

Each group is compared to the corresponding control group with a Bonferroni Test following a variance analysis (Anova, GraphPad Prism software version 6.0; GraphPad Software, San Diego, CA, USA)

** $P< 0.01$; *** $P< 0.001$

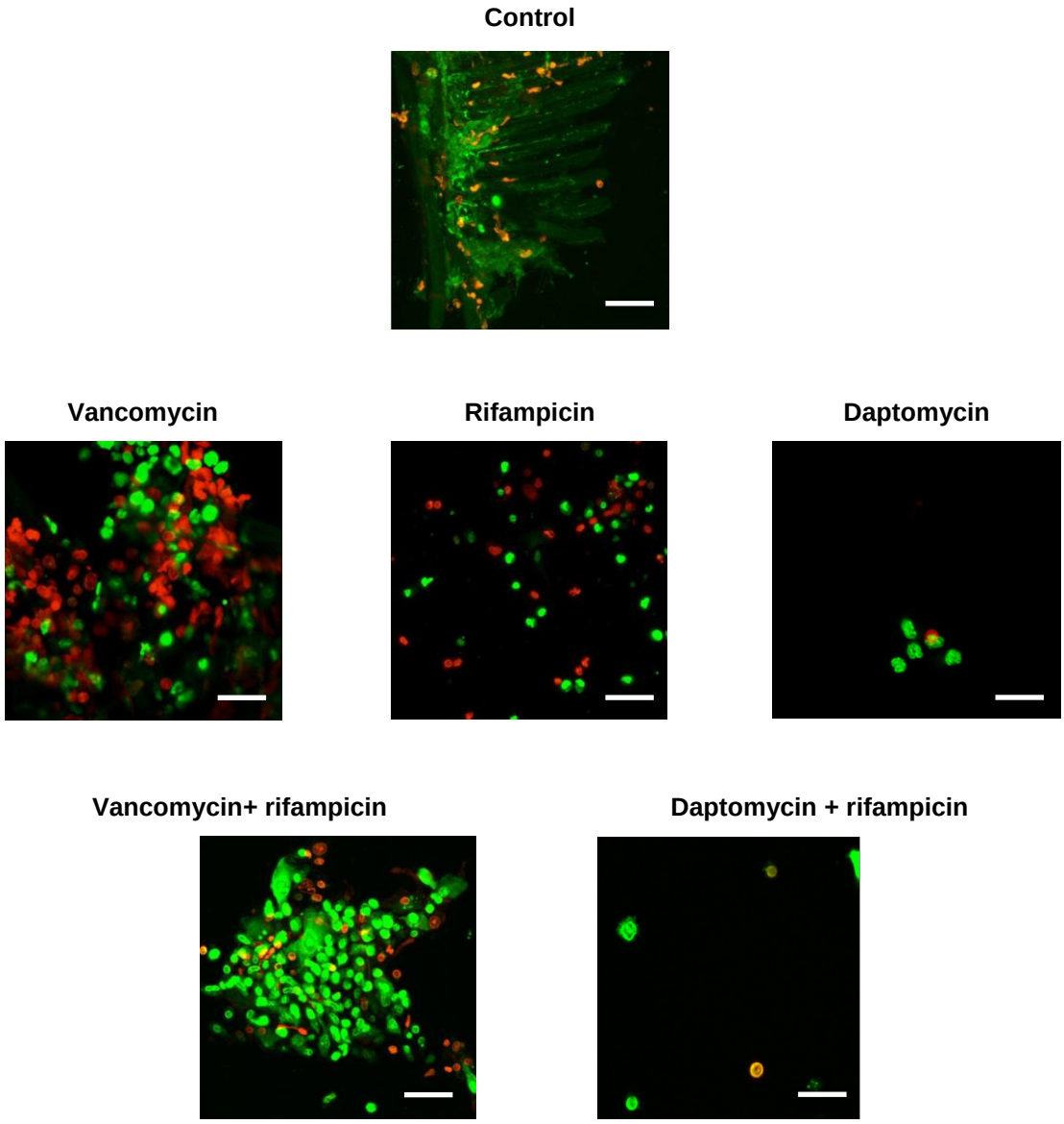

Figure S1: *Visualization of Dacron®-related MRSA BCB8 biofilm depending on treatment group by confocal laser scanning microscope. Green staining: Syto9® (Live cells), Red staining: propidium iodide (Dead cells)*

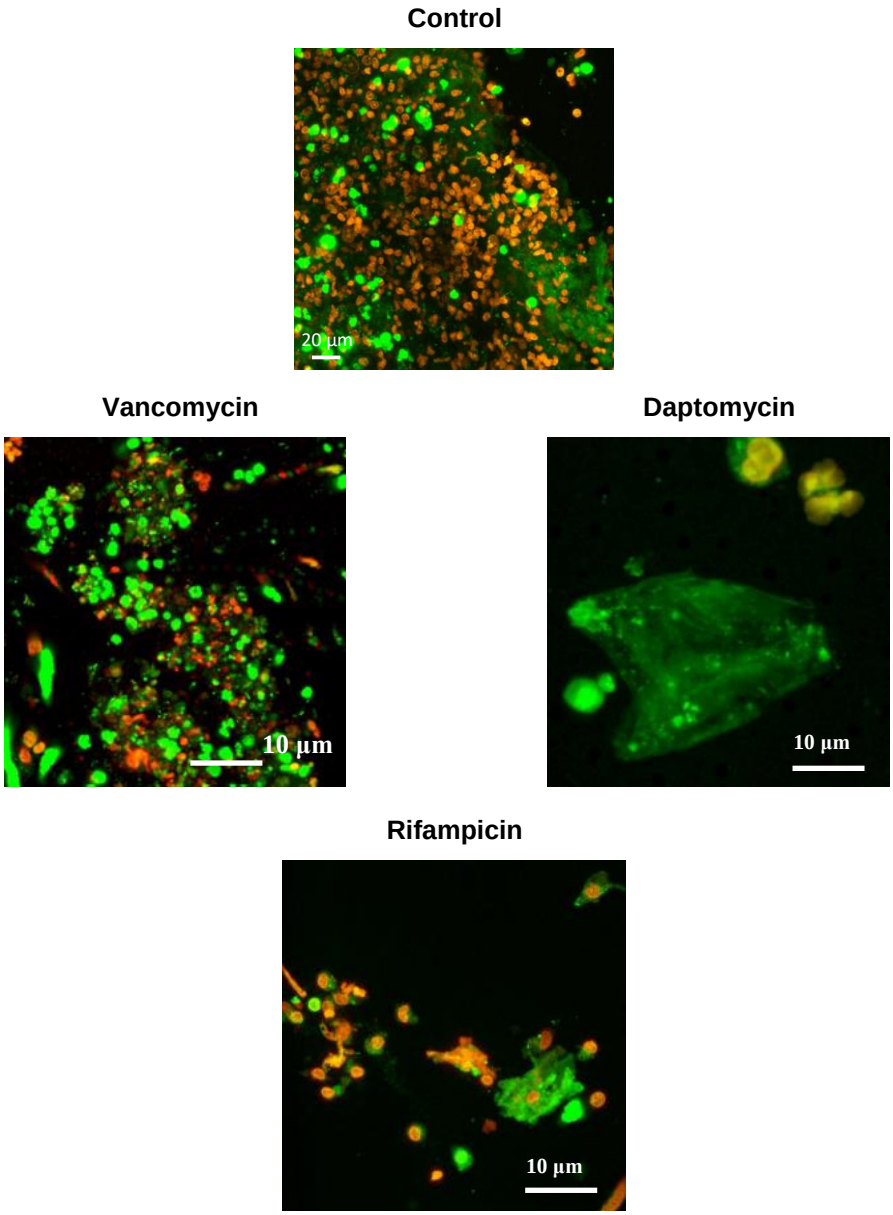

Figure S2: *Visualization of Dacron®-related MSSA 27217 biofilm depending on treatment group by confocal laser scanning microscope: monotherapies. Green staining: Syto9® (Live cells), Red staining: propidium iodide (Dead cells)*

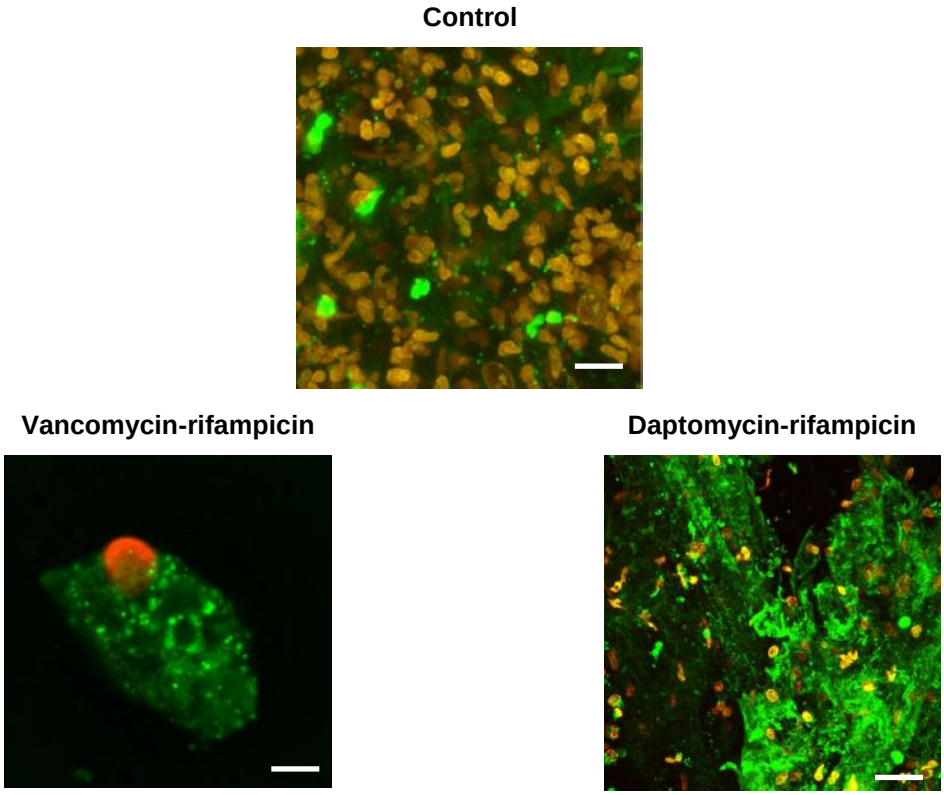

Figure S3: *Visualization of Dacron®-related MSSA 27217 biofilm depending on treatment group by confocal laser scanning microscope: combined therapies. Green staining: Syto9® (Live cells), Red staining: propidium iodide (Dead cells)*

Chapitre 4. Comment la spectroscopie et l'imagerie de fluorescence multimodale contribuent-elles à disséquer l'(in)efficacité des antibiotiques vis-à-vis des biofilms de *S. aureus in vitro* ?

Les données obtenues avec notre modèle d'infections sur implant chez l'animal ont révélé que les antibiotiques (vancomycine, daptomycine), qu'ils soient seuls ou en association avec la rifampicine et à des concentrations comparables à celles utilisées en clinique, ne permettaient pas d'éradiquer complètement les infections à biofilms de *S. aureus in vivo*. Comme vu dans le chapitre précédent, l'internalisation des bactéries au sein des cellules immunitaires joue un rôle important mais sans doute pas le seul. Alors, quels autres facteurs liés à l'organisation en biofilms seraient susceptibles d'expliquer l'inefficacité des antibiotiques ? C'est la question à laquelle nous avons tenté de répondre dans les chapitres qui suivent. Une des hypothèses émises suggère que la matrice d'exopolymères sécrétée par les bactéries jouerait un rôle de « barrière » à la pénétration et à la libre diffusion des antibiotiques. Dans ce contexte, l'équipe Biophysique/Biophotonique de l'ISMO, qui s'intéresse depuis plusieurs années à l'étude de la diffusion-réaction des antibiotiques au sein des biofilms staphylococciques, a développé une combinaison unique de méthodes d'imagerie de la dynamique de fluorescence. Parmi ces méthodes (détaillées dans le chapitre 2 de la synthèse bibliographique), l'imagerie time-lapse permet d'évaluer la pénétration et la diffusion des antibiotiques fluorescents et la FRAP (Fluorescence Recovery After Photobleaching) ainsi que l'imagerie de durées de vie de fluorescence (FLIM, Fluorescence Lifetime Imaging) donnent accès à leur biodisponibilité. Il a pu être démontré que le manque d'activité de l'antibiotique vancomycine ne provenait ni d'un défaut de sa diffusion, ni d'un manque de sa biodisponibilité au sein des biofilms. Néanmoins, il est suggéré dans la littérature que la pénétration des antibiotiques dans la biomasse est fortement dépendante du couple antibiotique/souche étudié et de la structure du biofilm.

Ainsi, dans la continuité des précédents travaux, ce travail de thèse porte sur (i) l'optimisation d'un nouveau modèle *in vitro* de biofilm de *S. aureus* se rapprochant du modèle sur implant *in vivo* et (ii) sur l'étude de la diffusion-réaction au sein de biofilms non seulement de la vancomycine mais aussi de la daptomycine, seules et en association avec la rifampicine. Les mêmes souches de *S. aureus* que celles étudiées dans le précédent chapitre (MRSA et MSSA, de collection et cliniques) ont été utilisées. Il faut noter que le panel d'outils d'imagerie de fluorescence précédemment décrit nécessite que les antibiotiques soient fluorescents. La vancomycine fonctionnalisée au BODIPY-FL est disponible commercialement et nous avons vérifié que son activité n'était pas modifiée par l'ajout du fluorophore. Concernant la molécule de BODIPY-FL-daptomycine, elle n'est pas commercialisée et nous avons pu bénéficier d'un contrat de transfert de matériel avec la société Cubist Pharmaceuticals pour réaliser ce travail de test. Nous avons, par ailleurs, initié une synthèse de NBD-daptomycine décrite dans la partie résultats complémentaires de ce chapitre.

Les résultats détaillés sont présentés sous forme de deux articles parus dans *Photochemical and Photobiological Science* (2017, doi: 10.1039/C7PP00079K), intitulé ***« How do fluorescence spectroscopy and multimodal fluorescence imaging help to dissect the enhanced efficiency of vancomycin-rifampin combination against Staphylococcus aureus infections? »*** et dans *Antimicrobial Agents and Chemotherapy* (2016, doi:10.1128/AAC.00735-16), intitulé « ***New insight into daptomycin bioavailability and localization in S. aureus biofilms by dynamic fluorescence imaging.*** »

Nous avons tout d'abord validé notre modèle de biofilms *in vitro* en nous assurant que l'activité des antibiotiques était similaire à celle obtenue pour le modèle animal et en particulier que l'éradication complète d'un biofilm n'était jamais atteinte. La combinaison des différentes méthodes d'imagerie dynamique de fluorescence (time-lapse, FRAP, FLIM) a démontré pour tous les cas d'étude que le manque d'activité des antibiotiques au sein des biofilms n'était pas lié à un défaut de leur pénétration, de leur diffusion ou de leur biodisponibilité. Un point intéressant que la spectroscopie de fluorescence a permis d'identifier est la formation d'un complexe entre la vancomycine et la rifampicine, complexe dont la pénétration au sein du biofilm est facilitée par rapport à la vancomycine seule mais dont la présence requiert d'adapter le ratio des concentrations des deux antibiotiques.

Pris dans leur ensemble, ces résultats suggèrent que c'est plus probablement la physiologie spécifique des bactéries incluses en biofilm que la matrice d'exopolymères qui doit être considérée pour expliquer la tolérance aux antibiotiques.

4.1. Article 4 : "How do fluorescence spectroscopy and multimodal fluorescence imaging help to dissect the enhanced efficiency of vancomycin-rifampin combination against *Staphylococcus aureus* infections?"

Rym Boudjemaa, Romain Briandet, Marie-Pierre Fontaine-Aupart, Karine Steenkeste

Photochemical and Photobiological Science, 2017

Photochemical & Photobiological Sciences

PAPER

How do fluorescence spectroscopy and multimodal fluorescence imaging help to dissect the enhanced efficiency of vancomycin-rifampin combination against *Staphylococcus aureus* infections?

Received 00th January 20xx,
Accepted 00th January 20xx

DOI: 10.1039/x0xx00000x

www.rsc.org/

Rym Boudjemaa,[a] Romain Briandet,[b] Marie-Pierre Fontaine-Aupart [a] and Karine Steenkeste [a]

Staphylococcus aureus is one of the most frequent pathogens responsible for biofilm-associated infections. Among current clinical antibiotics, very few enable long-term successful treatment. Thus, it becomes necessary to better understand antibiotics failures and successes in treating infections in order to master the use of proper antibiotic therapies. In this context, we took benefit from a set of fluorescence spectroscopic and imaging methods, with the support of conventional microbiological tools to better understand the vancomycin-rifampin combination (in)efficiency against *S. aureus* biofilms. It was shown that both antibiotics interacted by forming a complex. This latter allowed a fastened penetration of the drugs before dissociating from each other to interact with their respective biological targets. However, sufficiently high concentrations of free vancomycin should be maintained, either by increasing vancomycin concentration or by applying repetitive doses of the two drugs, in order to eradicate rifampin-resistant mutants.

Introduction

Staphylococcus aureus (*S. aureus*) is a pathogenic microorganism that represents one of the major causes of chronic and hospital-acquired infections, in part due to its well-described intrinsic genetic resistance to antibiotics.[1] Apart from specific genetic mechanisms, it is also recognized that 80% of human infections are linked to biofilm formation, involving physiological changes of bacterial cells.[2] Biofilms are dense microbial communities, adhering to surfaces and further secreting an extracellular matrix mainly composed of water, polysaccharides, DNA and proteins.[3] These three-dimensional structures confer to bacteria the ability to protect themselves from the action of antibiotics and to survive under treatment through tolerance mechanisms.[4–6] This phenomenon implies to employ a specific strategy about antibiotic therapy administration.

Literature data on *S. aureus* biofilms, both *in vitro* and in clinical practice, are equivocal about antibiotic therapies inefficacy when administered alone.[7–12] One proposed strategy to overcome monotherapy-related limitations and to enhance its use has been to combine antibiotics with the goal of broadening the spectrum of antibacterial activities, enhancing tissue and intracellular penetration, and preventing the emergence of resistance.[9,13] Among the most commonly-used antibiotic therapies in clinical practice against *S. aureus* biofilm-associated infections are vancomycin and rifampin used either alone or in combination.[14,15]

Rifampin is a lipophilic antibiotic that specifically inhibits bacterial RNA polymerase, the enzyme responsible for DNA transcription, by forming a stable drug-enzyme complex with a binding constant of 10^{-9} M at 37°C.[16] This drug acts very rapidly, exerting a high bactericidal activity during the first hours of treatment. However, it is also known for involving a significant emergence of rifampin-resistant *S. aureus* mutants.[16] Vancomycin is a hydrophilic molecule that inhibits the bacterial cell wall synthesis by targeting the D-alanyl-D-alanine moieties of the N-acetylmuramic acid (NAM) and N-acetylglucosamine (NAG) that form the backbone strands of the bacterial cell wall.[17] This latter being synthesized during cell division, vancomycin is shown to be only efficient against actively-dividing cells. Several studies revealed a synergistic effect between vancomycin and rifampin, leading to an enhanced therapeutic efficacy.[18–21] By contrast, other studies also showed that the addition of rifampin to vancomycin treatment might have an antagonistic effect (a decreased efficacy compared to monotherapies).[10,22–26] This reduced effectiveness has often been related to unrecognized drug-drug interactions, emergence of resistance and adverse drugs effects. However, these contradictory results have recently been suggested to be correlated with the antibiotics concentrations used.[27]

The purpose of this study is to provide a deeper insight into these antibiotics (in)efficiency against *S. aureus* biofilms with the further goal of proposing relevant antibiotics administration. To address this issue, we took benefit from fluorescence spectroscopic and imaging tools, complementarily with conventional microbiological methods, used here to control the biological activity of vancomycin, rifampin and their association. The potential drug-drug interaction was

[a] *Institut des Sciences Moléculaires d'Orsay (ISMO), CNRS, Univ. Paris-Sud, Université Paris-Saclay, F-91405 Orsay, France.*
[b] *Micalis Institute, INRA, AgroParisTech, Université Paris-Saclay, 78350 Jouy-en-Josas, France.*
Electronic Supplementary Information (ESI) available: [details of any supplementary information available should be included here]. See DOI: 10.1039/x0xx00000x

characterized by steady-state and dynamic fluorescence spectroscopy. In addition, a confocal microscope developed for multimodal fluorescence imaging techniques was used (i) to visualize the antibiotic(s) penetration throughout biofilms by time-lapse, and (ii) to provide accurate information about antibiotics bioavailability through biofilms depth by image-based fluorescence recovery after photobleaching (FRAP) and time-resolved fluorescence spectroscopy.

Experimental

Bacterial strains, culture medium and antimicrobial agents

The *S. aureus* strain tested in the present study is the methicillin-susceptible *S. aureus* [MSSA] collection strain named ATCC 27217. The strain was kept at –80°C in Tryptic Soy Broth (TSB, bioMérieux, France) containing 20% (vol/vol) glycerol. The frozen cells were subcultured twice in TSB (one 8-h culture, followed by an overnight culture) to constitute the stock cultures from which aliquots were kept at –20°C. Bacterial growth was conducted at 37°C. Clinically-meaningful concentrations of vancomycin (Sigma, France) and rifampin (Sigma, France) were chosen to be close to the expected free fraction of drug reached in the plasma of patients. Therefore, the final concentrations used in this study were either 20 or 40 µg/ml for vancomycin and 10 or 20 µg/ml for rifampin, as specified in the text. The stock solutions were prepared by diluting vancomycin and rifampin in sterile water (2 mg/ml), kept at –20°C, and further diluted in TSB. When combined, the antibiotics were mixed together before addition to bacterial suspensions or application above the biofilm surface.

For fluorescence imaging, the fluorescently-labeled version of vancomycin, BODIPY-FL-vancomycin (Invitrogen, France), was used. The lyophilizates were dissolved in sterile Milli-Q water to obtain stock solutions of 69 mM. These stock solutions, kept at –20°C before use, were then diluted to working concentrations. It must be noted that the BODIPY-FL grafting of vancomycin does not affect its activity.[28]

Characterization of the molecular interactions between the antibiotics by absorption and fluorescence spectroscopies

Absorption spectra of antibiotics alone and in combination were measured with a Varian's Cary®300 spectrophotometer (Agilent Technologies, France). The corresponding fluorescence emission spectra were recorded using a Fluorolog-3 fluorescence spectrophotometer mounted with a front-face detection geometry to prevent from diffusion processes (Jobin Yvon, Inc., France). The percentage of fluorescence quenching was obtained by calculating the areas under the emission bands. The measurements were made in quintuplicate on each sample. These steady-state experiments were supported by fluorescence lifetime measurements using the setup described below.

In vitro antibiotics activities against planktonic bacteria

Antibiotics activities were controlled against the MSSA ATCC 27217 strain in the exponential phase of growth after a 3-hour culture following the overnight culture. Bacterial suspensions were then centrifuged at 7000*g* during 10 minutes at ambient temperature. After eliminating the supernatant, the bacterial pellet was dispersed in sterile NaCl 150 mM and centrifuged again in the same conditions. The bacterial pellet obtained was dispersed in TSB. Optical density was measured at 600 nm and adjusted to get a bacterial concentration ~10^6 CFU/ml (CFU, Colony Forming Units). The bacterial solution was divided equitably into cell culture flasks where antibiotics solutions were added. Bacterial growth was also controlled with a sample without antibiotics, corresponding to the control experiment. Viable culturable bacteria were counted at regular interval times: 0 h (when antibiotics were added), 3, 6 and 24 h after antibiotics injection. For each time, 1.5 ml of bacterial culture was collected and centrifuged 10 min at 7000*g* to eliminate the excess of antibiotic. The bacterial pellet was dispersed in 1.5 ml sterile NaCl 150 mM, centrifuged again and dispersed in the same conditions. Successive decimal dilutions were then realized. For each dilution, six drops (10 µL) were deposited on Tryptic Soy Agar (TSA) plates (bioMérieux, France), and incubated at 37°C during 24 h. CFUs were counted and averaged for each dilution at each time. The limit detection of viable culturable cells using this method was 100 CFU/ml.

In vitro biofilm preparation and antibiotics activities

For the preparation of *S. aureus* biofilms, 250-µl portions of an overnight subculture adjusted to an optical density of 0.02 at 600 nm (corresponding to ~ 10^8 CFU/ml) were added to a 96-well microplate (µClear; Greiner Bio-One, France). After a 1.5-h adhesion period at 37°C, the wells were rinsed with a NaCl solution (150 mM) to remove non-adherent cells, refilled with sterile TSB and then incubated for 24 h at 37°C to allow biofilm growth.

To assess antibiotic activities, the 24-h biofilms were rinsed with a NaCl solution (150 mM) before adding the antibiotic solutions diluted in TSB as described previously. Viable culturable bacteria were then counted at regular intervals: 0 h (when antibiotics are added), 6, 24, 48 and 72 h after antibiotic injection. For each time point, bacterial cultures were centrifuged 10 min at 7000*g* to eliminate the excess of antibiotic. The bacterial pellet was suspended in a NaCl sterile saline solution (150 mM), centrifuged again, and suspended in the same conditions. Bacterial counting was then performed as described for planktonic cells.

Confocal Laser Scanning Microscopy (CLSM)

All fluorescence imaging measurements were recorded using the same confocal microscope Leica TCS SP5 (Leica Microsystems, Germany; implemented at the Centre de Photonique Biomédicale of Orsay) equipped with a 63 x high numerical aperture (1.4) oil immersion objective, and coupled with either continuous lasers for FRAP acquisitions and time-lapse imaging or a femtosecond titanium-sapphire laser (Chameleon-XR; Coherent, USA) running at a 80-MHz repetition rate and delivering 150-fs pulses for biphotonic time-resolved fluorescence spectroscopy. All these experiments were performed with BODIPY-FL-vancomycin 40 µg/ml alone or combined with rifampin 20 µg/ml, diluted in TSB.

(i) Visualization of biofilms structures and antibiotic activities against biofilms using LIVE/DEAD® staining. 24h-biofilms grown as described previously were observed 0, 24 and 48h after antibiotic addition. Prior to each observation, bacteria were stained with a LIVE/DEAD® kit including Syto9® (Life Technologies, France), a green cell-permeant nucleic acid dye, and Propidium Iodide (PI) (Life Technologies, France), a red nucleic acid dye that can only penetrate cells with damaged membranes (generally corresponding to dead bacteria). Syto9® and PI were sequentially excited at 488 nm and 543 nm respectively, and their fluorescence emissions were collected between 500 and 560 nm for Syto9® and between 640 and 750 nm for PI. Image stacks were recorded with a z-step of 1 µm; the size of confocal images was 512 by 512 pixels, with a 3x numerical zoom (82 × 82 µm²). For each biofilm, four typical regions were analyzed. Images were reconstructed in three dimensions (3D) using the freely available ICY imaging software. The subsequent calculated percentage of dead cells corresponds to the ratio between biovolumes of PI-stained and Syto9®-stained bacteria.

The advantage of CLSM imaging is that it allows preserving the native biofilm structures and thus avoiding the possible artefacts of the enumeration method: partial stalling of the biofilm, presence of cell aggregates, cell stress, etc. However, one limitation is the detection sensitivity: the quantifiable proportion of dead cells measured allows to visualize variations of bacterial populations of more than 2 log, whereas the plate enumeration method can cover more than 6 log.

(ii) Antibiotic penetration inside biofilms. To study the penetration of BODIPY-FL-vancomycin alone and combined with rifampin within 24-h biofilms, we employed time-lapse microscopy, as described before.[28,29] Briefly, the fluorescence intensity evolution over time was observed in a defined focal plane (5 µm above the substratum surface). As soon as BODIPY-FL-vancomycin alone or combined with rifampin diluted in TSB were added to the biofilm, fluorescence intensity images were acquired every second for 15 min. Simultaneously, transmission images were acquired to ensure that no structural alteration of the biofilm occurred during this process. BODIPY-FL-vancomycin was excited with a continuous argon laser line at 488 nm, and the emitted fluorescence was recorded within 500 and 600 nm. The corresponding diffusive penetration coefficients (D_p) through the biofilms were determined according to the relationship previously described by Stewart:[30]

$$D_p = 1.03 * L^2/t_{90}$$

where L is the biofilm thickness, and t_{90} is the time required to attain 90% of the equilibrium staining intensity at the deepest layers of the biofilm.

(iii) Antibiotic diffusion and bioavailability inside biofilms using FRAP and time-resolved fluorescence spectroscopy experiments.

FRAP. This method is based on a brief excitation of fluorescent molecules by a very intense light source in a user-defined region to irreversibly photobleach their fluorescence. Fluorescence recovery is then probed over time at a low light power in the same photobleached region.[28,29,31] For all FRAP experiments, the fluorescence intensity image size was fixed to 512 by 128 pixels with an 80-nm pixel size and recorded using a 12-bit resolution. The line scan rate was fixed at 1400 Hz, corresponding to a total time between frames of 265 ms. As determined previously,[32] the full widths at half maximum in xy and z (along the optical axis) of the bleached profile were 0.8 µm and 14 µm, respectively, allowing us to neglect diffusion along the axial/vertical axis and thus to consider only two-dimensional diffusion. Each FRAP experiment started with the acquisition of 50 images at 7% of laser maximum intensity (which was measured to be 7 µW at the object level) followed by a 200-ms single bleached spot at 100% laser intensity. A series of 450 single-section images was then collected with the laser power attenuated to its initial value (7% of the bleach intensity). The first image was recorded 365 ms after the beginning of bleaching. The time course of fluorescence intensity recovery was then analysed with mathematical models, giving the quantitative mobility of the fluorescent molecules and allowing to determine the diffusion coefficients.[32]

It must be noted that in these experiments, the fluorescence recovery curves were recorded in a defined photobleached region, chosen to be centered on a single bacterium, with limited contribution of the surrounding biofilm matrix.

Time-resolved fluorescence spectroscopy. BODIPY-FL-vancomycin was biphotonically excited at 930 nm. The laser beam was scanned on the sample surface at 400 Hz, with a mean acquisition time of 13 ms per pixel. The fluorescence signal was collected by using a PicoHarp 300 device based on time-correlated single-photon counting method. An 800-nm short-pass emission filter was used to remove any residual laser light, and the emitted fluorescence was recorded within a range of 400 to 800 nm. The observed time-resolved decays were deconvoluted with the instrumental response function obtained on a picric acid solution, with a 100-ps time resolution. It was possible here to fit all the fluorescence decays, either with a single or multi-exponential function giving the fluorescence lifetimes of the sample. The fitting equation used was the following: $I_f = \sum_i f_i * e^{-t/\tau_i}$, with I_f the total fluorescence intensity, f_i the fluorescence intensity of the i species and τ_i its corresponding fluorescence lifetime. The mean fluorescence lifetime τ_f was calculated as follows:

$$\tau_f = \frac{\sum_i f_i * \tau_i}{\sum_i f_i}$$

It is then possible to extract the amplitude-averaged population a_i of the i species by using the following equation:

$$a_i = \frac{f_i/\tau_i}{\sum_i f_i/\tau_i}$$

Results

Time-kill studies coupled with the spatiotemporal visualization of antibiotics effect against *S. aureus* cells

To assess antibiotics activities against *S. aureus* exponentially-growing bacteria (high rate of bacterial multiplication), we

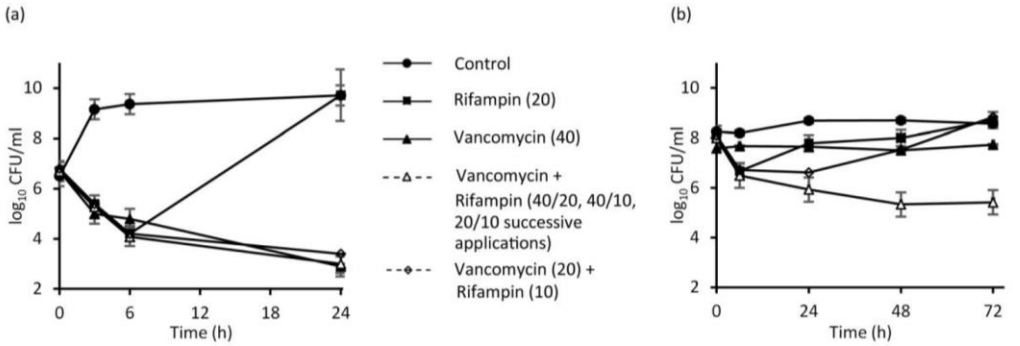

Fig. 1 Time-kill curves of vancomycin and rifampin alone and in combination against *S. aureus* (a) exponentially-growing cells and (b) biofilms. In parentheses, the antibiotics concentrations in µg/ml. The values are means ± standard deviations (error bars).

performed classical microbiological counts on agar plates. During the exponential growth phase (Fig. 1a), the three antibiotic treatments (vancomycin, rifampin and the combination of both) allowed to reach bactericidal activities within 6 h (defined as a ≥ 3-log reduction in bacterial counts compared to the initial bacterial concentration). However, while the bacterial concentrations continued decreasing until 24 h when the cells were treated with vancomycin and its combination to rifampin, regrowth was observed from 6 h to 24 h until reaching the same bacterial concentrations as the initial ones when treated with rifampin.

When *S. aureus* bacteria were grown to biofilms, fluorescence confocal laser scanning microscopy was first used to visualize in real time the antibiotics effects on the three-dimensional biostructures and bacteria killing over time (Fig. 2). Fluorescence images showed that the untreated biofilms (control) yielded compact three-dimensional structures, and their thicknesses were not significantly variable over time (27 ± 3 µm). When treated with vancomycin and rifampin alone, biofilms exhibited lower thicknesses (23 ± 2 µm and 19 ± 2 µm respectively), but only 10% of cell damage was quantified over time for both antibiotics. When rifampin was mixed with vancomycin, significantly higher cell damages were measured over time, achieving 70% at 48h, and correlated with a significant decrease in biofilms thicknesses (13 ± 4 µm). Another interesting observation resulting from the action of vancomycin-rifampin treatment is that damaged cells were observed over the whole biofilm depth, including the basal layer of cells in contact with the substratum. This strongly suggests an effective antibiotics diffusion through the whole biofilms depth.

These fluorescence imaging data were completed with time-kill curves obtained by agar counting measurements (Fig. 1b). By contrast with exponentially-growing cells (Fig. 1a), vancomycin inhibited the bacterial multiplication but was not able to decrease the bacterial loads over time. Similarly, rifampin decreased the bacterial counts by only 1.5 log within the first six hours but regrowth was observed between 6h and 72 h. When vancomycin and rifampin were administered in combination with doses of 20 µg/ml and 10 µg/ml respectively, the drugs activity was similar to that of rifampin alone during the first six hours before regrowth was observed from 24 to 72 h. By contrast, for concentrations of vancomycin and rifampin of 40/20 µg/ml and 40/10 µg/ml respectively, and for successive applications of combined antibiotics every 6 hours at respective concentrations of 20/10 µg/ml, the bacterial concentrations decreased gradually over time before reaching a 3-log reduction of the bacterial counts after 48h of treatment.

The observation of bacterial regrowth under rifampin exposure should be correlated with the emergence of antibiotic-resistant mutants. To confirm this hypothesis, *S. aureus* cells were grown on rifampin-enriched agar plates.

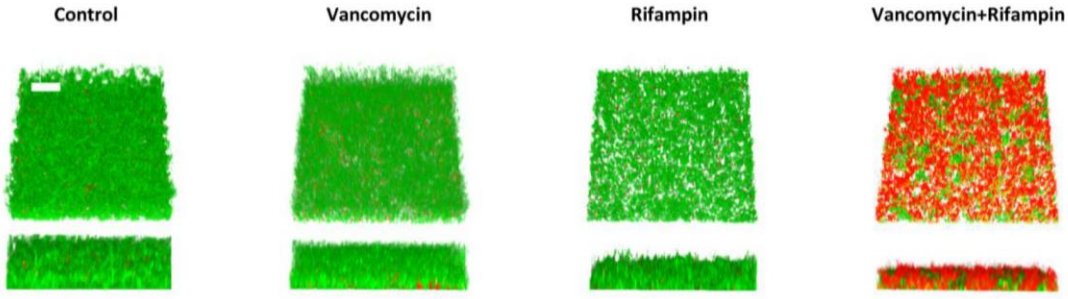

Fig. 2 24-hour *S. aureus* biofilms three-dimensional structures and distribution of both live and dead cells 48 h after the addition of vancomycin (40 µg/ml) and rifampin (20 µg/ml) alone or in combination. Living cells (green) and dead cells (red) were labeled with Syto9® (2-5 µM) and Propidium Iodide (PI) (30 µM) respectively. The scale bar represents 20 µm. Syto9® and PI were sequentially excited at 488 nm and 543 nm respectively, and their fluorescence emissions were collected between 500 and 560 nm for Syto9® and between 640 and 750 nm for PI.

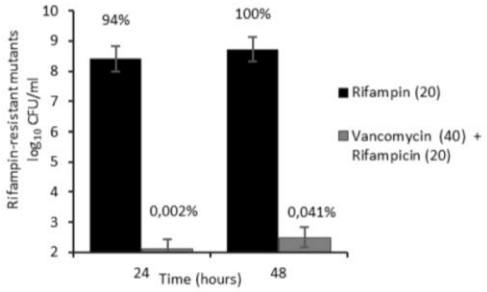

Fig. 3 Proportion of rifampin-resistant mutants over time when *S. aureus* cells were treated with rifampin (black) or with its combination to vancomycin (grey).

When the cells were treated with rifampin (20 µg/ml), 100% of bacteria were found to be resistant to rifampin (Fig. 3). However, when vancomycin (40 µg/ml) was added, only residual amounts of resistant mutants were counted, confirming that vancomycin could prevent the emergence of rifampin-resistant mutants (Fig. 3).

Spectroscopic characterization of the interaction between vancomycin and rifampin.

Fig. 4a illustrates the absorption spectra of vancomycin (without fluorescent labelling with BODIPY-FL), rifampin and their combination. It can be observed that the absorption of vancomycin was not influenced by the addition of rifampin. By contrast, in the presence of rifampin, the fluorescence emission intensity of vancomycin was quenched by ~ 80%, strongly suggesting an interaction between the antibiotics and involving more than one vancomycin molecule to one rifampin (the concentration vancomycin was double to that of rifampin) (Fig. 4b). This was also confirmed by fluorescence decay time analysis (Table 1). As we could not excite vancomycin itself, we measured the fluorescence lifetime of its labeled version, BODIPY-FL vancomycin. The fluorescence lifetime of BODIPY-FL-vancomycin remained unchanged in the presence of rifampin (5.7 ns) but a ~ 80% decrease of the initial photon count rate was measured in correlation with a very efficient non-radiative relaxation process.

Antibiotics penetration through the biofilms three-dimensional structures

Time-lapse imaging experiments were performed to compare the penetration of BODIPY-FL-vancomycin alone and mixed with rifampin. We found that the penetration rate of the antibiotics combination was 4 times enhanced compared to the one of BODIPY-FL-vancomycin alone (2.9 ± 0.2 µm²/s *vs* 0.7 ± 0.1 µm²/s) (Figure 5a). As shown in Fig. 5b, once the antibiotic penetrated throughout the deepest layers of *S. aureus* biofilms, the drug was localized at the bacterial cell surface whether used alone or mixed with rifampin.

Antibiotics bioavailability

Image-based FRAP focusing on one bacterium and its very close surrounding environment was performed to assess vancomycin bioavailability inside biofilms. As shown in Fig. 6, fluorescence recovery curves demonstrate that 40% ± 10% of BODIPY-FL-vancomycin molecules diffuse freely in the photobleached region around the single bacterium (with a diffusion coefficient of 0.89 ± 0.17 µm²/s) while 60% ± 10% of them are immobile and thus interact with the cell. When rifampin was mixed with BODIPY-FL-vancomycin, according to the precision of the experiments, similar diffusion coefficients and proportions of freely-diffusing and immobile molecules were found. As a control, we performed the same experiments with free BODIPY-FL (data not shown), and in this case, the fluorescence recovery was total after photobleaching, meaning that the fluorescent molecules were totally redistributed in the photobleached region surrounding the bacteria, freely diffusing and not interacting with the cell, in good agreement with our previous studies.[28,29]

Time-resolved fluorescence spectroscopy experiments were performed on both exponentially-growing bacteria and biofilms treated or not with vancomycin alone or with vancomycin-rifampin combination. The data are summarized in Table 1.

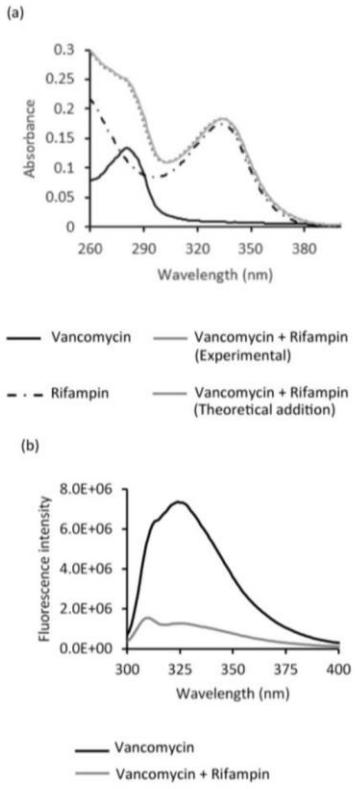

Fig. 4 Vancomycin and rifampin interact with each other, leading to the formation of a non-fluorescent complex. (a) Experimental absorption spectra of vancomycin (without fluorescent labelling with BODIPY-FL) 40 µg/ml (black straight line), rifampin 20 µg/ml (black dash-dotted line) and vancomycin 40 µg/ml-rifampin 20 µg/ml mixed together (grey straight line). The sum absorption spectrum of vancomycin 40 µg/ml and rifampin 20 µg/ml alone is represented in a grey dotted line. (b) Fluorescence emission spectra of vancomycin 40 µg/ml alone (black straight line) and mixed with rifampin 20 µg/ml (grey straight line). Vancomycin excitation wavelength: 270 nm (rifampin does not emit fluorescence).

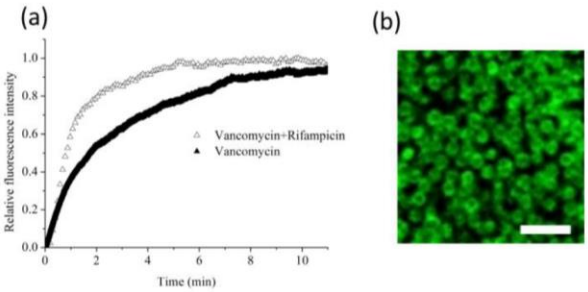

Fig. 5 BODIPY-FL-vancomycin, when mixed beforehand with rifampin, reaches more rapidly the biofilms deepest layers, and is further localized at the bacterial cell surface. (a) Typical time course of the penetration of BODIPY-FL-vancomycin alone (black triangles) and mixed beforehand with rifampin (white triangles) measured at the bottom of *S. aureus* biofilms (layers in contact with the substratum). The relative intensity corresponds to a normalization of the maximum intensity value to one. Time zero corresponds to the moment at which the antibiotic(s) was(were) added above the biofilm surface. The curves presented are representative of at least 5 biofilms probed. (b) A fluorescence intensity image of BODIPY-FL-vancomycin mixed with rifampin in *S. aureus* biofilms, obtained after 15 min incubation. The scale bar represents 5 µm. Excitation wavelength: 488 nm. Fluorescence emission range: 500-600 nm.

The best deconvolution of the fluorescence decay signals results in a ~ 0.5-ns component having the highest amplitude due to bacteria autofluorescence, a long lifetime component of 5.7 ns corresponding to free BODIPY-FL-vancomycin but also a shorter one, which can only be attributed to BODIPY-FL-vancomycin interacting with bacteria and/or biofilms components (τ_2 = 1.2-1.7 ns). Considering the ratio between free and bacteria-bound BODIPY-FL-vancomycin (a_1/a_2, Table 1), similar results are obtained whether the antibiotic is alone or combined with rifampin: free BODIPY-FL-vancomycin represents 14-18% in the presence of exponentially-growing cells and 7-8% inside biofilms, a difference that can be related to the different bacterial concentration (10^6 and 10^8 CFU/ml respectively).

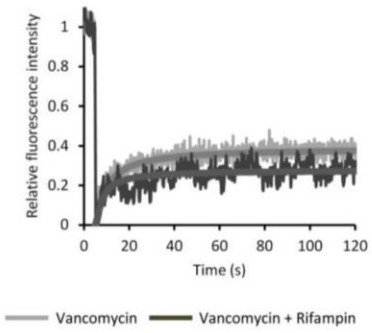

Fig. 6 Vancomycin and its association with rifampin interact with bacteria (60 and 70% ± 10% respectively) while the rest of the molecules (30 and 40% ± 10% respectively) freely diffuse in the cell vicinity. FRAP acquisitions for BODIPY-FL-vancomycin alone (light grey) and mixed beforehand with rifampin (dark grey) inside *S. aureus* biofilms and incubated 15 min. A typical fluorescence recovery curve representative of six different photobleached zones shown here and its fit (calculated using the model described in experimental section) is plotted in thick line. Excitation wavelength: 488 nm. Fluorescence emission range: 500-600 nm.

As reported above, a drastic decrease of the fluorescence photon counts was measured in solution between BODIPY-FL-vancomycin alone and associated with rifampin (Table 1), in agreement with the formation of a non-fluorescent complex. This was not observed in the presence of exponentially-growing bacteria: the decrease in fluorescence photon counts was strictly correlated to the one of the mean fluorescence lifetime (25%). By contrast, within biofilms, a 70% decrease of the fluorescence photon counts was observed between application of BODIPY-FL-vancomycin alone and associated with rifampin while the mean fluorescence lifetime only decreases from 1.7 ns to 1.2 ns (30%) revealing the persistence of non-fluorescent vancomycin-rifampin complexes.

Discussion

At a time when antimicrobial resistance represents a worldwide public health problem, it becomes necessary to better understand antibiotics failures and successes in treating infections in order to master the use of proper antibiotic therapies. To address this issue, we took benefit of fluorescence spectroscopic and imaging tools to provide a new insight into the vancomycin-rifampin combination (in)efficacy in treating *S. aureus* biofilm-associated infections.

We first controlled the activity of vancomycin and rifampin used alone against biofilms by comparison with planktonic cells. Several reports have pinpointed that despite the rapid bactericidal activity of rifampin for the first hours, resistant mutants emerge very quickly under the antibiotic exposure.[16,33] Our data obtained using conventional microbiology tools confirmed this observation where 100% of bacteria inside biofilms acquired resistance to rifampin after 48 h of treatment. However, this resistance occurred later than for exponentially-growing cells (24 h).

Another interesting result concerning rifampin activity is its reduced effectiveness against *S. aureus* biofilms compared to exponentially-growing cells during the first hours of treatment (before the appearance of rifampin-resistant mutants): only 1.5-log reduction in bacterial counts was measured within biofilms while a 3.0-log one was recorded for exponentially-growing bacteria. This can be explained by the well-established antibiotics-related horizontal genes transfer that occurs at a much higher frequency between cells in a biofilm than between their planktonic counterparts,[34] leading to rapid growth of resistant cells and thus to a reduced activity of rifampin.

Concerning vancomycin alone, its bactericidal activity in treating exponentially-growing *S. aureus* bacteria was not recovered against biofilms. In this case, only a bacteriostatic effect was recorded. Such result is in good agreement with vancomycin mechanism of action to eradicate preferentially actively-dividing cells than the slowly-growing bacteria in biofilms.[7,8]

Consistently with literature data,[9,17–21] the addition of adapted concentrations of vancomycin to rifampin (Fig. 1b) effectively prevented from rifampin-resistant bacteria. However, the large *S. aureus* bacterial eradication observed for exponentially-growing cells was far from being achieved for biofilms.

	Fluorescence photon counts	τ_f (ns)	τ_1 (ns)	τ_2 (ns)	τ_3 (ns)	a_1 (%)	a_2 (%)	a_3 (%)	a_1/a_2 (%)
TSB									
BODIPY-vancomycin	110 000	5.6	5.6	/	/	100	/	/	/
BODIPY-vancomycin+ rifampin	21 000	5.7	5.7	/	/	100	/	/	/
Exponential phase of growth									
Bacteria alone		0.5	/	/	0.5	/	/	100	/
BODIPY-vancomycin	41 000	1.8	5.7	1.5	0.5	2	11	87	18
BODIPY-vancomycin+ rifampin	31 000	1.4	5.7	1.2	0.5	1	7	92	14
Biofilms									
Bacteria alone		0.5	/	/	0.5	/	/	100	/
BODIPY-vancomycin	19 000	1.7	5.7	1.7	0.5	2	25	73	8
BODIPY-vancomycin+ rifampin	5 500	1.2	5.7	1.6	0.5	1	14	84	7

Table 1 Summary of the fluorescence lifetimes τ_i and the amplitude-averaged populations a_i of BODIPY-FL-vancomycin, alone and mixed with rifampin within exponentially-growing cells and inside biofilms. The data for free bacteria and free antibiotics are also reported as references. Fluorescence photon counts obtained during 10-min acquisition correspond to the areas under fluorescence decays. τ_f is the mean fluorescence lifetime. a_1/a_2 represents the ratio between free BODIPY-FL-vancomycin population and the one interacting with bacteria. All the fluorescence lifetimes and populations values are given with a 10% accuracy. Excitation wavelength: 930 nm. Fluorescence emission range: 400-800 nm

What is behind this differential efficacy of vancomycin-rifampin association between biofilms and exponentially-growing bacteria? We have first considered an eventual complex formation between both drugs and its behaviour in contact with bacteria.

Steady-state and dynamic fluorescence spectroscopies experiments revealed a static quenching process of vancomycin fluorescence in the presence of rifampin. The complexation between the two antibiotics is only possible if they are in proximity and well-oriented each other, generally corresponding to the formation of a strong π-stacking non-fluorescent complex. Furthermore, more than one vancomycin molecule interacted with each rifampin molecule. In agreement with an interaction between the two antibiotics, time-lapse measurements revealed a faster penetration rate of the drugs complex in biofilms by comparison with BODIPY-FL-vancomycin alone. This can be due to less non-specific interaction of vancomycin, in such a complex, with the biofilm matrix components.[28]

Interestingly, time-lapse experiments also highlighted that despite the occurrence of complex formation between the two antibiotics, the fluorescence intensity evolution of BODIPY-FL-vancomycin measured at the biofilm basis, in the absence and in the presence of rifampin, was similar. This result can only be explained considering a dissociation of the antibiotics complex at the bacterial site, a hypothesis supported by fluorescence lifetime results. Indeed, the large difference (80%) of the fluorescence photon counts between BODIPY-FL-vancomycin alone and added to rifampin in solution was not recovered anymore in the presence of exponentially-growing bacteria. This result can only be attributed to a dissociation of the drug complex at the bacterial cell surface, a consequence of the higher affinity of vancomycin for its biological target (the peptidoglycan). Rifampin is then free to penetrate the cell and reach its own target, ARN. This total dissociation of the antibiotics complex occurring in the presence of exponentially-growing bacteria was not as efficient within biofilms. As a matter of fact, biofilms cells secrete an extracellular polymeric matrix that is believed to retain some of the vancomycin-rifampin complexes, thus preventing them from reaching their bacterial target. Is this the cause of the reduced synergistic effect of the two drugs when added in biofilms by comparison to exponentially-growing bacteria?

Although the antibiotics reached the deepest layers of the biofilms (as revealed by time-lapse measurements, Fig. 5) and dead cells were homogeneously localized through the whole three-dimensional biostructure (Fig. 2), a possible lack of antibiotics bioavailability at the bacterial cell site must be considered. FRAP experiments, centered on a single bacterium, revealed that a significant percentage of non-complexed BODIPY-FL-vancomycin molecules (40% ± 10%) was freely diffusing in the cell vicinity, indicating an excess of antibiotic in addition to the concentration fixed on the cell surface. We can thus ascertain that the failure of the drugs association activity in biofilms is not due to a lack of vancomycin bioavailability at the concentration of 40 µg/ml. Nor is it caused by a too low concentration of rifampin (20 µg/ml) since similar drug association effect was observed with a twice lower rifampin concentration. Altogether, these results suggest that the lack of antibiotics efficiency against biofilms may rather be assigned to a specific physiology adopted by biofilm-embedded cells, allowing them to circumvent the drugs activity and which should further be studied.

Another important feature of this study concerns the proper concentrations and/or the administration mode of antibiotics. When a single application of vancomycin at 20 µg/ml and rifampin at 10 µg/ml was used, vancomycin concentration was insufficient to kill rifampin-resistant mutants beyond 24 h of drugs exposure. However, repetitive drug applications at regular interval times, as performed in clinical practice, led to a bactericidal activity maintained over time. Similar antibiotics efficacy was obtained for a single application of vancomycin at

40 μg/ml and rifampin 10 μg/ml. This strongly implies that vancomycin needs to be available over time for effectively eradicating rifampin-resistant mutants.

Conclusions

Taken together, the results of this work demonstrated that complementing conventional microbiological methods with the use of fluorescence spectroscopic and imaging tools allows to provide deeper insights into antibiotics (in)action against *S. aureus* biofilms. We showed that the combination of vancomycin and rifampin can be bactericidal against such biofilms, only if proper concentrations and administration mode of the antibiotics were used. Spectroscopic tools showed that both antibiotics interacted by forming a non-fluorescent complex. Fluorescence imaging revealed that this complex allowed a fastened penetration of the drugs before dissociating from each other to interact with their respective biological targets. To prevent effectively the newly-formed resistant mutants and thus enhance the combined drugs activity, sufficiently high concentrations of free vancomycin should be maintained, either by increasing vancomycin concentration or by applying repetitive doses of the two drugs.

Acknowledgements

The authors want to thank the Centre de Photonique Biomédicale (CPBM) of the Centre Laser de l'Université Paris-Sud (CLUPS/LUMAT FR2764, Orsay, France) for the confocal microscope and L2 microbiology facilities, and Rachel Méallet-Renault for the spectrofluorimeter facilities at the Ecole Normale Supérieure (ENS Cachan).

References

1 F. D. Lowy, *J Clin Invest.*, 2003, **111**, 1265–1273.
2 C. E. Edmiston, A. J. McBain, C. Roberts and D. Leaper, *Adv. Exp. Med. Biol.*, 2015, **830**, 47–67.
3 H.-C. Flemming and J. Wingender, *Nat. Rev. Microbiol.*, 2010, **8**, 623–633.
4 P. A. Smith and F. E. Romesberg, *Nat. Chem. Biol.*, 2007, **3**, 549–556.
5 H. Van Acker, P. Van Dijck and T. Coenye, *Trends Microbiol.*, 2014, **22**, 326–333.
6 I. Levin-Reisman, I. Ronin, O. Gefen, I. Braniss, N. Shoresh and N. Q. Balaban, *Science*, 2017, eaaj2191.
7 V. Kostenko, H. Ceri and R. J. Martinuzzi, *FEMS Immunol. Med. Microbiol.*, 2007, **51**, 277–288.
8 K. L. LaPlante and S. Woodmansee, *Antimicrob. Agents Chemother.*, 2009, **53**, 3880–3886.
9 S. Deresinski, *Clin. Infect. Dis.*, 2009, **49**, 1072–1079.
10 H.-J. Tang, C.-C. Chen, K.-C. Cheng, K.-Y. Wu, Y.-C. Lin, C.-C. Zhang, T.-C. Weng, W.-L. Yu, Y.-H. Chiu, H.-S. Toh, S.-R. Chiang, B. A. Su, W.-C. Ko and Y.-C. Chuang, *Antimicrob. Agents Chemother.*, 2013, **57**, 5717–5720.
11 O. Cirioni, F. Mocchegiani, R. Ghiselli, C. Silvestri, E. Gabrielli, E. Marchionni, F. Orlando, D. Nicolini, A. Risaliti and A. Giacometti, *Eur. J. Vasc. Endovasc. Surg.*, 2010, **40**, 817–822.
12 S. M. Jones, M. Morgan, T. J. Humphrey and H. Lappin-Scott, *The Lancet*, 2001, **357**, 40–41.
13 D. C. Bean and S. M. Wigmore, *mBio*, 2015, **6**, e00120-15.
14 G. N. Forrest and K. Tamura, *Clin. Microbiol. Rev.*, 2010, **23**, 14–34.
15 W. Zimmerli, R. Frei, A. F. Widmer and Z. Rajacic, *J. Antimicrob. Chemother.*, 1994, **33**, 959–967.
16 W. Wehrli, *Rev. Infect. Dis.*, 1983, **5**, S407–S411.
17 Barna JC and Williams DH, *Annu. Rev. Microbiol.*, 1984, **38**, 339–357.
18 J. A. Niska, J. H. Shahbazian, R. I. Ramos, K. P. Francis, N. M. Bernthal and L. S. Miller, *Antimicrob. Agents Chemother.*, 2013, **57**, 5080–5086.
19 D. C. Coraça-Huber, M. Fille, J. Hausdorfer, K. Pfaller and M. Nogler, *J. Appl. Microbiol.*, 2012, **112**, 1235–1243.
20 F. D. Lowy, D. S. Chang and P. R. Lash, *Antimicrob. Agents Chemother.*, 1983, **23**, 932–934.
21 P. Vergidis, M. S. Rouse, G. Euba, M. J. Karau, S. M. Schmidt, J. N. Mandrekar, J. M. Steckelberg and R. Patel, *Antimicrob. Agents Chemother.*, 2011, **55**, 1182–1186.
22 C. Watanakunakorn and J. C. Guerriero, *Antimicrob. Agents Chemother.*, 1981, **19**, 1089–1091.
23 A. H. Salem, W. F. Elkhatib and A. M. Noreddin, *J. Pharm. Pharmacol.*, 2011, **63**, 73–79.
24 G. L. Simon, R. H. Smith and M. A. Sande, *Rev. Infect. Dis.*, 1983, **5 Suppl 3**, S507-508.
25 S. Tremblay, T. T. Y. Lau and M. H. H. Ensom, *Ann. Pharmacother.*, 2013, **47**, 1045–1054.
26 D. J. Riedel, E. Weekes and G. N. Forrest, *Antimicrob. Agents Chemother.*, 2008, **52**, 2463–2467.
27 A. S. van der Horst, S. Medda, E. Ledbetter, A. Liu, P. Weinhold, D. J. Del Gaizo and L. Dahners, *J. Orthop. Res.*, 2015, **33**, 1320–1326.
28 S. Daddi Oubekka, R. Briandet, M.-P. Fontaine-Aupart and K. Steenkeste, *Antimicrob. Agents Chemother.*, 2012, **56**, 3349–3358.
29 R. Boudjemaa, R. Briandet, M. Revest, C. Jacqueline, J. Caillon, M.-P. Fontaine-Aupart and K. Steenkeste, *Antimicrob. Agents Chemother.*, 2016, **60**, 4983–4990.
30 P. S. Stewart, *J. Bacteriol.*, 2003, **185**, 1485–1491.
31 S. Daddi Oubekka, R. Briandet, F. Waharte, M.-P. Fontaine-Aupart and K. Steenkeste, in *Proc. SPIE 8087, Clinical and Biomedical Spectroscopy and Imaging II, 80871I*, eds. N. Ramanujam and J. Popp, Proc. SPIE 8087, Clinical and Biomedical Spectroscopy and Imaging II, 80871I, 2011, vol. Proc. SPIE 8087, Clinical and Biomedical Spectroscopy and Imaging II, 80871I, p. 80871I–80871I–7.
32 F. Waharte, K. Steenkeste, R. Briandet and M.-P. Fontaine-Aupart, *Appl. Environ. Microbiol.*, 2010, **76**, 5860–5869.
33 A. Tupin, M. Gualtieri, F. Roquet-Banères, Z. Morichaud, K. Brodolin and J.-P. Leonetti, *Int. J. Antimicrob. Agents*, 2010, **35**, 519–523.
34 N. Høiby, T. Bjarnsholt, M. Givskov, S. Molin and O. Ciofu, *Int. J. Antimicrob. Agents*, 2010, **35**, 322–332.

Fig. S1 Chemical structures of vancomycin, rifampin and BODIPY-FL-vancomycin

Vancomycin	Rifampin	BODIPY-FL-vancomycin
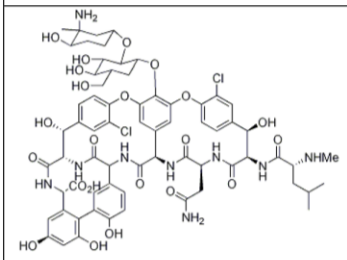	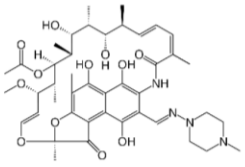	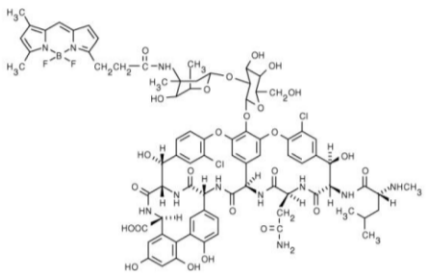

4.2. Article 5 : "New insight into daptomycin bioavailability and localization in *Staphylococcus aureus* biofilms by dynamic fluorescence imaging"

Rym Boudjemaa, Romain Briandet, Matthieu Revest, Cédric Jacqueline, Jocelyne Caillon, Marie-Pierre Fontaine-Aupart, Karine Steenkeste

Antimicrobial Agents and Chemotherapy, 2016

AMERICAN SOCIETY FOR MICROBIOLOGY | Antimicrobial Agents and Chemotherapy

New Insight into Daptomycin Bioavailability and Localization in *Staphylococcus aureus* Biofilms by Dynamic Fluorescence Imaging

Rym Boudjemaa,[a] Romain Briandet,[b] Matthieu Revest,[c,d] Cédric Jacqueline,[d] Jocelyne Caillon,[d] Marie-Pierre Fontaine-Aupart,[a] Karine Steenkeste[a]

Institut des Sciences Moléculaires d'Orsay (ISMO), CNRS, Université Paris-Sud, Université Paris-Saclay, Orsay, France[a]; Micalis Institute, INRA, AgroParisTech, Université Paris-Saclay, Jouy-en-Josas, France[b]; CHU Rennes, Rennes, France[c]; Université de Nantes, Faculté de Médecine, UPRES EA 3826, Nantes, France[d]

***Staphylococcus aureus* is one of the most frequent pathogens responsible for biofilm-associated infections (BAI), and the choice of antibiotics to treat these infections remains a challenge for the medical community. In particular, daptomycin has been reported to fail against implant-associated *S. aureus* infections in clinical practice, while its association with rifampin remains a good candidate for BAI treatment. To improve our understanding of such resistance/tolerance toward daptomycin, we took advantage of the dynamic fluorescence imaging tools (time-lapse imaging and fluorescence recovery after photobleaching [FRAP]) to locally and accurately assess the antibiotic diffusion reaction in methicillin-susceptible and methicillin-resistant *S. aureus* biofilms. To provide a realistic representation of daptomycin action, we optimized an *in vitro* model built on the basis of our recently published *in vivo* mouse model of prosthetic vascular graft infections. We demonstrated that at therapeutic concentrations, daptomycin was inefficient in eradicating biofilms, while the matrix was not a shield to antibiotic diffusion and to its interaction with its bacterial target. In the presence of rifampin, daptomycin was still present in the vicinity of the bacterial cells, allowing prevention of the emergence of rifampin-resistant mutants. Conclusions derived from this study strongly suggest that *S. aureus* biofilm resistance/tolerance toward daptomycin may be more likely to be related to a physiological change involving structural modifications of the membrane, which is a strain-dependent process.**

Staphylococcus aureus is a Gram-positive bacterial species shown to be the most frequent cause of biofilm-associated infections (BAI) (1) and one of the major causes of morbidity and mortality in hospitals and communities (2). Unlike planktonic cells, biofilms exhibit specific phenotypic traits allowing them to resist host defenses and antibiotic treatments (3), which frequently leads to chronic infections such as endocarditis, sinusitis, and osteomyelitis and also to implant-associated infections (4).

Among the most recent clinically used antibiotics, daptomycin is a cyclic lipopeptide approved for the treatment of serious staphylococcal infections such as bacteremia and implant-related infections (5). Daptomycin is a calcium-dependent antibiotic that acts by insertion into the Gram-positive cytoplasmic membranes where it forms oligomeric pores, causing potassium ion leakage and subsequent membrane depolarization, leading ultimately to cell death (6). As is the case for many antibiotics, daptomycin has been shown to exhibit a significant bactericidal activity against planktonic cells (7–9). However, the eradication of adherent bacteria is rarely achieved despite the large number of *in vitro* and animal studies in which daptomycin activity was evaluated (10–16). Besides the results of the literature that appear controversial (17), direct comparison between studies is not directly possible, since the biofilm growth and treatment protocols used differ greatly.

To obtain a realistic representation of daptomycin action against *S. aureus* biofilms, we developed an *in vitro* model built on the basis of our recently published *in vivo* study on *S. aureus* prosthetic vascular graft infections using the same strains (18). The interest of this approach was the possibility to use fluorescence imaging techniques that cannot be employed *in vivo* (confocal laser scanning microscopy [CLSM], time-lapse microscopy, and fluorescence recovery after photobleaching [FRAP]) to examine the penetration, diffusion, bioavailability, and localization of the fluorescently labeled antibiotic inside the biofilms. To validate this approach, we monitored for 72 h the activity of daptomycin against biofilms formed by methicillin-susceptible and methicillin-resistant clinical and collection strains. In addition, we enriched the culture medium with proteins and calcium to mimic the *in vivo* physiological conditions of our mouse model (18). The same experiments were performed in the presence of rifampin, an antibiotic that can be combined with daptomycin for recalcitrant *S. aureus* BAI.

MATERIALS AND METHODS

Bacterial strains. Four *S. aureus* strains were tested in the present study: two were collection strains (methicillin-susceptible *S. aureus* [MSSA] ATCC 27217 and methicillin-resistant *S. aureus* [MRSA] ATCC 33591), and two others were isolated from patients with *S. aureus* bloodstream infections (MSSA 176 and MRSA BCB8). All strains were kept at −80°C in tryptic soy broth (TSB) (bioMérieux, France) containing 20% (vol/vol) glycerol. The frozen cells were subcultured twice in TSB (one 8-h culture, followed by an overnight culture) to constitute the stock cultures from which aliquots were kept at −20°C. Bacterial growth and experiments were both conducted at 37°C.

Received 31 March 2016 Returned for modification 1 May 2016
Accepted 3 June 2016
Accepted manuscript posted online 13 June 2016
Citation Boudjemaa R, Briandet R, Revest M, Jacqueline C, Caillon J, Fontaine-Aupart M-P, Steenkeste K. 2016. New insight into daptomycin bioavailability and localization in *Staphylococcus aureus* biofilms by dynamic fluorescence imaging. Antimicrob Agents Chemother 60:4983–4990. doi:10.1128/AAC.00735-16.
Address correspondence to Rym Boudjemaa, rym.boudjemaa@u-psud.fr.
Supplemental material for this article may be found at http://dx.doi.org/10.1128/AAC.00735-16.

Antimicrobial agents and medium. Daptomycin and rifampin were both purchased from Sigma (France). The fluorescently labeled antibiotic BODIPY-FL-labeled daptomycin (BODIPY-FL-daptomycin) (BODIPY-FL is fluorescently labeled boron-dipyrromethene) was a kind gift from Cubist Pharmaceuticals (MA, USA), and BODIPY-FL was purchased from Invitrogen (France). According to the manufacturer's instructions, the stock solutions were prepared by diluting daptomycin and BODIPY-FL-daptomycin in dimethyl sulfoxide (1 mg/ml) and by diluting rifampin in sterile water (2 mg/ml), which were then kept at −20°C. Before the solutions were used, they were diluted in TSB enriched with proteins (bovine serum albumin[BSA], 36 g/liter; Sigma, France) and calcium ($CaCl_2 \cdot 2H_2O$, 50 mg/liter; Sigma, France) to mimic *in vivo* physiological levels. It has been determined that, under these conditions, the final concentration of dimethyl sulfoxide was noncytotoxic for the bacteria. Clinically meaningful concentrations were used in this study: 20 μg/ml for both daptomycin and rifampin. When combined, the antibiotics were mixed together before application to the biofilm surface.

Susceptibility testing. The MICs of daptomycin and rifampin were determined by the broth microdilution method in cation-adjusted Mueller-Hinton broth (CAMHB), according to the European Committee on Antimicrobial Susceptibility Testing (EUCAST). Media were supplemented with 50 mg/liter Ca^{2+} for daptomycin.

Characterization of molecular interactions between daptomycin and rifampin by absorption and fluorescence spectroscopies. Absorption spectra of antibiotics alone and in combination were measured with a Varian Cary 300 spectrophotometer (Agilent Technologies, France). The corresponding fluorescence emission spectra were recorded using a Fluorolog-3 (Jobin Yvon, Inc., France) fluorescence spectrophotometer mounted with front-face detection geometry by exciting daptomycin at 360 nm. The measurements were made five times on each sample.

***In vitro* biofilm preparation and antibiotic activities.** Biofilms were studied in a polystyrene microtiter plate-based assay since it has been shown that this material has physicochemical properties close to that of biomaterial surfaces such as polyethylene terephthalate, which is used in vascular grafts (19, 20). For the preparation of *S. aureus* biofilms, 250-μl portions of an overnight subculture adjusted to an optical density at 600 nm of 0.02 (corresponding to ~10^8 CFU/ml) were added to 96-well microplates (μClear; Greiner Bio-One, France). After a 1.5-h adhesion period at 37°C, the wells were rinsed with sterile physiological water (150 mM NaCl) in order to eliminate nonadherent cells, refilled with sterile TSB enriched with proteins and calcium (TSBpc) and then incubated for 24 h at 37°C to allow biofilm growth.

To assess antibiotic activities, the 24-h biofilms were rinsed with a 150 mM NaCl aqueous solution before adding the antibiotic solutions diluted in TSBpc as described previously. Viable culturable bacteria were then counted at time points at regular intervals: 0 h (when antibiotics are added), 24, 48, and 72 h after antibiotic injection. For each time point, bacterial cultures were centrifuged 10 min at 7,000 × *g* in order to eliminate excess antibiotic. The bacterial pellet was suspended in a 150 mM NaCl sterile saline solution, centrifuged again, and suspended in the same conditions. Successive decimal dilutions were then performed. For each dilution, 6 drops (10 μl) were deposited on tryptic soy agar (TSA) plates (bioMérieux, France) and incubated at 37°C during 24 h. CFU were counted and averaged for each dilution at each time point. The detection limit of viable culturable cells was 100 CFU/ml.

Percentages of rifampin-resistant mutants in biofilms. To determine the percentages of rifampin-resistant mutants, the antibiotic solutions (rifampin alone or combined with daptomycin) were added to 24-h biofilms. CFU were counted on TSA plates or TSA plates containing rifampin (20 μg/ml) at 24 and 48 h after antibiotic injections. The percentages were obtained by calculating the ratio between the number of CFU grown on rifampin-containing TSA plates and the number of CFU grown on rifampin-free TSA plates.

Statistical analysis. The mean $\log_{10}$ CFU/milliliter and biovolume for each therapy were compared with each other by analysis of variance (ANOVA). They were performed using the Statgraphics software (Manugistics, Rockville, MD, USA). Statistical significance was defined as a *P* value of less than 0.05 by a Fisher test.

Confocal laser scanning microscopy. (i) Visualization of antibiotic activities against biofilms using LIVE/DEAD staining. Biofilms grown for 24 h prepared as described previously were observed 24, 48, and 72 h after antibiotic addition using a Leica TCS SP5 confocal laser scanning microscope (Leica Microsystems, France) at the Centre de Photonique Biomédicale (CPBM) (Orsay, France). Prior to each observation, bacteria were stained with 2.5 μM Syto9 (Life Technologies, France), a green cell-permeant nucleic acid dye, and 30 μM propidium iodide (PI) (Life Technologies, France), a red nucleic acid dye that can penetrate cells with compromised membranes (dead cells) only. Syto9 and PI were sequentially excited at 488 nm and 543 nm, respectively, and their fluorescence emissions were collected between 500 and 600 nm for Syto9 and between 640 and 750 nm for PI. Images were acquired using a 63× oil immersion objective with a 1.4 numerical aperture. The size of the confocal images was 512 by 512 pixels (82 by 82 μm^2), recorded with a z-step of 1 μm. For each biofilm, four typical regions were analyzed. Images were reconstructed in three dimensions (3D) using ICY software.

(ii) Quantification of biovolumes and maximum biofilm thickness. Maximum biofilm thickness (in micrometers) was measured directly from xyz stacks. Biovolumes (in cubic micrometers) were calculated by binarizing images with a java script executed by ICY software as described previously (21). The biovolume was then defined as the overall volume of cells in the observation field. The percentage of dead cells corresponds to the ratio between biovolumes of PI-stained bacteria and Syto9-stained bacteria.

(iii) Antibiotic penetration and localization inside biofilms. To study the penetration of BODIPY-FL-daptomycin alone and combined with rifampin within 24-h biofilms, we employed time-lapse microscopy, as described before (22), using the same Leica TCS SP5 confocal microscope. Briefly, the fluorescence intensity evolution over time was observed in a defined focal plane (5 μm above the substratum surface). As soon as the TSBpc-diluted solutions of BODIPY-FL-daptomycin alone or combined with rifampin were added to the biofilm, fluorescence intensity images were acquired every second for 15 min. Simultaneously, transmission images were acquired to ensure that no structural alteration of the biofilm occurred during this process. The labeled antibiotic was excited with a continuous argon laser line at 488 nm through a 63× oil immersion objective, and the emitted fluorescence was recorded within 500 and 600 nm.

The corresponding diffusive penetration coefficients (D_p) through the biofilms were determined according to the relationship previously described by Stewart (23):

$$D_p = 1.03 \times L^2 / t_{90} \quad (1)$$

where *L* is the biofilm thickness and t_{90} is the time required to attain 90% of the equilibrium staining intensity at the deeper layers of the biofilm.

To observe the localization of the fluorescently labeled daptomycin within biofilms, bacteria were counterstained with the FM4-64 dye (Life Technologies, France): this dye was also excited at 488 nm, but its fluorescence emission was collected within the range 640 to 750 nm. The images (512 by 512 pixels) of both fluorophores were simultaneously recorded with a z-step of 1 μm.

(iv) Antibiotic diffusion and bioavailability inside biofilms using FRAP experiments. Image-based fluorescence recovery after photobleaching (FRAP) measurements was used to assess local diffusion and bioavailability of the fluorescently labeled daptomycin. Briefly, FRAP is based on a brief excitation of fluorescent molecules by a very intense light source in a user-defined region to irreversibly photobleach their fluorescence. Fluorescence recovery is then probed over time at a low light power in the same photobleached region (22, 24). All time-resolved measurements were obtained using the same confocal microscope. The time course of fluorescence intensity recovery was analyzed with mathematical models, giving us the quantitative mobility of the fluorescent molecules

TABLE 1 MICs of daptomycin and rifampin against the four *S. aureus* strains[a]

S. aureus strain	MIC (mg/liter) of:	
	Daptomycin	Rifampin
MSSA ATCC 27217	0.25	<0.06
MSSA 176	0.5	0.015
MRSA ATCC 33591	0.25	0.0075
MRSA BCB8	0.125	<0.06

[a] The standard deviations of the values are ±5%.

and allowing us to determine the diffusion coefficients. For all FRAP experiments, the fluorescence intensity image size was fixed to 512 by 128 pixels with an 80-nm pixel size and recorded using a 12-bit resolution. The line scan rate was fixed at 1,400 Hz, corresponding to a total time between frames of ~265 ms. As determined previously, the full widths at half maximum in xy and z (along the optical axis) of the bleached profile were 0.8 μm and 14 μm, respectively, allowing us to neglect diffusion along the axial/vertical axis and thus to consider only two-dimensional diffusion. Each FRAP experiment started with the acquisition of 50 images at 7% of laser maximum intensity (7 μW) followed by a 200-ms single bleached spot at 100% laser intensity. A series of 450 single-section images was then collected with the laser power attenuated to its initial value (7% of the bleach intensity). The first image was recorded 365 ms after the beginning of bleaching.

RESULTS

Susceptibility testing. The MICs obtained for daptomycin and rifampin against the four *S. aureus* strains are presented in Table 1. All isolates in planktonic conditions were susceptible to daptomycin and rifampin. The breakpoint values of drugs according to the European Committee on Antimicrobial Susceptibility Testing (EUCAST) in 2016 are as follows: 2 mg/liter for vancomycin; 1 mg/liter for daptomycin; for rifampin, sensitivity of ≤0.06 mg/liter and resistance of >0.5 mg/liter.

Spectroscopic characterization of the interaction between rifampin and daptomycin. Neither the photonic absorption properties nor the fluorescence emission spectrum of daptomycin were significantly influenced by the addition of rifampin (Fig. 1), revealing the absence of cross-reaction between the two antibiotics.

BODIPY-FL-daptomycin penetration, diffusion, bioavailability, and localization inside *S. aureus* biofilms. (i) Time-lapse imaging. Time-lapse experiments were performed to visualize *in situ* penetration of fluorescently labeled daptomycin alone and combined with rifampin throughout the deepest layers of *S. aureus* biofilms. By setting the focal plane 5 μm above the substratum surface, we demonstrated that BODIPY-FL-daptomycin penetrated the biofilms (~30-μm thickness) within a few minutes: fluorescence intensity was measured a few seconds after antibiotic addition and increased rapidly to reach 90% of the maximal intensity in 9 min (see Fig. S1 and Movie S4 in the supplemental material). The penetration coefficients obtained from equation 1 ranged from 2.5 $\mu m^2/s \pm 0.7$ $\mu m^2/s$ for *S. aureus* ATCC 27217, 176, and ATCC 33591 to 4.9 $\mu m^2/s \pm 0.7$ $\mu m^2/s$ for *S. aureus* BCB8. These values are both of the same order by comparison with BODIPY-FL alone for which the penetration coefficient was higher at 140 $\mu m^2/s$ (22). The coefficients were not statistically different in comparison with those of daptomycin in the presence of rifampin.

(ii) FRAP imaging. FRAP was used to measure the local diffusion of BODIPY-FL-daptomycin and its interaction with bacteria within biofilms. According to the FRAP principle (22, 24, 25), if the fluorescently labeled daptomycin molecules are allowed to move freely in the sample, total fluorescence recovery is observed, meaning that the fluorescence is redistributed in the defined region. Conversely, if the fluorescence recovery is not total after the photobleaching, it means that a fraction of molecules is not diffusing freely and thus interacts with its local environment. The other fraction diffuses and is thus bioavailable.

First, we checked that no bacterial movement occurred during image acquisition by representing kymograms, two-dimensional graphs of fluorescence intensity measured along a line (here a straight line drawn on the full width of the images) for each image of the FRAP series (Fig. 2a). A typical FRAP curve of BODIPY-FL-daptomycin in *S. aureus* biofilms is presented in Fig. 2b. Whatever the bacterial strains or the treatments used (daptomycin alone or in combination with rifampin), we demonstrated here that the fluorescence recovery was not total after photobleaching: only 20% of BODIPY-FL-daptomycin molecules interacted with the environment, meaning that a large excess of molecules (80%) were diffusing freely in the defined regions and thus bioavailable (mean local diffusion coefficient, 7.1 ± 0.6 $\mu m^2/s$).

(iii) Localization of the fluorescently labeled daptomycin alone or combined with rifampin depending on the surrounding environment. As daptomycin is known to be highly bound to serum proteins (90 to 93%) (26), we addressed the question of whether there could be a different localization of the fluorescently labeled daptomycin in a protein-enriched medium. As shown in Fig. 3, fluorescence intensity images were significantly different depending on the surrounding medium: regardless of the strain tested, the antibiotic appeared to be colocalized with the FM4-64 dye at the bacterial site when the surrounding medium was an aqueous NaCl solution supplemented with calcium, while the antibiotic localization appeared to be mainly extracellular when the medium was enriched with proteins (TSBpc). The addition of rifampin did not affect daptomycin localization in the biofilm.

Combining 3D fluorescence imaging and time-kill studies to assess *S. aureus* biofilm inactivation in the presence of daptomycin alone and in association with rifampin. We used confocal microscopy to describe the three-dimensional structures of biofilms and the temporal distribution of both live and dead cells throughout the biofilm thickness.

Fluorescence intensity images showed that the biofilms formed by the four strains yielded similar compact structures (controls in Fig. 4a and controls in Fig. S2 in the supplemental material). Their

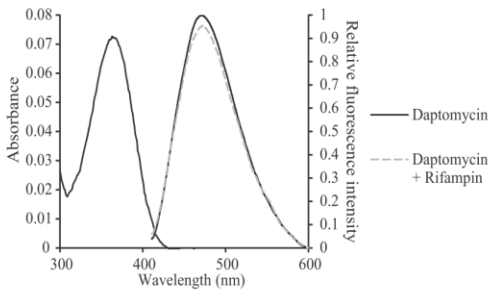

FIG 1 Absorption and fluorescence spectra of daptomycin (20 μg/ml) alone and combined with rifampin (20 μg/ml). The excitation wavelength was 360 nm.

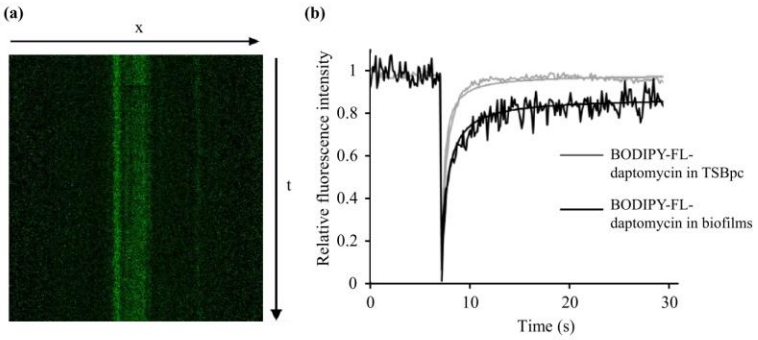

FIG 2 FRAP acquisitions for BODIPY-FL-daptomycin inside *S. aureus* biofilms. (a) Kymogram representation (x,t) of FRAP acquisitions. The line along which the kymogram was done is 38 μm. (b) Typical fluorescence recovery curves representative of six different zones for each condition: BODIPY-FL-daptomycin inside biofilms (black) and inside TSBpc without biofilm (gray). The kymogram and fluorescence recovery curve presented here are the ones obtained for MSSA ATCC 27217 biofilms, since they were representative of the data obtained for the other strains in the presence or absence of rifampin.

thicknesses were not significantly variable from one strain to another (25 to 29 μm; $P > 0.05$) or from one time point to another time point (24 h and 72 h). This is a reasonable result given that the culture medium (TSBpc) was renewed before the first observation but not over time: thus, biofilm development mainly occurred during the first 24 h.

When treated with daptomycin, biofilms exhibited more areas free of cells compared to the controls (Fig. 4a; see Fig. S2 in the supplemental material). This can be related to significant decreases in biofilm thicknesses (19 to 21 μm in the presence of daptomycin; $P < 0.05$) compared to the control biofilms. Moreover, in the presence of daptomycin, no statistically significant change in the proportion of cell death over time was quantified (10 to 30%; $P > 0.05$) (Fig. 4b). However, the MRSA clinical isolate (BCB8) was more susceptible to daptomycin: ~60% of cell death was quantified at 24 h, a value that decreased beyond 24 h (40% at 72 h; $P < 0.05$) due to cell regrowth (see below).

Compared to the monotherapy treatment, the structures and thicknesses of biofilms were not affected when they were treated with daptomycin in combination with rifampin. However, under these conditions, a significantly higher proportion of cell death was observed, achieving 85% at 72 h ($P < 0.01$) (Fig. 4b). For the two MSSA strains (ATCC 27217 and strain 176) and the MRSA collection strain (ATCC 33591), the antibiotic association activity (daptomycin plus rifampin) gradually increased over time (Fig. 4), while the maximum activity against the MRSA clinical strain (BCB8) was reached within 24 h.

Another observation of interest (Fig. 4a) is that upon daptomycin exposure, dead cells were observed over the whole biofilm depth, including the basal layer of cells in contact with the substratum, providing further evidence of the antibiotic penetration throughout the deepest layers of the biofilms. This result is even more pronounced for the BCB8 strain because of the greater proportion of dead cells involved by the action of daptomycin. This process was also observed when daptomycin was used in association with rifampin.

These data from fluorescence imaging were supported by CFU counts of suspended biofilms (Fig. 5). The results confirm that daptomycin alone was ineffective against biofilms formed by the two MSSA strains (ATCC 27217 and strain 176) and the MRSA collection strain (ATCC 33591). For the MRSA clinical isolate (BCB8), reduction in bacterial counts of only ~1 to 2 log units was measured at 24 h before regrowth was observed to reach the same values as for the MSSA biofilms.

In accordance with fluorescence imaging data, the activity of the combination of antibiotics was much greater than that of monotherapy. The sensitivity of the microbiological method allowed us to determine that the cell population decreased by ~4 log units after 72 h of treatment ($P < 0.05$). The emergence of rifampin-resistant mutants was verified. As presented in Fig. 6, daptomycin dramatically prevented the emergence of rifampin-resistant mutants when the combination of daptomycin and rifampin was used.

DISCUSSION

The choice of antibiotics to treat *S. aureus* BAI remains a challenge for the medical community. In this context, the ambivalence of the published results on daptomycin activity is a relevant example. Despite increasing data about daptomycin as an option to treat implant-associated *S. aureus* infections, as many failures (18, 27) as successes (7–9, 12) have been reported both in clinical practice and in laboratory models. This highlights that *S. aureus* BAI resistance/tolerance mechanisms to antimicrobials deserve more attention.

The biofilm-associated exopolymeric matrix may be considered to act as a shield to the antimicrobial diffusion reaction (28–32) by delaying its penetration and/or reducing its bioavailability. To verify this hypothesis noninvasively, we took advantage of dynamic fluorescence imaging methods: confocal microscopy, time-lapse imaging, and FRAP. For our biofilm model and whatever the bacterial strain, no failure of daptomycin penetrability or bioavailability was observed. The opposite finding described by Siala et al. (31) may be related to the conditions of fluorescence acquisition that were not well adapted to BODIPY-FL fluorescence. In this study, time-lapse fluorescence imaging experiments demonstrated that daptomycin rapidly reached the biofilm's deepest layers, while section views of fluorescence intensity images presented in Fig. 3 ascertain the presence of the fluorescently labeled antibiotic through the whole biofilm structure. Furthermore, FRAP results ascertained that only ~20% of the antibiotic molecules were immobilized. Thus, the majority of the antibiotic molecules were

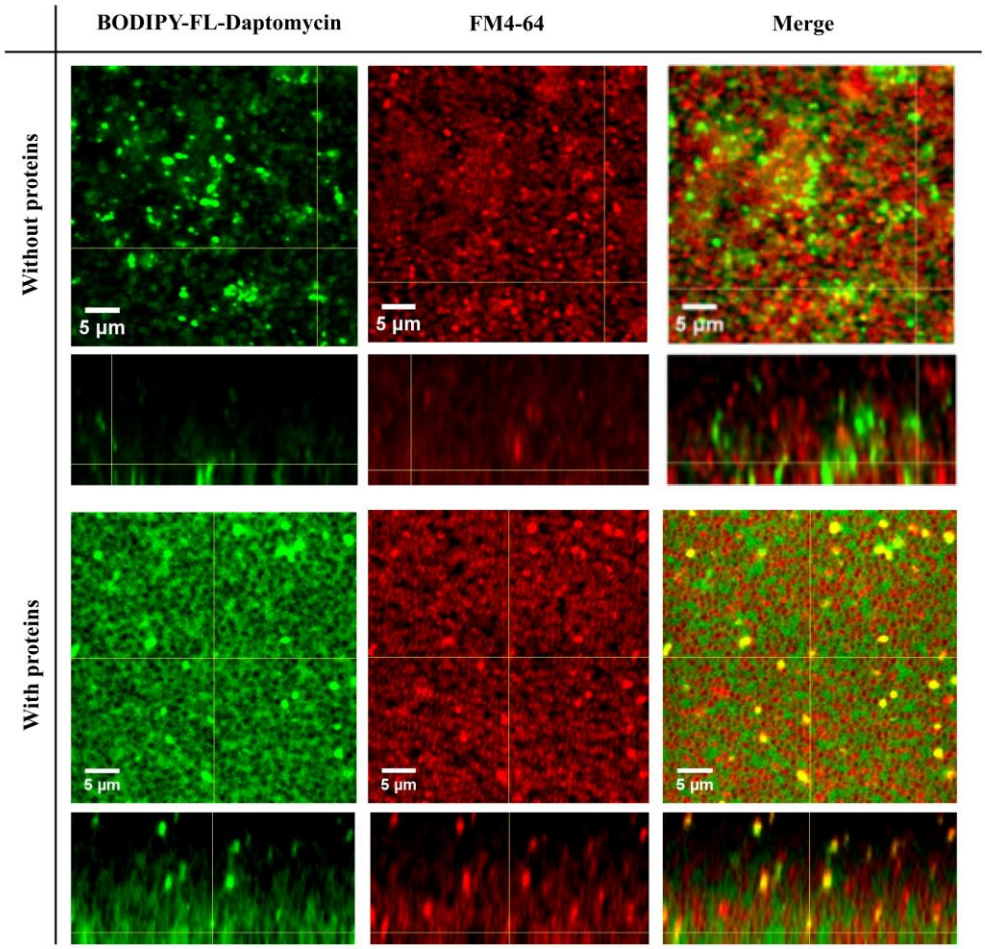

FIG 3 Fluorescence imaging of BODIPY-FL-daptomycin (green channel) and FM4-64 (red channel) in *S. aureus* biofilms. Merged images are also shown. In the top panels (Without proteins), the surrounding medium is an aqueous NaCl (150 mM) solution supplemented with calcium ions (50 mg/liter). In the bottom panels (With proteins), the surrounding medium is TSB enriched with proteins (36 g/liter) and calcium ions (50 mg/liter). Only images of MSSA ATCC 27217 biofilms are represented, since they were representative of all biofilms visualized for other strains in the presence or absence of rifampin.

in free movement and could be bioavailable through the biomass (~80% of nonimmobilized molecules).

We further addressed the question of whether or not daptomycin reached its bacterial target. Fluorescence intensity images provided interesting information, showing that the majority of fluorescently labeled antibiotic was distributed in the extracellular matrix rather than in the bacterial cell membranes (Fig. 3). This is in agreement with the well-known property of daptomycin to have a very high degree of protein binding, especially with serum albumin (90 to 93%) (26, 33) which is naturally present in physiological conditions. Nevertheless, the fluorescence recovery curves obtained by FRAP experiments in free medium and in the biofilms strongly suggested the reversibility of daptomycin protein binding (33, 34): the equilibrium between the bound and unbound states may conserve the apparent mobility of the antibiotic. Additional experiments were performed in a protein-free medium (a saline solution supplemented with calcium ions). In this case, bacterial cell membranes appeared as hot spots on fluorescence images, consistently with the described antibiotic interaction with its target (6). Surprisingly, whether the medium was protein-free or not, daptomycin exhibited the same lack of effectiveness, as revealed by time-kill studies performed by fluorescent LIVE/DEAD staining and conventional plating on agar (data in the absence of proteins not shown). Thus, the interaction with the matrix components cannot explain biofilm tolerance to the antibiotic.

Thus, the particular physiology of embedded bacteria should be considered, and more specifically, cells with low metabolic activity should be investigated. Previous studies using a bromodeoxyuridine (BrdU) immunofluorescent labeling technique demonstrated that the large majority of staphylococcal cells in a biofilm were actually in a low metabolic state (35, 36). Additionally, in the present study, the comparison of cell viability results obtained by CFU counts and fluorescence imaging highlighted a significant proportion of viable cells detected by LIVE/DEAD staining but not by CFU measurements. This subpopulation may

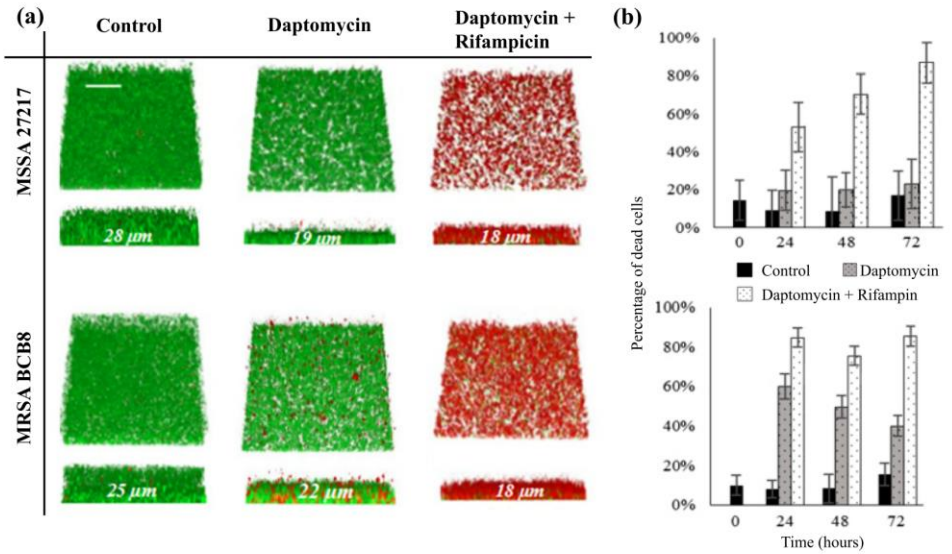

FIG 4 (a) Visualization of MSSA ATCC 27217 and MRSA BCB8 biofilms using 3D reconstruction to observe biofilm thickness. Images were collected without any drug exposure (control) and after 72-h exposure to unlabeled daptomycin (20 μg/ml) alone and in association with rifampin (20 μg/ml). Dead cells were stained red with propidium iodide, and all bacteria were stained green with Syto9. The acquisition was performed on the whole biofilm thickness with an axial displacement of 1 μm. The dimensions of the images are 82 by 82 μm^2. The mean thickness values of the biofilms over time (from 24 to 72 h) are written in white on each image. Bar, 20 μm. (b) Percentage of dead cells over time calculated from three series of biofilm images. The biofilms were not treated with daptomycin (control) or were treated with daptomycin (20 μg/ml) alone or combined with rifampin (20 μg/ml). The values are means ± standard deviations (error bars).

be considered viable but nonculturable (VBNC), a subpopulation known to have a slow metabolism (37–39). Moreover, it has been demonstrated that daptomycin is poorly effective against bacteria in stationary stage (7, 27). One can thus reasonably suggest that for bacteria with low metabolic activity, the cell membrane dysregulation induced by daptomycin may be slower and/or more difficult to attain due to structural modifications of the cell membrane. This assumption is supported by the reported data revealing that daptomycin displays a concentration-dependent bactericidal activity against dormant cells (7, 9, 12). In the present study, we tested a higher concentration (double) of daptomycin (40 μg/ml) on the different *S. aureus* biofilms, almost leading to bactericidal effects after 24 h of drug exposure (see Fig. S3 in the supplemental material) and showing no cell regrowth over time. However, biofilm clearance was not reached. This achievement was reported to occur at a daptomycin concentration equal to or greater than 100 μg/ml but may not be relevant in clinical practice (7, 9, 12).

Two distinctive findings in this study concern the BCB8 clinical isolate, which discriminated itself by a twofold-higher penetration coefficient compared to the other strains tested and a greater susceptibility as revealed by the observation of a larger proportion of dead cells over the whole biofilm thickness, including the basal layer in contact with the substratum. These results are in line with those obtained *in vivo* (18), which demonstrated a strain-dependent activity of daptomycin against *S. aureus* biofilms. In view of the antibiotic mechanism of action which is supposed to target the plasma membrane, the observed variable response depending on the bacterial strain may be due to a change in membrane composition or conformation from a strain to another.

Facing the lack of daptomycin efficiency in treating recalcitrant

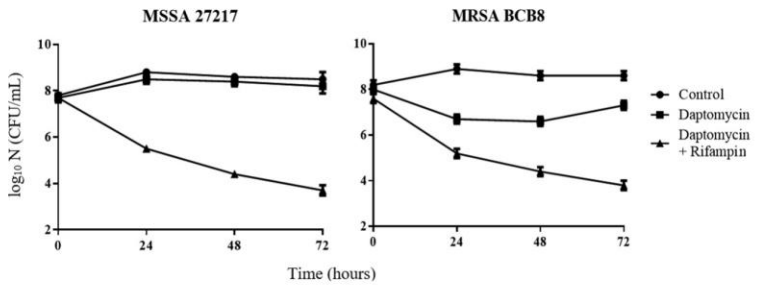

FIG 5 Time-kill curves of daptomycin (20 μg/ml) alone or combined or with rifampin (20 μg/ml) against MSSA ATCC 27217 and MRSA BCB8 biofilms. The values are means ± standard deviations (error bars).

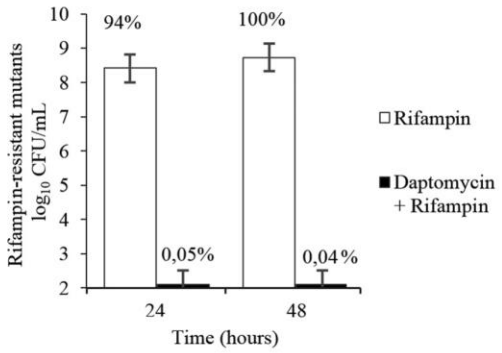

FIG 6 Number of rifampin-resistant mutants determined in MSSA ATCC 27217 biofilms counted on rifampin-containing TSA plates. The biofilms were treated with rifampin alone (20 μg/ml) or with the daptomycin-rifampin combination (20 μg/ml for both antibiotics). Above each bar is shown the percentage of rifampin-resistant mutants in *S. aureus* biofilms among the total bacterial population. Error bars represent the standard deviations.

S. aureus BAI, the addition of rifampin has raised great interest (10–13, 15, 40–42). In this study, we demonstrated that the combined therapy was indeed highly efficient against *S. aureus* biofilms but did not allow total bacterial clearance. Both antibiotics have been shown not to cross-react with each other, as evidenced by steady-state fluorescence spectroscopy. Moreover, the penetration, diffusion, and localization of the fluorescently labeled daptomycin were not affected by the presence of rifampin. We also proved here that rifampin-resistant mutants emerged when biofilms were treated with rifampin alone, but not when treated with the antibiotic combination. Altogether, the data presented here confirm that daptomycin prevents the emergence of rifampin-resistant mutants, allowing the bactericidal activity of rifampin to occur quickly, regardless of the cell physiological state.

In conclusion, consistently with the previous *in vivo* study aiming at evaluating the antibiotic efficacy in *S. aureus* prosthetic vascular graft infections (18), we demonstrated in the present *in vitro* model a strain-dependent lack of daptomycin activity toward biofilms. Dynamic fluorescence microscopy allowed discarding a lack of antibiotic availability and interaction with bacteria. Given the mode of action of daptomycin, these observations suggest a membrane-dependent factor of tolerance in such biofilms. Therefore, to provide a better understanding of the reduced activity of daptomycin against biofilms, the composition of the membrane should be analyzed.

ACKNOWLEDGMENTS

We thank the Centre de Photonique Biomédicale (CPBM) of the Centre Laser de l'Université Paris-Sud (CLUPS/LUMAT FR2764, Orsay, France) for allowing us to use the confocal microscope and L2 microbiology facilities, Rachel Méallet-Renault for allowing us to use the spectrofluorimeter facilities at the Ecole Normale Supérieure (ENS Cachan), and Jared Silverman (Cubist Pharmaceuticals) for providing BODIPY-FL-labeled daptomycin.

This work was supported by a grant from the Ministère de l'Education Nationale, de l'Enseignement Supérieur et de la Recherche, Université Paris-Sud, for Rym Boudjemaa's Ph.D. thesis (grant 2014-172).

FUNDING INFORMATION

This work, including the efforts of Rym Boudjemaa, was funded by Ministère de l'Enseignement Supérieur et de la Recherche, Université Paris-Sud (2014-172).

REFERENCES

1. **Sun F, Qu F, Ling Y, Mao P, Xia P, Chen H, Zhou D.** 2013. Biofilm-associated infections: antibiotic resistance and novel therapeutic strategies. Future Microbiol **8:**877–886. http://dx.doi.org/10.2217/fmb.13.58.
2. **Costerton JW, Stewart PS, Greenberg EP.** 1999. Bacterial biofilms: a common cause of persistent infections. Science **284:**1318–1322. http://dx.doi.org/10.1126/science.284.5418.1318.
3. **Lebeaux D, Ghigo J-M, Beloin C.** 2014. Tolérance des biofilms aux antibiotiques: comprendre pour mieux traiter. J Anti-Infect **16:**112–121. http://dx.doi.org/10.1016/j.antinf.2014.04.001.
4. **Costerton JW, Irvin RT, Cheng K-J, Sutherland IW.** 1981. The role of bacterial surface structures in pathogenesis. Crit Rev Microbiol **8:**303–338. http://dx.doi.org/10.3109/10408418109085082.
5. **Steenbergen JN, Alder J, Thorne GM, Tally FP.** 2005. Daptomycin: a lipopeptide antibiotic for the treatment of serious Gram-positive infections. J Antimicrob Chemother **55:**283–288. http://dx.doi.org/10.1093/jac/dkh546.
6. **Straus SK, Hancock REW.** 2006. Mode of action of the new antibiotic for Gram-positive pathogens daptomycin: comparison with cationic antimicrobial peptides and lipopeptides. Biochim Biophys Acta **1758:**1215–1223. http://dx.doi.org/10.1016/j.bbamem.2006.02.009.
7. **Mascio CTM, Alder JD, Silverman JA.** 2007. Bactericidal action of daptomycin against stationary-phase and nondividing Staphylococcus aureus cells. Antimicrob Agents Chemother **51:**4255–4260. http://dx.doi.org/10.1128/AAC.00824-07.
8. **Cotroneo N, Harris R, Perlmutter N, Beveridge T, Silverman JA.** 2008. Daptomycin exerts bactericidal activity without lysis of Staphylococcus aureus. Antimicrob Agents Chemother **52:**2223–2225. http://dx.doi.org/10.1128/AAC.01410-07.
9. **Silverman JA, Perlmutter NG, Shapiro HM.** 2003. Correlation of daptomycin bactericidal activity and membrane depolarization in Staphylococcus aureus. Antimicrob Agents Chemother **47:**2538–2544. http://dx.doi.org/10.1128/AAC.47.8.2538-2544.2003.
10. **Khasawneh FA, Ashcraft DS, Pankey GA.** 2008. In vitro testing of daptomycin plus rifampin against methicillin-resistant Staphylococcus aureus resistant to rifampin. Saudi Med J **29:**1726–1729.
11. **LaPlante KL, Woodmansee S.** 2009. Activities of daptomycin and vancomycin alone and in combination with rifampin and gentamicin against biofilm-forming methicillin-resistant Staphylococcus aureus isolates in an experimental model of endocarditis. Antimicrob Agents Chemother **53:**3880–3886. http://dx.doi.org/10.1128/AAC.00134-09.
12. **Parra-Ruiz J, Vidaillac C, Rose WE, Rybak MJ.** 2010. Activities of high-dose daptomycin, vancomycin, and moxifloxacin alone or in combination with clarithromycin or rifampin in a novel in vitro model of Staphylococcus aureus biofilm. Antimicrob Agents Chemother **54:**4329–4334. http://dx.doi.org/10.1128/AAC.00455-10.
13. **Olson ME, Slater SR, Rupp ME, Fey PD.** 2010. Rifampicin enhances activity of daptomycin and vancomycin against both a polysaccharide intercellular adhesin (PIA)-dependent and -independent Staphylococcus epidermidis biofilm. J Antimicrob Chemother **65:**2164–2171. http://dx.doi.org/10.1093/jac/dkq314.
14. **Nadrah K, Strle F.** 2011. Antibiotic combinations with daptomycin for treatment of *Staphylococcus aureus* infections. Chemother Res Pract **2011:**619321. http://dx.doi.org/10.1155/2011/619321.
15. **Cirioni O, Mocchegiani F, Ghiselli R, Silvestri C, Gabrielli E, Marchionni E, Orlando F, Nicolini D, Risaliti A, Giacometti A.** 2010. Daptomycin and rifampin alone and in combination prevent vascular graft biofilm formation and emergence of antibiotic resistance in a subcutaneous rat pouch model of staphylococcal infection. Eur J Vasc Endovasc Surg **40:**817–822. http://dx.doi.org/10.1016/j.ejvs.2010.08.009.
16. **Salem AH, Elkhatib WF, Noreddin AM.** 2011. Pharmacodynamic assessment of vancomycin–rifampicin combination against methicillin resistant Staphylococcus aureus biofilm: a parametric response surface analysis. J Pharm Pharmacol **63:**73–79. http://dx.doi.org/10.1111/j.2042-7158.2010.01183.x.
17. **John A-K, Schmaler M, Khanna N, Landmann R.** 2011. Reversible daptomycin tolerance of adherent staphylococci in an implant infection

model. Antimicrob Agents Chemother **55:**3510–3516. http://dx.doi.org/10.1128/AAC.00172-11.

18. **Revest M, Jacqueline C, Boudjemaa R, Caillon J, Le Mabecque V, Breteche A, Steenkeste K, Tattevin P, Potel G, Michelet C, Fontaine-Aupart MP, Boutoille D.** 2016. New in vitro and in vivo models to evaluate antibiotic efficacy in Staphylococcus aureus prosthetic vascular graft infection. J Antimicrob Chemother **71:**1291–1299. http://dx.doi.org/10.1093/jac/dkv496.
19. **Wang IW, Anderson JM, Jacobs MR, Marchant RE.** 1995. Adhesion of Staphylococcus epidermidis to biomedical polymers: contributions of surface thermodynamics and hemodynamic shear conditions. J Biomed Mater Res **29:**485–493. http://dx.doi.org/10.1002/jbm.820290408.
20. **Mafu AA, Plumety C, Deschênes L, Goulet J.** 2010. Adhesion of pathogenic bacteria to food contact surfaces: influence of pH of culture. Int J Microbiol **2011:**972494. http://dx.doi.org/10.1155/2011/972494.
21. **Sanchez-Vizuete P, Coq DL, Bridier A, Herry J-M, Aymerich S, Briandet R.** 2015. Identification of ypqP as a new Bacillus subtilis biofilm determinant that mediates the protection of Staphylococcus aureus against antimicrobial agents in mixed-species communities. Appl Environ Microbiol **81:**109–118. http://dx.doi.org/10.1128/AEM.02473-14.
22. **Daddi Oubekka S, Briandet R, Fontaine-Aupart M-P, Steenkeste K.** 2012. Correlative time-resolved fluorescence microscopy to assess antibiotic diffusion-reaction in biofilms. Antimicrob Agents Chemother **56:**3349–3358. http://dx.doi.org/10.1128/AAC.00216-12.
23. **Stewart PS.** 2003. Diffusion in biofilms. J Bacteriol **185:**1485–1491. http://dx.doi.org/10.1128/JB.185.5.1485-1491.2003.
24. **Daddi Oubekka S, Briandet R, Waharte F, Fontaine-Aupart M-P, Steenkeste K.** 2011. Image-based fluorescence recovery after photobleaching (FRAP) to dissect vancomycin diffusion-reaction processes in Staphylococcus aureus biofilms, p 80871I–80871I–7. *In* Ramanujam H, Popp J (ed), Proc SPIE 8087, Clinical and Biomedical Spectroscopy and Imaging II. SPIE, Bellingham, WA.
25. **Bridier A, Tischenko E, Dubois-Brissonnet F, Herry J-M, Thomas V, Daddi-Oubekka S, Waharte F, Steenkeste K, Fontaine-Aupart M-P, Briandet R.** 2011. Deciphering biofilm structure and reactivity by multiscale time-resolved fluorescence analysis. Adv Exp Med Biol **715:**333–349. http://dx.doi.org/10.1007/978-94-007-0940-9_21.
26. **Benvenuto M, Benziger DP, Yankelev S, Vigliani G.** 2006. Pharmacokinetics and tolerability of daptomycin at doses up to 12 milligrams per kilogram of body weight once daily in healthy volunteers. Antimicrob Agents Chemother **50:**3245–3249. http://dx.doi.org/10.1128/AAC.00247-06.
27. **Humphries RM, Pollett S, Sakoulas G.** 2013. A current perspective on daptomycin for the clinical microbiologist. Clin Microbiol Rev **26:**759–780. http://dx.doi.org/10.1128/CMR.00030-13.
28. **Pibalpakdee P, Wongratanacheewin S, Taweechaisupapong S, Niumsup PR.** 2012. Diffusion and activity of antibiotics against Burkholderia pseudomallei biofilms. Int J Antimicrob Agents **39:**356–359. http://dx.doi.org/10.1016/j.ijantimicag.2011.12.010.
29. **Singh R, Ray P, Das A, Sharma M.** 2010. Penetration of antibiotics through Staphylococcus aureus and Staphylococcus epidermidis biofilms. J Antimicrob Chemother **65:**1955–1958. http://dx.doi.org/10.1093/jac/dkq257.
30. **Jefferson KK, Goldmann DA, Pier GB.** 2005. Use of confocal microscopy to analyze the rate of vancomycin penetration through Staphylococcus aureus biofilms. Antimicrob Agents Chemother **49:**2467–2473. http://dx.doi.org/10.1128/AAC.49.6.2467-2473.2005.
31. **Siala W, Mingeot-Leclercq M-P, Tulkens PM, Hallin M, Denis O, Bambeke FV.** 2014. Comparison of the antibiotic activities of daptomycin, vancomycin, and the investigational fluoroquinolone delafloxacin against biofilms from Staphylococcus aureus clinical isolates. Antimicrob Agents Chemother **58:**6385–6397. http://dx.doi.org/10.1128/AAC.03482-14.
32. **Stewart PS, Davison WM, Steenbergen JN.** 2009. Daptomycin rapidly penetrates a Staphylococcus epidermidis biofilm. Antimicrob Agents Chemother **53:**3505–3507. http://dx.doi.org/10.1128/AAC.01728-08.
33. **Zeitlinger MA, Derendorf H, Mouton JW, Cars O, Craig WA, Andes D, Theuretzbacher U.** 2011. Protein binding: do we ever learn? Antimicrob Agents Chemother **55:**3067–3074. http://dx.doi.org/10.1128/AAC.01433-10.
34. **Schmidt S, Röck K, Sahre M, Burkhardt O, Brunner M, Lobmeyer MT, Derendorf H.** 2008. Effect of protein binding on the pharmacological activity of highly bound antibiotics. Antimicrob Agents Chemother **52:**3994–4000. http://dx.doi.org/10.1128/AAC.00427-08.
35. **Oubekka SD.** 2012. Dynamique réactionnelle d'antibiotiques au sein des biofilms de Staphylococcus aureus: apport de la microscopie de fluorescence multimodale. Ph.D. thesis. Université Paris Sud-Paris XI, Paris, France.
36. **Rani SA, Pitts B, Beyenal H, Veluchamy RA, Lewandowski Z, Davison WM, Buckingham-Meyer K, Stewart PS.** 2007. Spatial patterns of DNA replication, protein synthesis, and oxygen concentration within bacterial biofilms reveal diverse physiological states. J Bacteriol **189:**4223–4233. http://dx.doi.org/10.1128/JB.00107-07.
37. **Ayrapetyan M, Williams TC, Oliver JD.** 2015. Bridging the gap between viable but non-culturable and antibiotic persistent bacteria. Trends Microbiol **23:**7–13. http://dx.doi.org/10.1016/j.tim.2014.09.004.
38. **Li L, Mendis N, Trigui H, Oliver JD, Faucher SP.** 2014. The importance of the viable but non-culturable state in human bacterial pathogens. Front Microbiol **5:**258. http://dx.doi.org/10.3389/fmicb.2014.00258.
39. **Pasquaroli S, Citterio B, Cesare AD, Amiri M, Manti A, Vuotto C, Biavasco F.** 2014. Role of daptomycin in the induction and persistence of the viable but non-culturable state of Staphylococcus aureus biofilms. Pathogens **3:**759–768. http://dx.doi.org/10.3390/pathogens3030759.
40. **Credito K, Lin G, Appelbaum PC.** 2007. Activity of daptomycin alone and in combination with rifampin and gentamicin against Staphylococcus aureus assessed by time-kill methodology. Antimicrob Agents Chemother **51:**1504–1507. http://dx.doi.org/10.1128/AAC.01455-06.
41. **Garrigós C, Murillo O, Euba G, Verdaguer R, Tubau F, Cabellos C, Cabo J, Ariza J.** 2010. Efficacy of usual and high doses of daptomycin in combination with rifampin versus alternative therapies in experimental foreign-body infection by methicillin-resistant Staphylococcus aureus. Antimicrob Agents Chemother **54:**5251–5256. http://dx.doi.org/10.1128/AAC.00226-10.
42. **Stein C, Makarewicz O, Forstner C, Weis S, Hagel S, Löffler B, Pletz MW.** 21 January 2016. Should daptomycin-rifampin combinations for MSSA/MRSA isolates be avoided because of antagonism? Infection. Epub ahead of print.

SUPPLEMENTARY MATERIAL

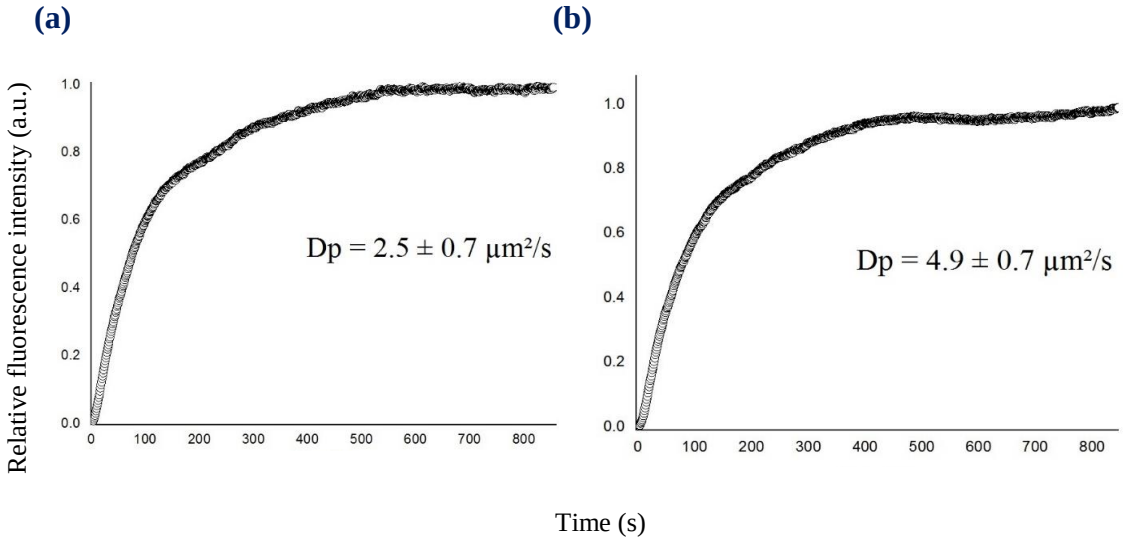

FIG S1 *Time course of BODIPY-FL®-daptomycin penetration measured at the bottom of* ***(a)*** *S. aureus 27217, 176 and 33591 and* ***(b)*** *S. aureus BCB8 biofilms. The relative intensity corresponds to a normalization of the maximum intensity value to one. Time zero corresponds to the moment at which BODIPY-FL®-daptomycin was added above biofilm.*

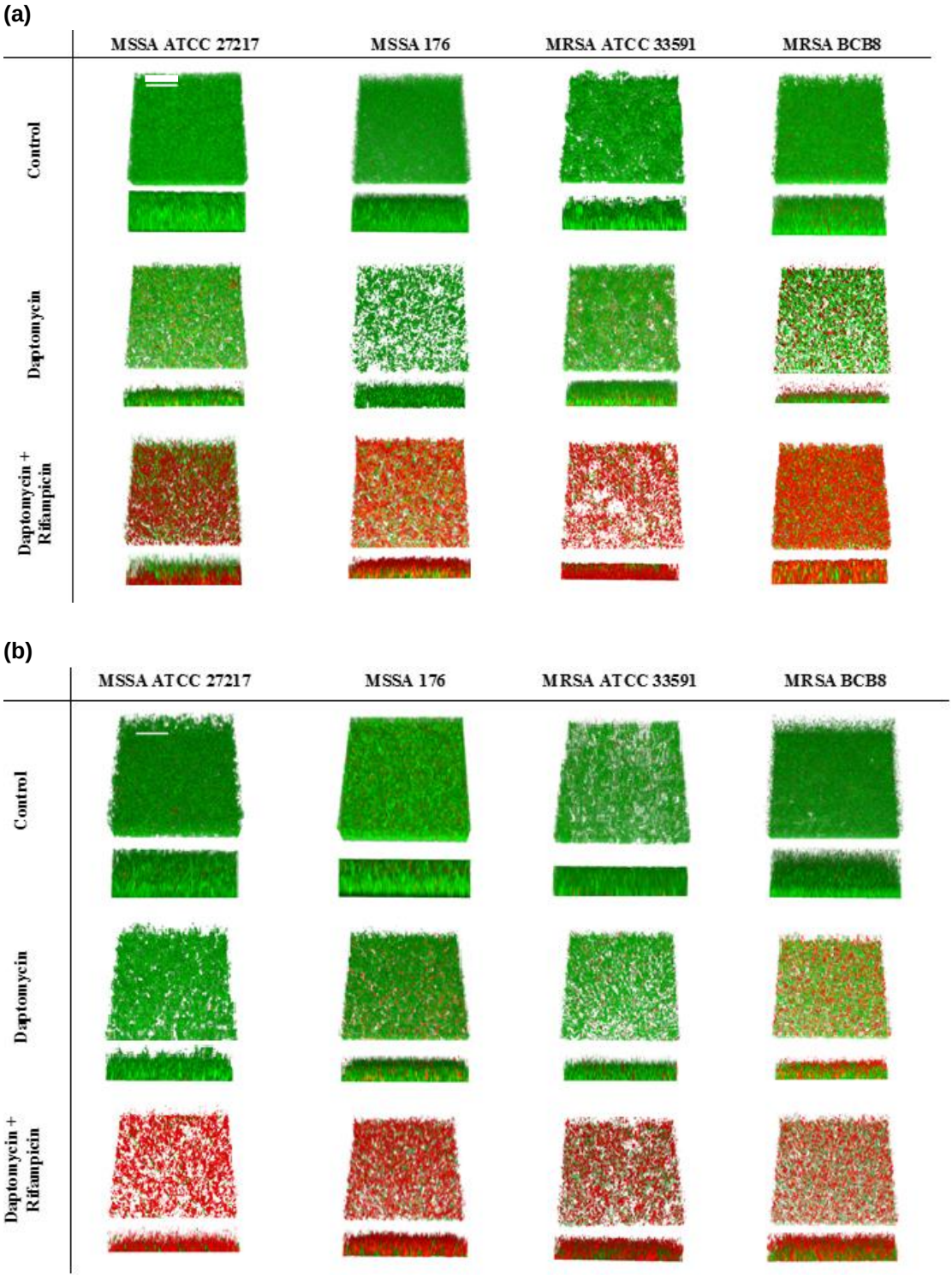

FIG S2 *Visualization of MSSA and MRSA biofilms using 3D reconstruction to observe biofilm thickness. Images were collected without any drug exposure (control) and after* ***(a)*** *24 h and* ***(b)*** *48 h exposure to daptomycin (20 µg/mL) alone and in association with rifampicin (20 µg/mL). Dead cells were stained red with PI and all bacteria were stained green with Syto9®. The acquisition was performed on the whole biofilm thickness with an axial displacement of 1 µm. Images dimension is 82x82µm². The scale bar corresponds to 20 µm.*

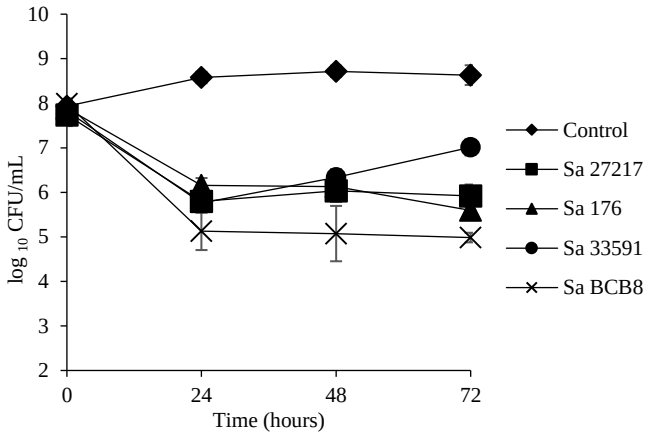

FIG S3 *Time-kill curves of daptomycin (40 µg/mL) against the four MSSA and MRSA biofilms. Since no statistically significant difference was observed between the four controls (P > 0.05), only one curve was represented. Filled diamonds: controls, filled squares: S. aureus 27217, filled triangles: S. aureus 176, filled circles: S. aureus 33591, crosses: S. aureus BCB8. Error bars represent the standard deviation.*

4.3. Résultats complémentaires

4.3.1. Sensibilité aux antibiotiques de biofilms de 24 h selon la nature du substrat.

Nous avons évalué l'influence de la nature du support – patch de Dacron ® (cf. Article 2) ou microplaque en polystyrène (cf. Article 3) – *in vitro* sur la croissance des biofilms et sur l'action des antibiotiques daptomycine et vancomycine seuls ou en association avec la rifampicine (**Figure 5**). La structure tridimensionnelle des biofilms, observée en imagerie de fluorescence confocale, s'est révélée être très différente : sur le Dacron®, la biostructure est beaucoup moins dense et plutôt organisée en amas de bactéries ne recouvrant pas toute la surface (cf. Article 2 JAC 2016) comparativement à une microsurface de polystyrène sur laquelle le biofilm se développe de façon uniforme sur toute la surface pour atteindre ~20 µm d'épaisseur au bout de 24 h. Néanmoins, l'activité des antibiotiques est très comparable dans les deux cas (**Figure 5**), ce qui révèle que l'(in)activité de ces antibiotiques est indépendante l'épaisseur du biofilm.,

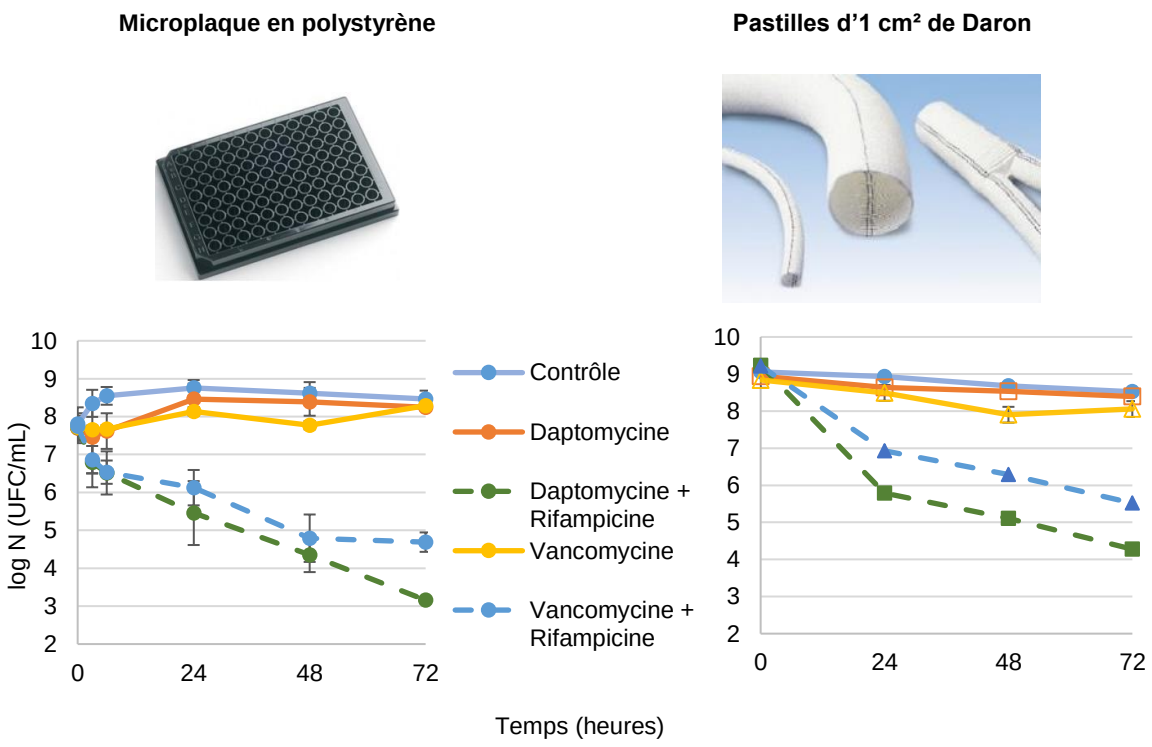

***Figure 5*. Cinétiques de bactéricidie des antibiotiques vis-à-vis des biofilms de S. aureus ATCC 27217 formés sur microplaque et sur Dacron®.** *Les pastilles de Dacron d'1 cm² sont pré-incubées une nuit dans de l'albumine de sérum bovin (BSA) 37 g/L pour se rapprocher des conditions de pré-implantation chez la souris. 1 mL de suspension bactérienne (10^6 CFU/ml) est alors déposé dans le puit d'une plaque de 24 puits contenant le Dacron de sorte à l'immerger complètement. Après incubation 1h30 à 37°C (adhésion), chacun des puits est rincé avec de l'eau physiologique 9 g/L et resupplémenté en Tryptic Soy Broth (TSB)+BSA+Ca^{2+}. 24h plus tard (formation de biofilm), les puits sont rincés à nouveau et resupplémenté cette fois en TSB+BSA+Ca^{2+} additionné ou non d'antibiotiques. La concentration finale en calcium est de 50 mg/L. Les dénombrements de bactéries viables cultivables sont alors réalisés après dilutions successives et dépôts sur milieux gélosés (TSA). Les concentrations d'antibiotiques sont de 40 µg/ml pour la vancomycine et de 20 µg/ml pour la daptomycine et la rifampicine.*

4.3.2. Marquage fluorescent de la daptomycine

La daptomycine est un antibiotique naturellement fluorescent (absorption : 360 nm, émission de fluorescence : 470 nm) mais son rendement de fluorescence est très faible. De ce fait, pour pouvoir suivre la dynamique de la daptomycine au sein des biofilms en imagerie de fluorescence, il était nécessaire de marquer l'antibiotique avec un fluorophore.

(i) Synthèse du NBD-daptomycine

Nous avons dans une première approche initié la synthèse du NBD-daptomycine en suivant le protocole décrit par Murai *et al.*[133,134] Le NBD-Cl (4-Chloro-7-nitrobenzofurazan) est couramment utilisé pour marquer des peptides, des protéines, des médicaments ou d'autres biomolécules. Il ne fluoresce que lorsqu'il réagit avec des groupes tels que les amines, les acides aminés, les peptides et les protéines. De plus, il a été démontré que son greffage à la daptomycine ne modifiait pas son activité de vis-à-vis des bactéries.[133]

Bien que nous soyons parvenus à synthétiser la molécule NBD-daptomycine, sa fluorescence, aux concentrations thérapeutiques d'antibiotique que nous avons utilisées (20 µg/ml), s'est avérée trop faible pour être visualisée correctement en microscopie confocale de fluorescence (**Figure 6**). C'est pourquoi nous avons choisi d'utiliser le BODIPY-FL-daptomycine, gracieusement fourni par la société américaine (Cubist Pharmaceuticals, aujourd'hui faisant partie du groupe Merck).

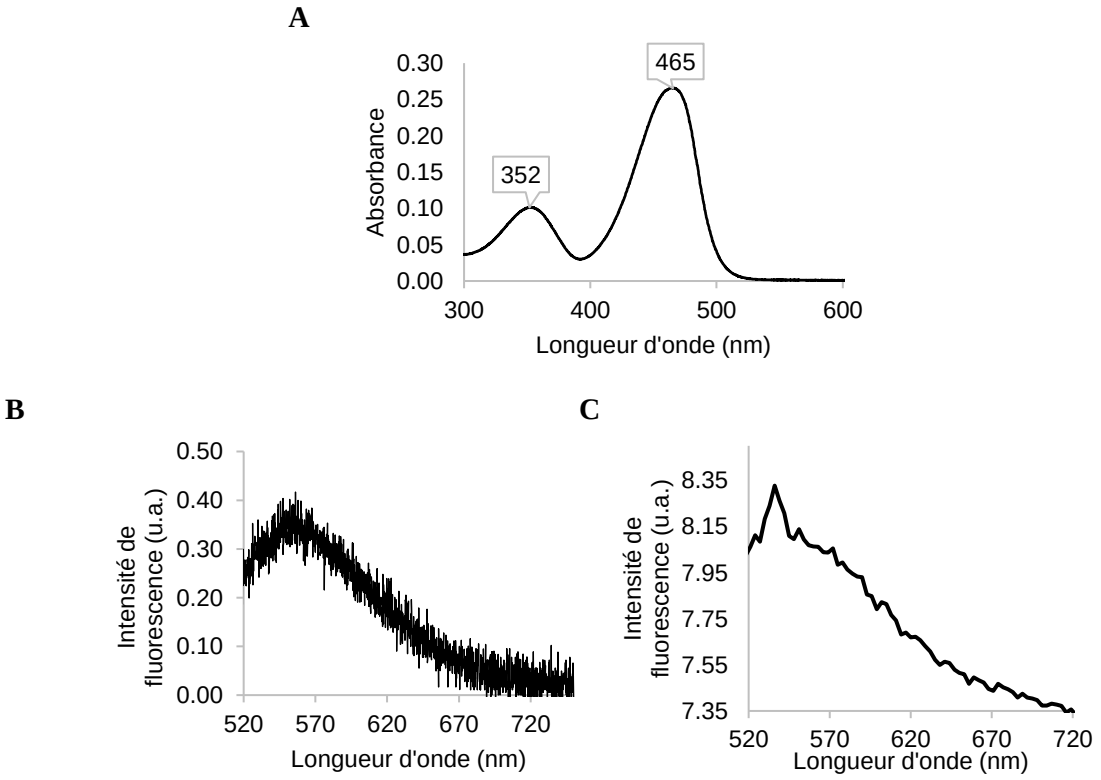

Figure 6. *Spectres d'absorption* ***(A)*** *et d'émission de fluorescence du NBD-daptomycine dans de l'eau physiologique 9 g/L* ***(B)*** *et au sein des biofilms de 24h de S. aureus ATCC 27217 (milieu : TSB+BSA+Ca^{2+})* ***(C).*** *Les spectres A et B sont acquis avec un spectrofluorimètre (Varian) tandis que le spectre C est acquis avec le microscope confocal de fluorescence Leica TCS SP5. Dans les deux cas, la longueur d'onde d'excitation est de 488 nm. La concentration du NBD-daptomycine est de 20 µg/ml.*

Chapitre 5. L'imagerie optique à résolution micro-nanométrique et les méthodes de (bio)chimie permettent d'identifier l'un des facteurs responsables de l'échec de la daptomycine

Dans le cadre de l'étude des facteurs responsables de l'inefficacité des antibiotiques vis-à-vis des biofilms de *S. aureus*, nos précédents résultats suggèrent que l'état physiologique des bactéries joue très probablement un rôle plus important que la matrice d'exopolymères dans notre modèle de biofilms. En effet, tel que décrit dans le chapitre 1, la majorité des bactéries constituant un biofilm de *S. aureus* serait dans un état de métabolisme très fortement ralenti. Ainsi, le manque d'efficacité de la vancomycine au sein des biofilms peut s'expliquer par son mécanisme d'action. En effet, il consiste à inhiber la synthèse de la paroi bactérienne et ce, en ciblant l'aminoacyl-D-alanyl-D-alanine, un processus qui ne se produit que sur des bactéries en phase de division cellulaire.

La daptomycine est un lipopeptide qui, en présence de calcium, s'insère dans les membranes des bactéries à Gram positif et s'oligomérise pour ensuite former des canaux par lesquels vont fuir les ions potassium intracellulaires ; la membrane est alors dépolarisée et la bactérie meurt. De ce fait, la molécule devrait être efficace indépendamment de la physiologie des bactéries. Les résultats décrits dans les deux premiers chapitres montrent que l'efficacité de la daptomycine dans les biofilms, aussi bien *in vivo* qu*'in vitro*, reste limitée. Quels facteurs de la physiologie des bactéries peuvent entrer en jeu ?

Pour ce faire, nous avons tiré parti de l'imagerie optique à résolution micro-nanométrique en combinaison avec des méthodes (bio)chimiques afin de (i) sonder les propriétés structurales et mécaniques de surface des bactéries dans leurs différentes phases de croissance, exposées ou non à la daptomycine et (ii) disséquer les différentes étapes du mécanisme d'action de l'antibiotique (insertion dans la membrane, formation de pores, fuite d'ions potassium), selon la phase de croissance bactérienne.

Cette partie du travail a nécessité des développements méthodologiques, tant pour les mesures de microscopie à force atomique, réalisées en collaboration avec Christian Marlière, que pour les mesures de microscopie de super-localisation de molécules uniques (DONALD) réalisées avec l'équipe de Sandrine Lévêque-Fort. La mise au point du protocole concernant cette dernière méthode est détaillée dans la partie résultats complémentaires du présent chapitre. Les mesures AFM en mode approche-retrait, quant à elles, requièrent une immobilisation/fixation des bactéries afin d'empêcher leur détachement lors du passage de la pointe. Les méthodes d'immobilisation/fixation rapportées dans la littérature impliquent souvent des procédés invasifs (piégeage mécanique par aspiration, fixation chimique, séchage,…) qui modifient la physiologie des bactéries.[135] Dans notre cas, l'immobilisation a été rendue possible par le simple dépôt des suspensions bactériennes sur des lames d'oxyde d'indium et d'étain (ITO). Ainsi, l'optimisation des conditions d'acquisition (force appliquée, …) a permis des observations sur des bactéries vivantes au cours du temps. Par ailleurs, l'injection d'antibiotique a pu être effectuée directement sous la pointe AFM sans retrait du substrat : il a alors été possible de sonder la surface d'une même bactérie avant et après ajout d'antibiotique. Néanmoins, notre étude présente une limite par rapport au milieu physiologique utilisé pour l'observation des bactéries : bien que cultivées et déposées dans un milieu de culture riche classique (TSB), les acquisitions ont été menées dans un milieu minimum (de l'eau physiologique NaCl, 9 g/L) pouvant « stresser » les bactéries sur des temps longs. De ce fait, les modifications structurales et mécaniques de surface des bactéries ont été

évaluées pour chacune des phases de croissance sur des temps ne dépassant pas les deux heures, en s'assurant que le milieu n'impactait pas la survie des bactéries (imagerie Live/Dead®).

Une première question était de savoir, lorsque la daptomycine n'est pas efficace (phase stationnaire, biofilms), si l'antibiotique atteint sa cible biologique, la membrane cytoplasmique. Grâce à l'apport de la méthode DONALD, nous avons confirmé que la daptomycine était effectivement localisée à la membrane des bactéries. Nous avons ensuite recherché par microscopie confocale de fluorescence et par microscopie à force atomique si l'antibiotique induisait des modifications de structure de la surface et de la membrane des bactéries. Ces modifications structurales ont été observées pour les seules bactéries en phase exponentielle de croissance (daptomycine active) mais pas pour les bactéries en phase stationnaire et en biofilms (inactive). Enfin, l'imagerie de fluorescence a aussi permis de contrôler la présence d'ions potassium dans le milieu extracellulaire, caractérisant l'action de la daptomycine. La présence de ces ions n'a pu être mise en évidence que lorsque la daptomycine est active (phase exponentielle de croissance).

Pour être efficace, la daptomycine doit aussi s'oligomériser au sein de la membrane bactérienne, un processus qui requiert une fluidité membranaire adaptée. Nous avons complété nos travaux par une analyse détaillée de la composition en acides gras de la membrane des bactéries de *S. aureus*. De manière générale, la membrane des bactéries est une bicouche lipidique composée notamment d'acides gras, dont la structure et l'agencement déterminent la rigidité/fluidité de la membrane. Alors que les acides gras saturés non-branchés confèrent aux membranes une rigidité importante, les acides gras saturés branchés et/ou insaturés sont représentatifs d'une fluidité plus importante, rendant la membrane plus perméable. L'analyse de la composition des membranes bactériennes en acides gras a été réalisée par des méthodes de (bio)chimie analytique (chromatographie en phase gazeuse et spectrométrie de masse) en collaboration avec Florence Dubois-Brissonnet et Romain Briandet à l'Institut Micalis de l'INRA. Les résultats obtenus ont mis en évidence une corrélation entre la rigidité des membranes et l'inefficacité de l'antibiotique. Ceci suggère que bien que l'antibiotique atteigne sa cible biologique au niveau de la membrane, il ne peut s'oligomériser du fait d'un encombrement stérique local en acide gras trop important et n'est donc pas actif.

Cette hypothèse a été vérifiée en enrichissant le milieu nutritif des bactéries avec un acide gras insaturé, que l'on retrouve en abondance dans toutes les huiles végétales et animales et qui permet d'induire une fluidité membranaire plus importante : dans ce cas, on recouvre une activité bactéricide de la daptomycine.

Les résultats détaillés de ce troisième chapitre sont présentés sous forme de deux articles en préparation, le premier intitulé : « ***Real-time atomic force microscopy analysis of live Staphylococcus aureus bacteria: from single sessile cell toward biofilm genesis*** » et le second intitulé : « ***Failure of daptomycin to inactivate S. aureus cells: the influence of the fatty acid composition of bacterial membranes.*** »

5.1. Article 6 : "Real-time atomic force microscopy analysis of live *Staphylococcus aureus* bacteria: from single sessile cell toward biofilm genesis"

Rym Boudjemaa, Christian Marlière, Romain Briandet Marie-Pierre Fontaine-Aupart, Karine Steenkeste

Article en préparation

Real-time atomic force microscopy analysis of live *Staphylococcus aureus*: from single sessile bacteria toward biofilm genesis

Rym Boudjemaa,[a] Christian Marlière,[a] Romain Briandet,[b] Marie-Pierre Fontaine-Aupart,[a] Karine Steenkeste[a]

[a] Institut des Sciences Moléculaires d'Orsay (ISMO), CNRS, Université Paris-Sud, Université Paris-Saclay, Orsay, France; [b] Micalis Institute, INRA, AgroParisTech, Université Paris-Saclay, Jouy-en-Josas, France

Introduction

Staphylococcus aureus (S. aureus) is a Gram-positive pathogen implicated in a wide range of hospital-acquired infections and often associated with biofilm formation on medical implants.[1] Biofilm growth involves bacterial adhesion to (a)biotic surfaces, followed by cell-cell interactions leading to microcolonies and further mature biofilms, encased in a self-secreted exopolymeric matrix.[2] Initial bacterial adhesion is associated with changes in phenotypic and physiologic changes, enabling bacteria to cope with antimicrobials aggression and thus rendering associated infections very difficult to treat.[3]

Among the key factors promoting bacterial adhesion, cell envelope constituents (cell-wall anchored proteins, exopolysaccharides, adhesins, …etc.) fulfill an important role in substrate and intercellular interactions involved in subsequent biofilm formation.[1–6] Indeed, it is now clear that these biocompounds are either covalently anchored or loosely-attached to *S. aureus* cell wall.[4,7] However, the mechanisms by which they are implicated from bacterial adhesion to biofilm formation remain unclear for now, likely due to the lack of high-resolution data.

In this context, Atomic Force Microscopy (AFM) offers the possibility to probe the nanoscale architecture of living cells surface in their native liquid environment, giving access to both visual and quantitative information.[8–11] Hence, extensive research has focused on the study of cells morphological and mechanical properties.[12–17] More recently, the combination of force spectroscopy with biospecific probes has proved very useful for the quantification of subcellular chemical heterogeneities but also for the characterization of bacterial interactions with each other, with immune cells or with specific molecules such as lectins, antimicrobials, antibodies, … etc.[18–22] Notably, recent studies evaluated some of the surface decorations that mediate cell-cell interactions (PIA, SraP, SdrC, SasG, …), revealing electrostatic and/or specific homophilic binding between proteins of the interacting cells.[4,19,23,24] However, little is currently known about the bacterial cells envelope modifications that drive aggregation and further biofilm formation.

In this context, we took benefit from AFM to study and quantify in real time and at sub-micrometric scale the evolution of structural and nanomechanical properties of live *S. aureus* cell surface from dividing processes occurring during exponential growth phase to the very first step of biofilm formation. The morphological and mechanical effects induced by a membrane-targeting antibiotic, daptomycin, were also investigated depending on the bacterial growth phase.

Results and discussion

S. aureus cell surface properties from bacterial division to the first steps of biofilm formation.

The structural and mechanical properties of *S. aureus* bacterial surface were investigated depending on their growth phase, whether in exponentially-growing or in late stationary phase (24-h culture). Each bacterial culture was adhered 1h30 before AFM acquisitions (see Materials and Methods section).

When probed in a large field of view (3 x 3 µm²), AFM height images revealed that exponentially-growing cells were most often dividing, by pairs or individualized (Figure 1 and 2). As shown in Fig. 1A, bacterial division could be observed in real-time during AFM scanning. Between 0 and 20 min, in line with electron microscopy observations,[25–27] a bridge linking the two dividing cells was observed (Figure 1A). Simultaneously, both space and depth between bacteria increased from 100 to 150 nm and 70 to 200 nm respectively, revealing the septum formation (Figure 1B). Interestingly, when focusing on a smaller area on the top of exponentially-growing cells (during division or not, 0.4 x 0.4 µm²), height images revealed that the bacterial surface was decorated with a regular distribution of three-dimensional herring-bone patterns (Figures 1A and 2B). Their lateral dimensions varied between 50 and 100 nm and the height between 10 and 15 nm. In a study on *Lactobacillus*, Francius *et al.* also highlighted a rough morphology decorated with waves, attributed to the production of extracellular polysaccharides.[18] However, to our knowledge, such structural observations have never been reported for *S. aureus* species. To explore the mechanical properties of these patterns, we determined Young moduli values, a parameter that reflects the elasticity of the cell (the lower are the values, the softer is the cell surface). To obtain these values, force curves were recorded over each image (128 x 128), converted into indentation curves and fitted with the Hertz model to generate elasticity maps (Figure 2C). From each map, resulting histograms were represented to depict the Young moduli distribution over each image (Figure S2). Elasticity maps and their corresponding histograms showed three major values (center of gaussian peaks), 0.35 ± 0.03 MPa, 0.95 ± 0.07 MPa and 2.3 ± 0.3 MPa (mean ± SD, *n* = 32 768 curves from three different cells

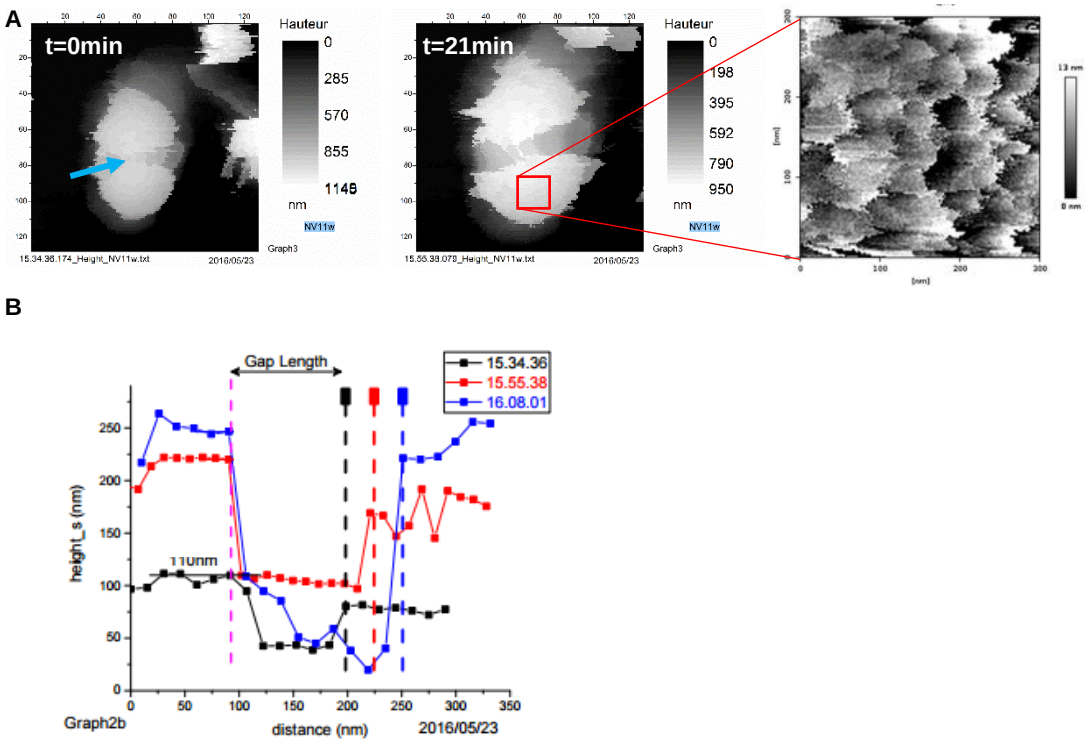

Figure 1. Real-time AFM imaging of *S. aureus* bacterial division. (A) Height images are represented at t0 and 21 min after the first acquisition. A high magnification image (0.3 x 0.3 µm²) is also represented on the right, to show the topographic structure on the top of the cell (indicated with the red square) (B) Cross-sections illustrating space and depth increase over time. The blue arrow indicates the bridge linking the two dividing cells.

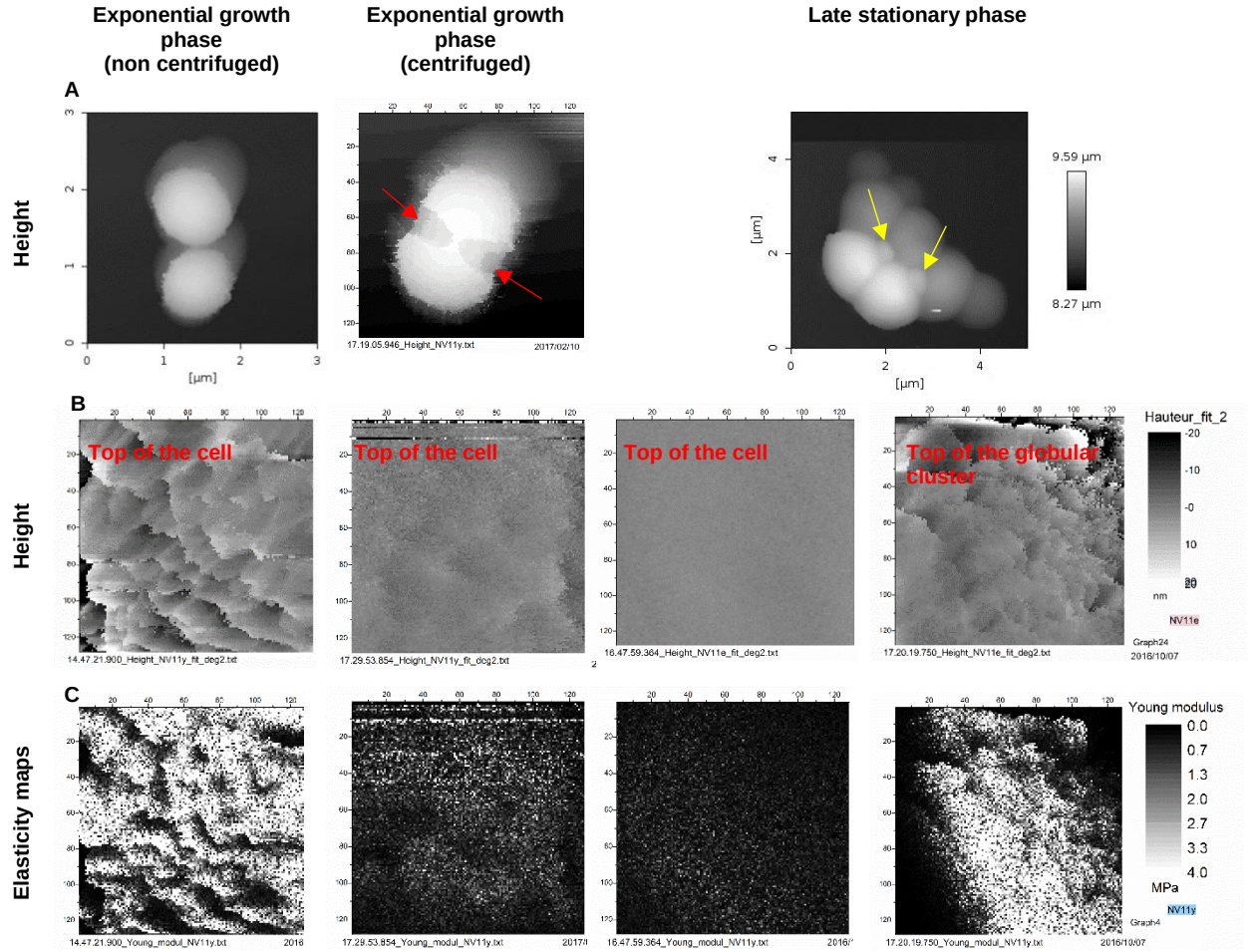

Figure 2**. AFM multiparametric imaging reveals the nanoscale structure and mechanical properties of *S. aureus* cell surface depending on its growth phase.** For each condition (exponential growth phase, centrifuged or not, and stationary phase), are represented (A) 3 x 3 µm² height images of *S. aureus* cells, (B) 0.4 x 0.4 µm² height images corrected from curvature radii, (C) elasticity maps over the same area. Similar results were obtained for at least four cells from different cultures. Red arrows point the bacterial septum and yellow ones indicate the globular clusters.

from two different cultures), with contributions (areas under the related peak) of: 17 ± 6%, 30 ± 5% and 53 ± 9 % (Figure 3D). Correlation between structural and elasticity properties indicated that the main stiff consituents (~ 2.3 MPa) corresponded to the upper patterns while the softer ones (~ 0.35 MPa) were deeper, thus likely attributed to the bacterial cell wall. Indeed, this ~ 0.35-MPa Young modulus is consistent with literature data, reportedly varying from 0.3 to 0.5 MPa for *S. aureus* cell wall.

To determine if this stiff extracellular layer covering the cells was firmly attached to the cell wall, we imaged exponentially-growing cells after centrifugation. The resulting height images and elasticity maps demonstrated that centrifuged cells exhibited a smooth (1.8 nm Root Mean Square (RMS) for an 0.3 x 0.3 µm² area) and softer surface (major peak centered at 0.3 MPa), revealing that the cells decorations were removed (Figure 2) and thus loosely-attached to the cell wall. In view of these results, this extracellular layer cannot be attributed to cell wall anchored proteins, components that should not be easily removable by centrifugation.

By contrast to exponentially-growing bacteria, when grown to late stationary phase (24-h culture), *S. aureus* cells were mostly aggregated

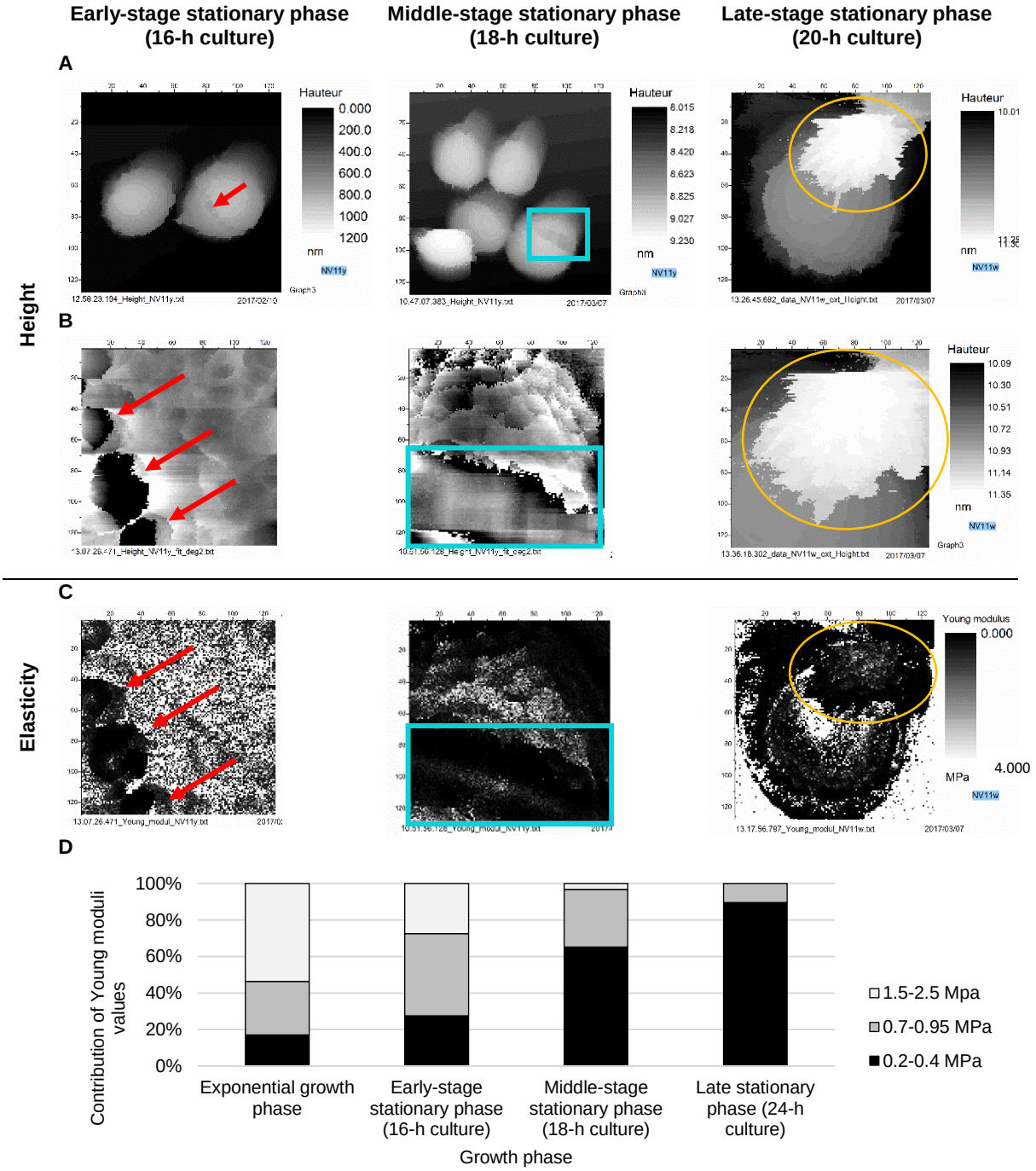

Figure 3. The stiff extracellular layer covering adhered exponentially-growing cells gets gradually removed with the growth phase aging. For each culture stage (16-, 18- and 20-h cultures) are represented (A) 3 x 3 µm² height images of *S. aureus* cells, (B) 0.4 x 0.4 µm² height images corrected from curvature radii, (C) elasticity maps over the same area, (D) contributions (%) of each Young modulus value depending on the bacterial growth phase. Similar results were obtained for at least four cells from different cultures. Red arrows indicate the holes formed (~0.4 MPa) at the bacterial surface. Blue squares indicate the 'zipper-like' pattern (~0.4 MPa). Yellow circles indicate the soft extracellular material (~50 kPa) secreted by bacteria.

and small globular clusters (200-nm high and 300-nm large) were observed between them (Figure 2A). In addition, no decorations were observed on their top (Figure 2B): while the surface of exponentially-growing cells was rough, the one of stationary phase bacteria appeared much smoother (4.7 and 0.5 nm RMS respectively for 0.3 x 0.3 µm² areas, Figure 2B). Consistently with

earlier AFM studies on *S. aureus*,[19,28] Young moduli histograms demonstrated for late stationary phase a homogenously soft cell surface (one peak centered at 0.17 ± 0.05 MPa, Figure 2C and S2). Strikingly, we found, by focusing (0.3 x 0.3 µm²) on the globular clusters present between bacteria, that they exhibited the same structural and mechanical properties as for exponentially-growing bacteria (Figure 2B, 2C and S2): highly stiff (major peak centered at 2.68 ± 0.07 MPa) herring bone patterns (~ 15-nm high) with a roughness of 2.6 nm RMS for an 0.3 x 0.3 µm² area. What happens then to this stiff extracellular layer when the bacterial cultures get older?

S. aureus cells have been well-described to produce a variety of extracellular biocompounds (proteins, polysaccharides, …etc) associated to the cell surface that promote cell-cell adhesion and further biofilm formation.[4,7] Among them, cell-wall anchored proteins are numerous. However, considering our observations (easy removal upon centrifugation), the extracellular stiff layer observed on the surface of exponentially-growing cells cannot be attributed to such firmly-attached proteins. Rather, the presence of a polysaccharidic capsule should be more consistent but needs to be further studied. In view of our results, it is then tempting to speculate that during exponential-to-late stationary phase transition, bacteria get rid of their stiff envelope layer, which further accumulates into globular clusters between cells to cement cell-cell adhesion and initiate subsequent biofilm formation.

To support this hypothesis, we further assessed the evolution of the cell surface structural and mechanical properties over time from exponential to late stationary phase (described above). To this end, we harvested cells at intermediate stages: 16- , 18- and 20-h cultures (Figure 3). AFM height images and elasticity maps obtained for early stationary phase cells (16-h culture) showed that the cell surface exhibited again herring-bone patterns with similar mechanical properties than exponentially-growing bacteria (~ 2 MPa, Figure S2). But in addition, multiple 60-nm large and 20-nm deep holes were observed (Figure 3B), yielding a low value (0.4 ± 0.2 MPa) for elasticity (Figures 3C and S2), similarly to the surface of late stationary phase cells (Figure 2D).

When grown for 18 h, bacteria were not anymore isolated but rather gathered within aggregates. Importantly, the holes extended to finally join each other, forming a zipper-like pattern (indicated with blue rectangles in Figure 3) on the cell surface in which Young moduli values were 0.4 ± 0.2 MPa while the rest of the surface was ~1.6-2 MPa (Figure S2), indicating a gradual removal of the stiff extracellular decorations.

Finally, bacteria harvested from 20-h cultures were no longer covered by the 2-MPa stiff decorations and displayed homogenously smooth and softer (0.4 MPa) surfaces (Figure 3). By contrast, at this growth stage, a very soft (~ 50 kPa) extracellular material, different from the 2-MPa stiff one, was shown to be slowly secreted by bacteria at a diffusion/secretion rate of 21 nm²/s (Figure 4). In a previous AFM study,[19] it

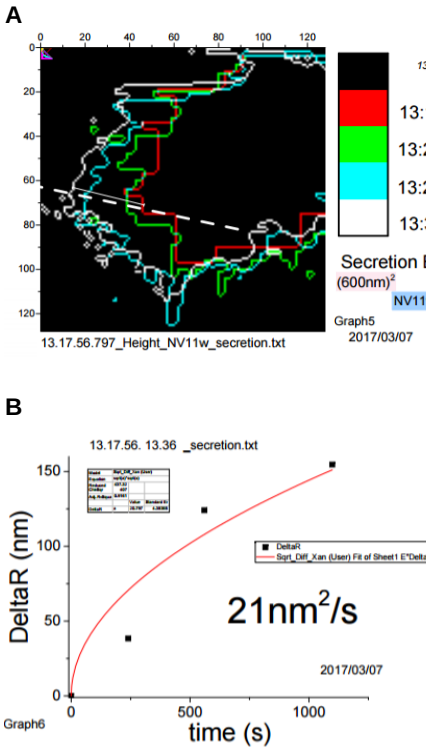

Figure 4. Diffusion measurement of the soft extracellular material (~ 50 kPa) secreted by *S. aureus* bacteria. (A) Secretion spread at different time points **(B)** Distance between the secretion spread curves as a function of time over the white dashed line.

has been shown that *S. aureus* can produce an extracellular soft layer that covers its surface and drastically increases the cell softness (~ 45 kPa instead of ~ 500 kPa for native cell), a finding attributed to the secretion of Polysaccharide Intercellular Adhesin (PIA), a major biofilm matrix component.

To provide quantitative information about the stiff extracellular layer removal as a function of the growth phase, we deduced from the Young moduli histograms the contributions (areas under peak) for each of the three values over time. Depicted in Figure 3D, they confirm that the contribution of the stiffer component drastically decreases from exponentially-growing cells to late stationary phase cells (53 to 0%). Inversely, the softer component (0.4 MPa) significantly increases from 17 to 60 %. This strongly provides evidence that bacterial cells progressively get rid of their stiff extracellular surface decorations from the dividing step to the late maturation of cells.

Daptomycin effect on *S. aureus* surface properties. Daptomycin is a membrane-targeting antibiotic that, in the presence of calcium, inserts into the cytoplasmic membrane where it oligomerizes, leading to pore formation, potassium ions leakage and ultimately to cell death.[29] Recently, it has also been shown that beside targeting the membrane, daptomycin action involves a delocalization of membranes-anchored proteins subsequently blocking the cell wall synthesis.[30] Here, we took benefit from AFM to analyze the topographic and mechanical properties of exponentially-growing and stationary phase *S. aureus* bacteria in the presence of daptomycin (20 µg/mL). But first, we assessed daptomycin activity over 24 h against exponentially-growing *S. aureus* cells, adhered to a surface in the same conditions that the ones used for AFM. To this end, bacterial counting on agar plates was performed, revealing that daptomycin was bactericidal against adherent cells for the first 6 h only (Figure S1). Interestingly, the same experiments performed on their planktonic counterparts showed that daptomycin maintained its bactericidal activity over the whole time course (24 h). The comparison between these two conditions strongly suggests that adhesion of *S. aureus* cells plays a major role on the antibiotic efficacy. Daptomycin activity assessment was also performed on planktonic stationary phase cells, demonstrating that this population was insensitive to daptomycin: only a slight reduction in bacterial counts was measured for the first 3 h of treatment (Figure S1). In this context, which impact does have the antibiotic on *S. aureus* cell surface depending on the growth phase?

When grown to late stationary phase cells, neither the structural nor the mechanical properties of *S. aureus* cells were affected by daptomycin presence (Figure 6B). By contrast, on exponentially-growing bacteria, addition of dapto-

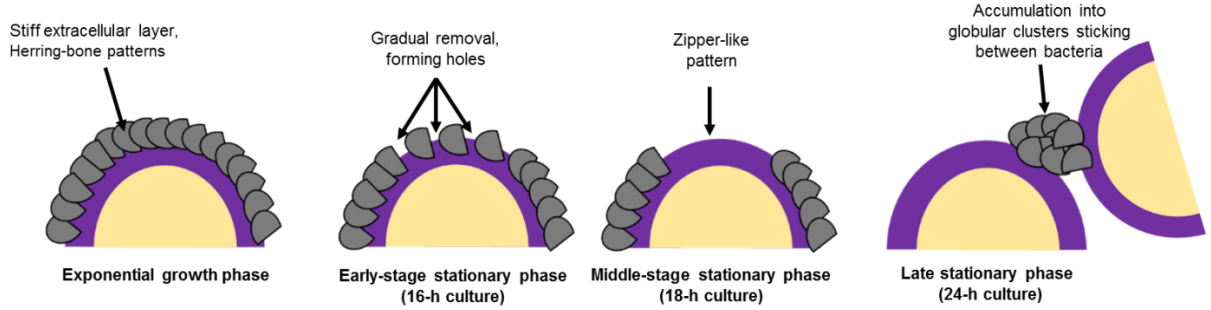

Figure 5. Schematic representation of the proposed dynamic for the stiff extracellular layer. In exponential growth phase, the cell surface is surrounded by a stiff extracellular layer characterized by herring-bone patterns. Along with phase aging, these patterns get gradually removed, first forming holes, second zipper-like patterns and finally accumulate into globular clusters sticking between bacteria. During this late stage, bacteria also secrete a very soft extracellular material, probably contributing to the matrix construction.

mycin strongly altered the structural and mechanical properties of the cell surface. The surface morphology, shown in Fig. 6B, was much rougher: 15 min after daptomycin injection, a drastic increase of the difference in major height values was measured (~1 to ~ 10.2 ± 1.7 nm) and remained stable over 2 h (Fig. 6A). The cell surface stiffness was lower: concomitantly to the sudden height variation, the highest Young modulus peak (2.5 MPa) slightly decreased to reach a mean value of 2.26 ± 0.05 MPa within 10 min. 90 min after that, this high elasticity peak, associated with the stiff extracellular layer completely disappeared: only the peaks at lower values, 0.37 ± 0.01 MPa and 0.90 ± 0.15 MPa (with a weight of 5% and 95% respectively) were still present. This sudden height and elasticity variation effect can reasonably be attributed to the deconstruction of the peptidoglycan wall, presumably a consequence of daptomycin insertion into the cytoplasmic membrane of exponentially-growing cells. In a recent study,[30] daptomycin was shown to have indirect effects on the cell wall structure upon insertion into the membrane: subsequently to its membrane insertion, daptomycin is believed to interfere with

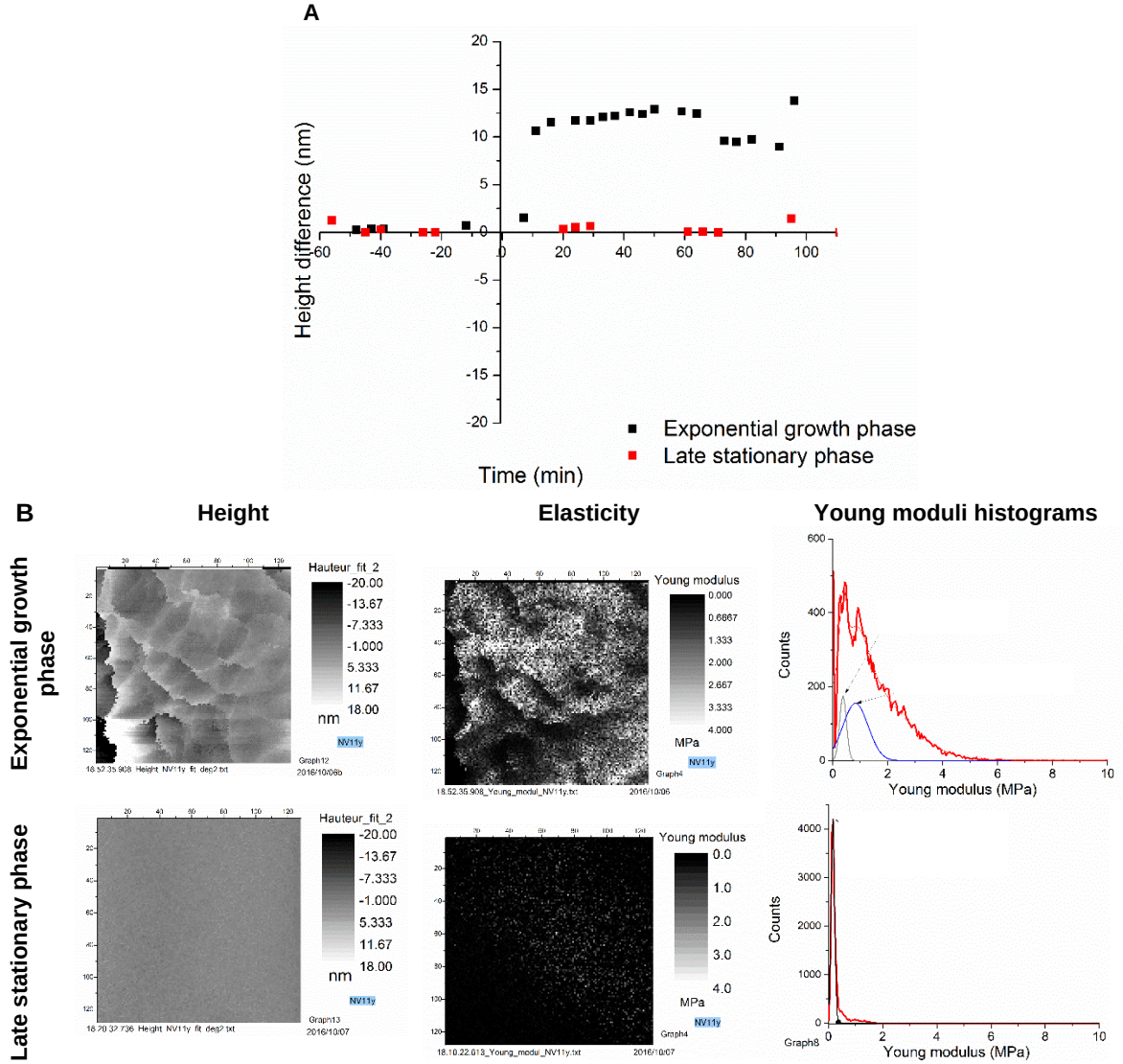

Figure 6. Daptomycin-induced nanoscale effect on *S. aureus* exponentially-growing and late stationary phase cells. (A) Height difference measurements over time before and after daptomycin addition (axe zero). (B) Height images, elasticity maps and Young moduli histograms.

the lipid organization of the cell membrane, further provoking the rapid detachment of specific membrane-associated proteins, and leading to cell wall alteration.[30]

In view of the poor or no activity of daptomycin reported against stationary phase cells, the differential effects observed with exponentially-growing bacteria are likely related to the daptomycin-induced action in this last case.

Conclusion

In conclusion, our live-cell AFM experiments enabled to analyze in real time the evolution of the structural and mechanical properties of *S. aureus* during exponential-to-stationary phase transition (or planktonic individualized cells to aggregates formation). Our data presented here demonstrate that exponentially-growing *S. aureus* exhibit a stiff extracellular layer, likely to play a crucial role in subsequent biofilm formation. Indeed, real-time analysis of the cells surface structural and mechanical modifications provide direct evidence that the stiff 15-nm layer covering the cells progressively detach during exponential-to-late stationary phase transition to agglomerate into globular deposits sticking between the cells, and thus promoting intercellular adhesion and aggregation.

Furthermore, we show here that addition of daptomycin profoundly alters the structural and mechanical properties of *S. aureus* cell surface in exponential growth phase. Our data emphasize the key role of daptomycin in cell wall deconstruction as a consequence of membrane insertion and further destabilization.

Methods.

Bacterial strain and culture conditions. The following *S. aureus* strain was used in this study: *S. aureus* ATCC 27217 (a methicillin-susceptible collection strain). Prior kept at –80°C in Trypticase Soy Broth (TSB, bioMérieux, France) containing 20% (vol/vol) glycerol, the frozen cells were then subcultured twice in TSB (one 8-h culture, followed by an overnight culture at 37°C) to constitute the stock cultures from which aliquots were kept at -20°C.

Following two further subcultures in TSB (one 8-h culture followed by an overnight culture), stationary phase cells were harvested after 16, 18, 20 or 24 h of the overnight culture while exponentially-growing cells were obtained with a third subculture in TSB.

AFM experiments.

(i) Bacterial immobilization and antibiotic addition. One fundamental requirement when using AFM is to avoid the sweeping away of bacteria from the scanned region by the AFM tip because of its lateral interactions with the poorly adhered bacteria. To cope with this limitation, several approaches have been employed to immobilize or fix cells (mechanical trapping into membrane pores, chemical coating of substrates,…).[10] Unfortunately, such strategies may induce stressful conditions but more importantly to alter the bacterial cell physiology and bias observations. To obtain the most realistic representation, we therefore imaged living bacteria spontaneously adhering on the substratum (RBS and $CaCO_3$-cleaned Indium-Tin Oxide (ITO) glass slides). 500 µL portions of the bacterial cultures, prepared as described previously, were deposited (without any centrifugation if not mentioned in the text) on the cleaned ITO for 1h30 at 37°C. Samples were then both rinsed and refilled with sterile NaCl (9 g/L) supplemented with $CaCl_2$, $2H_2O$ (50 mg/L).

For the experiments involving daptomycin, the antibiotic (purchased from Sigma Aldrich) was used at a therapeutic concentration of 20 mg/L, and injected directly into the sample in a way that prevents sample moving. For these experiments, the surface of a same bacterium was probed before and after daptomycin injection to control (i) that the tip didn't damage the cells and (ii) to prevent from intercellular variability.

All experiments were performed at least five cells from three independent cultures.

(ii) AFM imaging. AFM images were performed using a Nanowizard III AFM (JPK Instruments, Germany) coupled to a commercial inverted microscope (Zeiss, Germany). AFM data were acquired the Quantitative Imaging mode with CSC38 SiO_2 AFM tips were used (MikroMasch, nominal spring constant of 0.03 N/m). Force curves were acquired over 128 pixels x 128 pixels images were recorded with an applied force kept at 1.2 nN for all conditions at a constant approach/retract speed of 142 µm/s (z-range of 1 µm). Young's moduli were calculated using the Hertz model, in which the force (F), indentation (δ), and Young's modulus (E) follow the equation $F = \frac{2*E*\tan\alpha}{\pi(1-\nu^2)\delta^2}$, where α is the tip opening angle (40°) and ν the Poisson ratio (arbitrarily assumed to be 0.5). The cantilever spring constants were determined by the thermal noise method.

Raw data treatment was then performed using home-made Matlab programs and Origin Pro software.

Determination of daptomycin biological activity against *S. aureus*. Daptomycin activity was assessed against the *S. aureus* MSSA ATCC 27217 strain in exponential phase of growth (planktonic and adhere), stationary phase and 24 h biofilms.

(i) Planktonic cells. After two subcultures in TSB (one 8-h culture followed by an overnight culture), stationary phase cells were harvested directly using the overnight culture while exponentially-growing cells were obtained with a third subculture in TSB with shaking at 100 rpm during 3 h. Bacterial suspensions were washed twice in sterile NaCl (9 g/L) and resuspended in TSB. The bacterial solution was then divided equitably into cell culture flasks where daptomycin solution was added. Bacterial growth was also controlled with a sample without daptomycin that corresponds to the control experiment. Viable culturable bacteria were then counted at regular interval times: 0 h (when antibiotics were added), 3, 6 and 24 h after antibiotics injection. For each time, 1.5 mL of bacterial culture was collected and centrifuged 10 min at 7000*g* in order to eliminate the excess of antibiotic. The bacterial pellet was dispersed in 1.5 mL sterile NaCl (9 g/L) centrifuged again and dispersed in the same conditions. Successive decimal dilutions were then realized. For each dilution, six drops (10 µL) were deposited on Tryptic Soy Agar (TSA) plates (Biomérieux, France), incubated at 37°C during 24 h. CFUs were counted and averaged for each dilution at each time. The detection limit of viable culturable cells was here 100 CFU/mL.

(ii) Adhered exponentially-growing cells. Bacterial suspensions were obtained after three subcultures in TSB. 250 µL were then added to 96-well microplates (µClear; Greiner Bio-One, France). After a 1.5-h adhesion period at 37°C, the wells were rinsed with a NaCl solution (9 g/L) to eliminate non-adherent cells, refilled with sterile TSB supplemented with calcium and daptomycin (final concentrations: 50 mg/L and 20 µg/mL respectively). Viable culturable bacteria were then enumerated by serial dilutions and plating on TSA plates at regular interval times: 0 h (when daptomycin was added), 3, 6 and 24 h after the antibiotic injection. For each time, bacterial cultures were centrifuged twice, decimal dilutions were realized and CFUs were counted as for planktonic bacteria.

(iii) Biofilms. For the preparation of *S. aureus* biofilms, the same adhesion protocol as for adhered cells was followed. After the 1.5-h adhesion period at 37°C, the wells were rinsed with a NaCl solution (9 g/L) to eliminate non-adherent cells, refilled with sterile TSB and then incubated for 24 h at 37°C to allow biofilm growth. To assess daptomycin activity, the 24 h-biofilms were rinsed with a sterile NaCl solution (9 g/L) before adding daptomycin solution diluted in TSB as described previously. Viable culturable bacteria were then enumerated by serial dilutions and plating on TSA plates at regular interval times: 0 h (when daptomycin was added), 3, 6 and 24 h after the antibiotic injection. For each time, bacterial cultures were centrifuged twice, decimal dilutions were realized and CFUs were counted as for planktonic bacteria.

References

(1) Costerton, J. W.; Stewart, P. S.; Greenberg, E. P. Bacterial Biofilms: A Common Cause of Persistent Infections. *Science* **1999**, *284*, 1318–1322.

(2) Costerton, J. W.; Irvin, R. T.; Cheng, K.-J.; Sutherland, I. W. The Role of Bacterial Surface Structures in Pathogenesis. *Crit. Rev. Microbiol.* **1981**, *8*, 303–338.

(3) Otto, M. Staphylococcal Biofilms. *Curr. Top. Microbiol. Immunol.* **2008**, *322*, 207–228.

(4) Foster, T. J.; Geoghegan, J. A.; Ganesh, V. K.; Höök, M. Adhesion, Invasion and Evasion: The Many Functions of the Surface Proteins of Staphylococcus Aureus. *Nat. Rev. Microbiol.* **2014**, *12*, 49–62.

(5) Chan, Y. G.-Y.; Kim, H. K.; Schneewind, O.; Missiakas, D. The Capsular Polysaccharide of Staphylococcus Aureus Is Attached to Peptidoglycan by the LytR-CpsA-Psr (LCP) Family of Enzymes. *J. Biol. Chem.* **2014**, jbc.M114.567669.

(6) Paharik, A. E.; Horswill, A. R. The Staphylococcal Biofilm: Adhesins, Regulation, and Host Response. *Microbiol. Spectr.* **2016**, *4*.

(7) Speziale, P.; Pietrocola, G.; Foster, T. J.; Geoghegan, J. A. Protein-Based Biofilm Matrices in Staphylococci. *Front. Cell. Infect. Microbiol.* **2014**, *4*, 171.

(8) Dufrêne, Y. F. Towards Nanomicrobiology Using Atomic Force Microscopy. *Nat. Rev. Microbiol.* **2008**, *6*, 674–680.

(9) Müller, D. J.; Dufrêne, Y. F. Atomic Force Microscopy: A Nanoscopic Window on the Cell Surface. *Trends Cell Biol.* **2011**, *21*, 461–469.

(10) Louise Meyer, R.; Zhou, X.; Tang, L.; Arpanaei, A.; Kingshott, P.; Besenbacher, F. Immobilisation of Living Bacteria for AFM Imaging under Physiological Conditions. *Ultramicroscopy* **2010**, *110*, 1349–1357.

(11) Dufrêne, Y. F.; Ando, T.; Garcia, R.; Alsteens, D.; Martinez-Martin, D.; Engel, A.; Gerber, C.; Müller, D. J. Imaging Modes of Atomic Force Microscopy for Application in Molecular and Cell Biology. *Nat. Nanotechnol.* **2017**, *12*, 295–307.

(12) Formosa, C.; Grare, M.; Jauvert, E.; Coutable, A.; Regnouf-de-Vains, J. B.; Mourer, M.; Duval, R. E.; Dague, E. Nanoscale Analysis of the Effects of Antibiotics and CX1 on a Pseudomonas Aeruginosa Multidrug-Resistant Strain. *Sci. Rep.* **2012**, *2*.

(13) Formosa, C.; Herold, M.; Vidaillac, C.; Duval, R. E.; Dague, E. Unravelling of a Mechanism of Resistance to Colistin in Klebsiella Pneumoniae Using Atomic Force Microscopy. *J. Antimicrob. Chemother.* **2015**, *70*, 2261–2270.

(14) Longo, G.; Alonso-Sarduy, L.; Rio, L. M.; Bizzini, A.; Trampuz, A.; Notz, J.; Dietler, G.; Kasas, S. Rapid Detection of Bacterial Resistance to Antibiotics Using AFM Cantilevers as Nanomechanical Sensors. *Nat. Nanotechnol.* **2013**, *8*, 522–526.

(15) Longo, G.; Rio, L. M.; Trampuz, A.; Dietler, G.; Bizzini, A.; Kasas, S. Antibiotic-Induced Modifications of the Stiffness of Bacterial Membranes. *J. Microbiol. Methods* **2013**, *93*, 80–84.

(16) Longo, G.; Kasas, S. Effects of Antibacterial Agents and Drugs Monitored by Atomic Force Microscopy. *Wiley Interdiscip. Rev. Nanomed. Nanobiotechnol.* **2014**, *6*, 230–244.

(17) Scocchi, M.; Mardirossian, M.; Runti, G.; Benincasa, M. Non-Membrane Permeabilizing Modes of Action of Antimicrobial Peptides on Bacteria. *Curr. Top. Med. Chem.* **2016**, *16*, 76–88.

(18) Francius, G.; Lebeer, S.; Alsteens, D.; Wildling, L.; Gruber, H. J.; Hols, P.; Keersmaecker, S. D.; Vanderleyden, J.; Dufrêne, Y. F. Detection, Localization, and Conformational Analysis of Single Polysaccharide Molecules on Live Bacteria. *ACS Nano* **2008**, *2*, 1921–1929.

(19) Formosa-Dague, C.; Feuillie, C.; Beaussart, A.; Derclaye, S.; Kucharíková, S.; Lasa, I.; Van Dijck, P.; Dufrêne, Y. F. Sticky Matrix: Adhesion Mechanism of the Staphylococcal Polysaccharide Intercellular Adhesin. *ACS Nano* **2016**, *10*, 3443–3452.

(20) Chapot-Chartier, M.-P.; Vinogradov, E.; Sadovskaya, I.; Andre, G.; Mistou, M.-Y.; Trieu-Cuot, P.; Furlan, S.; Bidnenko, E.; Courtin, P.; Péchoux, C.; *et al.* Cell Surface of Lactococcus Lactis Is Covered by a Protective Polysaccharide Pellicle. *J. Biol. Chem.* **2010**, *285*, 10464–10471.

(21) El-Kirat-Chatel, S.; Beaussart, A.; Boyd, C. D.; O'Toole, G. A.; Dufrêne, Y. F. Single-Cell and Single-Molecule Analysis Deciphers the Localization, Adhesion, and Mechanics of the Biofilm Adhesin LapA. *ACS Chem. Biol.* **2014**, *9*, 485–494.

(22) Gilbert, Y.; Deghorain, M.; Wang, L.; Xu, B.; Pollheimer, P. D.; Gruber, H. J.; Errington, J.; Hallet, B.; Haulot, X.; Verbelen, C.; *et al.* Single-Molecule Force Spectroscopy and Imaging of the Vancomycin/D-Ala-D-Ala Interaction. *Nano Lett.* **2007**, *7*, 796–801.

(23) Formosa-Dague, C.; Speziale, P.; Foster, T. J.; Geoghegan, J. A.; Dufrêne, Y. F. Zinc-Dependent Mechanical Properties of Staphylococcus Aureus Biofilm-Forming Surface Protein SasG. *Proc. Natl. Acad. Sci. U. S. A.* **2016**, *113*, 410–415.

(24) Feuillie, C.; Formosa-Dague, C.; Hays, L. M. C.; Vervaeck, O.; Derclaye, S.; Brennan, M. P.; Foster, T. J.; Geoghegan, J. A.; Dufrêne, Y. F. Molecular Interactions and Inhibition of the Staphylococcal Biofilm-Forming Protein SdrC. *Proc. Natl. Acad. Sci. U. S. A.* **2017**, *114*, 3738–3743.

(25) Touhami, A.; Jericho, M. H.; Beveridge, T. J. Atomic Force Microscopy of Cell Growth and Division in Staphylococcus Aureus. *J. Bacteriol.* **2004**, *186*, 3286–3295.

(26) Matias, V. R. F.; Beveridge, T. J. Cryo-Electron Microscopy of Cell Division in Staphylococcus Aureus Reveals a Mid-Zone between Nascent Cross Walls. *Mol. Microbiol.* **2007**, *64*, 195–206.

(27) Monteiro, J. M.; Fernandes, P. B.; Vaz, F.; Pereira, A. R.; Tavares, A. C.; Ferreira, M. T.; Pereira, P. M.; Veiga, H.; Kuru, E.; VanNieuwenhze, M. S.; *et al.* Cell Shape Dynamics during the Staphylococcal Cell Cycle. *Nat. Commun.* **2015**, *6*, 8055.

(28) Perry, C. C.; Weatherly, M.; Beale, T.; Randriamahefa, A. Atomic Force Microscopy Study of the Antimicrobial Activity of Aqueous Garlic versus Ampicillin against Escherichia Coli and Staphylococcus Aureus. *J. Sci. Food Agric.* **2009**, *89*, 958–964.

(29) Humphries, R. M.; Pollett, S.; Sakoulas, G. A Current Perspective on Daptomycin for the Clinical Microbiologist. *Clin. Microbiol. Rev.* **2013**, *26*, 759–780.

(30) Müller, A.; Wenzel, M.; Strahl, H.; Grein, F.; Saaki, T. N. V.; Kohl, B.; Siersma, T.; Bandow, J. E.; Sahl, H.-G.; Schneider, T.; *et al.* Daptomycin Inhibits Cell Envelope Synthesis by Interfering with Fluid Membrane Microdomains. *Proc. Natl. Acad. Sci. U. S. A.* **2016**, *113*, E7077–E7086.

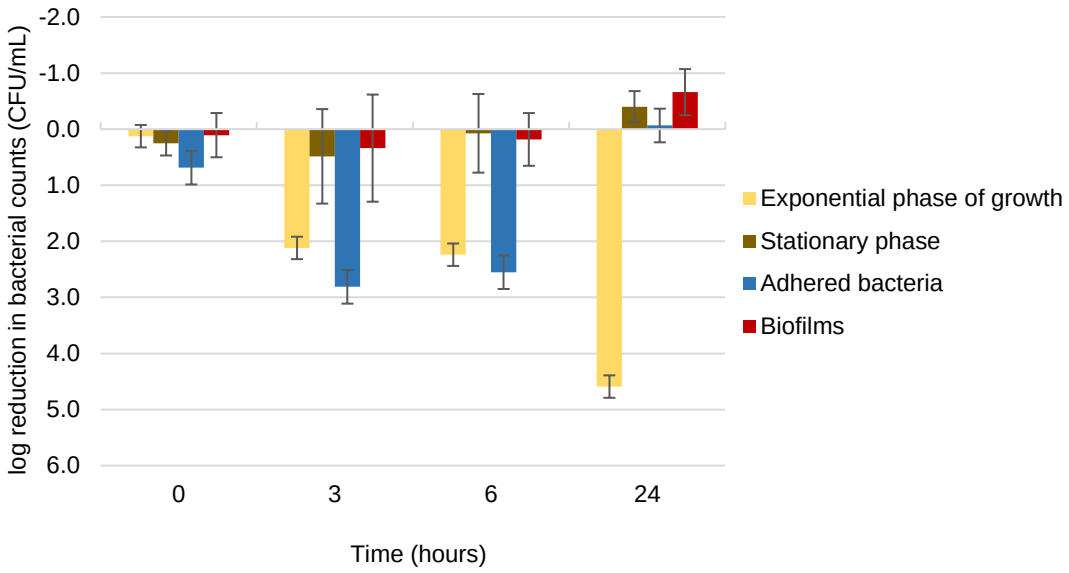

Figure S1. Daptomycin activity against *S. aureus* planktonic cells (exponential and stationary phase), adhered bacteria and biofilms.

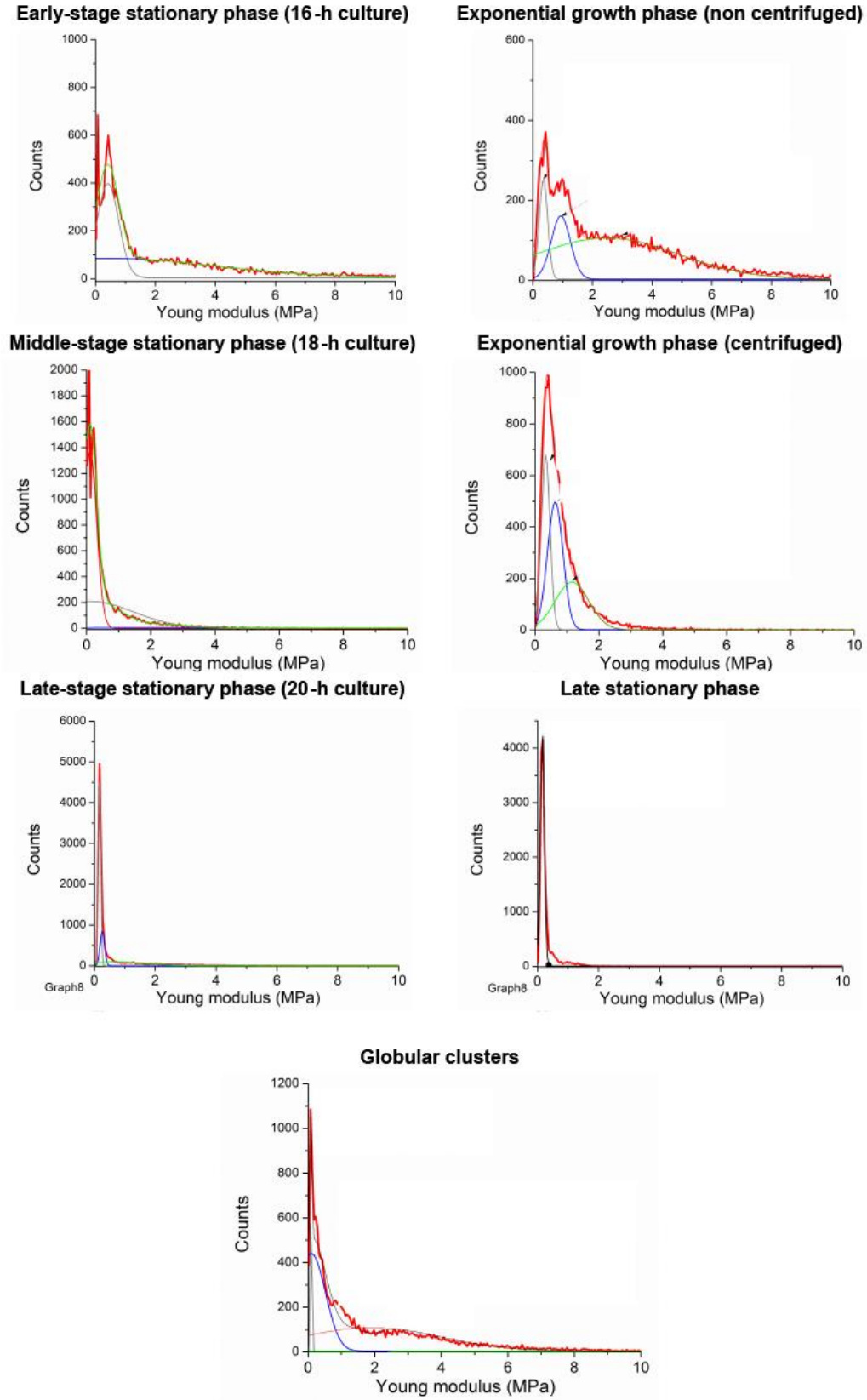

Figure S2. Young moduli histograms corresponding to the elasticity maps presented in Figures 2 and 3.

5.2. Article 7 : "Failure of daptomycin to inactivate *S. aureus* cells: the influence of the fatty acid composition of bacterial membranes"

Rym Boudjemaa, Clément Cabriel, Florence Dubois-Brissonnet, Nicolas Bourg, Guillaume Dupuis, Alexandra Gruss, Sandrine Lévêque-Fort, Romain Briandet, Marie-Pierre Fontaine-Aupart, Karine Steenkeste

Article soumis

Failure of daptomycin to inactivate *S. aureus* cells: the influence of the fatty acid composition of bacterial membranes

Rym Boudjemaa, [a] Clément Cabriel, [a] Florence Dubois-Brissonnet, [b] Nicolas Bourg, [a] Guillaume Dupuis, [c] Alexandra Gruss, [b] Sandrine Lévêque-Fort, [a] Romain Briandet, [b] Marie-Pierre Fontaine-Aupart, [a] Karine Steenkeste [a]

[a] Institut des Sciences Moléculaires d'Orsay (ISMO), CNRS, Université Paris-Sud, Université Paris-Saclay, Orsay, France; [b] Micalis Institute, INRA, AgroParisTech, Université Paris-Saclay, Jouy-en-Josas, France; [c] Centre Laser de l'Université Paris-Sud (CLUPS/LUMAT), Univ. Paris-Sud, CNRS, Université Paris-Saclay, F-91405 Orsay, France

Introduction

Staphylococcus aureus (*S. aureus*) is a major opportunistic human pathogen that causes a wide range of severe clinical infections, including bacteremia and endocarditis, as well as infections related to prosthetic implants.[1] These invasive diseases are often associated with biofilm formation.[2,3] The distinct properties of bacteria in biofilms, compared to their planktonic counterparts, render such infections particularly difficult to treat, resulting in severely restricted antimicrobial treatment options.[4]

Daptomycin was approved by the Food and Drug Administration in 2003 for the treatment of severe Gram-positive infections including those caused by methicillin-resistant *S. aureus* (MRSA).[5] This cyclic lipopeptide, comprising a hydrophilic depsipeptide covalently linked to a decanoyl fatty acid chain,[5,6] generally displays a rapid bactericidal activity by binding to the cytoplasmic membrane. Calcium ions (Ca^{2+}) enhance daptomycin amphiphilicity by assembling the charged amino acids on one side of the molecule and exposing its lipophilic tail on the other side, leading also to micelle formation. When in contact with bacterial membranes, daptomycin micelles undergo structural transitions, enabling the lipophilic tail to interact with the membrane, leading to pore formation and membrane destabilization, followed by potassium ion leakage and subsequent cell death.[7] Daptomycin aggregation in the membrane also interferes with membrane-associated processes, impairing cell envelope synthesis.[7–10]

Due to their multiple targeted mode of action, membrane-active antimicrobials such as daptomycin are believed to be bactericidal against slowly-growing or dormant bacteria as well as on biofilms.[6,11,12] However, daptomycin failure to treat *S. aureus* infections in clinical practice [5,13–22] reportedly vary between 10% and 40% depending on the site of infection treated.[20] Interestingly, while daptomycin treatment failure is frequent in clinical practice, it does not seem to correlate with resistance-based genetic mutations.[23,24] This might suggest that decreased susceptibility to daptomycin is an adaptive event independent on "classical resistance". In this context, daptomycin showed decreased activity against slowly-growing and biofilms cells without any concomitant increase in strains MICs (minimum antibiotic concentration required to inhibit bacterial growth, a parameter that defines the strain sensitivity/resistance).[20] We reasoned that as the bacterial membrane is the daptomycin target, an investigation of membrane biophysical properties would give insight on the parameters affecting bacterial unsusceptibility *versus* susceptibility. In particular, Dubois-Brissonnet *et al.* recently reported that slow-growing and biofilm bacteria exhibit more rigid membranes than actively-growing cells, which may be one reason for bacterial recalcitrance to daptomycin.[25]

The bacterial membrane equilibrium between rigidity and fluidity is driven by the structure and composition of phospholipid fatty acids.[26,27] In the case of *S. aureus*, bacterial membranes mainly consist of straight-chain and branched chain

saturated fatty acids. Straight-chains pack together to produce a bilayer with low permeability properties, while branched chain *iso* or *anteiso* methyl species promote a more fluid membrane structure.[26] Besides, the presence of exogenous fatty acids as found in the growth environment (serum, fluids, …etc.) can impact membrane composition and fluidity.[28]

Here we investigate the impact of growth phase and membrane composition on daptomycin efficacy against *S. aureus*.

Results

***S. aureus* sensitivity to daptomycin as a function of growth state and strains.** Daptomycin activity was assessed against two methicillin-susceptible (MSSA ATCC 27217 and 176) and two methicillin-resistant (MRSA ATCC 33591 and BCB8) *S. aureus* strains, all of which scored as daptomycin-sensitive in standard MIC tests (Minimum Inhibitory Concentrations (MICs) below the breakpoint value, which is 1 mg/L according to EUCAST 2016).[29] These strains were then examined for sensitivity to daptomycin as a function of growth phase (Fig. 1).

Three of the four strains (Fig. 1) showed accrued sensitivity during exponential growth when treated with a therapeutic daptomycin concentration (20 µg/mL, Fig. 1). In strong contrast, daptomycin had only a primarily bacteriostatic effect on cells maintained in the stationary phase or included in biofilms (Fig. 1).

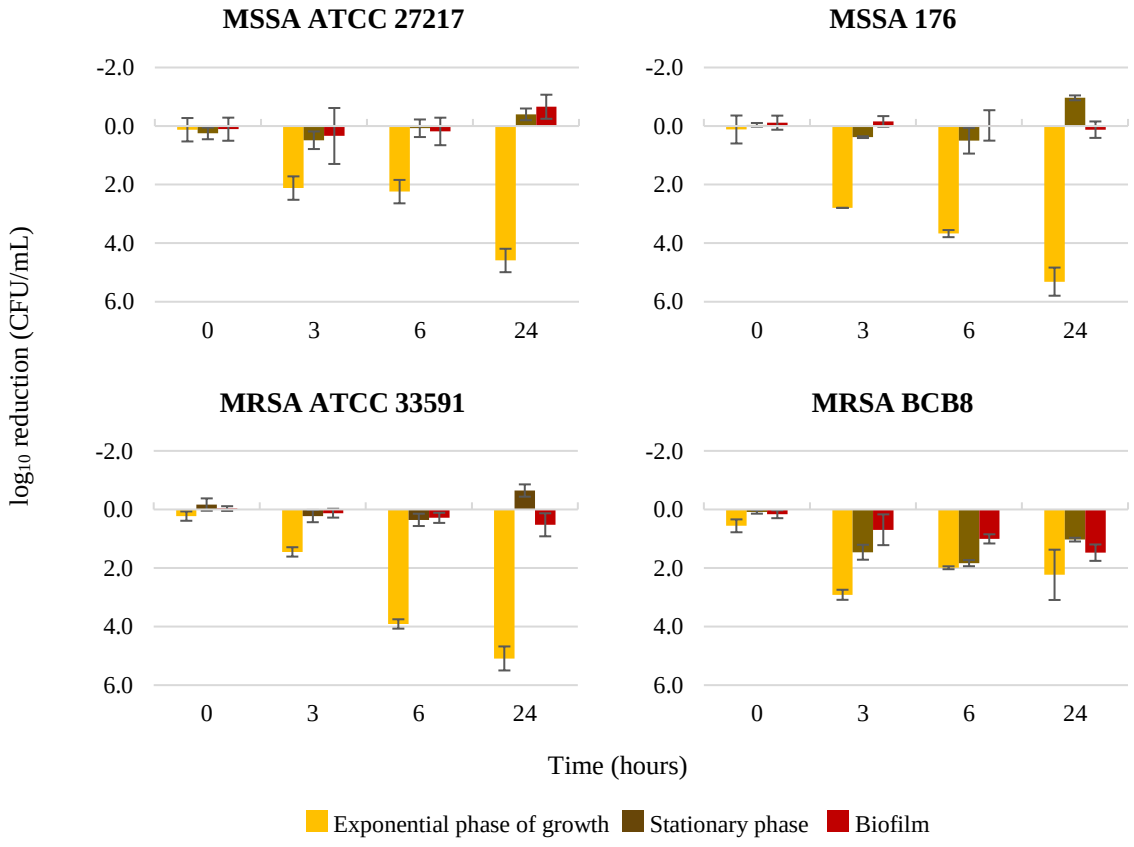

Fig. 1. Daptomycin activity over time against four *S. aureus* strains depending on their phase of growth. Each graph represents daptomycin-induced reduction in bacterial counts over time at regular time points (0, 3, 6 and 24 h) for each strain. MSSA ATCC 27217 and MRSA ATCC 33591 are two collection strains. MSSA 176 and MRSA BCB8 are clinical strains isolated from bloodstream infections in patients. Error bars represent the ANOVA based on at least 4 independent experiments ($P < 0.05$).

One clinical isolate, MRSA BCB8, responded differently to daptomycin compared to the other tested strains. This latter was less sensitive to daptomycin for exponential growth cells, but was less affected for cells in the stationary phase or inside biofilms (Fig. 1).

These results show that *S. aureus* sensitivity to daptomycin activity varies not only with the growth state but also with the strain.

Daptomycin is bioavailable and interacts with stationary phase *S. aureus* cells. We investigated whether the failure of daptomycin to eradicate *S. aureus* stationary phase and biofilm cells was simply due to a loss of binding by comparison to exponential phase cells. To this purpose, we performed image-based Fluorescence Recovery After Photobleaching (FRAP) to measure daptomycin diffusion and bioavailability within planktonic cells, either during exponential growth or in stationary phase and compare to the results already obtained with biofilm-encased cells in [29]. Fluorescence recovery curves were equivalent regardless of the bacteria growth phase. The *S. aureus*-bound fluorescent BODIPY-FL-daptomycin was ~ 60 ± 5%, (*vs* only 20% inside biofilms) while 40% (respectively 80% inside biofilms) remained bioavailable over the 30-s observation period (Fig. 2A). The local diffusion coefficient at equilibrium (D), determined using the Braga mathematical model,[30] was 11.0 ± 1.2 µm²/s, and was independent of the growth phase (to be compare to 7.1 ± 0.6 µm²/s in biofilms). As a control, BODIPY-FL alone did not associate with bacteria, and fluorescence was fully recovered after photobleaching (100% freely-diffusing molecules); its local diffusion coefficient was ~ 180 ± 60 µm²/s (data published in [30]). Daptomycin binding to stationary phase staphylococci was also imaged by fluorescence Confocal Laser Scanning Microscopy (CLSM) (Fig. 2B). Altogether, these results demonstrate that daptomycin interacts with *S. aureus* independently of the cell state, suggesting that the drug is cell-associated, but inactive against stationary phase and biofilm cells.

Daptomycin reaches its cytoplasmic membrane target in stationary phase *S. aureus*. We asked whether cell-bound daptomycin actually reached its target, the cytoplasmic membrane, in stationary phase cells. Due to the thin *S. aureus* cell membrane, fluorescence CLSM did not provide

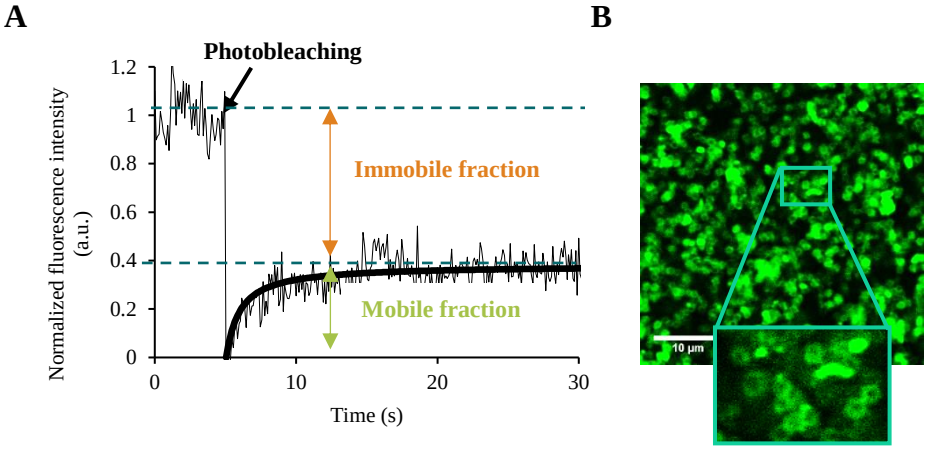

Fig. 2. Daptomycin interacts with exponentially-growing and stationary phase cells and 40% of free molecules are still bioavailable. (A) A typical fluorescence recovery curve obtained for BODIPY-FL-daptomycin within exponentially-growing and stationary phase MSSA ATCC 27217 cells. The normalized fluorescence intensity is represented as a function of the time. In orange is shown the immobile fraction and in green the mobile fraction. **(B)** A typical image acquired for stationary phase cells deposited 5 min prior to observation on a coverslip, in the presence of BODIPY-FL-daptomycin. The inset allows to visualize that BODIPY-FL-daptomycin appeared homogenously localized at the surface of bacterial cells.

significant resolution to discriminate between wall or membrane location of daptomycin (200-nm resolution, versus ~ 40-nm thickness for the cell wall and 10-15 nm for the cell membrane).[31–33] We therefore performed Direct Optical Nanoscopy with Axially Localized Detection (DONALD) to determine antibiotic 3D localization with a nanometric precision (10-nm in lateral and 15-20 nm in axial).[34] For this experiment, the antibiotic was fluorescently labelled by means of a 10-12 nm antibodies-based construction (shown in Fig. 3A and detailed in Materials and Methods section). Inside the cell wall, antibiotic localization would expectedly be random, and hence distribute over the ~ 40 nm thickness. In contrast, antibiotic molecules inserted into the membrane would be expected to localize at ~ 30 nm from the coverslip surface – considering the 10-12 nm fluorescent labeling together with the cell wall thickness (Fig. 3B). It should be noted that the antibodies-based labelling construction is on the cyclic decapeptide core of daptomycin, such that the lipid tail is kept free to interact with the lipid bilayer. Data processing of DONALD acquisitions (see details in Material and Methods section), allowed to determine the mean height of the fluorophores from the coverslip surface (z) and represented it as a function of the bacterium fluorophore radial position (ρ) (Fig. 3D). These results showed that the labelled daptomycin was localized around 33 nm (between 28 and 38 nm) above the substratum. Considering the length of the antibodies-based construction linked to daptomycin (10-12 nm) and their random orienta-

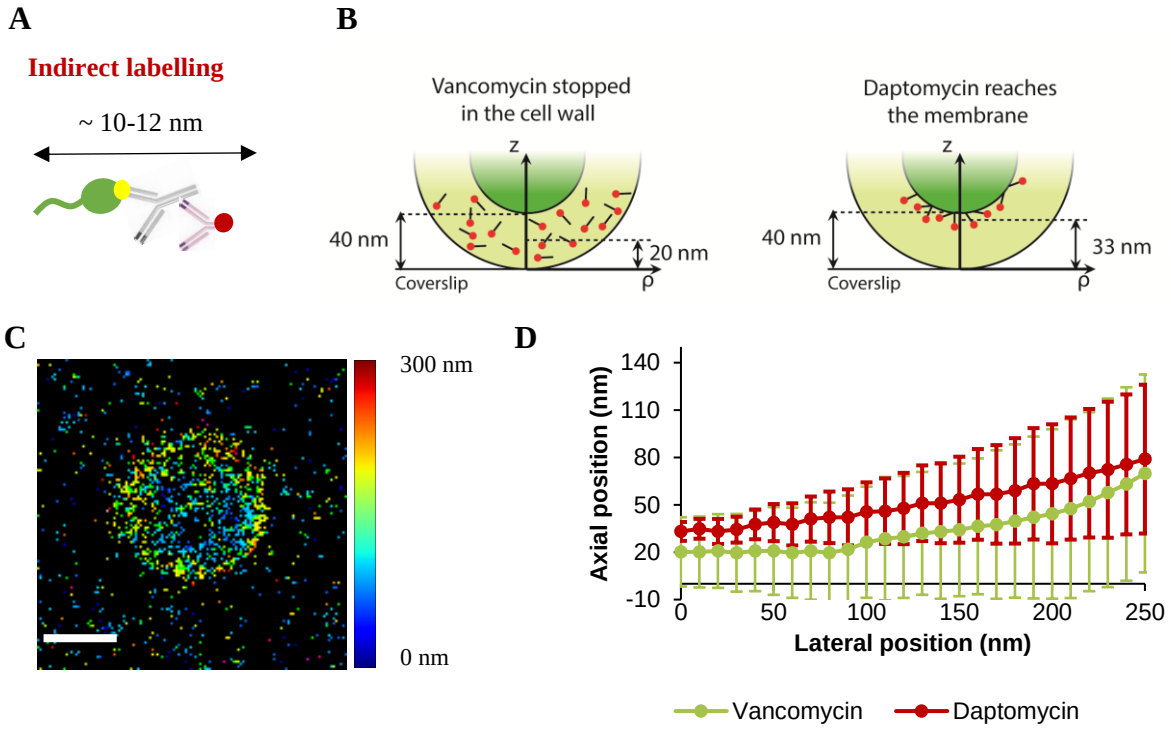

Fig. 3. Daptomycin reaches the cytoplasmic membrane of stationary phase cells. (A) Antibodies-based construction used to label daptomycin: in green daptomycin, in yellow the BODIPY-FL grafted on the cyclic decapeptide core of daptomycin, in grey the anti-BODIPY-FL rabbit antibody and in red the AF647-fragment of goat antibody. **(B)** The two cases considered here: either localization within the cell wall (vancomycin) or at the cell membrane (daptomycin). **(C)** A typical 3D DONALD image acquired for stationary phase cells. The color scale bar represents the z position in nanometers and the white horizontal scale bar represents 500 nm. **(D)** Daptomycin (red) and vancomycin (green) localization curves representing the axial positions of the fluorescently-labelled antibiotics as a function of their lateral positions. Error bars represent ± twice the standard deviation of the fluorescent probes distribution. It must be noted that TIRF depth detection (~300 nm) limits observations to the bottom side of each bacterium deposited on the substratum.

tion, the results obtained indicate that the antibiotic itself is localized ~ 40 nm above the coverslip, corresponding to a membrane localization (Fig. 3B and D).

As a control, we performed the same experiments in the same conditions with vancomycin, a cell-wall targeting antibiotic that was labelled with the same antibodies-based construction. In this last case, the labelled vancomycin was found to be localized between 0 and 40 nm (20 ± 22 nm) above the coverslip (Fig. 3D), characterizing a random localization of vancomycin within the bacterial cell wall.

These results confirm that daptomycin effectively reaches the cell membrane in stationary phase cells.

Daptomycin induces lower membrane damage in stationary phase and biofilm staphylococci than in growing cells. Pore-forming ability of daptomycin was evaluated using propidium iodide (PI). Due to the large-size of this cationic fluorescent dye, PI is excluded from cells with intact cytoplasmic membranes but can penetrate damaged-membrane bacteria if pores of sufficient size are created. PI was able to penetrate the high amounts of exponentially-growing cells just 10 min after daptomycin treatment (~ 40%). By contrast, only few cells were PI-positive (~ 5%) in stationary phase and biofilms, revealing significantly lower membrane damage (Fig. 4). Pore formation was also controlled 3h after daptomycin treatment: exponentially-growing cells were all PI-positive (100%), whereas stationary phase and biofilms cells were predominantly negative (~ 5-10%).

Daptomycin-triggered release of potassium ions is lower in stationary phase and biofilm staphylococci than in growing cells. Daptomycin-induced release of potassium ions was evaluated using the membrane-impermeant K^+ fluorescent probe APG-2 (Fig. 5). Within 1 min after daptomycin addition to exponentially-

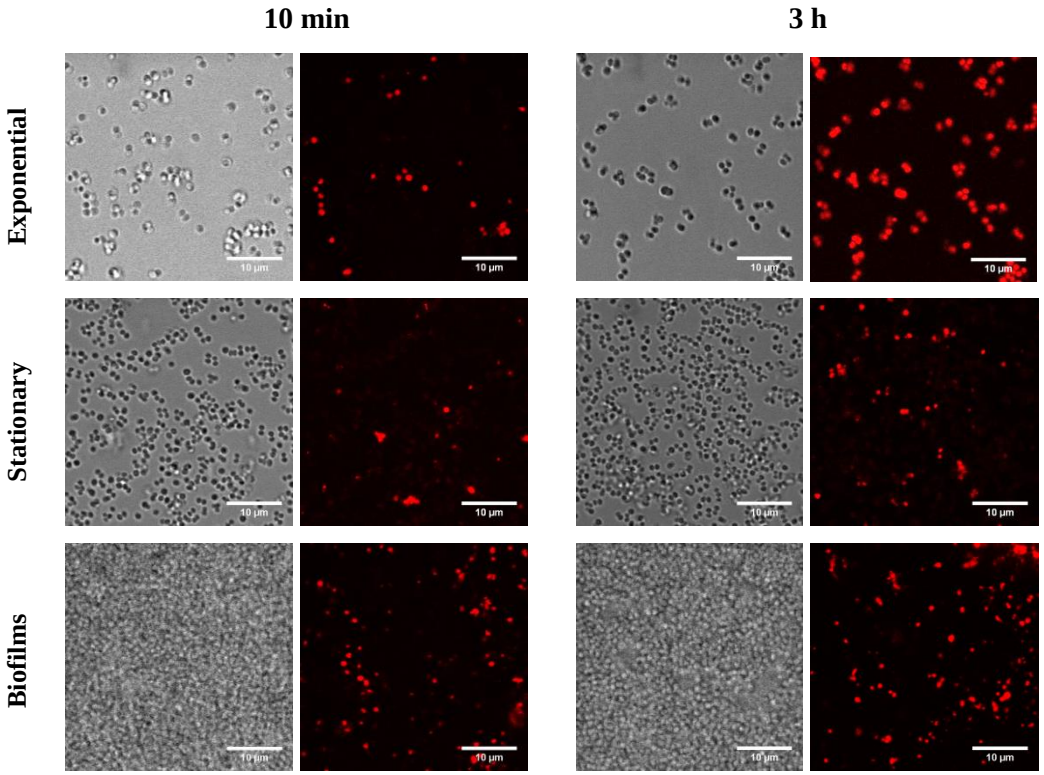

Fig. 4. Pore-forming ability of daptomycin: significant membrane damage only occurs within exponentially-growing cells. Transmission images show all the bacterial cells in the field of observation and corresponding fluorescence images show the bacterial cell membrane damage highlighted by PI labelling after 10 min and 3 h of treatment with daptomycin. Note that while biofilm cell density is very high the proportion of PI-labelled cells is minor.

growing bacteria the fluorescence signal increased from a baseline of 200 a.u. to 700 a.u., revealing a rapid release of K^+ ions into the surrounding medium. By contrast, the fluorescence intensity measured within stationary phase cells was comparable before and after antibiotic injection. For biofilms, a slight increase was observed after daptomycin addition before reaching a plateau within 1 min (400 a.u.). Three hours after daptomycin incubation within bacterial cells in presence of APG-2, extracellular fluorescence intensity continued to increase for exponentially-growing cells while it remained stable for stationary phase and biofilm bacteria.

Membrane fatty-acid composition is a determinant of daptomycin efficacy. We considered that membrane modifications, in particular those affecting membranes fluidity/ rigidity, could impact daptomycin activity. We thus investigated *S. aureus* fatty acid composition as a determinant of membrane fluidity on all strains (MSSA 176, 27217 and MRSA 33591, BCB8) (Fig. 1) and during different growth phases (Fig. S4). The data were compiled together with daptomycin-sensitivity results (Table 1 and Fig 6) using variance analyses, to determine whether daptomycin activity correlated with the ratios of fatty acids constituting bacterial membranes. Significantly, poor daptomycin activity correlated with higher percentages of saturated fatty acids (SFA) and *iso* form fatty acids, with a concomitant overall decrease in *anteiso* species ($P < 0.05$) (Table 1). These results suggest that high percentages of SFA and *iso* fatty acid forms may be a determining factor in poor efficiency of daptomycin against *S. aureus*, leading us to suggest that daptomycin action may depend upon bacterial membrane composition.

Afterward, we correlated more precisely the strain susceptibility towards daptomycin (regardless the growth phase) to *S. aureus* membrane fatty acid content (Fig. 7). Variance analysis showed that more resistant strains (*i.e.*, the tested MSSA isolates) had more SFA-rich membranes whereas more sensitive strains (MRSA isolates) had higher *anteiso* BFA contents ($P < 0.05$).

To further confirm the impact of bacterial membrane rigidity on daptomycin inactivity, we manipulated the membrane fatty acid content by adding different exogenous fatty acids. Stearic acid (C18) is a long-chain SFA that rigidifies membranes, while oleic acid (C18:1) is a long-chain unsaturated fatty acid that fluidifies membranes.[25,26] Bacterial growth was simultaneously determined in the presence of either C18 or C18:1 without daptomycin to check that no fatty acid-induced toxicity occurred in the test conditions (Fig. S2 and S3). While C18 incorporation led to a decreased or equal activity of daptomycin in all growth phases, C18:1 incorporation led to a significant increase in daptomycin sensitivity (Fig. 8A). Indeed, a 4.3 log reduction in bacterial survival was measured at 6 h in exponentially-growing cells (a 100-fold increase in sensitivity compared to a non-supplemented culture, Fig. 8A). Interestingly, while stationary phase cultures were totally insensitive to daptomycin in TSBpc (Fig. 8A), C18:1 addition led to a 2500-fold reduction in bacterial counts after 6 h of treatment. Biofilm bacteria were also sensitized to daptomycin by C18:1 addition but to a lesser extent (~10-fold reduction, Fig. 8A). Fatty-acid profiles determined

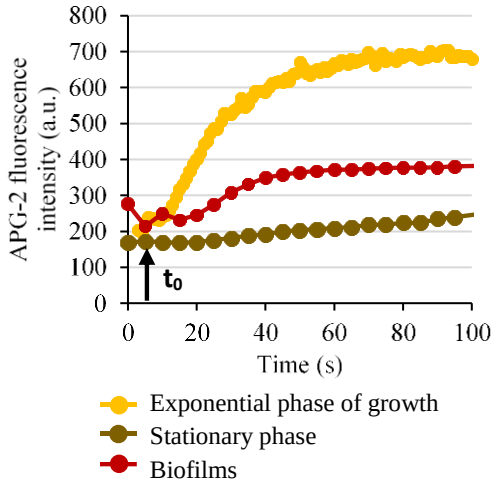

Fig. 5. Potassium ions release after daptomycin injection. Bacteria were incubated 10 min with APG-2 (a membrane-impermeant K+ ions marker) to check the fluorescence intensity signal. t_0 corresponds to daptomycin injection (indicated with the black arrow).

Fatty acid	% of each fatty acid when		
	Daptomycin is active ǂ	Daptomycin is inactive ǂ	Statistically significant difference
Saturated Fatty acids	46	52	*
Iso Branched-chain Fatty Acids	21	20	*
Anteiso Branched-chain Fatty Acids	33	28	*

This table represents the ratios of each type of fatty acid present in the membrane when daptomycin is either active or inactive. The results shown here consider all the data obtained, independently on the strain and the phase of growth.
* represents a statistically significant difference between fatty acids percentages whether daptomycin is active or not ($P < 0.05$)
ǂ In order to classify the different experiments according to daptomycin susceptibility, we considered that daptomycin was active when the log reduction in bacterial counts was positive (a decrease in bacterial populations) and *a contrario* that daptomycin was inactive when the log reduction in bacterial counts was negative or zero (an increase in bacterial counts).

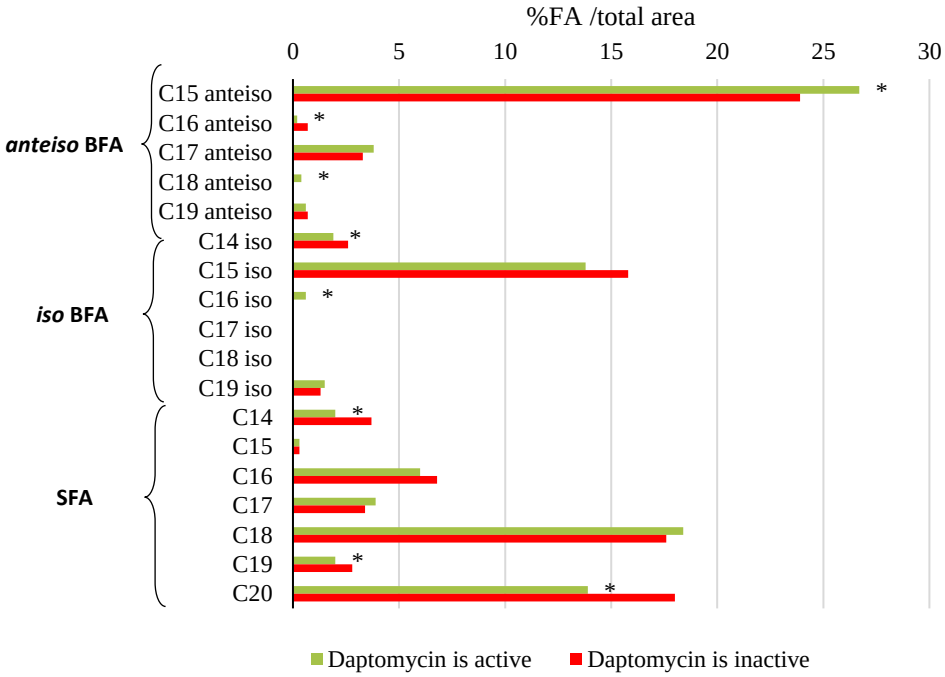

Fig. 6. Daptomycin inactivity is correlated with higher ratios of SFA and *iso* BFA and lower ratios of *anteiso* BFA. This figure represents the ratio of each fatty acid present in the membrane when daptomycin is either active (a reduction in bacterial counts > 0) or inactive (a reduction in bacterial counts ≥ 0)
* represents a statistically significant difference between fatty acids percentages whether daptomycin is active or not ($P < 0.05$)

for C18:1-supplemented bacterial cultures (Fig. 8B) demonstrated that stationary phase cells incorporated oleic acid to reach 43% of the whole bacterial membranes contents while biofilms cells only incorporated 4%. This latter result is in good agreement with the lower enhancement of daptomycin sensitivity in biofilms by contrast with stationary phase cells (Figure 8A).

Discussion

Daptomycin is a last-resort antibiotic used to treat infections due to multi-antibiotic-resistant bacteria.[5] However, daptomycin efficacy in *S. aureus* is diminished in stationary phase and biofilm cells.[12,35] The physical basis for conditional *S. aureus* daptomycin-resistance has remained an unsolved question. Our main findings identify the step at which daptomycin activity fails, and provide a means of restoring its efficacy.

Previous studies suggested that daptomycin resistance of stationary and biofilm cells was due to poor access to its membrane target and consequent lack of bioavailability.[6,36] Our results

disprove this hypothesis: first, daptomycin diffuses throughout the biofilm structure and interacts with bacteria.[29] Second, daptomycin was shown here to interact with the cell membrane of tolerant stationary phase cells and biofilms. Thus, limited antibiotic access does not explain daptomycin resistance in these cell states. To our knowledge, this is the first report in which an antibiotic is localized with such precision in live *S. aureus* cells. Previous studies of antibiotic localization were performed on larger targets, e.g., *Bacillus subtilis* or giant unilamellar vesicles.[37,38]

Antimicrobial activity of daptomycin is attributed to its aggregation in the membrane; this leads to pore formation and subsequent potassium ion release, as was shown in exponentially growing cells.[39] Our results reveal that pore formation fails to occur in stationary and biofilm daptomycin-resistant cells, which did not undergo membrane damage or potassium ion leakage. Taken together, our results reveal that daptomycin reaches its membrane target in stationary and biofilm cells, and that oligomerization for pore formation is the crucial missing step.

Stationary and biofilm *S. aureus* cell membranes have previously shown to be more rigid than exponentially-growing cells,[25] leading us to hypothesize that membrane fluidity could be a determining factor for whether daptomycin could form membrane-permeabilizing pores. Unsaturated fatty acids generate kinks that generate greater fluidity of membrane phospholipids.[6] Adding free exogenous fatty acids is an effective means of altering membrane composition, such that membrane fluidity can be manipulated.[25,28,40,41] Remarkably, we found that unsaturated fatty acid supplementation greatly increased daptomycin sensitivity of *S. aureus* regardless of its growth state. The restoration of daptomycin sensitivity correlated with the efficiency of oleic acid incorporation, which varied with the bacterial growth state.[25] These results lead us to suggest that membrane fluidity is a crucial determinant of daptomycin activity.

The above findings indicate that daptomycin pore formation is facilitated in fluid membranes, as obtained by oleic acid addition (Fig. 8). We suggest that enhanced membrane fluidity due to oleic acid incorporation in phospholipids gives more space for daptomycin oligomerization, as suggested by enhanced cell death. Additional effects of oleic acid might also be considered in view of a recent study showing that daptomycin efficacy is attenuated in *S. aureus agr* mutants.[42]

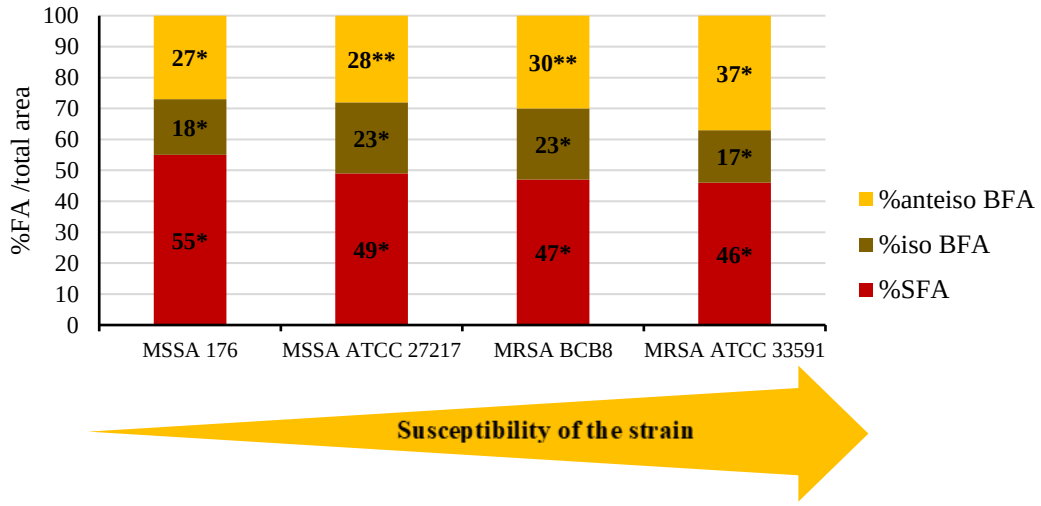

Fig. 7. Correlation between the fatty acid percentages and the susceptibility of the strain. The results shown here consider the four strains susceptibility independently on the phase of growth. In each bar are represented the percentage values for each type of fatty acid.

* SFA and *iso* BFA percentages were statistically different between the four strains ($P < 0.05$)

** *anteiso* BFA percentages were statistically not different between the two strains ($P < 0.05$)

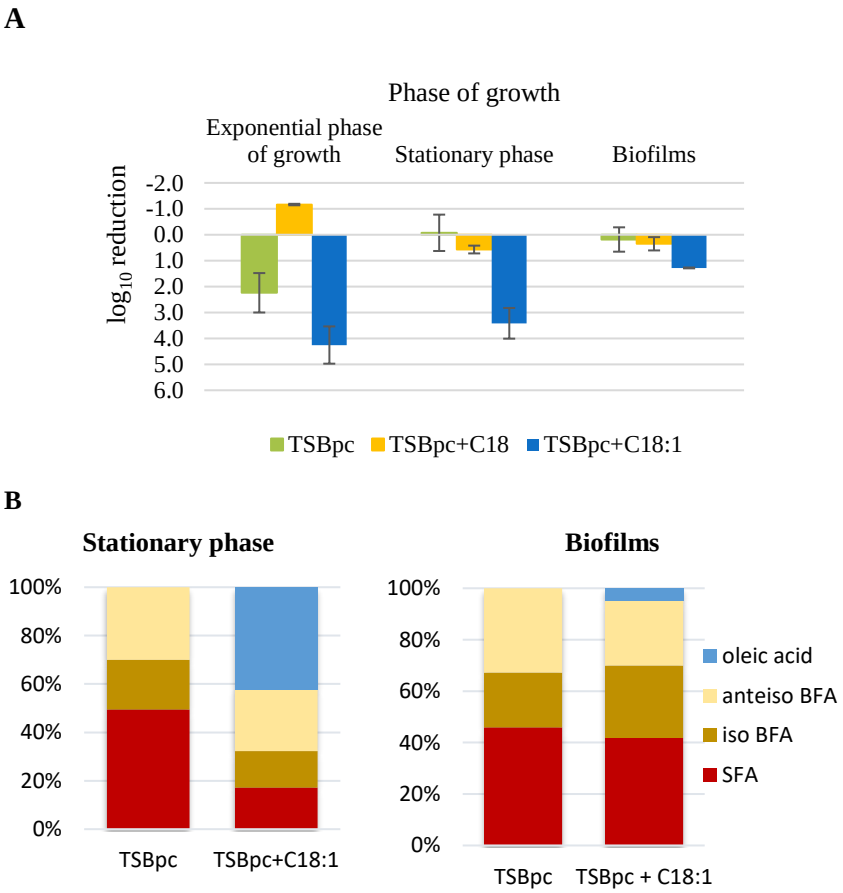

Fig. 8. Incorporation of oleic acid (C18:1) into *S. aureus* bacterial membranes increases daptomycin sensitivity while the incorporation of stearic acid (C18) decreases the antibiotic activity. (A) represents the number of log reduction in bacterial counts after 6h of daptomycin treatment compared with the initial bacterial concentration. TSBpc is the medium used to grow *S. aureus* cells without fatty acids, TSBpc+C18 corresponds to the stearic acid-supplemented medium and TSBpc+C18:1 corresponds to the oleic acid-supplemented medium. Error bars represent the standard deviation. **(B)** represents the fatty acids composition of bacterial membranes when the growth medium is supplemented with oleic acid.

Authors showed that an *S. aureus agr* mutant forms vesicles that are shed from membranes, which sequester daptomycin to lower its effective concentration.[42] Interestingly, oleic acid reportedly stimulates *agr* gene transcription.[43] It is therefore tempting to speculate that blebbing would not occur when *agr* expression is high, thus leaving cells daptomycin-sensitive. This provocative hypothesis remains to be tested.

Interestingly, fatty acid supplementation led to an opposite effect in a recent study on *Enterococcus faecalis*, *i.e.*, these bacteria become more daptomycin-resistant in the presence of exogenous fatty acids or lipid containing fluids, including bile. Those effects did not correlate with membrane fluidity.[41] These results suggest that species-specific differences might account for different responses. Alternatively, co-treatment with fatty acids and daptomycin could lead to titration of the antibiotic into micelles. In the present study, daptomycin was added to fatty-acid-loaded, but washed cells, which might account for the observed differences.

In summary, results of this study show that daptomycin reaches its membrane target in *S. aureus* regardless of growth state, and that the key parameter for daptomycin sensitivity *versus* tolerance is likely to depend on its capacity to form pores, as a function of membrane composition. Staphylococcal sensitivity to daptomycin can be manipulated, which could open the way to novel strategies of antibiotic treatment, such as its

encapsulation within fatty acids [44] or the use of bi-therapies including daptomycin and membrane-fluidizing agents.

Materials and methods.

Bacterial strains. Four *S. aureus* strains were tested in the present study: two were collection strains (methicillin-susceptible *S. aureus* [MSSA] ATCC 27217 and methicillin-resistant *S. aureus* [MRSA] ATCC 33591), and two others were isolated from patients with *S. aureus* bloodstream infections (MSSA 176 and MRSA BCB8). All strains were kept at -80°C in tryptic soy broth (TSB) (BioMérieux, France) containing 20% (vol/vol) glycerol. The frozen cells were sub-cultured once in TSB (overnight culture) to constitute the stock cultures from which aliquots were kept at -20°C. Bacterial growth and experiments were both conducted at 37°C.

Antibiotic and culture medium. Daptomycin was purchased from Sigma (France) and the fluorescently labelled antibiotic BODIPY-FL-labelled daptomycin (BODIPY-FL-daptomycin) (BODIPY-FL is fluorescently labelled boron-dipyrromethene) was kindly provided by Cubist Pharmaceuticals (MA, USA). According to the manufacturer's instructions, the stock solutions were prepared by diluting daptomycin and BODIPY-FL-daptomycin in dimethyl sulfoxide (1 mg/ml), which was then kept at -20°C. Before the solutions were used, they were diluted in TSB enriched with proteins (bovine serum albumin [BSA], 36 g/L; Sigma, France) and calcium ($CaCl_2 \cdot 2H_2O$, 50 mg/L; Sigma, France) to mimic *in vivo* physiological levels. It has been determined that, under these conditions, the final concentration of dimethyl sulfoxide was noncytotoxic for the bacteria. A clinically meaningful concentration was used in this study: 20 µg/ml for daptomycin.

When indicated, an exogenous fatty acid was added to the culture medium: either stearic acid (C18, +99%puriss, Larodan, a saturated fatty acid) or oleic acid (C18:1cis9, +99% puriss, Larodan, a monounsaturated fatty acid). 100-mM stocks solutions of exogenous fatty acids were prepared in dimethylsulfoxide (final concentrations of DMSO did not induce bacterial toxicity). Final concentrations of fatty acids were 0.25 mM in the growth medium.

Determination of daptomycin activity against *S. aureus*. Daptomycin activity was assessed against the four *S. aureus* strains in exponential phase of growth, stationary phase and 24 h biofilms.

(i) Planktonic cells. After two subcultures in TSB (one 8-h culture followed by an overnight culture), stationary phase cells were harvested directly using the overnight culture while exponentially-growing cells were obtained with a third subculture in TSB enriched with proteins and calcium (TSBpc) with shaking at 100 rpm during 3 h. Bacterial suspensions were washed twice in sterile NaCl (150 mM) and resuspended in TSBpc. Optical density was measured at 600 nm to control the initial bacterial concentration. The bacterial solution was then divided equitably into cell culture flasks where daptomycin solution was added. Bacterial growth was also controlled with a sample without daptomycin that corresponds to the control experiment. Viable culturable bacteria were then counted at regular interval times: 0 h (when antibiotics were added), 3, 6 and 24 h after antibiotics injection. For each time, 1.5 mL of bacterial culture was collected and centrifuged 10 min at 7000*g* in order to eliminate the excess of antibiotic. The bacterial pellet was dispersed in 1.5 mL sterile NaCl 150 mM, centrifuged again and dispersed in the same conditions. Successive decimal dilutions were then realized. For each dilution, six drops (10 µL) were deposited on Tryptic Soy Agar (TSA) plates (Biomérieux, France), incubated at 37°C during 24 h. CFUs were counted and averaged for each dilution at each time. The detection limit of viable culturable cells was here 100 CFU/mL.

(ii) Biofilms. For the preparation of *S. aureus* biofilms, 250 µL of an overnight subculture were added to 96-well microplates (µClear; Greiner Bio-One, France). After a 1.5-h adhesion period at

37°C, the wells were rinsed with a NaCl solution (150 mM) to eliminate non-adherent cells, refilled with sterile TSBpc and then incubated for 24 h at 37°C to allow biofilm growth. To assess daptomycin activity, the 24 h-biofilms were rinsed with a sterile NaCl solution (150 mM) before adding daptomycin solution diluted in TSBpc as described previously. Viable culturable bacteria were then enumerated by serial dilutions and plating on tryptic soy agar (TSA) plates at regular interval times: 0 h (when daptomycin was added), 3, 6 and 24 h after the antibiotic injection. For each time, bacterial cultures were centrifuged twice, decimal dilutions were realized and CFUs were counted as for planktonic bacteria.

Antibiotic diffusion and bioavailability inside biofilms using FRAP experiments. Image-based fluorescence recovery after photobleaching (FRAP) measurements were performed on MSSA ATCC 27217 planktonic cells. Bacterial cultures were either grown to exponential phase of growth or stationary phase as described previously. Then, 250 µL of these cultures were deposited 5 min on 96-well polystyrene microtiter plates prior to observations. All the time-resolved measurements were obtained using a Leica TCS SP5 confocal laser scanning microscope (Leica Microsystems, France) implemented at the Centre de Photonique Biomédicale (CPBM) (Orsay, France). The microscope is equipped with a 63x high numerical aperture (1.4) oil immersion objective and coupled with continuous lasers. BODIPY-FL-daptomycin was excited at 488 nm and fluorescence emission was recorded between 500 and 600 nm. As described previously in [29,30,45], FRAP experiments were conducted as follows. BODIPY-FL-daptomycin molecules were excited with a very intense light source in a user-defined region (a bacterium in our case) to irreversibly photobleach their fluorescence. Fluorescence recovery is then probed over time at a low light power in the same photobleached region. The time course of fluorescence intensity recovery was analyzed with mathematical models, giving us the quantitative mobility of the fluorescent molecules and allowing us to determine the diffusion coefficients. For all FRAP experiments, the fluorescence intensity image size was fixed to 512 by 128 pixels with an 80-nm pixel size and recorded using a 16-bit resolution. The line scan rate was fixed at 1 400 Hz, corresponding to a total time between frames of 265 ms. The full widths at half maximum in *xy* and *z* (along the optical axis) of the bleached profile were 0.8 µm and 14 µm, respectively, allowing us to neglect diffusion along the axial/vertical axis and thus to consider only two-dimensional diffusion. Each FRAP experiment started with the acquisition of 50 images at 7% of laser maximum intensity (7 µW) followed by a 200-ms single bleached spot at 100% laser intensity. A series of 450 single-section images was then collected with the laser power attenuated to its initial value (7% of the bleach intensity). The first image was recorded 365 ms after the beginning of bleaching.

DONALD. This technique, described in detail in [34], relies on the localization of individual fluorescent molecules and requires them to be fluorescent only a fraction of time so that they can be localized separately. To achieve this temporal separation, a reversible blinking (*i.e.* oscillation between bright and dark states) of the fluorescent molecules is induced by the addition of chemicals in the imaging buffer to influence their photophysical properties. One limitation, however, is that the mechanisms responsible for this chemically-induced blinking has only been identified for a few dyes [46]. Among them, Alexa Fluor (AF) 647 together with its imaging buffer (an enzymatic oxygen scavenging system to prevent from photobleaching) have widely been used to perform dSTORM imaging [47,48]. Thus, to allow the antibiotic localization in our experiments, we designed a specific fluorescent labelling construction in order to detect AF647 fluorescence.

(i) Daptomycin labelling and buffer. The labelling consisted in grafting a primary rabbit antibody (8nm) that specifically targets BODIPY-FL and quenches its fluorescence. Then, a secondary goat anti-rabbit antibody fragment (5 nm) labelled with AF647 was used to target the

rabbit antibody. The advantage of using such antibodies-based labelling is their rigid structure that allows to ascertain a precise size and orientation of the whole structure [49]. The fluorophore detected and imaged here was then Alexa Fluor 647 which was excited at 637 nm. To select the fluorescence emission of this latter dye only, a quad band 446-523-600-677 (Semrock) filter was used. Acquisitions were performed using a thiol-based buffer (dSTORM super resolution buffer Smart Kit, Abbelight). We ensured that bacteria stayed alive during the time of acquisition by using PI to label damaged-membrane cells.

(ii) Localization, data processing and statistical analysis. Using a Total Internal Reflection Fluorescence (TIRF) excitation to reduce background noise, most of the fluorophores were induced in a dark state until a sufficient density was obtained (typically 1 molecule per bacterium per frame). Images were acquired with 50 ms exposure time and 150 Electron-Multiplying Charged Coupled Device (EMCCD) gain. The frames were then processed using a home-written Python code detecting the lateral position and the absolute depth of each spot. This detection relies on the Direct Optical Nanoscopy with Axially Localized Detection (DONALD) technique, which couples both Single Molecule Localization Microscopy (SMLM) and Supercritical Angle Fluorescence (SAF) using a Nikon Eclipse Ti-E microscope [34]. SAF detection is based on the comparison of the far-field emission and the part of the near-field emission that is coupled into propagative waves at the sample/glass coverslip interface due to the refractive index mismatch. Since the near-field amplitude decays exponentially before it reaches the interface, an intensity measurement yields the absolute axial positions (z) of the fluorophores.

In order to determine the position of the antibiotic in bacteria, the data were processed as follows. First, the center (x_0, y_0) of each bacterium was measured. Then the lateral position ρ of each fluorophore (x, y, z) was calculated: $\rho = \sqrt{(x - x_0)^2 + (y - y_0)^2}$. The localization results were pooled over approximately 80 bacteria for a total amount of 60 000 localizations. The results were then integrated radially and divided in ρ slices of 10 nm width, and the mean depth $< z >$ of each ρ slice was displayed alongside with its uncertainty (± 2 standard deviation). The value ρ = 0 corresponds to the contact point between the bacterium and the coverslip, and gives the position of the fluorophore in the 40 nm thick cell wall. The advantage of measuring fluorophores heights at the contact point with the coverslip is that no assumption on the size (*i.e.*, the radius) or the shape (whether they flatten out near the contact point or not) of bacteria is required. It is worth noting that this does not immediately yield the position of the antibiotic since the labelling process creates an antibody structure in which the fluorophore is 10-12 nm away from the antibiotic, which was taken into account in the analysis of our results.

Pore formation and potassium ions release assays. Exponentially-growing and stationary phase MSSA ATCC 27217 bacteria (250 µL portions of each), cultured as described previously, were deposited in 96-well microtiter plates 5 min before observation to allow sedimentation and further microscopy observations. 24-h biofilms, grown as described previously, were rinsed with sterile NaCl (150 mM) and refilled with TSBpc, Fluorescence imaging was then performed using the same confocal microscope.

(i) Pore formation. After daptomycin was added in each well to a final concentration of 20 µg/mL, 30-µM propidium iodide (PI, Sigma) was added to observe pore formation within cytoplasmic membranes. The fluorescent dye was excited at 543 nm and fluorescence emission was collected between 640 and 750 nm. Transmission and fluorescence images were acquired 10 min and 3 h after daptomycin injection in the same wells.

(**ii) Potassium ions release by bacterial cells.** To measure daptomycin-induced potassium ions release by bacterial cells, Asante Potassium Green

(APG-2 TMA+ salt, Abcam), a membrane-impermeant dye that fluoresces upon extracellular K+ ions chelation was used. The dye was excited at 488 nm and its fluorescence emission was recorded between 500 and 600 nm. After addition of APG-2 to a final concentration of 2 µM in each bacterial sample, the fluorescence intensity was first controlled without antibiotic over 5 min. Fluorescence intensity images were then recorded each second during 100 s to observe the fluorescence intensity evolution over time. Daptomycin was injected ~5 s after the beginning of the acquisition.

Membrane fatty acid analysis. Bacteria were grown to exponential or stationary growth phases and biofilms as described previously. Planktonic suspensions were washed twice in sterile NaCl (150 mM) or 0.1% triton X-100 when exogenous fatty acids were added in the medium. Entire biofilms were rinsed twice *in-situ* with 150 mM NaCl or triton before analysis. Extraction and methylation of fatty acids were carried out directly on bacterial pellets or entire biofilms as described in [25]. Briefly, fatty acids of bacterial pellets or scratched biofilm cells were directly saponified and esterified by methanolic NaOH and methanolic HCl (1 mL NaOH 3.75 mol/l in 50% v/v methanol solution for 30 min at 100°C; addition of 2 mL HCl 3.25 mol/l in 45% v/v methanol solution for 10 min at 80°C). Fatty acid methyl esters were extracted with a diethyl ether/cyclohexane solution (1:1 v/v) and the organic phase was washed with a dilute base (NaOH 0.3 mol/l). Analytical gas chromatography of fatty acid methyl esters was carried out on a 6890HP system (Agilent Technologies, Santa Clara, CA, USA) equipped with a 0.25 µm BPX70 capillary column (25m, 0.22 mm i.d.) (SGE, Ring Wood, Victoria, Australia) and a flame-ionization detector. Column temperature was set at 100°C for 1 min and then increased to 170°C at the rate of 2°C/min. Data were acquired using a HPCORE ChemStation system (Agilent Technologies, Santa Clara, CA, USA) and expressed as a percentage of the total area. Fatty acids were identified using fatty acid methyl ester standards and grouped in three classes: saturated fatty acids (SFA), *iso* branched-chain fatty acids (BFA) and *anteiso* BFA. Results are the average of at least six profiles (two injections of three extractions from independent cultures) for each condition.

Statistics. For daptomycin activity results and fatty acid compositions of bacterial membranes, analyses of variance (ANOVA) were performed using Statgraphics software (Manugistic™, Rockville, MD, USA). Evaluated factors were considered as statistically significant when *P*-values associated with the Fischer test were below 0.05.

Acknowledgements

The authors want to thank Cynthia Arnassalom Apalama for performing membrane fatty acid analysis, and the Centre de Photonique Biomédicale (CPBM) of the Centre Laser de l'Université Paris-Sud (CLUPS/LUMAT FR2764, Orsay, France) for the confocal microscope and L2 microbiology facilities.

References

1. Lowy, F. D. Staphylococcus aureus Infections. *N. Engl. J. Med.* **339,** 520–532 (1998).
2. Davies, D. Understanding biofilm resistance to antibacterial agents. *Nat. Rev. Drug Discov.* **2,** 114–122 (2003).
3. Lebeaux, D., Ghigo, J.-M. & Beloin, C. Biofilm-Related Infections: Bridging the Gap between Clinical Management and Fundamental Aspects of Recalcitrance toward Antibiotics. *Microbiol. Mol. Biol. Rev.* **78,** 510–543 (2014).
4. Shopsin, B., Kaveri, S. V. & Bayry, J. Tackling Difficult Staphylococcus aureus Infections: Antibodies Show the Way. *Cell Host Microbe* **20,** 555–557 (2016).
5. Humphries, R. M., Pollett, S. & Sakoulas, G. A Current Perspective on Daptomycin for the Clinical Microbiologist. *Clin. Microbiol. Rev.* **26,** 759–780 (2013).

6. Mingeot-Leclercq, M.-P. & Décout, J.-L. Bacterial lipid membranes as promising targets to fight antimicrobial resistance, molecular foundations and illustration through the renewal of aminoglycoside antibiotics and emergence of amphiphilic aminoglycosides. *MedChemComm* **7,** 586–611 (2016).
7. Straus, S. K. & Hancock, R. E. W. Mode of action of the new antibiotic for Gram-positive pathogens daptomycin: Comparison with cationic antimicrobial peptides and lipopeptides. *Biochim. Biophys. Acta BBA - Biomembr.* **1758,** 1215–1223 (2006).
8. Muthaiyan, A., Silverman, J. A., Jayaswal, R. K. & Wilkinson, B. J. Transcriptional Profiling Reveals that Daptomycin Induces the Staphylococcus aureus Cell Wall Stress Stimulon and Genes Responsive to Membrane Depolarization. *Antimicrob. Agents Chemother.* **52,** 980–990 (2008).
9. Mengin-Lecreulx, D., Allen, N. E., Hobbs, J. N. & Heijenoort, J. van. Inhibition of peptidoglycan biosynthesis in Bacillus megaterium by daptomycin. *FEMS Microbiol. Lett.* **69,** 245–248 (1990).
10. Müller, A. *et al.* Daptomycin inhibits cell envelope synthesis by interfering with fluid membrane microdomains. *Proc. Natl. Acad. Sci. U. S. A.* **113,** E7077–E7086 (2016).
11. Mascio, C. T. M., Alder, J. D. & Silverman, J. A. Bactericidal Action of Daptomycin against Stationary-Phase and Nondividing Staphylococcus aureus Cells. *Antimicrob. Agents Chemother.* **51,** 4255–4260 (2007).
12. Lamp, K. C., Rybak, M. J., Bailey, E. M. & Kaatz, G. W. In vitro pharmacodynamic effects of concentration, pH, and growth phase on serum bactericidal activities of daptomycin and vancomycin. *Antimicrob. Agents Chemother.* **36,** 2709–2714 (1992).
13. Fowler, V. G. *et al.* Daptomycin versus Standard Therapy for Bacteremia and Endocarditis Caused by Staphylococcus aureus. *N. Engl. J. Med.* **355,** 653–665 (2006).
14. Mariani, P. G., Sader, H. S. & Jones, R. N. Development of decreased susceptibility to daptomycin and vancomycin in a Staphylococcus aureus strain during prolonged therapy. *J. Antimicrob. Chemother.* **58,** 481–483 (2006).
15. Julian, K. *et al.* Characterization of a daptomycin-nonsusceptible vancomycin-intermediate Staphylococcus aureus strain in a patient with endocarditis. *Antimicrob. Agents Chemother.* **51,** 3445–3448 (2007).
16. Lamp, K. C., Friedrich, L. V., Mendez-Vigo, L. & Russo, R. Clinical Experience with Daptomycin for the Treatment of Patients with Osteomyelitis. *Am. J. Med.* **120,** S13–S20 (2007).
17. Sharma, M., Riederer, K., Chase, P. & Khatib, R. High rate of decreasing daptomycin susceptibility during the treatment of persistent Staphylococcus aureus bacteremia. *Eur. J. Clin. Microbiol. Infect. Dis.* **27,** 433–437 (2008).
18. Levy, D. T. *et al.* Successful treatment of a left ventricular assist device infection with daptomycin non-susceptible methicillin-resistant Staphylococcus aureus: case report and review of the literature. *Transpl. Infect. Dis. Off. J. Transplant. Soc.* **14,** E89-96 (2012).
19. Moise, P. A. *et al.* Multicenter Evaluation of the Clinical Outcomes of Daptomycin with and without Concomitant β-Lactams in Patients with Staphylococcus aureus Bacteremia and Mild to Moderate Renal Impairment. *Antimicrob. Agents Chemother.* **57,** 1192–1200 (2013).
20. Daptomycin Failures in Prosthetic Joint Infections and Bone... : Infectious Diseases in Clinical Practice. *LWW* Available at: http://journals.lww.com/infectdis/Fulltext/2008/09000/Daptomycin_Failures_in_Prosthetic_Joint_Infections.14.aspx. (Accessed: 18th April 2017)

21. Stefani, S. *et al.* Insights and clinical perspectives of daptomycin resistance in Staphylococcus aureus: A review of the available evidence. *Int. J. Antimicrob. Agents* **46,** 278–289 (2015).
22. Seaton, R. A. *et al.* Evaluation of Effectiveness and Safety of High-Dose Daptomycin: Results from Patients Included in the European Cubicin® Outcomes Registry and Experience. *Adv. Ther.* **32,** 1192–1205 (2015).
23. Jones, T. *et al.* Failures in Clinical Treatment of Staphylococcus aureus Infection with Daptomycin Are Associated with Alterations in Surface Charge, Membrane Phospholipid Asymmetry, and Drug Binding. *Antimicrob. Agents Chemother.* **52,** 269–278 (2008).
24. Skiest, D. J. Treatment failure resulting from resistance of Staphylococcus aureus to daptomycin. *J. Clin. Microbiol.* **44,** 655–656 (2006).
25. Dubois-Brissonnet, F., Trotier, E. & Briandet, R. The Biofilm Lifestyle Involves an Increase in Bacterial Membrane Saturated Fatty Acids. *Front. Microbiol.* **7,** (2016).
26. Zhang, Y.-M. & Rock, C. O. Membrane lipid homeostasis in bacteria. *Nat. Rev. Microbiol.* **6,** 222–233 (2008).
27. Denich, T. J., Beaudette, L. A., Lee, H. & Trevors, J. T. Effect of selected environmental and physico-chemical factors on bacterial cytoplasmic membranes. *J. Microbiol. Methods* **52,** 149–182 (2003).
28. Morvan, C. *et al.* Environmental fatty acids enable emergence of infectious Staphylococcus aureus resistant to FASII-targeted antimicrobials. *Nat. Commun.* **7,** (2016).
29. Boudjemaa, R. *et al.* New Insight into Daptomycin Bioavailability and Localization in Staphylococcus aureus Biofilms by Dynamic Fluorescence Imaging. *Antimicrob. Agents Chemother.* **60,** 4983–4990 (2016).
30. Daddi Oubekka, S., Briandet, R., Fontaine-Aupart, M.-P. & Steenkeste, K. Correlative time-resolved fluorescence microscopy to assess antibiotic diffusion-reaction in biofilms. *Antimicrob. Agents Chemother.* **56,** 3349–3358 (2012).
31. Cui, L. *et al.* Cell Wall Thickening Is a Common Feature of Vancomycin Resistance in Staphylococcus aureus. *J. Clin. Microbiol.* **41,** 5–14 (2003).
32. Cui, L., Tominaga, E., Neoh, H. & Hiramatsu, K. Correlation between Reduced Daptomycin Susceptibility and Vancomycin Resistance in Vancomycin-Intermediate Staphylococcus aureus. *Antimicrob. Agents Chemother.* **50,** 1079–1082 (2006).
33. Matias, V. R. F. & Beveridge, T. J. Native Cell Wall Organization Shown by Cryo-Electron Microscopy Confirms the Existence of a Periplasmic Space in Staphylococcus aureus. *J. Bacteriol.* **188,** 1011–1021 (2006).
34. Bourg, N. *et al.* Direct optical nanoscopy with axially localized detection. *Nat. Photonics* **9,** 587–593 (2015).
35. Sauermann, R., Rothenburger, M., Graninger, W. & Joukhadar, C. Daptomycin: A Review 4 Years after First Approval. *Pharmacology* **81,** 79–91 (2008).
36. Oldfield, E. & Feng, X. Resistance-Resistant Antibiotics. *Trends Pharmacol. Sci.* **35,** 664–674 (2014).
37. Pogliano, J., Pogliano, N. & Silverman, J. A. Daptomycin-Mediated Reorganization of Membrane Architecture Causes Mislocalization of Essential Cell Division Proteins. *J. Bacteriol.* **194,** 4494–4504 (2012).
38. Chen, Y.-F., Sun, T.-L., Sun, Y. & Huang, H. W. Interaction of Daptomycin with Lipid Bilayers: A Lipid Extracting Effect. *Biochemistry (Mosc.)* **53,** 5384–5392 (2014).

39. Silverman, J. A., Perlmutter, N. G. & Shapiro, H. M. Correlation of Daptomycin Bactericidal Activity and Membrane Depolarization in Staphylococcus aureus. *Antimicrob. Agents Chemother.* **47,** 2538–2544 (2003).
40. Brinster, S. *et al.* Type II fatty acid synthesis is not a suitable antibiotic target for Gram-positive pathogens. *Nature* **458,** 83–86 (2009).
41. Saito, H. E., Harp, J. R. & Fozo, E. M. Incorporation of Exogenous Fatty Acids Protects Enterococcus faecalis from Membrane-Damaging Agents. *Appl. Environ. Microbiol.* **80,** 6527–6538 (2014).
42. Pader, V. *et al.* Staphylococcus aureus inactivates daptomycin by releasing membrane phospholipids. *Nat. Microbiol.* **2,** 16194 (2016).
43. Kenny, J. G. *et al.* The Staphylococcus aureus Response to Unsaturated Long Chain Free Fatty Acids: Survival Mechanisms and Virulence Implications. *PLoS ONE* **4,** (2009).
44. Nanocapsules lipidiques comprenant un antibiotique et leurs utilisations en therapie.
45. Daddi Oubekka, S., Briandet, R., Waharte, F., Fontaine-Aupart, M.-P. & Steenkeste, K. Image-based fluorescence recovery after photobleaching (FRAP) to dissect vancomycin diffusion-reaction processes in Staphylococcus aureus. in *Proc. SPIE 8087, Clinical and Biomedical Spectroscopy and Imaging II, 80871I* (eds. Ramanujam, N. & Popp, J.) **Proc. SPIE 8087, Clinical and Biomedical Spectroscopy and Imaging II, 80871I,** 80871I–80871I–7 (Proc. SPIE 8087, Clinical and Biomedical Spectroscopy and Imaging II, 80871I, 2011).
46. Olivier, N., Keller, D., Rajan, V. S., Gönczy, P. & Manley, S. Simple buffers for 3D STORM microscopy. *Biomed. Opt. Express* **4,** 885–899 (2013).
47. Dempsey, G. T., Vaughan, J. C., Chen, K. H., Bates, M. & Zhuang, X. Evaluation of fluorophores for optimal performance in localization-based super-resolution imaging. *Nat. Methods* **8,** 1027–1036 (2011).
48. Lin, Y. *et al.* Effect of laser intensity on Alexa Fluor 647 photoswitching kinetics. (2015). doi:10.1371/journal.pone.0128135.g006
49. van de Linde, S. *et al.* Direct stochastic optical reconstruction microscopy with standard fluorescent probes. *Nat. Protoc.* **6,** 991–1009 (2011).

SUPPLEMENTARY DATA

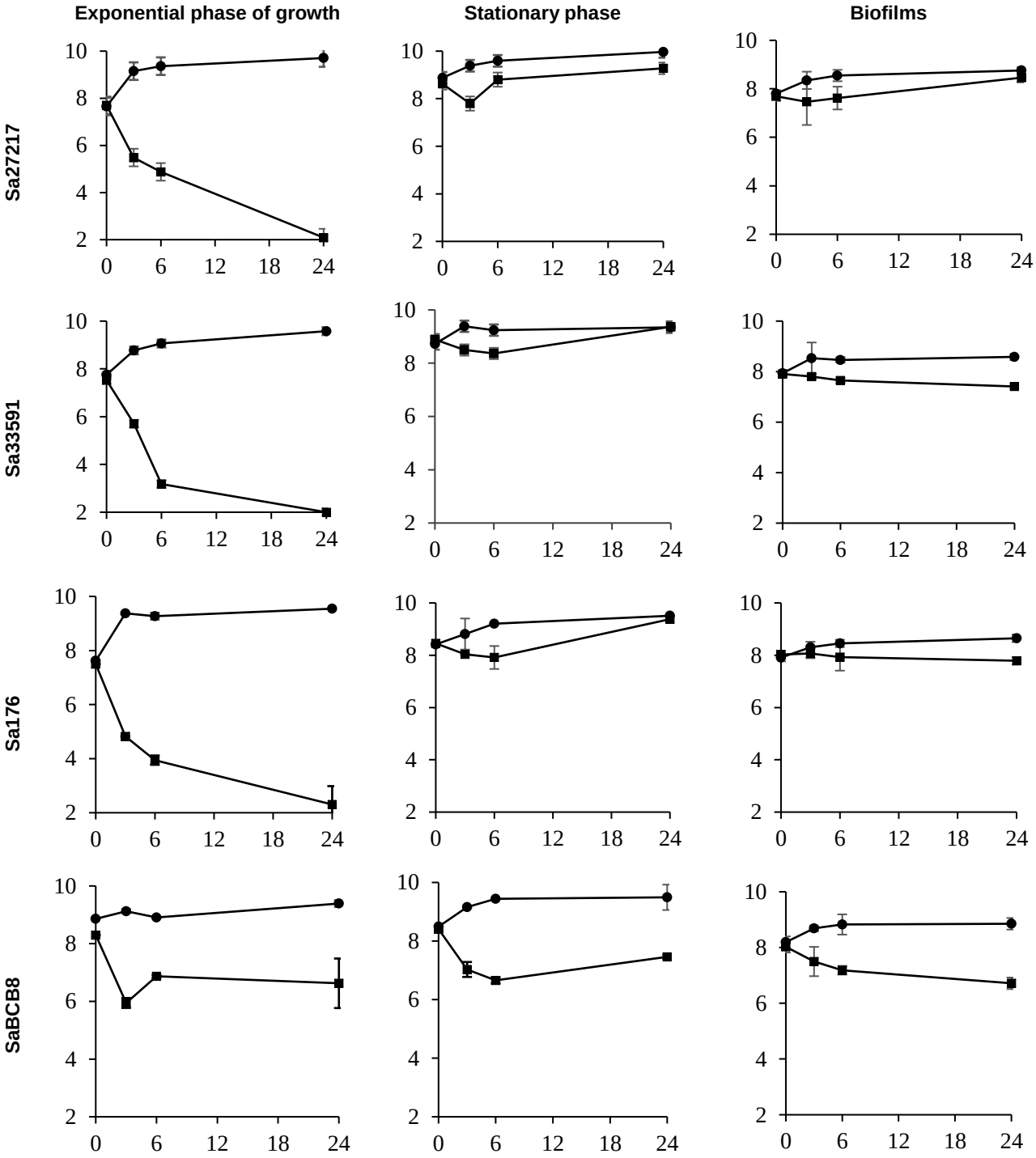

Fig. S1. Detailed time-kill studies of daptomycin against the four *S. aureus* strains in the three phases of growth.

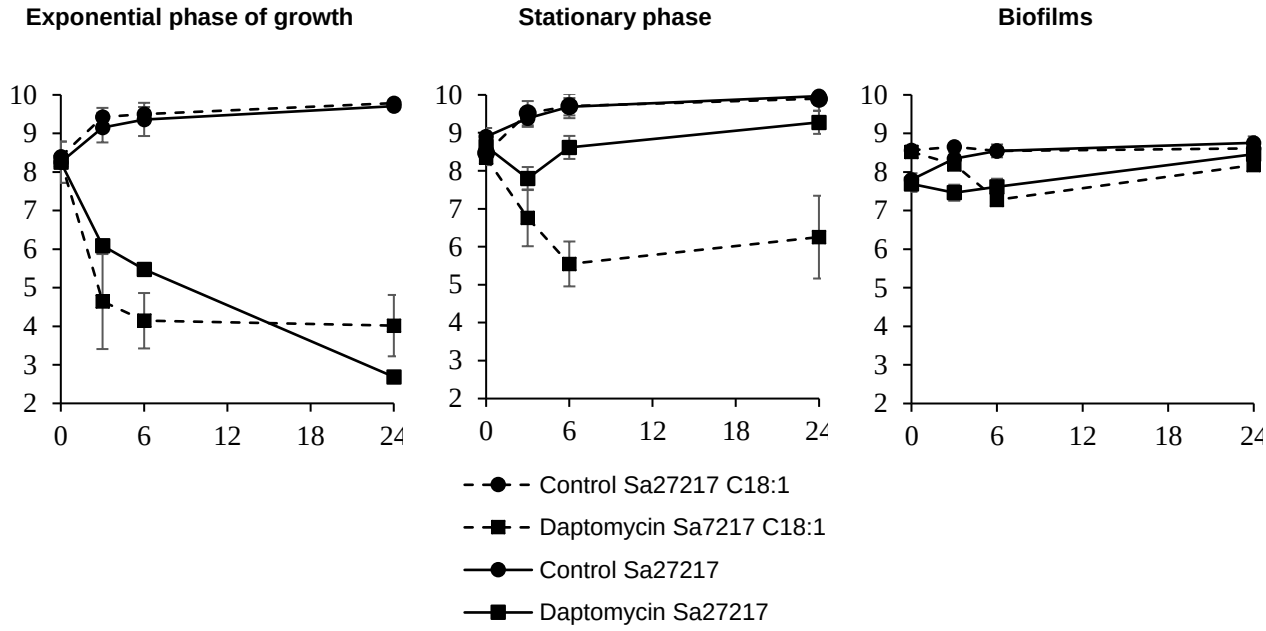

Fig. S2. Daptomycin activity against MSSA ATCC 27217 cultivated in TSBpc medium supplemented with oleic acid (C18:1). In black lines, the fatty acid-free medium and in dashed lines the fatty-acid-supplemented medium

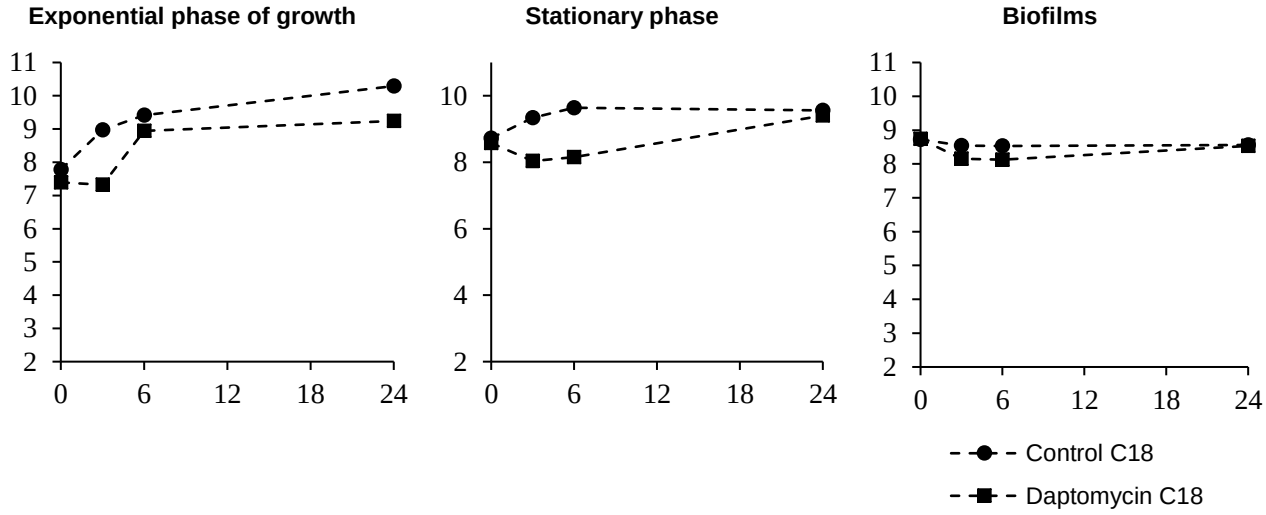

Fig. S3. Daptomycin activity against MSSA ATCC 27217 cultivated in TSBpc medium supplemented with stearic acid (C18). The fatty acid free medium results are presented in the precedent figure.

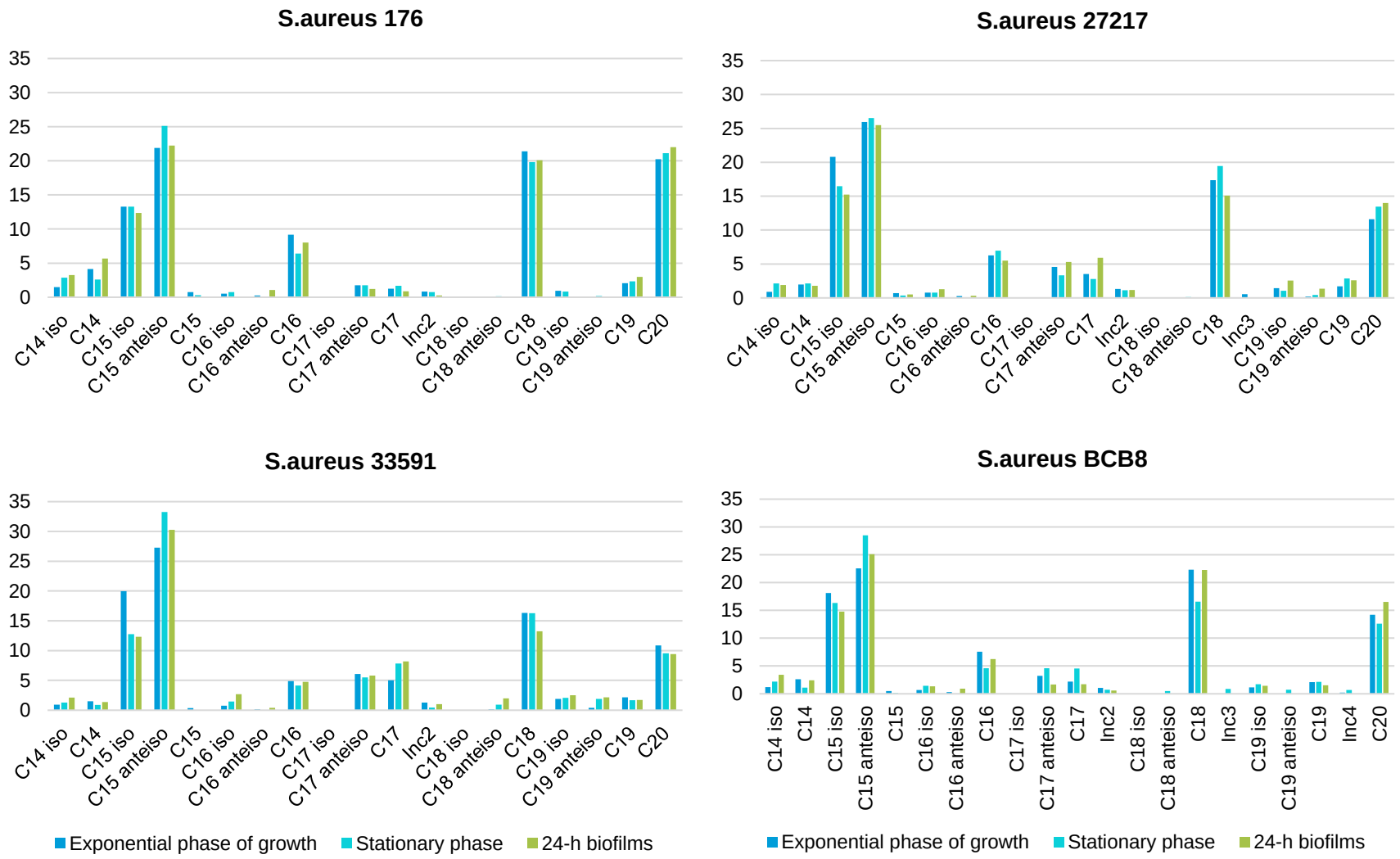

Fig. S4. Detailed membrane fatty acid composition for each *S. aureus* strain depending on the growth phase (exponential, stationary, 24-h biofilms).

5.3. Résultats complémentaires

Adaptation du marquage de la daptomycine à la méthode DONALD (Direct Optical Nanoscopy With Axially Localized Detection)

La méthode DONALD est une méthode optique à résolution nanoscopique qui repose sur la localisation de molécules fluorescentes individuelles. Celles-ci doivent fluorescer pendant un temps très court (clignotement) afin d'être localisées individuellement. Ce clignotement réversible (oscillation entre les états fluorescents et sombres, dits « dark ») peut être atteint de différentes manières selon la méthode optique concernée. On distingue : le PALM (Photo-activated Localization Microscopy) où l'on utilise des molécules photoactivables telles que des protéines fluorescentes ; le PAINT (Point Accumulation for Imaging in Nanoscale Topography) méthode qui utilise des fluorophores qui se lient de manière réversible à leur cible biologique (molécule souvent non fluorescente en solution) ; et le dSTORM (direct Stochastic Optical Resolution Microscopy) où l'on utilise des fluorophores classiques mais mis en solution dans un tampon chimique spécial qui permet aux molécules de « clignoter » entre des états fluorescents et des états sombres. Une limitation repose, cependant, sur le fait que les mécanismes responsables de l'induction de ce clignement chimique n'ont été identifiés que pour quelques sondes fluorescentes. Parmi eux, l'Alexa Fluor (AF) 647 ainsi que son tampon d'imagerie (un système enzymatique permettant de quencher l'oxygène pour empêcher les réactions chimiques avec O_2) ont largement été utilisés pour effectuer de l'imagerie dSTORM. L'inconvénient principal de ce tampon d'imagerie repose sur le fait qu'il est constitué, entre autres, de thiols, souvent toxiques pour les bactéries et empêchant alors de garder les bactéries vivantes.

Ainsi, pour effectuer les mesures dans des conditions physiologiques optimales pour les bactéries, nous nous sommes affranchis de ce tampon en utilisant les antibiotiques marqués au BODIPY-FL seulement conjointement avec un marqueur de la membrane bactérienne, le Nile Red. Ce dernier est une sonde fluorescente qui se lie réversiblement à la membrane des bactéries, capable de produire l'état de clignotement recherché. Les images obtenues avec ce marqueur sans antibiotiques ont été concluantes (**Figure 7B**). En revanche, concernant les antibiotiques marqués au BODIPY-FL, les résultats se sont révélés beaucoup moins probants car le clignotement était très faible dans ce cas, ne permettant pas d'obtenir un signal de fluorescence suffisant (**Figure 7C**). Ainsi, nous nous sommes orientés vers l'optimisation d'un marquage indirect à base d'anticorps (détaillé dans l'article 7).

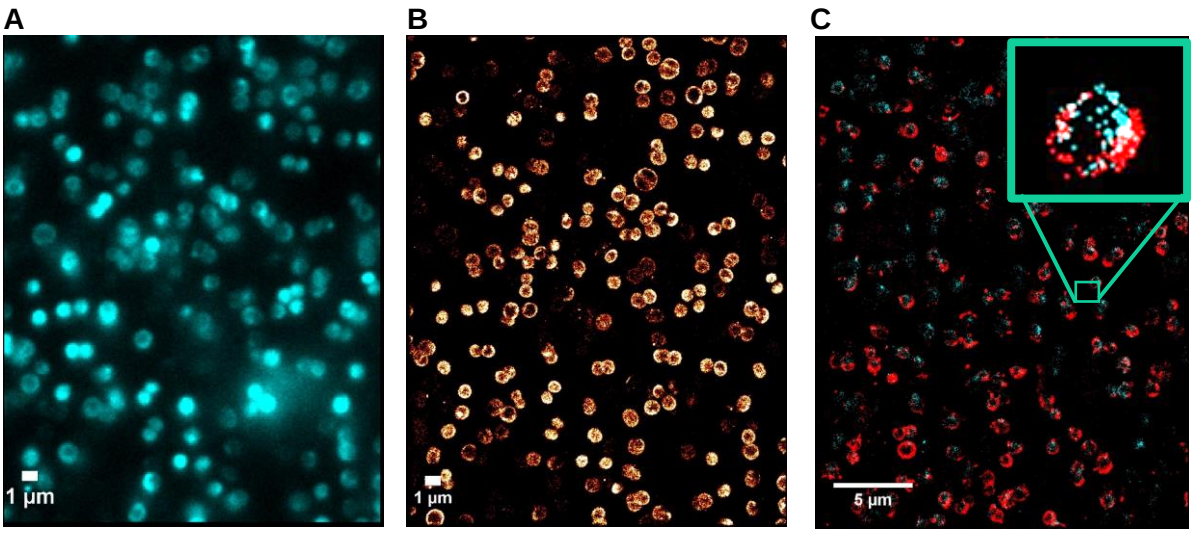

Figure 7. ***(A)*** *Image d'intensité de fluorescence des bactéries marquées au Nile Red obtenue à l'aide d'un microscope à épifluorescence.* ***(B)*** *Image équivalente obtenue en utilisant la technique DONALD* ***(C)*** *Image DONALD des bactéries marquées au Nile Red (rouge) et au BODIPY-FL-daptomycine (cyan). Longueur d'onde d'excitation du Nile Red : 540 nm. Longueur d'onde d'excitation du BODIPY-FL-daptomycine : 488 nm.*

SYNTHESE GENERALE

L'implication et l'importance des biofilms dans les environnements naturels, industriels et médicaux sont aujourd'hui largement démontrées par la communauté scientifique. En médecine humaine plus particulièrement, la prévalence des infections associées aux biofilms attire considérablement l'attention du fait de l'inefficacité des traitements thérapeutiques. Dans ce contexte, la compréhension des mécanismes impliqués notamment dans l'échec de l'antibiothérapie est devenue un challenge, aussi bien de la recherche médicale que de la recherche fondamentale.

Derrière cet échec, on distingue deux phénomènes distincts : la résistance et la tolérance aux antibiotiques. La résistance implique des mutations génétiques des micro-organismes leur permettant d'inhiber l'action des antibiotiques par de multiples mécanismes (modification de la cible attaquée, destruction ou modification de l'antibiotique, efflux ou altération de la perméabilité à l'antibiotique, …) et donc de se multiplier en présence d'un biocide.[210,211] La tolérance, quant à elle, est une des caractéristiques les plus remarquables du biofilm, qualifiée de réversible, phénotypique et non héritée.[14,84] Ainsi, les biofilms bactériens survivent à des doses d'antibiotiques jusqu'à 1000 fois supérieures à la concentration minimale inhibitrice nécessaire pour éradiquer les mêmes bactéries planctoniques.[212] Génétiquement identiques aux bactéries en suspension sensibles, les bactéries tolérantes ont adopté un état physiologique spécifique qui leur permet de contrer l'activité des antibiotiques.[14]

C'est dans ce contexte que s'inscrit ce travail de thèse dans lequel nous avons tenté d'apporter des éléments de compréhension à la tolérance aux antibiotiques des biofilms de *S. aureus.* Le but final est, à plus long terme, de proposer des améliorations de l'utilisation des thérapies actuelles et/ou des alternatives à l'antibiothérapie.

L'approche choisie pour initier cette recherche s'est fondée sur un modèle original d'infections à biofilm de *S. aureus* sur prothèse vasculaire implantable chez la souris, qui nous a servi à optimiser un modèle de biofilms *in vitro,* compatible avec une étude utilisant l'imagerie optique à résolution micro-nanométrique.

Apport du modèle animal dans l'évaluation de protocoles thérapeutiques.

Malgré une fréquence non négligeable et une gravité certaine, les infections de prothèses vasculaires manquent souvent d'une prise en charge médicale adaptée, faute de connaissances sur la nature des biofilms formés *in vivo* et sur leur sensibilité aux antibiotiques. Dans ce domaine, nous avons apporté des données nouvelles grâce à l'utilisation d'un modèle d'implant vasculaire chez la souris, infecté par *S. aureus* et traité par différents antibiotiques.

Plusieurs études de la littérature rapportent l'action d'antibiotiques sur des biofilms en présence de cellules immunitaires, mais uniquement à travers des modèles de cocultures *in vitro*.[213,214] Notre apport a été d'accéder à ces données par analyse du matériel vasculaire explanté.

En utilisant des concentrations d'antibiotiques compatibles avec un traitement clinique, nous avons pu mettre en évidence qu'en aucun cas une éradication totale des biofilms n'était observée et ce, malgré une faible épaisseur des biostructures formées *in vivo.* Par ailleurs, grâce à un polymarquage fluorescent adapté aux cellules immunitaires, aux bactéries et aux antibiotiques, il a été possible d'identifier (i) la présence des macrophages et des polynucléaires

sur le site de l'infection, (ii) que ces cellules étaient le « refuge » de bactéries de *S. aureus* vivantes et (iii) que les antibiotiques ne pénétraient pas à l'intérieur des macrophages. Ces résultats, dans leur ensemble, n'avaient jamais été mis en évidence par imagerie de fluorescence *in situ* et peuvent être corrélés avec l'(in)efficacité des antibiotiques : moins le traitement est efficace, plus la quantité de bactéries intracellulaires est importante. Il apparait donc que les cellules immunitaires constituent un « réservoir » de bactéries pathogènes pouvant être à l'origine de (i) l'efficacité limitée des traitements antibiotiques et (ii) la résurgence des infections chroniques.

On pourrait objecter que notre modèle animal présente une faiblesse du fait du lieu d'implantation de la prothèse vasculaire. Plutôt qu'en sous-cutané au niveau dorsal, il eut été préférable d'implanter la prothèse directement sur le réseau vasculaire de l'animal, qui aurait pu impacter différemment la structure du biofilm et l'action du système immunitaire. Cependant, une telle procédure s'est révélée complexe du fait de difficultés chirurgicales. Il faut aussi considérer que les systèmes immunitaires humain et murin ne sont pas complètement superposables.

Au regard de ces résultats, il serait intéressant de poursuivre ce travail par un suivi de l'évolution de l'infection directement chez la souris (sans explantation du matériel) et donc en présence des fluides biologiques. On citera en particulier les dispositifs de chambre dorsale et le marquage des microorganismes (bioluminescence, telles que décrites au Chapitre 2 – paragraphe 3.2.) qui permettent de suivre par imagerie optique l'évolution de l'infection et l'action des antibiotiques sur des temps longs (jusqu'à un mois).

Inefficacité d'antibiotiques au sein des biofilms de *S. aureus* : rôle de la matrice extracellulaire *vs* de la physiologie des bactéries.

Parmi les facteurs évoqués dans la littérature pour expliquer l'efficacité limitée des antibiotiques au sein des biofilms, la matrice extracellulaire sécrétée par les bactéries est souvent indiquée comme un frein à la diffusion des molécules antibiotiques, permettant une adaptation progressive de la physiologie des bactéries.[215] Cette hypothèse a pu être vérifiée dans le cas de l'action de la tobramycine dans les biofilms de *Pseudomonas aeruginosa* par exemple.[216] Au contraire, d'autres études [186,217–220] et celles réalisées dans le cadre de cette thèse affirment que les antibiotiques diffusent et sont biodisponibles au sein de biofilms de *S. aureus*. Le seul exemple où la matrice d'exopolymères joue un rôle de rétention est l'association de la vancomycine à la rifampicine. Nos travaux ont permis de montrer la formation d'un complexe entre ces deux antibiotiques en solution. Sa dissociation au niveau des bactéries, permettant à chacune des molécules d'atteindre sa cible biologique (le peptidoglycane et l'ARN), est cependant moins efficace au sein des biofilms. Une explication peut provenir de la composition de la matrice exopolymérique chez *S. aureus*, qui contient des N-acetylglucosamine (NAG) en concentrations élevées, pour lesquels la vancomycine a une grande affinité. De ce fait, une fraction du complexe vancomycine-rifampicine est retenue dans la matrice du biofilm et réduit l'activité des antibiotiques.

A l'exception de ce cas particulier, la présence de la matrice d'exopolymères ne peut seule expliquer l'inefficacité des antibiotiques mesurée dans nos modèles d'études. C'est sans aucun doute la physiologie des bactéries dans les biofilms qui joue un rôle fondamental. En effet, la

majeure partie des bactéries du biofilm ne sont pas en division active mais ont, au contraire, un métabolisme ralenti. Comme déjà mentionné au Chapitre 4, cet état physiologique des bactéries permet d'expliquer l'inefficacité de la vancomycine.

Le mode d'action de la daptomycine laissait supposer une activité quel que soit l'état physiologique des bactéries. C'était sans compter sur la composition en acides gras des membranes cellulaires, reflet de la fluidité membranaire et qui diffère selon l'état physiologique des bactéries de *S. aureus*.[181] Nos travaux montrent pour la première fois une corrélation directe entre la composition en acides gras des membranes des bactéries en biofilms et la perte d'activité de la daptomycine. Ces résultats méritent d'être consolidés en testant un plus large panel d'acides gras (acide palmitoléique, acide linoléique, acide γ-linolénique par exemple) mais ouvrent cependant des pistes pour l'amélioration de cette antibiothérapie**.** En effet, une perspective qui apparaît prometteuse consisterait à moduler la fluidité membranaire des bactéries. Comment ? En agissant sur le milieu environnant du site d'infection. Si on se rapproche de notre modèle *in vivo* d'infection sur implant chez la souris, on pourrait envisager d'injecter localement au niveau de l'implant des acides gras ou de préconditionner la zone infectée. Une autre approche intéressante serait de modifier l'alimentation de l'animal en l'enrichissant en acides gras insaturés et de mesurer son impact sur l'efficacité de la daptomycine. Auparavant, il serait intéressant de tester de nouveaux nanovecteurs de la daptomycine, constitués de liposomes à base d'acides gras. Ces entités ont été développées pour permettre une meilleure délivrance d'antibiotique au sein d'infections ostéoarticulaires. Mais ils pourraient aussi fluidifier la membrane des bactéries et rendre les cellules immunitaires perméables à la pénétration des antibiotiques.[204]

Cette démarche pour améliorer l'efficacité de la daptomycine pourrait être mise en perspective pour d'autres agents antibactériens tels que les désinfectants couramment utilisés pour la décontamination des surfaces (composés d'ammonium quaternaires), ou les antimicrobiens naturels (composés phénoliques d'origine végétale, bactériocines), dont la cible majeure est la membrane cytoplasmique.

Les infections associées aux biofilms de *S. aureus* : comment contourner l'antibiothérapie ?

Comme rapporté dans le premier chapitre de ce document, face à la difficulté d'éradiquer les biofilms par antibiothérapie, il est important de continuer la recherche et le développement concernant la maîtrise des surfaces dans le but d'empêcher l'adhésion bactérienne ou de faciliter l'éradication des bactéries adhérées.

Dans le cadre de mes travaux de thèse, j'ai pu contribuer à des projets de recherche dans ce sens. L'équipe de Raphael Schneider, du Laboratoire de Réactions et Génie des Procédés de Nancy, a développé la synthèse de quantum dots (QD) non toxiques ZCIS. Il s'agit de nanoparticules dont le cœur est constitué de Cuivre, Indium et Soufre ($CuInS_2$) et la coquille de sulfure de zinc (ZnS). Ces QD ont été fonctionnalisées avec de l'acide mercaptopropionique (MPA, **Figure 8A**). Ainsi, sous irradiation solaire, ces nanoparticules sont capables de générer des espèces réactives de l'oxygène, en majeure partie de l'oxygène singulet. Nous avons pu montrer que ces nanoparticules, appliquées sur une couche de bactéries de *S. aureus* adhérées, empêchait la formation du biofilm (**Figure 8B**).

Les propriétés phototoxiques de ces QD excluent leur utilisation *in vivo* mais pourraient être utilisés comme des décontaminants de surface non polluants et de faible coût de fabrication.

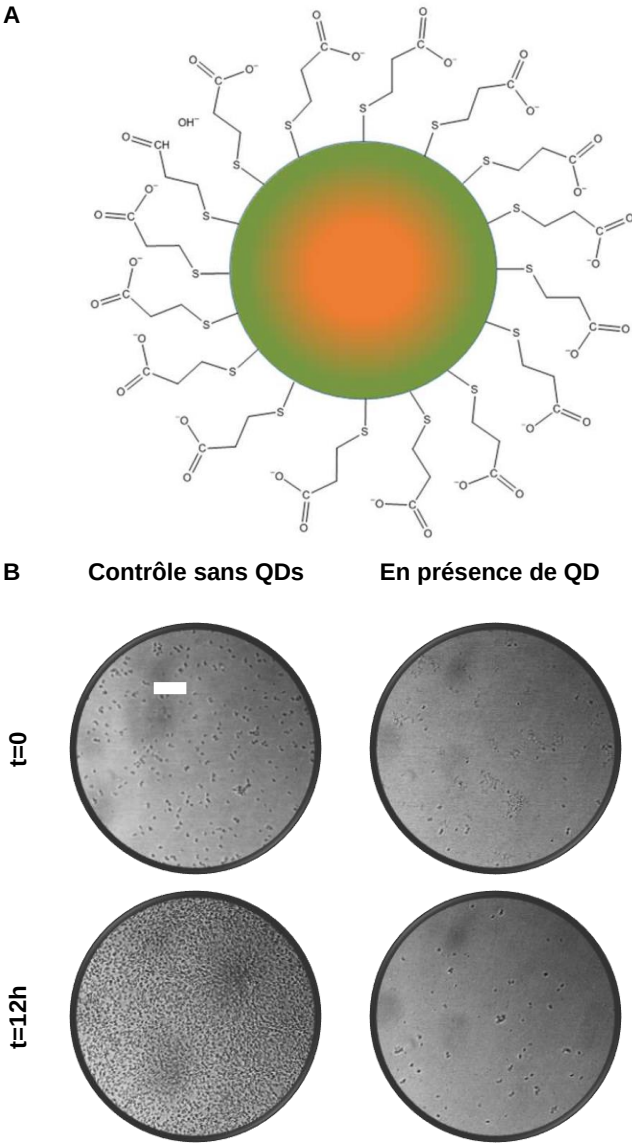

Figure 8. ***(A)*** *Structure des QD ZCIS fonctionnalisées au MPA.* ***(B)*** *Images en transmission des bactéries adhérées de S. aureus en présence ou non de QD et à lumière ambiante. L'échelle correspond à 10 µm.*

Dans une autre étude, menée en collaboration avec Pascal Thébault du Laboratoire Polymères, Biopolymères, Surfaces de l'Université de Rouen, nous avons testé l'efficacité d'un peptide antimicrobien, la nisine, immobilisé de façon covalente sur des surfaces d'or fonctionnalisées avec de l'acide mercaptoundécanoique (MUA, **Figure 9A**). Les résultats préliminaires obtenus permettent de démontrer une efficacité combinée anti-adhésive et toxique vis-à-vis des bactéries de *S. aureus* (**Figure 9B**).

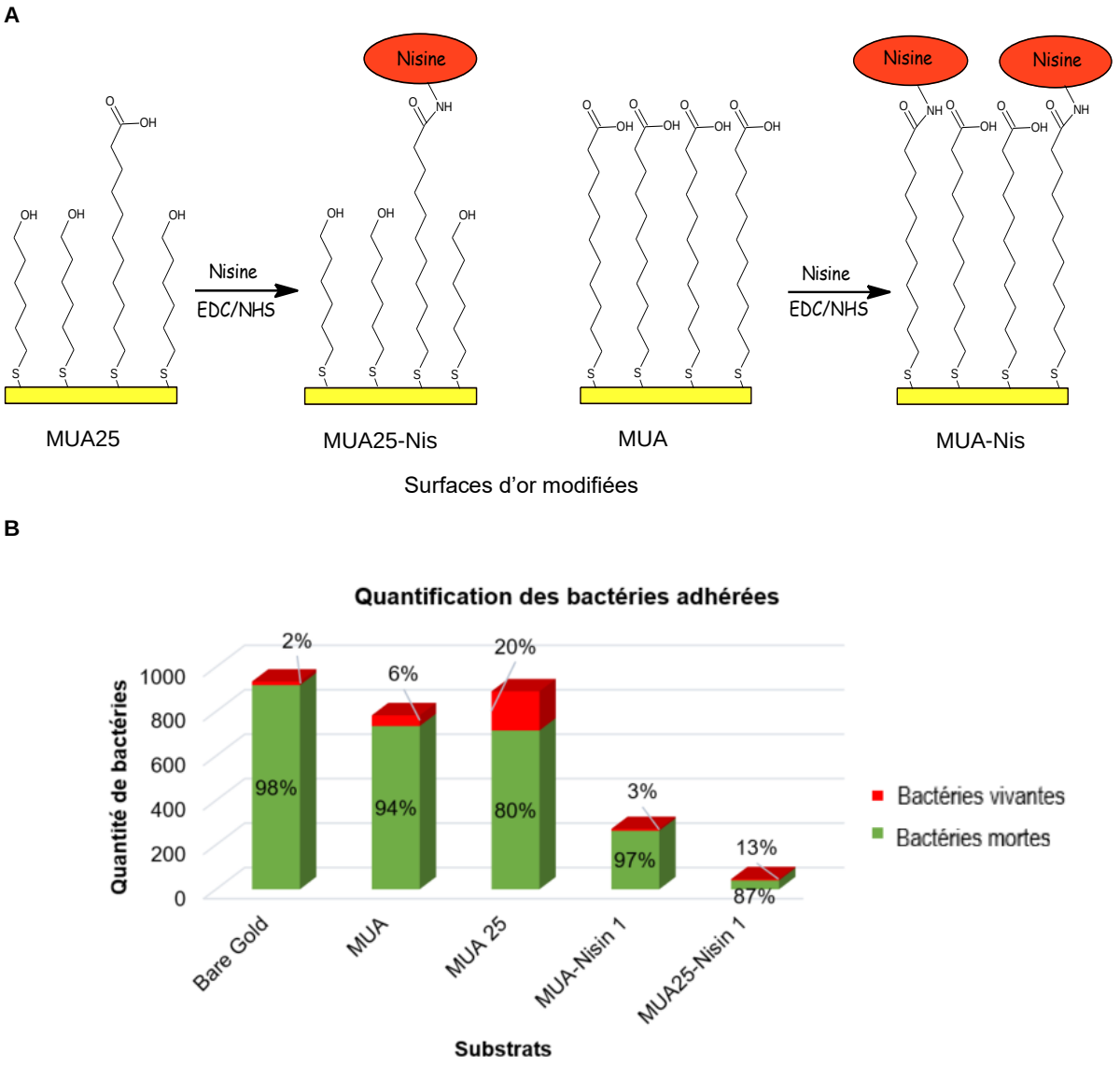

Figure 9. ***(A)*** *Substrats d'or fonctionnalisés avec de l'acide MUA et de la nisine (Nis).* ***(B)*** *Quantification des bactéries de S. aureus adhérées aux substrats.*

En conclusion, ce travail de thèse permet de démontrer l'intérêt d'une approche transdisciplinaire (microbiologie, imagerie multimodale, physicochimie) pour appréhender une problématique clinique, la tolérance aux antibiotiques. Nous avons contribué à une meilleure compréhension des mécanismes responsables de l'inefficacité des antibiotiques vis-à-vis des biofilms de *S. aureus*. Ces travaux ouvrent la voie à des perspectives d'amélioration et/ou d'alternative à l'antibiothérapie actuelle.

REFERENCES

1. Henrici, A. T. Studies of Freshwater Bacteria I. A Direct Microscopic Technique. *J. Bacteriol.* **25,** 277–287 (1933).
2. Zobell, C. E. & Allen, E. C. The Significance of Marine Bacteria in the Fouling of Submerged Surfaces. *J. Bacteriol.* **29,** 239–251 (1935).
3. McCoy, W. F., Bryers, J. D., Robbins, J. & Costerton, J. W. Observations of fouling biofilm formation. *Can. J. Microbiol.* **27,** 910–917 (1981).
4. Costerton, J. W., Irvin, R. T., Cheng, K.-J. & Sutherland, I. W. The Role of Bacterial Surface Structures in Pathogenesis. *Crit. Rev. Microbiol.* **8,** 303–338 (1981).
5. Mah, T.-F. C. & O'Toole, G. A. Mechanisms of biofilm resistance to antimicrobial agents. *Trends Microbiol.* **9,** 34–39 (2001).
6. Høiby, N. A short history of microbial biofilms and biofilm infections. *APMIS* **125,** 272–275 (2017).
7. Locci, R., Peters, G. & Pulverer, G. Microbial colonization of prosthetic devices. I. Microtopographical characteristics of intravenous catheters as detected by scanning electron microscopy. *Zentralbl. Bakteriol. Mikrobiol. Hyg. [B]* **173,** 285–292 (1981).
8. Christensen, G. D., Baddour, L. M. & Simpson, W. A. Phenotypic variation of Staphylococcus epidermidis slime production in vitro and in vivo. *Infect. Immun.* **55,** 2870–2877 (1987).
9. Marrie, T. J., Nelligan, J. & Costerton, J. W. A scanning and transmission electron microscopic study of an infected endocardial pacemaker lead. *Circulation* **66,** 1339–1341 (1982).
10. Thammavongsa, V., Kim, H. K., Missiakas, D. & Schneewind, O. Staphylococcal manipulation of host immune responses. *Nat. Rev. Microbiol.* **13,** 529–543 (2015).
11. Archer, N. K. *et al.* Staphylococcus aureus biofilms: properties, regulation, and roles in human disease. *Virulence* **2,** 445–459 (2011).
12. Hall-Stoodley, L., Costerton, J. W. & Stoodley, P. Bacterial biofilms: from the Natural environment to infectious diseases. *Nat. Rev. Microbiol.* **2,** 95–108 (2004).
13. Tong, S. Y. C., Davis, J. S., Eichenberger, E., Holland, T. L. & Fowler, V. G. Staphylococcus aureus Infections: Epidemiology, Pathophysiology, Clinical Manifestations, and Management. *Clin. Microbiol. Rev.* **28,** 603–661 (2015).
14. Lebeaux, D., Ghigo, J.-M. & Beloin, C. Tolérance des biofilms aux antibiotiques : comprendre pour mieux traiter. *J. Anti-Infect.* **16,** 112–121 (2014).
15. O'Toole, G., Kaplan, H. B. & Kolter, R. Biofilm formation as microbial development. *Annu. Rev. Microbiol.* **54,** 49–79 (2000).
16. Kostakioti, M., Hadjifrangiskou, M. & Hultgren, S. J. Bacterial Biofilms: Development, Dispersal, and Therapeutic Strategies in the Dawn of the Postantibiotic Era. *Cold Spring Harb. Perspect. Med.* **3,** (2013).
17. Busscher, H. J. & Weerkamp, A. H. Specific and non-specific interactions in bacterial adhesion to solid substrata. *FEMS Microbiol. Lett.* **46,** 165–173 (1987).

18. An, Y. H. & Friedman, R. J. Concise review of mechanisms of bacterial adhesion to biomaterial surfaces. *J. Biomed. Mater. Res.* **43,** 338–348 (1998).

19. Boks, N. P., Busscher, H. J., van der Mei, H. C. & Norde, W. Bond-strengthening in staphylococcal adhesion to hydrophilic and hydrophobic surfaces using atomic force microscopy. *Langmuir ACS J. Surf. Colloids* **24,** 12990–12994 (2008).

20. Garrett, T. R., Bhakoo, M. & Zhang, Z. Bacterial adhesion and biofilms on surfaces. *Prog. Nat. Sci.* **18,** 1049–1056 (2008).

21. Busscher, H. J. & Van Der Mei, H. C. Physico-Chemical Interactions in Initial Microbial Adhesion and Relevance for Biofilm Formation. *Adv. Dent. Res.* **11,** 24–32 (1997).

22. Costerton, J. W., Stewart, P. S. & Greenberg, E. P. Bacterial Biofilms: A Common Cause of Persistent Infections. *Science* **284,** 1318–1322 (1999).

23. Foster, T. J., Geoghegan, J. A., Ganesh, V. K. & Höök, M. Adhesion, invasion and evasion: the many functions of the surface proteins of Staphylococcus aureus. *Nat. Rev. Microbiol.* **12,** 49–62 (2014).

24. Otto, M. Staphylococcal Biofilms. *Curr. Top. Microbiol. Immunol.* **322,** 207–228 (2008).

25. Arciola, C. R., Campoccia, D., Ravaioli, S. & Montanaro, L. Polysaccharide intercellular adhesin in biofilm: structural and regulatory aspects. *Front. Cell. Infect. Microbiol.* **5,** (2015).

26. Chan, Y. G.-Y., Kim, H. K., Schneewind, O. & Missiakas, D. The capsular polysaccharide of Staphylococcus aureus is attached to peptidoglycan by the LytR-CpsA-Psr (LCP) family of enzymes. *J. Biol. Chem.* jbc.M114.567669 (2014). doi:10.1074/jbc.M114.567669

27. Paharik, A. E. & Horswill, A. R. The Staphylococcal Biofilm: Adhesins, regulation, and host response. *Microbiol. Spectr.* **4,** (2016).

28. Arciola, C. R., Campoccia, D., Speziale, P., Montanaro, L. & Costerton, J. W. Biofilm formation in Staphylococcus implant infections. A review of molecular mechanisms and implications for biofilm-resistant materials. *Biomaterials* **33,** 5967–5982 (2012).

29. Mack, D. *et al.* The intercellular adhesin involved in biofilm accumulation of Staphylococcus epidermidis is a linear beta-1,6-linked glucosaminoglycan: purification and structural analysis. *J. Bacteriol.* **178,** 175–183 (1996).

30. Lasa, I. & Penadés, J. R. Bap: a family of surface proteins involved in biofilm formation. *Res. Microbiol.* **157,** 99–107 (2006).

31. Taglialegna, A. *et al.* Staphylococcal Bap Proteins Build Amyloid Scaffold Biofilm Matrices in Response to Environmental Signals. *PLoS Pathog.* **12,** (2016).

32. Cucarella, C. *et al.* Bap, a Staphylococcus aureus surface protein involved in biofilm formation. *J. Bacteriol.* **183,** 2888–2896 (2001).

33. Hartford, O., McDevitt, D. & Foster, T. J. Matrix-binding proteins of Staphylococcus aureus: functional analysis of mutant and hybrid molecules. *Microbiol. Read. Engl.* **145 (Pt 9),** 2497–2505 (1999).

34. O'Neill, E. *et al.* A Novel Staphylococcus aureus Biofilm Phenotype Mediated by the Fibronectin-Binding Proteins, FnBPA and FnBPB. *J. Bacteriol.* **190,** 3835–3850 (2008).

35. Abraham, N. M. & Jefferson, K. K. Staphylococcus aureus clumping factor B mediates biofilm formation in the absence of calcium. *Microbiol. Read. Engl.* **158,** 1504–1512 (2012).

36. Flemming, H.-C. & Wingender, J. The biofilm matrix. *Nat. Rev. Microbiol.* **8,** 623–633 (2010).

37. Branda, S. S., Vik, Å., Friedman, L. & Kolter, R. Biofilms: the matrix revisited. *Trends Microbiol.* **13,** 20–26 (2005).

38. Das, T., Sharma, P. K., Busscher, H. J., Mei, H. C. van der & Krom, B. P. Role of Extracellular DNA in Initial Bacterial Adhesion and Surface Aggregation. *Appl. Environ. Microbiol.* **76,** 3405–3408 (2010).

39. Schwartz, K., Ganesan, M., Payne, D. E., Solomon, M. J. & Boles, B. R. Extracellular DNA facilitates the formation of functional amyloids in Staphylococcus aureus biofilms. *Mol. Microbiol.* **99,** 123–134 (2016).

40. Schwartz, K., Syed, A. K., Stephenson, R. E., Rickard, A. H. & Boles, B. R. Functional Amyloids Composed of Phenol Soluble Modulins Stabilize Staphylococcus aureus Biofilms. *PLoS Pathog* **8,** e1002744 (2012).

41. Cheung, G. Y. C., Joo, H.-S., Chatterjee, S. S. & Otto, M. Phenol-soluble modulins – critical determinants of staphylococcal virulence. *FEMS Microbiol. Rev.* **38,** 698–719 (2014).

42. Kaplan, J. B. Biofilm Dispersal. *J. Dent. Res.* **89,** 205–218 (2010).

43. Joo, H.-S. & Otto, M. Molecular basis of in-vivo biofilm formation by bacterial pathogens. *Chem. Biol.* **19,** 1503–1513 (2012).

44. Lebeaux, D., Chauhan, A., Rendueles, O. & Beloin, C. From in vitro to in vivo Models of Bacterial Biofilm-Related Infections. *Pathogens* **2,** 288–356 (2013).

45. Bjarnsholt, T. *et al.* The in vivo biofilm. *Trends Microbiol.* **21,** 466–474 (2013).

46. Stewart, P. S. & Franklin, M. J. Physiological heterogeneity in biofilms. *Nat. Rev. Microbiol.* **6,** 199–210 (2008).

47. Costerton, J. W. *et al.* Biofilms, the customized microniche. *J. Bacteriol.* **176,** 2137–2142 (1994).

48. de Beer, D., Stoodley, P., Roe, F. & Lewandowski, Z. Effects of biofilm structures on oxygen distribution and mass transport. *Biotechnol. Bioeng.* **43,** 1131–1138 (1994).

49. Xu, K. D., Stewart, P. S., Xia, F., Huang, C. T. & McFeters, G. A. Spatial physiological heterogeneity in Pseudomonas aeruginosa biofilm is determined by oxygen availability. *Appl. Environ. Microbiol.* **64,** 4035–4039 (1998).

50. Rani, S. A. *et al.* Spatial Patterns of DNA Replication, Protein Synthesis, and Oxygen Concentration within Bacterial Biofilms Reveal Diverse Physiological States. *J. Bacteriol.* **189,** 4223–4233 (2007).

51. Wood, T. K., Knabel, S. J. & Kwan, B. W. Bacterial Persister Cell Formation and Dormancy. *Appl. Environ. Microbiol.* **79,** 7116–7121 (2013).

52. Ayrapetyan, M., Williams, T. C. & Oliver, J. D. Bridging the gap between viable but non-culturable and antibiotic persistent bacteria. *Trends Microbiol.* **23,** 7–13 (2014).

53. Ramamurthy, T., Ghosh, A., Pazhani, G. P. & Shinoda, S. Current Perspectives on Viable but Non-Culturable (VBNC) Pathogenic Bacteria. *Front. Public Health* **2,** (2014).

54. Lewis, K. Persister cells, dormancy and infectious disease. *Nat. Rev. Microbiol.* **5,** 48–56 (2007).

55. Pascoe, B. *et al.* Dormant Cells of Staphylococcus aureus Are Resuscitated by Spent Culture Supernatant. *PLoS ONE* **9,** e85998 (2014).

56. Lewis, K. Persister cells and the riddle of biofilm survival. *Biochem. Biokhimiia* **70,** 267–274 (2005).

57. Prax, M. & Bertram, R. Metabolic aspects of bacterial persisters. *Front. Cell. Infect. Microbiol.* **4,** (2014).

58. Bergkessel, M., Basta, D. W. & Newman, D. K. The physiology of growth arrest: uniting molecular and environmental microbiology. *Nat. Rev. Microbiol.* **14,** 549–562 (2016).

59. Pasquaroli, S. *et al.* Antibiotic pressure can induce the viable but non-culturable state in Staphylococcus aureus growing in biofilms. *J. Antimicrob. Chemother.* **68,** 1812–1817 (2013).

60. Pasquaroli, S. *et al.* Role of Daptomycin in the Induction and Persistence of the Viable but Non-Culturable State of Staphylococcus Aureus Biofilms. *Pathogens* **3,** 759–768 (2014).

61. Scherr, T. D., Heim, C. E., Morrison, J. M. & Kielian, T. Hiding in Plain Sight: Interplay between Staphylococcal Biofilms and Host Immunity. *Front. Immunol.* **5,** (2014).

62. Hanke, M. L. & Kielian, T. Deciphering mechanisms of staphylococcal biofilm evasion of host immunity. *Front. Cell. Infect. Microbiol.* **2,** 62 (2012).

63. Foster, T. J. Immune evasion by staphylococci. *Nat. Rev. Microbiol.* **3,** 948–958 (2005).

64. Spaan, A. N., Surewaard, B. G. J., Nijland, R. & van Strijp, J. A. G. Neutrophils versus Staphylococcus aureus: a biological tug of war. *Annu. Rev. Microbiol.* **67,** 629–650 (2013).

65. Verdrengh, M. & Tarkowski, A. Role of macrophages in Staphylococcus aureus-induced arthritis and sepsis. *Arthritis Rheum.* **43,** 2276–2282 (2000).

66. Verdrengh, M. & Tarkowski, A. Role of neutrophils in experimental septicemia and septic arthritis induced by Staphylococcus aureus. *Infect. Immun.* **65,** 2517–2521 (1997).

67. Nauseef, W. M. How human neutrophils kill and degrade microbes: an integrated view. *Immunol. Rev.* **219,** 88–102 (2007).

68. Baselga, R., Albizu, I. & Amorena, B. Staphylococcus aureus capsule and slime as virulence factors in ruminant mastitis. A review. *Vet. Microbiol.* **39,** 195–204 (1994).

69. O'Riordan, K. & Lee, J. C. Staphylococcus aureus Capsular Polysaccharides. *Clin. Microbiol. Rev.* **17,** 218–234 (2004).

70. Clarke, S. R. Phenol-Soluble Modulins of Staphylococcus aureus Lure Neutrophils into Battle. *Cell Host Microbe* **7,** 423–424 (2010).

71. Fraunholz, M. & Sinha, B. Intracellular staphylococcus aureus: Live-in and let die. *Front. Cell. Infect. Microbiol.* **2,** (2012).

72. Butler, M. S., Blaskovich, M. A. & Cooper, M. A. Antibiotics in the clinical pipeline at the end of 2015. *J. Antibiot. (Tokyo)* (2016). doi:10.1038/ja.2016.72

73. Fux, C. A., Costerton, J. W., Stewart, P. S. & Stoodley, P. Survival strategies of infectious biofilms. *Trends Microbiol.* **13,** 34–40 (2005).

74. Rayner, C. & Munckhof, W. J. Antibiotics currently used in the treatment of infections caused by Staphylococcus aureus. *Intern. Med. J.* **35,** S3–S16 (2005).

75. Ciofu, O., Rojo-Molinero, E., Macià, M. D. & Oliver, A. Antibiotic treatment of biofilm infections. *APMIS* **125,** 304–319 (2017).

76. Forrest, G. N. & Tamura, K. Rifampin Combination Therapy for Nonmycobacterial Infections. *Clin. Microbiol. Rev.* **23,** 14–34 (2010).

77. Jørgensen, N. P. *et al.* Rifampicin-containing combinations are superior to combinations of vancomycin, linezolid and daptomycin against Staphylococcus aureus biofilm infection in vivo and in vitro. *Pathog. Dis.* **74,** ftw019 (2016).

78. Fair, R. J. & Tor, Y. Antibiotics and Bacterial Resistance in the 21st Century. *Perspect. Med. Chem.* **6,** 25–64 (2014).

79. Ventola, C. L. The Antibiotic Resistance Crisis. *Pharm. Ther.* **40,** 277–283 (2015).

80. Davies, J. & Davies, D. Origins and Evolution of Antibiotic Resistance. *Microbiol. Mol. Biol. Rev. MMBR* **74,** 417–433 (2010).

81. Lowy, F. D. Antimicrobial resistance: the example of Staphylococcus aureus. *J Clin Invest.* **111,** 1265–1273 (2003).

82. Fuda, C. C. S., Fisher, J. F. & Mobashery, S. Beta-lactam resistance in Staphylococcus aureus: the adaptive resistance of a plastic genome. *Cell. Mol. Life Sci. CMLS* **62,** 2617–2633 (2005).

83. Stewart, P. S. Antimicrobial Tolerance in Biofilms. *Microbiol. Spectr.* **3,** (2015).

84. Brauner, A., Fridman, O., Gefen, O. & Balaban, N. Q. Distinguishing between resistance, tolerance and persistence to antibiotic treatment. *Nat. Rev. Microbiol.* **14,** 320–330 (2016).

85. Kahlmeter, G. *et al.* European harmonization of MIC breakpoints for antimicrobial susceptibility testing of bacteria. *J. Antimicrob. Chemother.* **52,** 145–148 (2003).

86. Levin-Reisman, I. *et al.* Antibiotic tolerance facilitates the evolution of resistance. *Science* eaaj2191 (2017). doi:10.1126/science.aaj2191

87. Wu, H., Moser, C., Wang, H.-Z., Høiby, N. & Song, Z.-J. Strategies for combating bacterial biofilm infections. *Int. J. Oral Sci.* **7,** 1–7 (2015).

88. Lebeaux, D., Ghigo, J.-M. & Beloin, C. Biofilm-Related Infections: Bridging the Gap between Clinical Management and Fundamental Aspects of Recalcitrance toward Antibiotics. *Microbiol. Mol. Biol. Rev.* **78,** 510–543 (2014).

89. Lebeaux, D., Ghigo, J.-M. & Lortholary, O. [Infections related to implanted medical devices: the down-side of medical progress]. *Rev. Prat.* **64,** 617–619 (2014).

90. Lebeaux, D. & Ghigo, J.-M. [Management of biofilm-associated infections: what can we expect from recent research on biofilm lifestyles?]. *Med. Sci. MS* **28,** 727–739 (2012).

91. Bhattacharya, M., Wozniak, D. J., Stoodley, P. & Hall-Stoodley, L. Prevention and treatment of Staphylococcus aureus biofilms. *Expert Rev. Anti Infect. Ther.* **13,** 1499–1516 (2015).

92. Safdar, N., Handelsman, J. & Maki, D. G. Does combination antimicrobial therapy reduce mortality in Gram-negative bacteraemia? A meta-analysis. *Lancet Infect. Dis.* **4,** 519–527 (2004).

93. LaPlante, K. L. & Woodmansee, S. Activities of Daptomycin and Vancomycin Alone and in Combination with Rifampin and Gentamicin against Biofilm-Forming Methicillin-Resistant

Staphylococcus aureus Isolates in an Experimental Model of Endocarditis. *Antimicrob. Agents Chemother.* **53,** 3880–3886 (2009).

94. Chauhan, A., Lebeaux, D., Ghigo, J.-M. & Beloin, C. Full and Broad-Spectrum In Vivo Eradication of Catheter-Associated Biofilms Using Gentamicin-EDTA Antibiotic Lock Therapy. *Antimicrob. Agents Chemother.* **56,** 6310–6318 (2012).

95. Del Pozo, J. L. *et al.* Effectiveness of teicoplanin versus vancomycin lock therapy in the treatment of port-related coagulase-negative staphylococci bacteraemia: a prospective case-series analysis. *Int. J. Antimicrob. Agents* **34,** 482–485 (2009).

96. Fernandez-Hidalgo, N. *et al.* Antibiotic-lock therapy for long-term intravascular catheter-related bacteraemia: results of an open, non-comparative study. *J. Antimicrob. Chemother.* **57,** 1172–1180 (2006).

97. Qu, Y., Istivan, T. S., Daley, A. J., Rouch, D. A. & Deighton, M. A. Comparison of various antimicrobial agents as catheter lock solutions: preference for ethanol in eradication of coagulase-negative staphylococcal biofilms. *J. Med. Microbiol.* **58,** 442–450 (2009).

98. Rijnders, B. J., Van Wijngaerden, E., Vandecasteele, S. J., Stas, M. & Peetermans, W. E. Treatment of long-term intravascular catheter-related bacteraemia with antibiotic lock: randomized, placebo-controlled trial. *J. Antimicrob. Chemother.* **55,** 90–94 (2005).

99. Allison, K. R., Brynildsen, M. P. & Collins, J. J. Metabolite-enabled eradication of bacterial persisters by aminoglycosides. *Nature* **473,** 216–220 (2011).

100. Barraud, N., Buson, A., Jarolimek, W. & Rice, S. A. Mannitol Enhances Antibiotic Sensitivity of Persister Bacteria in Pseudomonas aeruginosa Biofilms. *PLOS ONE* **8,** e84220 (2013).

101. Lister, J. L. & Horswill, A. R. Staphylococcus aureus biofilms: recent developments in biofilm dispersal. *Front. Cell. Infect. Microbiol.* **4,** (2014).

102. Boles, B. R. & Horswill, A. R. Staphylococcal biofilm disassembly. *Trends Microbiol.* **19,** 449–455 (2011).

103. Kaplan, J. B., Ragunath, C., Velliyagounder, K., Fine, D. H. & Ramasubbu, N. Enzymatic Detachment of Staphylococcus epidermidis Biofilms. *Antimicrob. Agents Chemother.* **48,** 2633–2636 (2004).

104. Kaplan, J. B. *et al.* Genes involved in the synthesis and degradation of matrix polysaccharide in Actinobacillus actinomycetemcomitans and Actinobacillus pleuropneumoniae biofilms. *J. Bacteriol.* **186,** 8213–8220 (2004).

105. Donelli, G. *et al.* Synergistic activity of dispersin B and cefamandole nafate in inhibition of staphylococcal biofilm growth on polyurethanes. *Antimicrob. Agents Chemother.* **51,** 2733–2740 (2007).

106. Mann, E. E. *et al.* Modulation of eDNA release and degradation affects Staphylococcus aureus biofilm maturation. *PloS One* **4,** e5822 (2009).

107. Kaplan, J. B. *et al.* Recombinant human DNase I decreases biofilm and increases antimicrobial susceptibility in staphylococci. *J. Antibiot. (Tokyo)* **65,** 73–77 (2012).

108. Kumar Shukla, S. & Rao, T. S. Dispersal of Bap-mediated Staphylococcus aureus biofilm by proteinase K. *J. Antibiot. (Tokyo)* **66,** 55–60 (2013).

109. Chaignon, P. *et al.* Susceptibility of staphylococcal biofilms to enzymatic treatments depends on their chemical composition. *Appl. Microbiol. Biotechnol.* **75,** 125–132 (2007).

110. Swartjes, J. J. T. M. *et al.* Current Developments in Antimicrobial Surface Coatings for Biomedical Applications. *Curr. Med. Chem.* **22,** 2116–2129 (2015).

111. Lu, Y., Yue, Z., Wang, W. & Cao, Z. Strategies on designing multifunctional surfaces to prevent biofilm formation. *Front. Chem. Sci. Eng.* **9,** 324–335 (2015).

112. Li, J. *et al.* Hydrophobic Liquid-Infused Porous Polymer Surfaces for Antibacterial Applications. *ACS Appl. Mater. Interfaces* **5,** 6704–6711 (2013).

113. Privett, B. J. *et al.* Antibacterial fluorinated silica colloid superhydrophobic surfaces. *Langmuir ACS J. Surf. Colloids* **27,** 9597–9601 (2011).

114. Epstein, A. K., Wong, T.-S., Belisle, R. A., Boggs, E. M. & Aizenberg, J. Liquid-infused structured surfaces with exceptional anti-biofouling performance. *Proc. Natl. Acad. Sci.* **109,** 13182–13187 (2012).

115. Wong, T.-S. *et al.* Bioinspired self-repairing slippery surfaces with pressure-stable omniphobicity. *Nature* **477,** 443–447 (2011).

116. Hu, C. *et al.* Micro-/Nanometer Rough Structure of a Superhydrophobic Biodegradable Coating by Electrospraying for Initial Anti-Bioadhesion. *Adv. Healthc. Mater.* **2,** 1314–1321 (2013).

117. Forsgren, J., Brohede, U., Strømme, M. & Engqvist, H. Co-loading of bisphosphonates and antibiotics to a biomimetic hydroxyapatite coating. *Biotechnol. Lett.* **33,** 1265–1268 (2011).

118. Takigami, I. *et al.* Two-stage revision surgery for hip prosthesis infection using antibiotic-loaded porous hydroxyapatite blocks. *Arch. Orthop. Trauma Surg.* **130,** 1221–1226 (2010).

119. Guillaume, O., Garric, X., Lavigne, J.-P., Van Den Berghe, H. & Coudane, J. Multilayer, degradable coating as a carrier for the sustained release of antibiotics: preparation and antimicrobial efficacy in vitro. *J. Control. Release Off. J. Control. Release Soc.* **162,** 492–501 (2012).

120. Jose, B., Antoci, V., Zeiger, A. R., Wickstrom, E. & Hickok, N. J. Vancomycin covalently bonded to titanium beads kills Staphylococcus aureus. *Chem. Biol.* **12,** 1041–1048 (2005).

121. Hickok, N. J. & Shapiro, I. M. Immobilized antibiotics to prevent orthopaedic implant infections. *Adv. Drug Deliv. Rev.* **64,** 1165–1176 (2012).

122. Swanson, T. E., Cheng, X. & Friedrich, C. Development of chitosan-vancomycin antimicrobial coatings on titanium implants. *J. Biomed. Mater. Res. A* **97,** 167–176 (2011).

123. Shukla, A., Fang, J. C., Puranam, S. & Hammond, P. T. Release of vancomycin from multilayer coated absorbent gelatin sponges. *J. Controlled Release* **157,** 64–71 (2012).

124. Ganz, T. Defensins: antimicrobial peptides of innate immunity. *Nat. Rev. Immunol.* **3,** 710–720 (2003).

125. Onaizi, S. A. & Leong, S. S. J. Tethering antimicrobial peptides: current status and potential challenges. *Biotechnol. Adv.* **29,** 67–74 (2011).

126. Humblot, V. *et al.* The antibacterial activity of Magainin I immobilized onto mixed thiols Self-Assembled Monolayers. *Biomaterials* **30,** 3503–3512 (2009).

127. Yala, J.-F. *et al.* Elaboration of antibiofilm materials by chemical grafting of an antimicrobial peptide. *Appl. Microbiol. Biotechnol.* **89,** 623–634 (2011).

128. Holmberg, K. V. *et al.* Bio-inspired stable antimicrobial peptide coatings for dental applications. *Acta Biomater.* **9,** 8224–8231 (2013).

129. Kazemzadeh-Narbat, M. *et al.* Multilayered coating on titanium for controlled release of antimicrobial peptides for the prevention of implant-associated infections. *Biomaterials* **34,** 5969–5977 (2013).

130. Mu, H. *et al.* Potent Antibacterial Nanoparticles against Biofilm and Intracellular Bacteria. *Sci. Rep.* **6,** 18877 (2016).

131. Liu, Y. *et al.* The antimicrobial and osteoinductive properties of silver nanoparticle/poly (DL-lactic-co-glycolic acid)-coated stainless steel. *Biomaterials* **33,** 8745–8756 (2012).

132. Stevens, K. N. J. *et al.* The relationship between the antimicrobial effect of catheter coatings containing silver nanoparticles and the coagulation of contacting blood. *Biomaterials* **30,** 3682–3690 (2009).

133. Muraih, J. K., Pearson, A., Silverman, J. & Palmer, M. Oligomerization of daptomycin on membranes. *Biochim. Biophys. Acta BBA - Biomembr.* **1808,** 1154–1160 (2011).

134. Muraih, J. K. Mode of Action of Daptomycin, a Lipopeptide Antibiotic. (2013).

135. Kailas, L. *et al.* Immobilizing live bacteria for AFM imaging of cellular processes. *Ultramicroscopy* **109,** 775–780 (2009).

136. Speziale, P., Pietrocola, G., Foster, T. J. & Geoghegan, J. A. Protein-based biofilm matrices in Staphylococci. *Front. Cell. Infect. Microbiol.* **4,** 171 (2014).

137. Dufrêne, Y. F. Towards nanomicrobiology using atomic force microscopy. *Nat. Rev. Microbiol.* **6,** 674–680 (2008).

138. Müller, D. J. & Dufrêne, Y. F. Atomic force microscopy: a nanoscopic window on the cell surface. *Trends Cell Biol.* **21,** 461–469 (2011).

139. Louise Meyer, R. *et al.* Immobilisation of living bacteria for AFM imaging under physiological conditions. *Ultramicroscopy* **110,** 1349–1357 (2010).

140. Dufrêne, Y. F. *et al.* Imaging modes of atomic force microscopy for application in molecular and cell biology. *Nat. Nanotechnol.* **12,** 295–307 (2017).

141. Formosa, C. *et al.* Nanoscale analysis of the effects of antibiotics and CX1 on a Pseudomonas aeruginosa multidrug-resistant strain. *Sci. Rep.* **2,** (2012).

142. Formosa, C., Herold, M., Vidaillac, C., Duval, R. E. & Dague, E. Unravelling of a mechanism of resistance to colistin in Klebsiella pneumoniae using atomic force microscopy. *J. Antimicrob. Chemother.* **70,** 2261–2270 (2015).

143. Longo, G. *et al.* Rapid detection of bacterial resistance to antibiotics using AFM cantilevers as nanomechanical sensors. *Nat. Nanotechnol.* **8,** 522–526 (2013).

144. Longo, G. *et al.* Antibiotic-induced modifications of the stiffness of bacterial membranes. *J. Microbiol. Methods* **93,** 80–84 (2013).

145. Longo, G. & Kasas, S. Effects of antibacterial agents and drugs monitored by atomic force microscopy. *Wiley Interdiscip. Rev. Nanomed. Nanobiotechnol.* **6,** 230–244 (2014).

146. Scocchi, M., Mardirossian, M., Runti, G. & Benincasa, M. Non-Membrane Permeabilizing Modes of Action of Antimicrobial Peptides on Bacteria. *Curr. Top. Med. Chem.* **16,** 76–88 (2016).

147. Francius, G. *et al.* Detection, Localization, and Conformational Analysis of Single Polysaccharide Molecules on Live Bacteria. *ACS Nano* **2,** 1921–1929 (2008).

148. Formosa-Dague, C. *et al.* Sticky Matrix: Adhesion Mechanism of the Staphylococcal Polysaccharide Intercellular Adhesin. *ACS Nano* **10,** 3443–3452 (2016).

149. Chapot-Chartier, M.-P. *et al.* Cell surface of Lactococcus lactis is covered by a protective polysaccharide pellicle. *J. Biol. Chem.* **285,** 10464–10471 (2010).

150. El-Kirat-Chatel, S., Beaussart, A., Boyd, C. D., O'Toole, G. A. & Dufrêne, Y. F. Single-Cell and Single-Molecule Analysis Deciphers the Localization, Adhesion, and Mechanics of the Biofilm Adhesin LapA. *ACS Chem. Biol.* **9,** 485–494 (2014).

151. Gilbert, Y. *et al.* Single-Molecule Force Spectroscopy and Imaging of the Vancomycin/d-Ala-d-Ala Interaction. *Nano Lett.* **7,** 796–801 (2007).

152. Formosa-Dague, C., Speziale, P., Foster, T. J., Geoghegan, J. A. & Dufrêne, Y. F. Zinc-dependent mechanical properties of Staphylococcus aureus biofilm-forming surface protein SasG. *Proc. Natl. Acad. Sci. U. S. A.* **113,** 410–415 (2016).

153. Feuillie, C. *et al.* Molecular interactions and inhibition of the staphylococcal biofilm-forming protein SdrC. *Proc. Natl. Acad. Sci. U. S. A.* **114,** 3738–3743 (2017).

154. Touhami, A., Jericho, M. H. & Beveridge, T. J. Atomic force microscopy of cell growth and division in Staphylococcus aureus. *J. Bacteriol.* **186,** 3286–3295 (2004).

155. Matias, V. R. F. & Beveridge, T. J. Cryo-electron microscopy of cell division in Staphylococcus aureus reveals a mid-zone between nascent cross walls. *Mol. Microbiol.* **64,** 195–206 (2007).

156. Monteiro, J. M. *et al.* Cell shape dynamics during the staphylococcal cell cycle. *Nat. Commun.* **6,** 8055 (2015).

157. Perry, C. C., Weatherly, M., Beale, T. & Randriamahefa, A. Atomic force microscopy study of the antimicrobial activity of aqueous garlic versus ampicillin against Escherichia coli and Staphylococcus aureus. *J. Sci. Food Agric.* **89,** 958–964 (2009).

158. Humphries, R. M., Pollett, S. & Sakoulas, G. A Current Perspective on Daptomycin for the Clinical Microbiologist. *Clin. Microbiol. Rev.* **26,** 759–780 (2013).

159. Müller, A. *et al.* Daptomycin inhibits cell envelope synthesis by interfering with fluid membrane microdomains. *Proc. Natl. Acad. Sci. U. S. A.* **113,** E7077–E7086 (2016).

160. Lowy, F. D. Staphylococcus aureus Infections. *N. Engl. J. Med.* **339,** 520–532 (1998).

161. Davies, D. Understanding biofilm resistance to antibacterial agents. *Nat. Rev. Drug Discov.* **2,** 114–122 (2003).

162. Shopsin, B., Kaveri, S. V. & Bayry, J. Tackling Difficult Staphylococcus aureus Infections: Antibodies Show the Way. *Cell Host Microbe* **20,** 555–557 (2016).

163. Mingeot-Leclercq, M.-P. & Décout, J.-L. Bacterial lipid membranes as promising targets to fight antimicrobial resistance, molecular foundations and illustration through the renewal of aminoglycoside antibiotics and emergence of amphiphilic aminoglycosides. *MedChemComm* **7,** 586–611 (2016).

164. Straus, S. K. & Hancock, R. E. W. Mode of action of the new antibiotic for Gram-positive pathogens daptomycin: Comparison with cationic antimicrobial peptides and lipopeptides. *Biochim. Biophys. Acta BBA - Biomembr.* **1758,** 1215–1223 (2006).

165. Muthaiyan, A., Silverman, J. A., Jayaswal, R. K. & Wilkinson, B. J. Transcriptional Profiling Reveals that Daptomycin Induces the Staphylococcus aureus Cell Wall Stress Stimulon and Genes Responsive to Membrane Depolarization. *Antimicrob. Agents Chemother.* **52,** 980–990 (2008).

166. Mengin-Lecreulx, D., Allen, N. E., Hobbs, J. N. & Heijenoort, J. van. Inhibition of peptidoglycan biosynthesis in Bacillus megaterium by daptomycin. *FEMS Microbiol. Lett.* **69,** 245–248 (1990).

167. Mascio, C. T. M., Alder, J. D. & Silverman, J. A. Bactericidal Action of Daptomycin against Stationary-Phase and Nondividing Staphylococcus aureus Cells. *Antimicrob. Agents Chemother.* **51,** 4255–4260 (2007).

168. Lamp, K. C., Rybak, M. J., Bailey, E. M. & Kaatz, G. W. In vitro pharmacodynamic effects of concentration, pH, and growth phase on serum bactericidal activities of daptomycin and vancomycin. *Antimicrob. Agents Chemother.* **36,** 2709–2714 (1992).

169. Fowler, V. G. *et al.* Daptomycin versus Standard Therapy for Bacteremia and Endocarditis Caused by Staphylococcus aureus. *N. Engl. J. Med.* **355,** 653–665 (2006).

170. Mariani, P. G., Sader, H. S. & Jones, R. N. Development of decreased susceptibility to daptomycin and vancomycin in a Staphylococcus aureus strain during prolonged therapy. *J. Antimicrob. Chemother.* **58,** 481–483 (2006).

171. Julian, K. *et al.* Characterization of a daptomycin-nonsusceptible vancomycin-intermediate Staphylococcus aureus strain in a patient with endocarditis. *Antimicrob. Agents Chemother.* **51,** 3445–3448 (2007).

172. Lamp, K. C., Friedrich, L. V., Mendez-Vigo, L. & Russo, R. Clinical Experience with Daptomycin for the Treatment of Patients with Osteomyelitis. *Am. J. Med.* **120,** S13–S20 (2007).

173. Sharma, M., Riederer, K., Chase, P. & Khatib, R. High rate of decreasing daptomycin susceptibility during the treatment of persistent Staphylococcus aureus bacteremia. *Eur. J. Clin. Microbiol. Infect. Dis.* **27,** 433–437 (2008).

174. Levy, D. T. *et al.* Successful treatment of a left ventricular assist device infection with daptomycin non-susceptible methicillin-resistant Staphylococcus aureus: case report and review of the literature. *Transpl. Infect. Dis. Off. J. Transplant. Soc.* **14,** E89-96 (2012).

175. Moise, P. A. *et al.* Multicenter Evaluation of the Clinical Outcomes of Daptomycin with and without Concomitant β-Lactams in Patients with Staphylococcus aureus Bacteremia and Mild to Moderate Renal Impairment. *Antimicrob. Agents Chemother.* **57,** 1192–1200 (2013).

176. Daptomycin Failures in Prosthetic Joint Infections and Bone... : Infectious Diseases in Clinical Practice. *LWW* Available at: http://journals.lww.com/infectdis/Fulltext/2008/09000/Daptomycin_Failures_in_Prosthetic_Joint_Infections.14.aspx. (Accessed: 18th April 2017)

177. Stefani, S. *et al.* Insights and clinical perspectives of daptomycin resistance in Staphylococcus aureus: A review of the available evidence. *Int. J. Antimicrob. Agents* **46,** 278–289 (2015).

178. Seaton, R. A. *et al.* Evaluation of Effectiveness and Safety of High-Dose Daptomycin: Results from Patients Included in the European Cubicin® Outcomes Registry and Experience. *Adv. Ther.* **32,** 1192–1205 (2015).

179. Jones, T. *et al.* Failures in Clinical Treatment of Staphylococcus aureus Infection with Daptomycin Are Associated with Alterations in Surface Charge, Membrane Phospholipid Asymmetry, and Drug Binding. *Antimicrob. Agents Chemother.* **52,** 269–278 (2008).

180. Skiest, D. J. Treatment failure resulting from resistance of Staphylococcus aureus to daptomycin. *J. Clin. Microbiol.* **44,** 655–656 (2006).

181. Dubois-Brissonnet, F., Trotier, E. & Briandet, R. The Biofilm Lifestyle Involves an Increase in Bacterial Membrane Saturated Fatty Acids. *Front. Microbiol.* **7,** (2016).

182. Zhang, Y.-M. & Rock, C. O. Membrane lipid homeostasis in bacteria. *Nat. Rev. Microbiol.* **6,** 222–233 (2008).

183. Denich, T. J., Beaudette, L. A., Lee, H. & Trevors, J. T. Effect of selected environmental and physico-chemical factors on bacterial cytoplasmic membranes. *J. Microbiol. Methods* **52,** 149–182 (2003).

184. Morvan, C. *et al.* Environmental fatty acids enable emergence of infectious Staphylococcus aureus resistant to FASII-targeted antimicrobials. *Nat. Commun.* **7,** (2016).

185. Boudjemaa, R. *et al.* New Insight into Daptomycin Bioavailability and Localization in Staphylococcus aureus Biofilms by Dynamic Fluorescence Imaging. *Antimicrob. Agents Chemother.* **60,** 4983–4990 (2016).

186. Daddi Oubekka, S., Briandet, R., Fontaine-Aupart, M.-P. & Steenkeste, K. Correlative time-resolved fluorescence microscopy to assess antibiotic diffusion-reaction in biofilms. *Antimicrob. Agents Chemother.* **56,** 3349–3358 (2012).

187. Cui, L. *et al.* Cell Wall Thickening Is a Common Feature of Vancomycin Resistance in Staphylococcus aureus. *J. Clin. Microbiol.* **41,** 5–14 (2003).

188. Cui, L., Tominaga, E., Neoh, H. & Hiramatsu, K. Correlation between Reduced Daptomycin Susceptibility and Vancomycin Resistance in Vancomycin-Intermediate Staphylococcus aureus. *Antimicrob. Agents Chemother.* **50,** 1079–1082 (2006).

189. Matias, V. R. F. & Beveridge, T. J. Native Cell Wall Organization Shown by Cryo-Electron Microscopy Confirms the Existence of a Periplasmic Space in Staphylococcus aureus. *J. Bacteriol.* **188,** 1011–1021 (2006).

190. Bourg, N. *et al.* Direct optical nanoscopy with axially localized detection. *Nat. Photonics* **9,** 587–593 (2015).

191. Sauermann, R., Rothenburger, M., Graninger, W. & Joukhadar, C. Daptomycin: A Review 4 Years after First Approval. *Pharmacology* **81,** 79–91 (2008).

192. Friedman, L., Alder, J. D. & Silverman, J. A. Genetic changes that correlate with reduced susceptibility to daptomycin in Staphylococcus aureus. *Antimicrob. Agents Chemother.* **50,** 2137–2145 (2006).

193. Hayden, M. K. *et al.* Development of Daptomycin resistance in vivo in methicillin-resistant Staphylococcus aureus. *J. Clin. Microbiol.* **43,** 5285–5287 (2005).

194. Mangili, A., Bica, I., Snydman, D. R. & Hamer, D. H. Daptomycin-resistant, methicillin-resistant Staphylococcus aureus bacteremia. *Clin. Infect. Dis. Off. Publ. Infect. Dis. Soc. Am.* **40,** 1058–1060 (2005).

195. Marty, F. M. *et al.* Emergence of a clinical daptomycin-resistant Staphylococcus aureus isolate during treatment of methicillin-resistant Staphylococcus aureus bacteremia and osteomyelitis. *J. Clin. Microbiol.* **44,** 595–597 (2006).

196. Helaine, S. & Kugelberg, E. Bacterial persisters: formation, eradication, and experimental systems. *Trends Microbiol.* **22,** 417–424 (2014).

197. Oldfield, E. & Feng, X. Resistance-Resistant Antibiotics. *Trends Pharmacol. Sci.* **35,** 664–674 (2014).

198. Chen, Y.-F., Sun, T.-L., Sun, Y. & Huang, H. W. Interaction of Daptomycin with Lipid Bilayers: A Lipid Extracting Effect. *Biochemistry (Mosc.)* **53,** 5384–5392 (2014).

199. Hachmann, A.-B. *et al.* Reduction in membrane phosphatidylglycerol content leads to daptomycin resistance in Bacillus subtilis. *Antimicrob. Agents Chemother.* **55,** 4326–4337 (2011).

200. Pogliano, J., Pogliano, N. & Silverman, J. A. Daptomycin-Mediated Reorganization of Membrane Architecture Causes Mislocalization of Essential Cell Division Proteins. *J. Bacteriol.* **194,** 4494–4504 (2012).

201. Silverman, J. A., Perlmutter, N. G. & Shapiro, H. M. Correlation of Daptomycin Bactericidal Activity and Membrane Depolarization in Staphylococcus aureus. *Antimicrob. Agents Chemother.* **47,** 2538–2544 (2003).

202. Brinster, S. *et al.* Type II fatty acid synthesis is not a suitable antibiotic target for Gram-positive pathogens. *Nature* **458,** 83–86 (2009).

203. Saito, H. E., Harp, J. R. & Fozo, E. M. Incorporation of Exogenous Fatty Acids Protects Enterococcus faecalis from Membrane-Damaging Agents. *Appl. Environ. Microbiol.* **80,** 6527–6538 (2014).

204. Nanocapsules lipidiques comprenant un antibiotique et leurs utilisations en therapie.

205. Daddi Oubekka, S., Briandet, R., Waharte, F., Fontaine-Aupart, M.-P. & Steenkeste, K. Image-based fluorescence recovery after photobleaching (FRAP) to dissect vancomycin diffusion-reaction processes in Staphylococcus aureus. in *Proc. SPIE 8087, Clinical and Biomedical Spectroscopy and Imaging II, 80871I* (eds. Ramanujam, N. & Popp, J.) **Proc. SPIE 8087, Clinical and Biomedical Spectroscopy and Imaging II, 80871I,** 80871I–80871I–7 (Proc. SPIE 8087, Clinical and Biomedical Spectroscopy and Imaging II, 80871I, 2011).

206. Olivier, N., Keller, D., Rajan, V. S., Gönczy, P. & Manley, S. Simple buffers for 3D STORM microscopy. *Biomed. Opt. Express* **4,** 885–899 (2013).

207. Dempsey, G. T., Vaughan, J. C., Chen, K. H., Bates, M. & Zhuang, X. Evaluation of fluorophores for optimal performance in localization-based super-resolution imaging. *Nat. Methods* **8,** 1027–1036 (2011).

208. Lin, Y. *et al.* Effect of laser intensity on Alexa Fluor 647 photoswitching kinetics. (2015). doi:10.1371/journal.pone.0128135.g006

209. van de Linde, S. *et al.* Direct stochastic optical reconstruction microscopy with standard fluorescent probes. *Nat. Protoc.* **6,** 991–1009 (2011).

210. Blair, J. M. A., Webber, M. A., Baylay, A. J., Ogbolu, D. O. & Piddock, L. J. V. Molecular mechanisms of antibiotic resistance. *Nat. Rev. Microbiol.* **13,** 42–51 (2015).

211. Debabov, D. Antibiotic resistance: Origins, mechanisms, approaches to counter. *Appl. Biochem. Microbiol.* **49,** 665–671 (2013).

212. Dhar, N. & McKinney, J. D. Microbial phenotypic heterogeneity and antibiotic tolerance. *Curr. Opin. Microbiol.* **10,** 30–38 (2007).

213. Lehar, S. M. *et al.* Novel antibody–antibiotic conjugate eliminates intracellular S. aureus. *Nature* **527,** 323–328 (2015).

214. Nadzam, G. S., De La Cruz, C., Greco, R. S. & Haimovich, B. Neutrophil Adhesion to Vascular Prosthetic Surfaces Triggers Nonapoptotic Cell Death. *Ann. Surg.* **231,** 587–599 (2000).

215. Singh, R., Sahore, S., Kaur, P., Rani, A. & Ray, P. Penetration barrier contributes to bacterial biofilm-associated resistance against only select antibiotics, and exhibits genus-, strain- and antibiotic-specific differences. *Pathog. Dis.* ftw056 (2016). doi:10.1093/femspd/ftw056

216. Cao, B. *et al.* Diffusion Retardation by Binding of Tobramycin in an Alginate Biofilm Model. *PLoS ONE* **11,** (2016).

217. Jefferson, K. K., Goldmann, D. A. & Pier, G. B. Use of Confocal Microscopy To Analyze the Rate of Vancomycin Penetration through Staphylococcus aureus Biofilms. *Antimicrob. Agents Chemother.* **49,** 2467–2473 (2005).

218. Darouiche, R. O. *et al.* Vancomycin Penetration Into Biofilm Covering Infected Prostheses And Effect On Bacteria. *J. Infect. Dis.* **170,** 720–723 (1994).

219. Stewart, P. S., Davison, W. M. & Steenbergen, J. N. Daptomycin Rapidly Penetrates a Staphylococcus epidermidis Biofilm. *Antimicrob. Agents Chemother.* **53,** 3505–3507 (2009).

220. Zheng, Z. & Stewart, P. S. Penetration of Rifampin through Staphylococcus epidermidis Biofilms. *Antimicrob. Agents Chemother.* **46,** 900–903 (2002).

VALORISATION SCIENTIFIQUE

Publications scientifiques

1. Boudjemaa R, Briandet R, Steenkeste K, Fontaine-Aupart MP, *"*Taking advantage of fluorescent-based tools to puzzle out successes and failures of antibiotics to inactivate infectious bacteria", *Encyclopedia of Analytical Chemistry (EAC)* **2017**

2. Boudjemaa R, Briandet R, Fontaine-Aupart MP, Steenkeste K, "How do fluorescence spectroscopy and multimodal fluorescence imaging help to dissect the enhanced efficiency of vancomycin-rifampin combination against *Staphylococcus aureus* infections?", *Photophysical and Photobiological Sciences (PPS)* **2017**

3. Boudjemaa R, Briandet R, Revest M, Jacqueline C, Caillon J, Fontaine-Aupart M-P, Steenkeste K, *"*New insight into daptomycin bioavailability and localization in *S. aureus* biofilms by dynamic fluorescence imaging", *Antimicrobial Agents and Chemotherapy (AAC)* **2016**

4. Revest M, Jacqueline C, **Boudjemaa R**, Caillon J, Le Mabecque V, Breteche A, Steenkeste K, Tattevin P, Potel G, Michelet C, Fontaine-Aupart M-P, Boutoille D, "New *in vitro* and *in vivo* models to evaluate antibiotic efficacy in *S. aureus* prosthetic vascular graft infection", *Journal of Antimicrobial Chemotherapy (JAC)* **2016**

5. Boudjemaa R *et al. "*Intramacrophagic *Staphylococcus aureus* in prosthetic vascular graft infections as potential responsible of antibiotic therapy failure: observations of an ex-vivo mouse model", *soumis*

6. Boudjemaa R *et al. "*Real-time atomic force microscopy analysis of live *Staphylococcus aureus* bacteria: from single sessile cell toward biofilm genesis", *en vue d'être soumis*

7. Boudjemaa R *et al.* "Failure of daptomycin to inactivate *S. aureus* cells: the influence of the fatty acid composition of bacterial membranes", *soumis*

8. Boudjemaa R *et al.* "Design of new functionalized ZCIS QDs photosensitizers for singlet oxygen: taking advantage face to *S. aureus* bacteria adhered to surfaces", *en préparation*

9. Moran G, **Boudjemaa R** *et al.* "Highly Efficient Fluorescent Superhydrophobic Polypyrene Films towards Prevention of *Staphylococcus aureus* and *Pseudomonas aeruginosa* Biofilm Formation", *soumis*

Séminaire invité

1. Boudjemaa R. "Un exemple d'études *in vitro* et *in vivo* pour une infection à *S. aureus* sur implants cardiovasculaires : comment l'imagerie optique à résolution micro-nanométrique permet-elle d'éclairer les mécanismes de tolérance bactérienne aux antibiotiques ? ", *Laboratoire de Thérapeutique Expérimentale et Clinique des Infections*, **2017**, Nantes, France

Communications orales

1. Boudjemaa R, Briandet R, Revest M, Jacqueline C, Caillon J, Cabriel C, Bourg N, Dupuis G, Leveque-Fort S, Fontaine-Aupart MP, Steenkeste K "Micro to nanometric optical imaging resolution to better understand bacterial biofilms persistence: *in vitro* and *in vivo* visualization and characterization of antibiotics action", *Joint congress of French and Italian Photochemists and Photobiologists* **2016**, Bari, Italie

2. Boudjemaa R, Cabriel C, Bourg N, Dupuis G, Leveque-Fort S, Briandet R, Fontaine-Aupart MP, Steenkeste K, "Micro to nanometric optical imaging to ascertain antibiotic target localization: why are these antimicrobials not effective?", *Biofilms 7* **2016**, Porto, Portugal

3. Boudjemaa R, Briandet R, Revest M, Jacqueline C, Cabriel C, Bourg N, Dupuis G, Leveque-Fort S, Fontaine-Aupart MP, Steenkeste K, "L'inefficacité des antibiotiques contre des biofilms bactériens cliniques : visualiser et quantifier à l'échelle subcellulaire pour mieux comprendre" au *Réseau National Biofilms* **2015**, Toulouse, France et à la *Journée de l'Ecole Doctorale,* Ecole polytechnique, **2015**, France

4. Steenkeste K, **Boudjemaa R,** Briandet R, Revest M, Jacqueline C, Caillon J, Fontaine-Aupart MP, "Diffusion, localization and bioavailability of clinically-used antibiotics in staphylococcus aureus biofilms: toward a better understanding of bacterial biofilms tolerance?", *Physical Chemistry of the Cell* **2015**, Orsay, France

5. Boudjemaa R, Revest M, Jacqueline C, Caillon J, Briandet R, Fontaine-Aupart MP, Steenkeste K, "Diffusion, bioavailability and reactivity of antibiotics against *staphylococcus aureus* biofilms: a new approach by dynamic fluorescence imaging", *International Conference on Antimicrobial Research (ICAR)* **2014**, Madrid, Espagne

Posters

1. Boudjemaa R, Dubois-Brissonnet F, Gruss A, Briandet R, Fontaine-Aupart MP, Steenkeste K, "Membrane fatty acid composition runs *S. aureus* tolerance to daptomycin", *Eurobiofilms* **2017**, Amsterdam, Pays-Bas

2. Boudjemaa R, Marlière C, Briandet R, Fontaine-Aupart MP, Steenkeste K, "Real-Time changes of cell surface nanotopography in biofilm genesis", *Eurobiofilms* **2017**, Amsterdam, Pays-Bas

3. Cabriel C, Bourg N, **Boudjemaa R,** Steenkeste K, Fontaine-Aupart M-P, Dupuis G, Fort E, Lévêque-Fort S *"*Combining axial single molecule localization strategies to enhance 3D imaging of antibiotic in bacteria", *Single Molecule Localization Microscopy congress* **2016**, Lausanne, Suisse

4. **Boudjemaa R,** Briandet R, Revest M, Jacqueline C, Caillon J, Fontaine-Aupart M-P, Steenkeste K, *"Staphylococcus aureus* adhesion on prosthetic vascular grafts: an *in vivo* visualization and characterization of antibiotics efficiency" at *Biofilms 7* **2016**, Porto, Portugal

5. Thebault P, **Boudjemaa R,** Steenkeste K, Marlière C, Fontaine-Aupart M-P, "New insight on antibacterial mechanism of immobilized antimicrobial peptides", *Biofilms 7* **2016**, Porto, Portugal

6. **Boudjemaa R,** Briandet R, Revest M, Jacqueline C, Caillon J, Fontaine-Aupart M-P, Steenkeste K, "Visualization and quantification of *Staphylococcus aureus* biofilms inactivation by antibiotics to provide a better understanding of bacterial biofilms tolerance", *American Society for Microbiology conference on biofilms* **2015,** Chicago, Etats-Unis

7. Revest M, Jacqueline C, **Boudjemaa R**, Caillon J, Steenkeste K, Tattevin P, Potel G, Michelet C, Fontaine-Aupart M-P, Boutoille D, "Comparative efficacy of cloxacillin, vancomycin, daptomycin whether or not combined with rifampin in a mouse model of *Staphylococcus aureus* vascular material infection", *54th Interscience Conference on Antimicrobial Agents and Chemotherapy (ICAAC)* **2014**, Washington, Etats-Unis

8. **Boudjemaa R,** Revest M, Jacqueline C, Caillon J, Briandet R, Fontaine-Aupart M-P, Steenkeste K, "Diffusion, Bioavailability and Reactivity of Antibiotics against *Staphylococcus aureus* Biofilms: a New Approach by Dynamic Fluorescence Imaging", *54th Interscience Conference on Antimicrobial Agents and Chemotherapy (ICAAC)* **2014**, Washington, Etats-Unis

Mission et formation hors-recherche

1. Mission de doctorant-conseil chez VitaDX, start-up spécialisée dans le diagnostic précoce du cancer de la vessie (recherche bibliographique pour mettre au point un programme d'expériences R&D)

2. Suivi des cours d'un DU (Diplôme Universitaire) en ingénierie biomédicale : valorisation de la recherche et innovation biomédicale